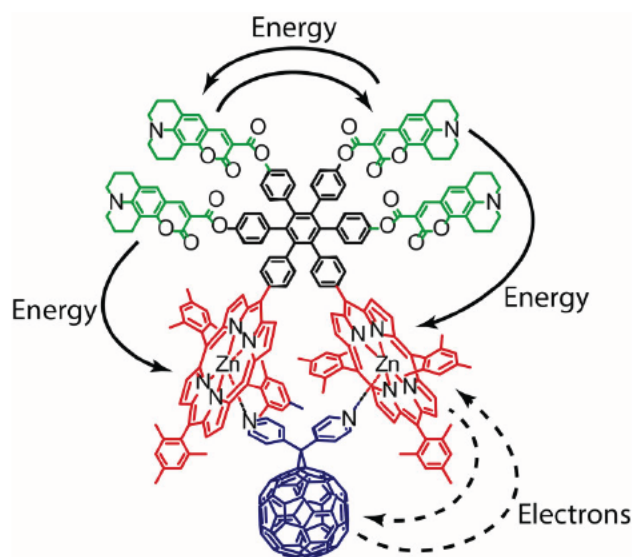
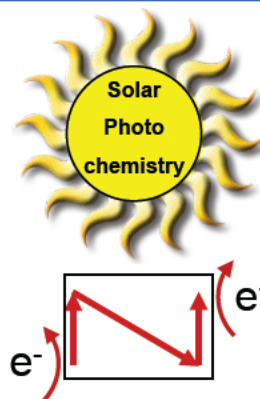
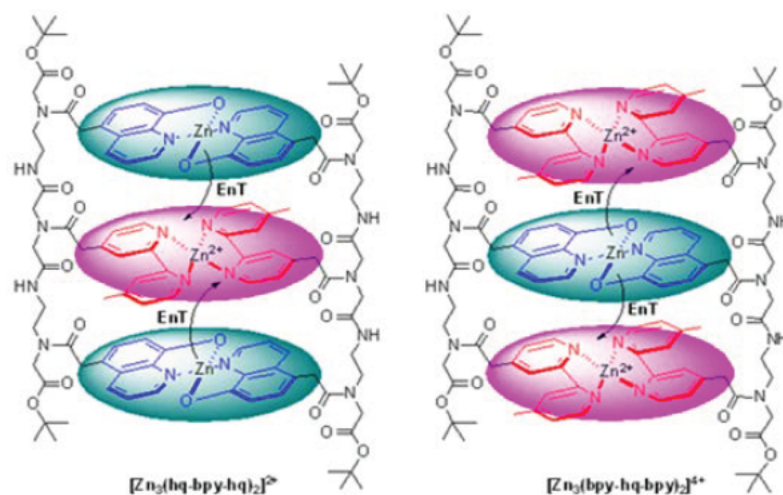
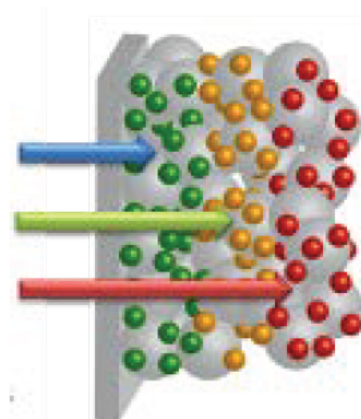


Westin Annapolis Hotel
Annapolis, MD
June 2-5, 2013



Proceedings of the
**Thirty-Fifth
DOE Solar Photochemistry
Research Meeting**



Sponsored by:

**Chemical Sciences, Geosciences, and Biosciences Division
Office of Basic Energy Sciences, U.S. Department of Energy**

Program and Abstracts

Solar Photochemistry Program Research Meeting

Westin Annapolis Hotel
Annapolis, Maryland
June 2-5, 2013

Chemical Sciences, Geosciences, and Biosciences Division
Office of Basic Energy Sciences
Office of Science
U.S. Department of Energy

Cover Graphics:

The cover figures are drawn from the abstracts of this meeting. One represents a stratified sensitization of a TiO₂ nanocrystalline electrode by quantum dots (Kamat., p. 46). Another depicts light harvesting and electron transfer in a unified molecular complex (Moore *et al.*, p. 65). A third shows a multifunctional energy and electron transfer structure (Gallagher *et al.*, p. 156).

FOREWORD

The 35th Department of Energy Solar Photochemistry Research Meeting, sponsored by the Chemical Sciences, Geosciences, and Biosciences Division of the Office of Basic Energy Sciences, is being held June 2-5, 2013 at the Westin Annapolis Hotel in Annapolis, Maryland. These proceedings include the meeting agenda, abstracts of the formal presentations and posters of the conference, and an address list for the participants.

This Conference is composed of the grantees who perform research in solar photochemical energy conversion with the support of the Chemical Sciences, Geosciences, and Biosciences Division. The purpose of the meeting is to foster collaboration, cooperation, and the exchange of new concepts and ideas between these researchers. This interaction has played an essential role in maintaining the high quality of research that has sustained this Program over the years.

This particular Solar Photochemistry Research Meeting has a distinct character. Its attendees represent the subset of the researchers supported by the Program that focus on the absorption of light, separation and transport of charge and its harvest as electrical power. The resultant meeting is smaller, but is hoped to allow for a more effective communication between participants. As a guest speaker, Professor Michael McGehee of Stanford University will open the conference sessions with a presentation on issues of power generation from organic solar cells that involve both basic as well as applied research. In the sessions that follow there will be presentations on photo-induced electron transfer in organic donor acceptor couples, between quantum dots, and at sensitized semiconductor surfaces. Further discussions on energy and electron transfer in model photosynthetic systems will be made and the topic of singlet fission in excited organic chromophores will be explored

I would like to express my appreciation to Diane Marceau of the Division of Chemical Sciences, Geosciences, and Biosciences, and Connie Lansdon of the Oak Ridge Institute of Science and Education for their assistance with the the logistics of this meeting. I must also thank all of the researchers whose enthusiasm, energy, and dedication to scientific inquiry have enabled these advances in solar photoconversion and made this meeting possible.

Mark T. Spitler
Chemical Sciences, Geosciences,
and Biosciences Division
Office of Basic Energy Sciences

Solar Photochemistry Research Conference Overview					
Time	Sunday, June 2	Monday, June 3	Tuesday, June 4	Wednesday, June 5	
7:15 AM					7:15 AM
7:30 AM		Breakfast	Breakfast	Breakfast	7:30 AM
7:45 AM		7:15-8:15	7:15-8:30	7:15-8:30	7:45 AM
8:00 AM					8:00 AM
8:15 AM		Opening Remarks			8:15 AM
8:30 AM					8:30 AM
8:45 AM		Session I	Session IV	Session VII	8:45 AM
9:00 AM		Opening Speaker	Solar Photoconversion with Quantum Dots	Inorganic Homogeneous Catalysis	9:00 AM
9:15 AM					9:15 AM
9:30 AM		BREAK			9:30 AM
9:45 AM		9:30 - 10:00			9:45 AM
10:00 AM			BREAK	BREAK	10:00 AM
10:15 AM		Session II	10:00 - 10:30	10:00 - 10:30	10:15 AM
10:30 AM					10:30 AM
10:45 AM		Photo-Induced Electron Transfer, Transport, and Fission	Session V Mostly Carbon	Session VIII Computational and Model Interfaces	10:45 AM
11:00 AM					11:00 AM
11:15 AM					11:15 AM
11:30 AM					11:30 AM
11:45 AM				Session IX	11:45 AM
12:00 PM					12:00 PM
12:15 PM		LUNCH	LUNCH	LUNCH	12:15 PM
12:30 PM		12:00 - 1:00	12:00 - 1:00	12:00 - 1:00	12:30 PM
12:45 PM					12:45 PM
1:00 PM					1:00 PM
1:15 PM				Session IX (cont.)	1:15 PM
1:30 PM				Dye Sensitized Interfaces and Systems	1:30 PM
1:45 PM					1:45 PM
2:00 PM					2:00 PM
2:15 PM		Individual Time			2:15 PM
2:30 PM			Individual Time	Closing Remarks	2:30 PM
2:45 PM					2:45 PM
3:00 PM					3:00 PM
3:15 PM					3:15 PM
3:30 PM					3:30 PM
3:45 PM					3:45 PM
4:00 PM					4:00 PM
4:15 PM	Registration				4:15 PM
4:30 PM	3:00 - 6:00		Session VI		4:30 PM
4:45 PM		Session III	Photosynthetic Systems Artificial and Real		4:45 PM
5:00 PM					5:00 PM
5:15 PM	No-Host Reception	Coupled			5:15 PM
5:30 PM	5:30 - 6:30	Donors and Acceptors			5:30 PM
5:45 PM	at the bar				5:45 PM
6:00 PM					6:00 PM
6:15 PM			DINNER		6:15 PM
6:30 PM		DINNER	on the town		6:30 PM
6:45 PM		6:15 - 7:30			6:45 PM
7:00 PM	DINNER		5:30 - 8:00		7:00 PM
7:15 PM	6:30 - 7:45				7:15 PM
7:30 PM					7:30 PM
7:45 PM	Welcome				7:45 PM
8:00 PM		Posters			8:00 PM
8:15 PM	After Dinner Session	odd numbers (1-45)	Posters even numbers (2-44)		8:15 PM
8:30 PM					8:30 PM
8:45 PM					8:45 PM
9:00 PM					9:00 PM
9:15 PM	Reception Continues	7:30 - 10:00			9:15 PM
9:30 PM	9:00 - 10:00		8:00 - 10:00		9:30 PM
9:45 PM	at the bar				9:45 PM
10:00 PM					10:00 PM

Table of Contents

TABLE OF CONTENTS

Foreword	iii
Overview	iv
Program	xiv

Abstracts of Oral Presentations

Sunday Evening - After Dinner Speakers

The Center for Interface Science: Solar Electric Materials (CISSEM) Neal R. Armstrong , University of Arizona	3
Quantum Confined Semiconductors for Photovoltaics The Center for Advanced Solar Photophysics (CASP) Matthew C. Beard , National Renewable Energy Laboratory	4

Session I – Opening Session

How the Morphology of Polymer Bulk Heterojunction Solar Cells Determines the Charge Separation Efficiency Jonathan A. Bartelt, Sean Sweetnam, Zach M. Beiley, Eric T. Hoke, William R. Mateker, Kenneth R. Graham, Jason Bloking, Alberto Salleo, Michael F. Toney, and Michael D. McGehee , Stanford University	7
--	---

Session II – Photo-Induced Electron Transfer, Transport, and Fission

Charge Transport and Transfer for Molecular Energy Conversion John Miller , Brookhaven National Laboratory	11
Dynamics and Efficiency of Photoinduced Charge Transport in DNA Frederick D. Lewis , Northwestern University	14
Singlet Fission in 1,3-Diphenylisobenzofuran: Chromophore Coupling and Excited State Evolution in Dimers and Solids Justin Johnson , National Renewable Energy Laboratory	17
Efficient Singlet Fission in Polycrystalline Perylenediimides and Related Perylene Dyes Michael R. Wasielewski , Northwestern University	20

Session III – Coupled Donors and Acceptors

Tetrapyrrolic Architectures for Fundamental Studies of Light Harvesting and Energy Transduction David F. Bocian, Dewey Holten, Christine Kirmaier, and Jonathan S. Lindsey , The University of California, Riverside, Washington University and North Carolina State University.....	29
I. Use of time resolved infrared to evaluate charge transfer excited states and intramolecular electron transfer in Re(I) dimethylaminobenzonitrile complexes; II. Triplet states and photoreactions of Sn(IV) N [^] N [^] O Schiff base complexes. Russell Schmehl , Tulane University.....	33

Session IV – Solar Photoconversion with Quantum Dots

Strongly Coupled Quantum Dot-Ligand Systems Emily A. Weiss , Northwestern University.....	39
Dependence of Size, Composition, and Doping on the Multiple Exciton Generation Efficiency in Quantum Dots Matthew C. Beard , National Renewable Energy Laboratory.....	42
Modulation of Light Harvesting Properties of Semiconductor Quantum Dot Assemblies Prashant Kamat , Notre Dame Radiation Laboratory.....	46

Session V – Mostly Carbon

Interfacial Exciton Dissociation in Organic Heterojunction Blends with Highly Enriched Semiconducting Single-Walled Carbon Nanotubes Jeff Blackburn , National Renewable Energy Laboratory.....	53
Ultrafast Optical Microscopy of Multi-Scale Energy Flow Libai Huang , Notre Dame Radiation Laboratory.....	56
Graphene: Charge Transfer, Spectroscopy and “Hot” Electrons Louis Brus , Columbia University.....	60

Session VI – Photosynthetic Systems – Artificial and Real

Interchromophore Interactions in Artificial Photosynthesis Ana L. Moore, Thomas A. Moore, Devens Gust , Arizona State University.....	65
Light Harvesting Dynamics Graham R. Fleming , Lawrence Berkeley National Laboratory.....	69

Session VII – Inorganic Homogeneous Photocatalysis

Mechanistic Understanding of Proton-Coupled Electron Transfer In Artificial Photosynthesis Dmitry E. Polyansky , Brookhaven National Laboratory	75
Critical Steps in Water Oxidation by Ru Blue Dimer Catalysts: Insights into the Electronic Requirements of Water Activation for Artificial Photosynthesis Yulia Pushkar , Purdue University.....	80
Electrochemical Water Oxidation by Homogenous Co Catalyst Linda H. Doerr , Boston University.....	83

Session VIII – Computational and Model Interfaces

Quantum Chemical Modeling of Systems for Solar Energy Conversion Richard Friesner , Columbia University.....	87
Time-Domain Ab Initio Studies of Light-Harvesting and Charge Transfer in Nanoscale Systems for Solar Photoconversion Oleg Prezhdo , Rochester University	90

Session IX – Dye Sensitized Interfaces and Systems

Sensitization of Single Crystal Semiconductor Electrodes with Dyes, Quantum Dots and Polymers Bruce Parkinson , University of Wyoming.....	94
Bisphenanthrolinecopper(I) in Photoinduced Charge Separation and DSSC Dyes C. Michael Elliott , Colorado State University.....	99
Model Dyes for Study of Molecule/Metal Oxide Interfaces and Electron Transfer Processes Elena Galoppini and Robert A. Bartynski , Rutgers University.....	102
Fundamental Studies of Light-induced Charge Transfer, Energy Transfer, and Energy Conversion with Supramolecular Systems Joseph T. Hupp , Northwestern University.....	106

Poster Abstracts (by poster number)

1.	Electronic Transport via Stokes-Shifted Dark States in Colloidal Quantum Dot Solids <u>John B. Asbury</u>	113
2.	Diode Linkers for the Covalent Attachment of Mn Catalysts to TiO ₂ Surfaces Christian Negre, Laura J. Allen, Rebecca L. Milot, Karin Brumback, Gary W. Brudvig, Charles A. Schmuttenmaer, Robert H. Crabtree and <u>Victor S. Batista</u>	114
3.	Electron Dynamics in pyrrolidinium bis(trifluoromethylsulfonyl)amid ionic liquids Benjamin FitzPatrick, Andrew T. Healy, Francesc Molins, and <u>David A. Blank</u>	115
4.	Semiconductor-electrocatalyst contacts: theory, experiment, and applications to solar water photoelectrolysis <u>Shannon W. Boettcher</u> , Fuding Lin, Thomas J. Mills.....	116
5.	Photoelectrochemical Oxidation of a Turn-On Fluorescent Probe Mediated by a Surface MnII Catalyst Covalently Attached to TiO ₂ Nanoparticles Alec C. Durrell, Gonghu Li, Matthieu Koepf, Christian F. A. Negre, Laura J. Allen, William R. McNamara, Hee-eun Song, Victor S. Batista, Robert H. Crabtree, and <u>Gary W. Brudvig</u>	117
6.	Towards Solar Fuels Enabling Cuprous Phenanthroline Complexes Catherine E. McCusker and <u>Felix N. Castellano</u>	118
7.	Photo-Induced Electron Transfer and Solute-Ion Interactions in Ionic Liquids Sufia Khatun, Min Liang, Marie F. Thomas and <u>Edward W. Castner, Jr.</u>	119
8.	Physical Properties of Doped and Sensitized Polyoxotitanate Nanostructures <u>Philip Coppens</u> , Jesse Sokolow, Yang Chen and Elzbieta Trzop.....	120
9.	Modular assembly of high-potential Zn porphyrin sensitizers attached to TiO ₂ with a series of anchoring groups Lauren A. Martini, Gary F. Moore, Rebecca L. Milot, Lawrence Z. Cai, Stafford W. Sheehan, Charles A. Schmuttenmaer, Gary W. Brudvig, and <u>Robert H. Crabtree</u>	121
10.	Computational and Experimental Strategies to Achieve, Control, and Understand Singlet Fission in Molecular and Thin Film Systems <u>Niels H. Damrauer</u> , Paul Vallett, Jamie Snyder, Bijan Paul, Jasper Cook, Thomas Carey, and Ryan Michael.....	122
11.	Multicomponent Arrays for Multiple-Redox and Multiple-Excited-State Interactions in Molecular Aggregates <u>Marye Anne Fox</u> and James K Whitesell.....	123
12.	PCET of Small Molecule Activation by Hangman Catalysts <u>Daniel G. Nocera</u>	124

13.	Effects of Water on the Charge-Carrier Dynamics, Photoelectrochemical Properties, and Stability of Dye-Sensitized Solar Cells Kai Zhu, Song-Rim Jang, and <u>Arthur J. Frank</u>	125
14.	Excited State Quenching Mechanism of a Terthiophene Acid Dye Bound to Monodisperse CdS Nanocrystals: Electron Transfer vs. Concentration Quenching Rajan Vatassery, Jon Hinke, Antonio Sanchez-Diaz, Ryan Hue, Kent R. Mann, David A. Blank, and <u>Wayne L. Gladfelter</u>	126
15.	Molecular and Material Approaches to Overcome Kinetic and Energetic Constraints in Dye-Sensitized Solar Cells Jesse Ondersma, Yuling Xie, Suraj Soman, Dhritabrata Mandal and <u>Thomas W. Hamann</u>	127
16.	Two-Catalyst Assemblies and Mixtures for Photochemical CO ₂ Reduction Davis B. Moravec, Nathan La Porte, and <u>Michael D. Hopkins</u>	128
17.	2D Electronic Spectra of PbSe Quantum Dots in the Short-Wave Infrared Samuel D. Park, Dmitry Baranov, Byungmoon Cho, Vivek Tiwari, and <u>David M. Jonas</u>	129
18.	Effects of Stranski-Krastanov Shells in the Charge Transfer Dynamics of ZnTe/CdSe Nanocrystals Zhong-Jie Jiang and <u>David F. Kelley</u>	130
19.	Neutral Carotenoid Radicals in Photoprotection Adam Magyar, Michael K. Bowman, Peter Molnar, and <u>Lowell D. Kispert</u>	131
20.	Photoexcited Excitons in Charged Single Walled Carbon Nanotubes Nicole M. Cogan, Sebastian Shaffer, Michael Odoi, Bradford Loesch, Julie Smyder, and <u>Todd D. Krauss</u>	132
21.	Exciton Dissociation Dynamics in Colloidal Triadic CdSe-CdS-Pt Nanorods Kaifeng Wu, Haiming Zhu and <u>Tianquan Lian</u>	133
22.	Photochemical and Photovoltaic Properties of Conjugated Ionomers Stephen Robinson, Ethan Walker, Chris Weber, and <u>Mark Loneragan</u>	134
23.	Controlled seeding and growth of Ta:TiO ₂ nanoforest and its performance as photoanode for dye sensitized solar cell devices Yukihiro Hara, Timothy Garvey, Leila Alibabaei, Rudresh Ghosh, <u>Rene Lopez</u>	135
24.	Sensitization of p-GaP Photoelectrodes with CdSe Quantum Dots: Light Stimulated Hole Injection Zhijie Wang, Junsi Gu, Sabrina Peczonczyk, and <u>Stephen Maldonado</u>	136
25.	Nanostructured Photocatalytic Water Splitting Systems Nella M. Vargas-Barbosa, John R. Swierk, Yixin Zhao, Nicholas McCool, Timothy P. Saunders, Jennifer L. Dysart, and <u>Thomas E. Mallouk</u>	137

26.	Rotational Dynamics in Ionic Liquids – NMR & MD Studies Anne Kaintz, Chris Rumble, Sharad K. Yadav, Claudio Margulis, and <u>Mark Maroncelli</u>	138
27.	Progress toward the Development of Iron-based Chromophores for Use In Solar Energy Conversion Strategies Lindsey L. Jamula, Allison M. Brown, and <u>James K. McCusker</u>	139
28.	Electron Transfer Dynamics in Efficient Molecular Solar Cells Atefeh Taheri, William Ward, Byron Farnum, and <u>Gerald J. Meyer</u>	140
29.	Metal-to-Ligand Charge Transfer Excited States on Surfaces and in Rigid Media. Application to Energy Conversion Akitaka Ito, John M. Papanikolas and <u>Thomas J. Meyer</u>	141
30.	Design of Structures Optimal for Singlet Fission <u>Josef Michl</u>	142
31.	Design of supramolecular cobaloxime-based photocatalyst assemblies <u>Karen L. Mulfort</u> , Anusree Mukherjee, Oleksandr Kokhan, Jier Huang, Jens Niklas, Lin X. Chen, David M. Tiede.....	143
32.	Control of Optical Transitions in Colloidal Indium Nitride Nanocrystals via Chemical Oxidation Peter K. B. Palomaki and <u>Nathan R. Neale</u>	144
33.	Formulation of D/A Coupling and the Role of Orthogonality <u>Marshall D. Newton</u>	145
34.	New Approaches to Generating and Utilizing Multiple Excitons from Single Photons for Enhanced Photoconversion Efficiency <u>A.J. Nozik</u> , J.C. Johnson, and M.C. Beard.....	146
35.	Single Molecule and Nanoparticle Spectroelectrochemistry for Understanding Interfacial Charge Transfer Events Caleb M. Hill, Daniel A. Clayton, Jia Liu and <u>Shanlin Pan</u>	147
36.	Photoinduced Charge Separation Processes: From Natural Photosynthesis to Organic Bulk Hetrojunctions <u>Oleg Poluektov</u> , Jens Niklas.....	148
37.	Miniature dispersive XES spectrometer for time resolved analysis of charge transfer K. Davis, J. Seidler, <u>Y. Pushkar</u>	149
38.	Photo-induced electron transfer in polymer solar photoconversion systems <u>Garry Rumbles</u> , Obadiah Reid, Nikos Kopidakis, Bryon Larson, Andrew Ferguson.....	150
39.	Formation and Characterization of Semiconductor Nanorod/Oxide Nanoparticle Hybrid Solids: Toward Vectoral Electron Transport <u>Neal R. Armstrong</u> , Jeffrey Pyun, S. Scott Saavedra.....	151

40.	Carrier Injection and Dynamics from Photoexcited Transition Metal Containing Porphyrins Rebecca L. Milot, Gary F. Moore, Lauren A. Martini, Christian A. F. Negre, Victor S. Batista, Robert H. Crabtree, Gary W. Brudvig, and <u>Charles A. Schmuttenmaer</u>	152
41.	Fluence-Dependent Singlet Biexciton Dynamics in Chirality-Enriched Single-Wall Carbon Nanotubes Jaehong Parka, Pravas Deria, Jean-Hubert Olivier, and <u>Michael J. Therien</u>	153
42.	Amorphous Oxides as Models for the Design of Molecular Catalysts for Artificial Photosynthesis <u>David M. Tiede</u> , Pingwu Du, Olesandr Kokhan, Karena Chapman, Peter Chupas, and Karen L. Mulfort.....	154
43.	Fast Current Blinking in Semiconductor Quantum Dots Klara Maturova, Sanjini U. Nanayakkara, Joseph M. Luther, and <u>Jao van de Lagemaat</u>	155
44.	Tuning Photochemical Function of Multimetallic Assemblies Linked by Artificial Oligopeptide Scaffolds Joy A. Gallagher, Meng Zhang, Sha Sun, Benjamin M. Biber and <u>Mary Elizabeth Williams</u>	156
45.	Bimolecular Electron Transfer Reactions in Ionic Liquids: Effects of Charge and Structure Masao Gohdo and <u>James F. Wishart</u>	157
46.	Dynamics of Excess Electrons and Other Solutes in Room-Temperature Ionic Liquids Jorge Kohanoff, Changhui Xu, Aleksander Durumeric, Hemant K. Kashyap, Sharad K. Yadav, Anne Kaintz, Chris Rumble, Mark Maroncelli, and <u>Claudio J. Margulis</u>	158
47.	Perovskite Oxynitrides and Pyrochlore Oxides: Light Harvesting and Surface Chemistry of Complex Semiconductors Polina Burmistrova, Limin Wang, Andrew Malingowski, and <u>Peter Khalifah</u>	159
	LIST OF PARTICIPANTS	161

Program

**35th DOE SOLAR PHOTOCHEMISTRY
RESEARCH MEETING**

June 2-5, 2013

**Westin Hotel
Annapolis, Maryland**

PROGRAM

Sunday, June 2

- 3:00 – 6:00 p.m. Registration
- 5:30 – 6:30 p.m. No Host Reception
- 6:30 – 7:45 p.m. Dinner

After Dinner Session – EFRCs and Solar Photochemistry
Mark T. Spitler, Chair

- 7:45 p.m. Welcome
- 8:00 p.m. The Center for Interface Science: Solar Electric Materials (CISSEM)
Neal R. Armstrong, University of Arizona
- 8:30 p.m. Quantum Confined Semiconductors for Photovoltaics
The Center for Advanced Solar Photophysics (CASP)
Matthew C. Beard, National Renewable Energy Laboratory

Monday Morning, June 3

- 7:15 a.m. Continental Breakfast
- 8:15 a.m. Opening Remarks
John C. Miller and **Mark Spitler**, U. S. Department of Energy

SESSION I
Opening Session
Mark T. Spitler, Chair

- 8:30 a.m. How the Morphology of Polymer Bulk Heterojunction Solar Cells Determines the Charge Separation Efficiency
Jonathan A. Bartelt, Sean Sweetnam, Zach M. Beiley, Eric T. Hoke, William R. Mateker, Kenneth R. Graham, Jason Bloking, Alberto Salleo, Michael F. Toney, and **Michael D. McGehee**, Stanford University
- 9:30 a.m. Coffee Break

Session II
Photo-induced Electron Transfer, Transport, and Fission
Mary Beth Williams, Chair

- 10:00a.m. Charge Transport and Transfer for Molecular Energy Conversion
John Miller, Brookhaven National Laboratory
- 10:30 a.m. Dynamics and Efficiency of Photoinduced Charge Transport in DNA
Frederick D. Lewis, Northwestern University
- 11:00 a.m. Singlet Fission in 1,3-Diphenylisobenzofuran: Chromophore Coupling and Excited State Evolution in Dimers and Solids
Justin Johnson, National Renewable Energy Laboratory
- 11:30 a.m. Efficient Singlet Fission in Polycrystalline Perylenediimides and Related Perylene Dyes
Michael R. Wasielewski, Northwestern University

Monday Afternoon, June 3

- 12:00 p.m. Lunch

Monday Evening, June 3

Session III
Coupled Donors and Acceptors
Marye Anne Fox, Chair

- 4:30 p.m. Tetrapyrrolic Architectures for Fundamental Studies of Light Harvesting and Energy Transduction
David F. Bocian, Dewey Holten, Christine Kirmaier, and Jonathan S. Lindsey, The University of California, Riverside, Washington University and North Carolina State University
- 5:15 p.m. I. Use of time resolved infrared to evaluate charge transfer excited states and intramolecular electron transfer in Re(I) dimethylaminobenzonitrile complexes;
II. Triplet states and photoreactions of Sn(IV) N^NO Schiff base complexes.
Russell Schmehl, Tulane University
- 6:15 p.m. Dinner
- 7:30 p.m. **Posters: Odd numbers, Posters 1 - 45**

Tuesday Morning, June 4

7:15 a.m. Continental Breakfast

SESSION IV Solar Photoconversion with Quantum Dots Arthur Nozik, Chair

- 8:30 a.m. Strongly Coupled Quantum Dot-Ligand Systems
Emily A. Weiss, Northwestern University
- 9:00 a.m. Dependence of Size, Composition, and Doping on the Multiple Exciton
Generation Efficiency in Quantum Dots
Matthew C. Beard, National Renewable Energy Laboratory
- 9:30 a.m. Modulation of Light Harvesting Properties of Semiconductor Quantum Dot
Assemblies
Prashant Kamat, Notre Dame Radiation Laboratory
- 10:00 a.m. Coffee Break

SESSION V Mostly Carbon Todd Krauss, Chair

- 10:30 a.m. Interfacial Exciton Dissociation in Organic Heterojunction Blends with Highly
Enriched Semiconducting Single-walled Carbon Nanotubes
Jeff Blackburn, National Renewable Energy Laboratory
- 11:00 a.m. Ultrafast Optical Microscopy of Multi-Scale Energy Flow
Libai Huang, Notre Dame Radiation Laboratory
- 11:30 a.m. Graphene: Charge Transfer, Spectroscopy and “Hot” Electrons
Louis Brus, Columbia University

Tuesday Afternoon, June 4

12:00 p.m. Lunch

Tuesday Evening, June 4

SESSION VI Photosynthetic Systems – Artificial and Real David Tiede, Chair

- 4:15 p.m. Interchromophore Interactions in Artificial Photosynthesis
Ana L. Moore, Thomas A. Moore, Devens Gust, Arizona State University
- 5:00 p.m. Light Harvesting Dynamics
Graham R. Fleming, Lawrence Berkeley National Laboratory

5:30 p.m. Dinner on the town

8:00 p.m. **Posters: Even numbers, Posters 2 - 44**

Wednesday Morning, June 5

7:15 a.m. Continental Breakfast

Session VII Inorganic Homogeneous Photocatalysis Tom Meyer, Chair

8:30 a.m. Mechanistic Understanding of Proton-Coupled Electron Transfer
In Artificial Photosynthesis
Dmitry E. Polyansky, Brookhaven National Laboratory

9:00 a.m. Critical Steps in Water Oxidation by Ru Blue Dimer Catalysts: Insights into the
Electronic Requirements of Water Activation for Artificial Photosynthesis
Yulia Pushkar, Purdue University

9:30 a.m. Electrochemical Water Oxidation by Homogenous Co Catalyst
Linda H. Doerr, Boston University

10:00 a.m. Coffee Break

Session VIII Computational and Model Interfaces Marshall Newton, Chair

10:30 a.m. Quantum Chemical Modeling of Systems for Solar Energy Conversion
Richard Friesner, Columbia University

11:00 a.m. Time-Domain Ab Initio Studies of Light-Harvesting and Charge Transfer in
Nanoscale Systems for Solar Photoconversion
Oleg Prezhdo, Rochester University

Session IX Dye Sensitized Interfaces and Systems Arthur Frank, Chair

11:30 p.m. Sensitization of Single Crystal Semiconductor Electrodes with Dyes, Quantum
Dots and Polymers
Bruce Parkinson, University of Wyoming

Wednesday Afternoon, June 5

12:00 p.m. Lunch

Session IX
Dye Sensitized Interfaces and Systems
(continued)

- 1:00 p.m. Bisphenanthrolinecopper(I) in Photoinduced Charge Separation and DSSC Dyes
C. Michael Elliott, Colorado State University
- 1:30 p.m. Model Dyes for Study of Molecule/Metal Oxide Interfaces and Electron Transfer
Processes
Elena Galoppini and Robert A. Bartynski, Rutgers University
- 2:00 p.m. Fundamental Studies of Light-induced Charge Transfer, Energy Transfer, and
Energy Conversion with Supramolecular Systems
Joseph T. Hupp, Northwestern University
- 2:30 p.m. Closing Remarks and Announcements
Mark T. Spitler

Sunday Evening

After Dinner Session

The Center for Interface Science: Solar Electric Materials (CISSEM)*

Neal R. Armstrong,¹ Jean-Luc Brédas,² Joseph J. Berry,³ David S. Ginger,⁴ David S. Ginley,³ Samuel Graham,⁵ Antoine Kahn,⁶ Bernard Kippelen,⁷ Seth R. Marder,² Dominic V. McGrath,¹ Oliver A.L. Monti,¹ Dana C. Olson,³ Jeanne E. Pemberton,¹ S. Scott Saavedra¹

¹ Department of Chemistry and Biochemistry, University of Arizona, Tucson, AZ 85721

² Department of Chemistry and Biochemistry, Georgia Tech, Atlanta, GA 30332

³ National Renewable Energy Laboratory, Golden, CO 80401

⁴ Department of Chemistry, University of Washington, Seattle, WA 98195

⁵ School of Mechanical Engineering, Georgia Tech, Atlanta, GA 30332

⁶ Department of Electrical Engineering, Princeton University, Princeton, NJ 08544

⁷ School of Electrical and Computer Engineering, Georgia Tech, Atlanta, GA 30332

Thin-film photovoltaic (PV) solar cells are increasing in efficiency at the highest rates of all PV platforms, although our understanding of the processes that dictate efficiency is still inadequate to ensure that low-cost, scalable energy conversion platforms are achieved that compete effectively with mature PV technologies. One of the key challenges in every solar cell platform is to realize efficient harvesting of photogenerated electrons and holes, and this is typically accomplished by implementation of “interlayers” that (in theory) provide both thermodynamic and kinetic charge selectivity at the contacts, and enhance power conversion efficiency. In the latest embodiments of organic and nanocrystalline solar cells, understanding and controlling interfacial processes at the boundaries between the active layer and interlayers/contacts is especially important: photogeneration of charges often occurs homogeneously throughout the active layer and the internal fields generated via the work function differences in the contacts are typically not sufficient to ensure that charge harvesting competes effectively with recombination.

The Center for Interface Science: Solar Electric Materials (CISSEM) is focused on developing new theoretical models and new characterization tools building on use-inspired material sets, which in combination provide an integrated nano- to meso-scale understanding of the relationships between contact/interlayer composition, atomic/molecular structure, interface energetics and the resultant electronic properties and efficiencies of charge harvesting at organic/oxide and organic/metal interfaces. These new understandings have recently led to some novel thin-film PV platforms.



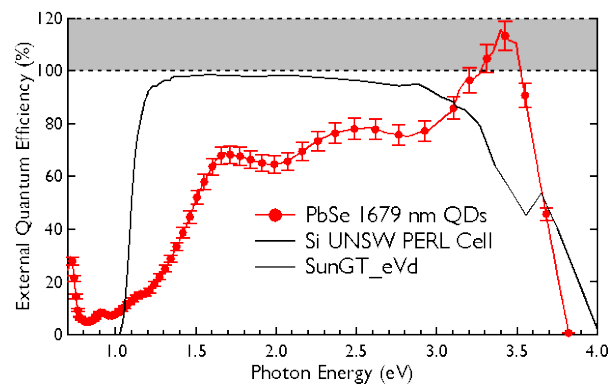
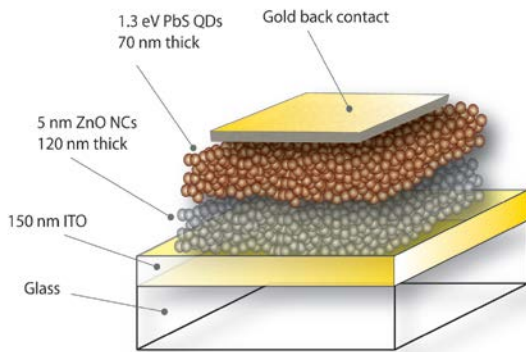
This talk will provide an overview of just a few of these new activities, highlighting several recent insights into how interface composition and energetics affect both hole- and electron-harvesting across oxide-only versus molecularly-modified interlayers. Some of the tools developed to provide insight into charge harvesting efficiencies over multiple length and time scales will also be described, which may be of interest for a broader range of energy conversion platforms.

* The Center for Interface Science: Solar Electric Materials is an Energy Frontier Research Center funded by the U.S. Department of Energy, Office of Science, Office of Basic Energy Sciences, under Award Number DE-SC0001084

Quantum Confined Semiconductors for Photovoltaics

Matthew C. Beard
Center for Advanced Solar Photophysics
National Renewable Energy Laboratory
Golden, CO, 80401

Nanomaterials are a flexible material platform that has great promise for providing new ways to approach solar energy conversion. The synthesis, investigation, and utilization of these novel nanostructures lie at the interface between chemistry, physics, materials science and engineering. The Center for Advanced Solar Photophysics (CASP) is an Energy Frontier Research Center that brings together a diverse set of scientist that are focused on exploring the unique attributes of colloidal quantum-confined semiconductor nanostructures for solar energy conversion. Semiconductor nanostructures, where at least one dimension is small enough to produce quantum confinement effects, provide new pathways for controlling energy flow and therefore have the potential to increase the efficiency of the primary photo conversion step. In this discussion, I will present the current status of CASP research efforts towards utilizing the unique properties of colloidal quantum dots (NCs confined in three dimensions) in prototype solar cells and demonstrate that these unique systems have the potential to bypass the Shockley-Queisser single-junction limit for solar photon conversion. The solar cells (left panel below) are constructed using a low temperature solution based deposition of PbS or PbSe QDs as the absorber layer. Different chemical treatments of the QD layer are employed in order to obtain good electrical communication while maintaining the quantum-confined properties of the QDs. The QD-layer exhibits p-type behavior and forms a p-n junction with solution deposited n-type ZnO nanocrystals. A unique aspect of our devices is that the QDs exhibit multiple exciton generation with an efficiency that is ~ 2 to 3 times greater than the parental bulk semiconductor. CASP efforts have resulted in a solar cell that can harvest these extra carriers (see below, right).



Session I

Opening Session

How the Morphology of Polymer Bulk Heterojunction Solar Cells Determines the Charge Separation Efficiency

Jonathan A. Bartelt, Sean Sweetnam, Zach M. Beiley, Eric T. Hoke, William R. Mateker, Kenneth R. Graham, Jason Bloking, Alberto Salleo, Michael F. Toney, and Michael D. McGehee*

Materials Science and Engineering
Stanford University
Palo Alto, CA 94301

Research by us and others over the past few years have shown that there are three phases in most polymer-fullerene bulk heterojunctions used to make solar cells – pure fullerene; pure, either crystalline or well aggregated polymer; and mixed regions of fullerene within the amorphous polymer (Fig. 1). The photocurrent generation process can be divided in two steps. The initial splitting of the exciton is governed by the molecular properties of the polymer, which acts as an electron donor (D) and the fullerene, which acts as an electron acceptor (A). Important aspects of the D-A couple include the energy levels, orbital overlap, molecular conformation and relative orientation. Once the free charges are initially generated, they need to reach the electrodes. This second step is largely governed by the film morphology, which provides pathway for holes and electrons to the electrodes. It is critically important to have three different kinds of percolative pathways for charge carriers. There must be a pathway for holes to travel through the polymer crystals as well as a pathway for electrons to travel through the fullerene clusters. These pathways are present when there is a sufficient volume fraction of these two phases. Additionally there must be enough of the fullerene molecules in the mixed phase for electrons to travel out of it and into the pure fullerene clusters. We find that many solar cells cease to work well after they are annealed because the fullerenes are driven out of the mixed phase. The fullerenes that are left behind act as charge traps. We are currently investigating the factors that determine the miscibility of fullerenes in polymers.

Solar cells with the three-phase morphology can have remarkably high quantum efficiency for charge separation because there are energetic offsets between the mixed phase and the pure phases that push charge carriers into the pure phases and keep them there. We have measured the energetic offsets using ultraviolet photoelectron spectroscopy and cyclical voltammetry. We are determining the extent to which the offsets are determined by the bandgap difference between crystalline and amorphous materials versus dipole formation.

We have performed Monte Carlo simulations to determine the extent to which the presence of mixed interfaces with energetic offsets can assist in charge separation. We find that carriers can escape from 10-nm wide mixed regions as long as the hole mobility is 10000 times higher than the electron mobility. We hypothesize that the hole mobility is in fact quite high because holes can travel through just one polymer chain to the nearest polymer crystal.

We have developed non-fullerene electronic acceptors and obtained power conversion efficiency as high as 3.7%. Detailed studies show that the currents are low because of geminate

recombination. We believe that separating charge is difficult in these systems because there is not a mixed phase like the one shown in figure 1 and there are no energetic offsets to help separate the carriers into different regions of the device and keep them separated from each other.

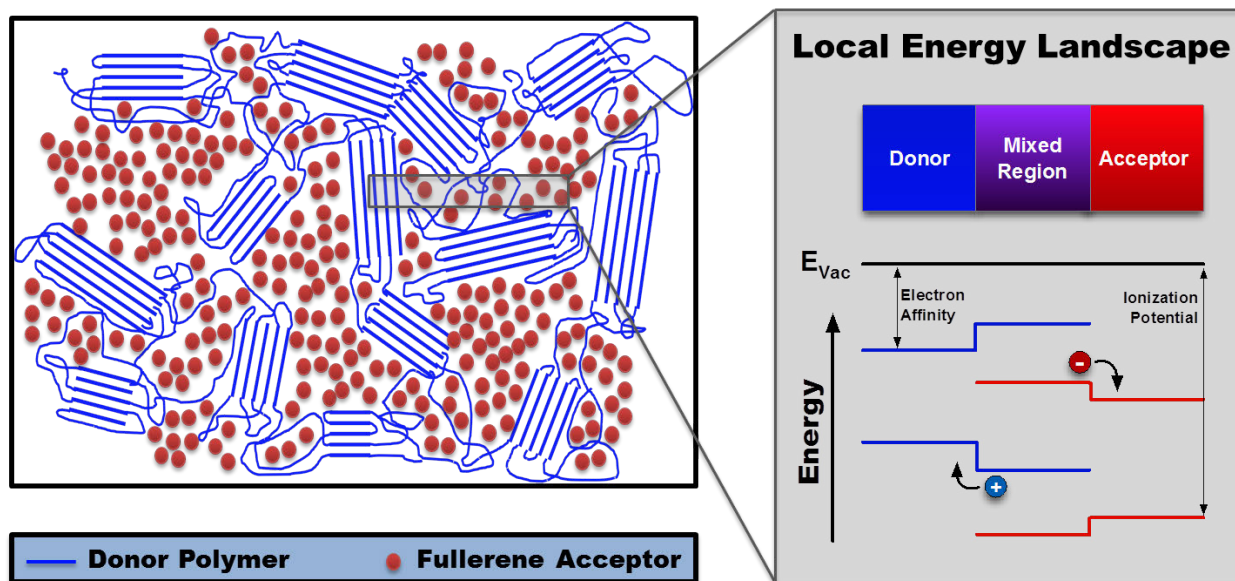


Figure 1: A schematic of a polymer-fullerene bulk heterojunction that could be used in a solar cell. The pure donor and acceptor regions have different energy levels than the mixed region. Charge carriers formed in the mixed region travel to the pure regions and stay there because of an energetic barrier.

References

1. “The Importance of Fullerene Percolation in the Mixed Regions of Polymer-Fullerene Bulk Heterojunction Solar Cells,” J.A. Bartelt, Z.M. Beiley, E.T. Hoke, W.R. Mateker, J.D. Douglas, B. Collins, J. Tumbleston, K.R. Graham, A. Amassian, H. Ade, J. Frechet, M.F. Toney, and M.D. McGehee, *Advanced Energy Materials*, 2012, DOI: 10.1002/aenm.201200637.
2. “Use of X-Ray Diffraction, Molecular Simulations, and Spectroscopy to Determine the Molecular Packing in a Polymer-Fullerene Bimolecular Crystal,” N.C. Miller, E. Cho, M.J.N. Junk, R. Gysel, C. Risko, D. Kim, S. Sweetnam, C.E. Miller, L.J Richter, R.J. Kline, M. Heeney, I. McCulloch, A. Amassian, D. Acevedo-Feliz, C. Knox, M.R. Hansen, D. Dudenko, B.F. Chmelka, M.F. Toney, J.L. Bredas, M.D. McGehee, *Advanced Materials*, 24 (2012) p. 6071-+.

Session II

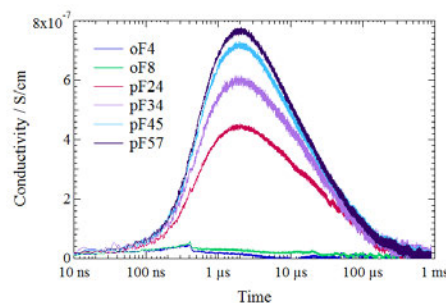
Photo-induced Electron Transfer, Transport, and Fission

Charge Transport and Transfer for Molecular Energy Conversion

John R. Miller, Andrew R. Cook, Matthew Bird, Hung-Cheng Chen, Matibur Zamadar, Garry Rumbles^b, Obadiah Reid^b

^aChemistry Department, Brookhaven National Laboratory, Upton, NY 11973
and ^bNational Renewable Energy Laboratory, Golden CO, 80401

This work investigates molecules, especially conjugated oligomers and polymers, for properties and principals of potential use in energy capture from sunlight. Our principal focus has been transport of charges and excitons over distances of tens of nm to examine the hypothesis that single chains have potential for outstanding transport that could underpin new, highly-efficient methods of solar energy conversion. One important technique is the use of electron pulses from accelerators which are almost unique in their ability to rapidly inject charges onto large conjugated molecular chains. Recent work adds three experimental techniques. Figure 1 (at right) shows transient microwave conductivity (TRMC) of holes in dilute solutions of a polyfluorene in benzene. The data was obtained with an instrument assembled at NREL and further developed at BNL. The data in Figure 1 and additional data will provide a deeper insight into the dependence of TRMC signal intensities on chain length, and hence the nature of hole transport. The electrodeless TRMC technique, developed to a high level at the University of Delft (Siebbeles,.; Grozema,.; de Haas,.; Warman,., *Radiat. Phys. Chem.* 2005, 72, 85-91) measures absorption of microwaves to determine conductivity, typically finding high intrachain mobilities.



A second new development is determination of infrared absorption bands and intensities (extinction coefficients, ϵ) for electrons and holes in conjugated polymers and oligomers. Figure 2 pictures the infrared spectrum of $F_2^{\bullet-}$. While extinction coefficients ϵ of 200 are considered strong infrared bands, this radical anion has infrared bands with $\epsilon > 3000$. Other ions have bands ten times as intense. IR transitions computed with a DFT method are found to provide a good description of polaron¹⁰ spectra are shown on the top axis. The calculations describe the observed spectra approximately. The spectra probably arise principally from ion-pairs.

The optical fiber single-shot (OFSS) detection system at LEAF has been further developed to give an improved time range. It finds impressive capture of electrons or holes by long, conjugated molecules, even when their concentrations are low. Figure 3 shows data with the OFSS and conventional detection that examines transport of electrons to traps at the ends of polyfluorene (pF) chains of different lengths in repeat units. Fits of this data find that

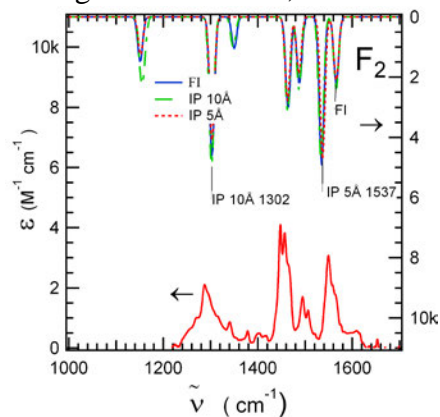
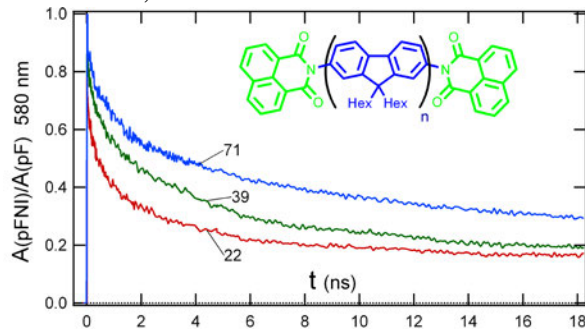


Figure 3 shows data with the OFSS and conventional detection that examines transport of electrons to traps at the ends of polyfluorene (pF) chains of different lengths in repeat units. Fits of this data find that



transport to the trap groups can be described with two exponential decays of approximately equal amplitude. Time constants for both decays change approximately linearly with chain length (Figure 4), a behavior not consistent with random diffusion along the chains. These observations may be a sign of transport hindered by defects. In this way information on transport to end traps may give a more microscopic description as well as characterizing transport over long distances.

Experiments adding triplet excitons to >100 nm long polyfluorene chains found that the triplets transferred completely or almost completely to trap groups at the ends within 40 ns.⁶ Time resolution is determined by the slowness of the bimolecular triplet injection.

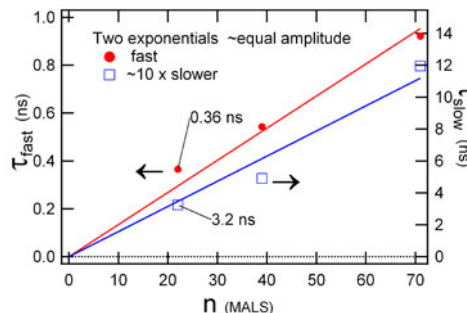
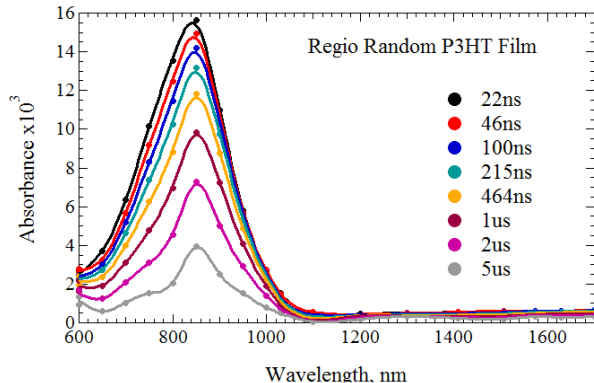


Figure 5 shows transient absorption spectra of a 100 μM polythiophene film ionized by 9 MeV electron pulses from the LEAF accelerator. Production of these relatively thick films enables the



use of pulse radiolysis of conjugated polymer films. Compared to photoexcitation this electron excitation should more readily yield ionization, but it has not been applied and no method is available to determine yields. These early results find readily-measurable transient absorptions. More difficult is to determine identities of the species. Likely candidates are a) electrons and holes or b) triplet excited states.

Planned Work We will seek experiments and

theory that will simultaneously describe transport as observed by TRMC and transient absorption (OFSS) on the same material under the same conditions, to provide unique insight into processes limiting charge transport. At first these will be on single-chain transport in liquids, but we hope to expand this to behavior of similar materials in solid films, making use of that developing capability.

For the films themselves we will compare photo-induced and electron-pulse induced transient absorptions on the same polymer thick film samples, while also comparing photo-induced experiments on the thick films to thin films such as those produced by spin coating. . We will attempt to apply doping techniques to selectively capture one or more species (electrons, holes, triplets). We will apply transient mid-infrared detection to distinguish electron and holes from excited states. We hope to apply OFSS to extend time resolution for vis/NIR experiments.

We will develop methods to rapidly produce triplets in conjugated chains and seek basic knowledge of the mechanism of fast production of triplets. We will use LEAF/OFSS to detect triplets at short times and determine their transport to trap groups.

We will explore whether infrared absorptions can provide sensitive and definitive measurement of delocalized electrons and holes and will seek the possibility of dynamic IR.

DOE Sponsored Publications 2010-2013

1. Shibano, Y.; Imahori, H.; Sreearunothai, P.; Cook, A. R.; Miller, J. R., "Conjugated "Molecular Wire" for Excitons", *J. Phys. Chem. Lett.* **2010**, *1*, 1492-1496.
2. Grills, D. C.; Cook, A. R.; Fujita, E.; George, M. W.; Preses, J. M.; Wishart, J. F., "Application of External-Cavity Quantum Cascade Infrared Lasers to Nanosecond Time-Resolved Infrared Spectroscopy of Condensed-Phase Samples Following Pulse Radiolysis", *Appl. Spectrosc.* **2010**, *64*, 563-570.
3. Schwerin, A. F.; Johnson, J. C.; Smith, M. B.; Sreearunothai, P.; Popovic, D.*et. al.*, "Toward Designed Singlet Fission: Electronic States and Photophysics of 1,3-Diphenylisobenzofuran", *J. Phys. Chem. A* **2010**, *114*, 1457-1473.
4. Cook, A. R.; Sreearunothai, P.; Asaoka, S.; Miller, J. R., "Sudden, "Step" Electron Capture by Conjugated Polymers", *J. Phys. Chem. A* **2011**, *115*, 11615-11623.
5. Keller, J. M.; Glusac, K. D.; Danilov, E. O.; McIlroy, S.; Sreearunothai, P.; Cook, A. R.; Jiang, H.; Miller, J. R.; Schanze, K. S., "Negative Polaron and Triplet Exciton Diffusion in Organometallic "Molecular Wires"", *J. Am. Chem. Soc.* **2011**, *133*, 11289-11298.
6. Sreearunothai, P.; Estrada, A.; Asaoka, S.; Kowalczyk, M.; Jang, S.; Cook, A. R.; Preses, J. M.; Miller, J. R., "Triplet Transport to and Trapping by Acceptor End Groups on Conjugated Polyfluorene Chains", *J. Phys. Chem. C* **2011**, *115*, 19569-19577.
7. Musat, R. M.; Cook, A. R.; Renault, J. P.; Crowell, R. A., "Nanosecond Pulse Radiolysis of Nanoconfined Water", *J. Phys. Chem. C* **2012**, *116*, 13104-13110.
8. Takeda, N.; Miller, J. R., "Poly(3-decylthiophene) Radical Anions and Cations in Solution: Single and Multiple Polarons and Their Delocalization Lengths in Conjugated Polymers", *J. Phys. Chem. B* **2012**, *116*, 14715-14723.
9. Wishart, J. F.; Funston, A. M.; Szreder, T.; Cook, A. R.; Gohdo, M., "Electron solvation dynamics and reactivity in ionic liquids observed by picosecond radiolysis techniques", *Faraday Discuss.* **2012**, *154*, 353-363.
10. Zaikowski, L.; Kaur, P.; Gelfond, C.; Selvaggio, E.; Asaoka, S.*et. al.*, "Polarons, Bipolarons, and Side-By-Side Polarons in Reduction of Oligofluorenes", *J. Am. Chem. Soc.* **2012**, *134*, 10852-10863.
11. Zamadar, M.; Cook, A. R.; Lewandowska-Andralojc, A.; Holroyd, R.; Jiang, Y.; Bikalis, J.; Miller, J. R., "Electron Transfer by Excited Benzoquinone Anions: Slow Rates for Two-Electron Transitions", *J. Phys. Chem. C* **2013**, *submitted*.

Dynamics and Efficiency of Photoinduced Charge Transport in DNA

Frederick D. Lewis

Department of Chemistry
Northwestern University
Evanston, IL 60208

The objective of this project is to investigate the mechanism and dynamics of photoinduced charge separation processes in systems which possess electron donor and electron acceptor chromophores separated by DNA base pairs. The hydrogen-bonded base pairs which constitute the core of duplex DNA form an extended one-dimensional π -stacked array with an average stacking distance of 3.4 Å. The possibility that these base pairs might serve as a pathway for charge transport was advanced 50 years ago. Our approach to the study of electron transfer in DNA is based on the use of synthetic conjugates in which a chromophore serves as a linker or capping group in stable hairpin or capped hairpin structures. Selective excitation of a chromophore can affect the injection of positive or negative charge (a hole or electron) into the base pair domain. The chromophores also serve as reporters for the dynamics and efficiency of charge separation in these “smart” hairpin and structures.

We recently reported the measurement of distance- and temperature-dependent rate constants for charge separation in capped hairpins in which a stilbene hole acceptor and hole donor are separated by an A_n or A_3G_n diblock polypurine sequence consisting of 3 adenines and 1-19 guanines (Figure 1a,b). The short A_3 block serves as a rectifier, preventing charge recombination once the hole has entered the G_n block (Figure 2). The longer diblock systems obey the simplest model for an unbiased random walk, providing for direct measurement of $k_{\text{hop}} = 4.3 \times 10^9 \text{ s}^{-1}$ for a single reversible G-to-G hole hopping step. This is somewhat faster than the value of $1.2 \times 10^9 \text{ s}^{-1}$ calculated from our data for A-tract hole hopping in A_n systems using a kinetic model. The temperature dependence for hopping in A_3G_{13} provides values of $E_{\text{act}} = 2.8 \text{ kcal/mol}$ and $A = 7 \times 10^9 \text{ s}^{-1}$, consistent with a weakly-activated, conformationally-gated process. Significantly slower rate constants are observed for hopping in alternating or random base sequences. Thus DNA hole transport via naturally occurring base pair sequences is a slow process, at best.

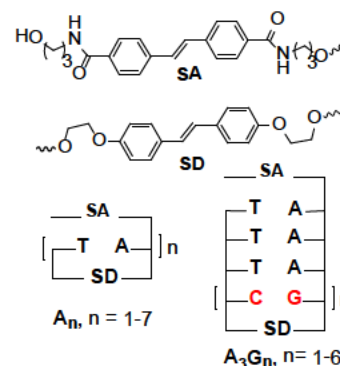
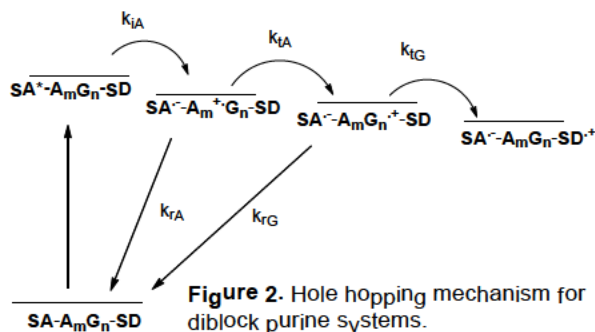


Figure 1. Structures of SA/SD capped hairpin structures for A_n and A_3G_n .



The effect of replacing the natural purine base A with 7-deazaadenine, Z (Figure 3a), on the dynamics and efficiencies of hole transport has been investigated in several SA- A_mZ_n -SD diblock and SA- $A_mZ_mG_m$ -SD triblock polypurine systems (Figure 3a). Comparison of the results for the diblock A_3Z_6 system with the

corresponding A_3G_6 system shows a decrease in the charge separation time τ_{cs} and increase in the efficiency of charge separation Φ_{cs} upon replacement of G with Z (Figure 3b). The decrease in τ_{cs} requires that the Z-to-Z hopping rate constant be faster than that for G-to-G. Assuming similar hopping rate constants within the short A-block and a unbiased random walk in the Z-block, a value of $k_{ht} \sim 4.2 \times 10^{10} \text{ s}^{-1}$ can be estimated for Z-block hopping, an order of magnitude faster than that for G-block hopping. We have attributed increased hole mobility to a decrease in minor groove solvation which results in increased duplex conformational mobility. No further increase in hole transport dynamics is observed when the A_3Z_6 diblock system is replaced with the triblock sequence $A_3Z_3G_3$, which presents an energy gradient for hole transport.

Experiments designed to further explore the effects of duplex conformational mobility on hole transport dynamics have been initiated. Increased backbone rigidity can be achieved by replacement of deoxyribose with a rigid bicyclic ribose known as a locked nucleic acid (LNA, Figure 4a). Results for diblock SA/SD

systems possessing LNA bases are shown in Figure 4b. Replacement of natural nucleotides with locked nucleotides in either the A-block or G-block results in a decrease in Φ_{cs} and a slight increase in τ_{cs} (Figure 4b). Decreases in the efficiency and rate constants for charge separation are attributed to the increased rigidity of the LNA bases in these DBA systems.

We are continuing our efforts to determine the dynamics of excess electron transport in DNA. Hairpins possessing an Sd linker electron donor separated from a PDI base pair surrogate electron acceptor by four base pairs have been prepared. Preliminary studies of the transient absorption spectra for the T_4A_4 sequence indicate that very little electron transport to PDI occurs following selective excitation of Sd. The use of diblock sequences with energy gradients will be explored in order to increase the efficiency of electron transport. We are also exploring the use of a triplet electron donor in hopes of obtaining a longer-lived contact radical ion pair.

Future plans include studies of the following: (a) the effects of backbone modifications which increase the conformational mobility of DNA or render it soluble in organic solvents, (b) the effects of base substitutions designed to increase the mobility of holes or electrons in DNA, and (c) separation of the electronically excited chromophore from the adjacent base pair by a artificial base pair capable of functioning as a tunneling barrier. We also will continue collaboration and dialog with theoreticians interested in DNA electron transfer.

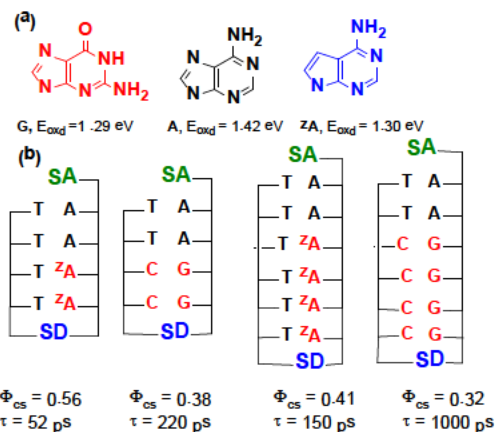


Figure 3. Comparison of charge separation efficiency and dynamics in $A_2Z_nA_n$ vs. A_2G_n systems.

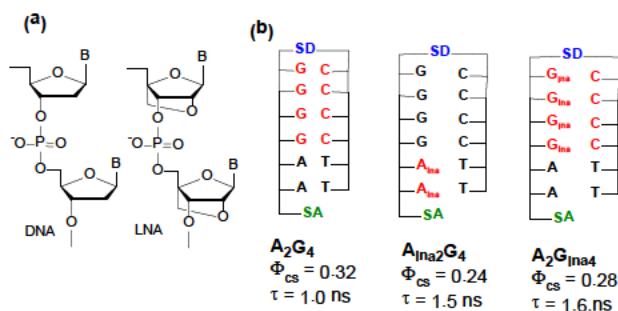


Figure 4. Comparison of charge separation efficiency and dynamics in DNA vs. LNA-containing diblock polypurine sequences.

DOE Sponsored Publications 2010-2013¹⁻⁸

- (1) Daublain, P.; Thazhathveetil, A. K.; Shafirovich, V.; Wang, Q. A.; Trifonov, A.; Fiebig, F.; Lewis, F. D.: Dynamics and efficiency of electron injection and transport in DNA using pyrenecarboxamide as an electron donor and 5-bromouracil as an electron acceptor. *J. Phys. Chem. B* **2010**, *114*, 14265-14272.
- (2) Lewis, F. D.; Thazhathveetil, A. K.; Zeidan, T. A.; Vura-Weis, J.; Wasielewski, M. R.: Dynamics of ultrafast singlet and triplet charge transfer in anthraquinone–DNA conjugates. *J. Am. Chem. Soc.* **2010**, *132*, 444-445.
- (3) Mickley Conron, S. M.; Thazhathveetil, A. K.; Wasielewski, M. R.; Burin, A. L.; Lewis, F. D.: Direct measurement of the dynamics of hole hopping in extended DNA G-tracts. An unbiased random walk. *J. Am. Chem. Soc.* **2010**, *132*, 14388-14390.
- (4) Thazhathveetil, A. K.; Trifonov, A.; Wasielewski, M. R.; Lewis, F. D.: Increasing the speed limit for hole transport in DNA. *J. Am. Chem. Soc.* **2011**, *133*, 11485-11487.
- (5) Vura-Weis, J.; Lewis, F. D.; Ratner, M. A.; Wasielewski, M. R.: Base Pair Sequence and Hole Transfer through DNA: Rational Design of Molecular Wires. In *Charge and Exciton Transport in Molecular Wires*; Grozema, F., Siebbeles, L., Eds.; Wiley-VCH: Weinheim, 2011; pp 133-156.
- (6) Thazhathveetil, A. K.; Vura-Weis, J.; Trifonov, A. A.; Wasielewski, M. R.; Lewis, F. D.: Dynamics and efficiency of hole transport in LNA:DNA hybrid diblock oligomers. *J. Am. Chem. Soc.* **2012**, *134*, 16434-16440.
- (7) Lewis, F. D.; Wasielewski, M. R.: Dynamics and efficiency of photoinduced charge transport in DNA: Toward the elusive molecular wire. *Pure Appl. Chem.* **2013**, in press.
- (8) Lewis, F. D.: Distance-dependent electronic interactions across DNA base pairs. Charge transport, exciton coupling, and energy transfer. *Israel J. Chem.* **2013**, in press.

Singlet Fission in 1,3-Diphenylisobenzofuran: Chromophore Coupling and Excited State Evolution in Dimers and Solids

Justin Johnson,[†] Joel Schrauben,[†] Joe Ryerson,^{†,‡} Kai Zhu,[†] Josef Michl,[†] Arthur Nozik^{†,‡}

[†]National Renewable Energy Laboratory, 15013 Denver West Pkwy, Golden, CO 80401

[‡]Dept. of Chemistry and Biochemistry, University of Colorado, Boulder, CO 80309

Singlet fission is an excited state molecular process by which two triplets are formed after one initial photoexcitation into a singlet state. The phenomenon was discovered and described theoretically in a few select molecular crystals (primarily polyacenes) several decades ago but a more comprehensive theory or discovery in a broad variety of systems was not pursued until very recently. Perfectly efficient singlet fission results in a 200% triplet yield, which could be useful in some types of photoelectrochemical and photovoltaic schemes aimed at breaking the conventional limits of conversion efficiency.¹

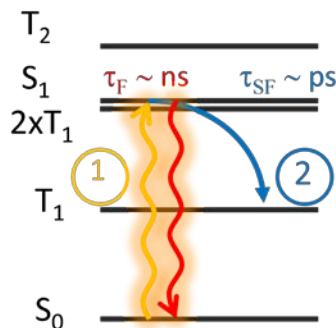


Fig. 1. The process of singlet fission (steps 1 and 2), which can be made to

After some initial efforts toward identifying and screening classes of chromophores that are most likely to exhibit singlet fission,² the focus of our efforts over the past several years has been to develop a detailed understanding of how chromophore coupling affects singlet fission in a model system. The system we have studied most extensively, 1,3-diphenylisobenzofuran (DPIBF), has a triplet energy T_1 that lies nearly midway between the ground state S_0 and first excited singlet S_1 , which nearly fulfills the ideal condition of slightly exoergic singlet fission but minimal loss into T_2 , which lies above S_1 (Figure 1).

More than a dozen covalent dimer compounds containing two DPIBF chromophores have been synthesized at CU-Boulder, with the goal of producing a series of structures with systematically varying strengths and geometries of interchromophore coupling. Most dimers have relatively weak and nearly linear coupling between the monomers, which we have shown induces charge transfer excitations and triplets in polar solvents at the expense of the fluorescence decay channel. However, the triplet yield remains relatively small (<15%) and cannot easily be identified as arising from singlet fission vs. crossing from a charge transfer intermediate. Theoretically, this is not altogether surprising as matrix elements of the model Hamiltonian for singlet fission are minimized under conditions of linear coupling.³ Some more strongly coupled dimer systems exhibit behavior that implies the formation of a nonpolar and high-spin intermediate, which could represent a direct observation of the precursor to singlet fission but requires further characterization. These studies on dimers have been highly valuable from a mechanistic standpoint but have not been successful in demonstrating efficient singlet fission.

The highest triplet yields have been observed in particular types of solid thin films of DPIBF. We have discovered at least two crystalline polymorphs of DPIBF that exhibit very different excited state dynamics. The films of one type, labeled A, exhibit 200% triplet quantum yield at 80 K and significantly above 100% at room temperature. Films of the other type, labeled B,

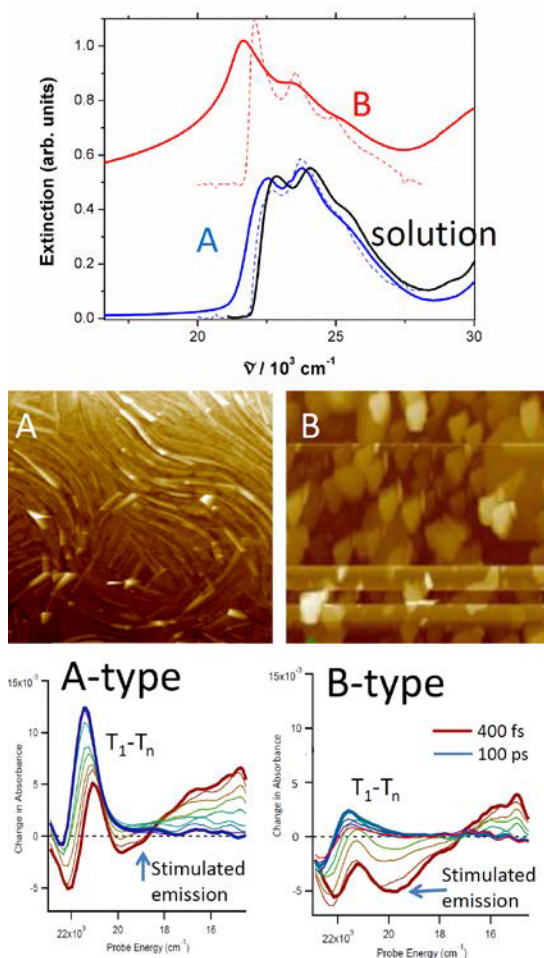


Fig. 2. (Top) UV/VIS absorption, (middle) AFM images, and (bottom) transient absorption of A- and B-type DPIBF films.

We have also begun efforts to observe photoinduced electron transfer from DPIBF to nanocrystalline TiO_2 and other substrates. Photocurrent studies suggest highly efficient charge injection and collection and minimal recombination as the molecules self-assemble onto the TiO_2 surface, which bodes well for demonstration of photocurrent enhanced by singlet fission. Injection specifically from the triplet state after singlet fission is being investigated as a function of DPIBF deposition conditions, acceptor conduction band energy, and covalent vs. noncovalent binding.

1. Hanna, M.; Nozik, A.J.; *J. Appl. Phys.* **2006**, *100*, 074510.
2. Paci, I. et al. *J. Amer. Chem. Soc.* **2006**, *128*, 16546.

show vanishingly small triplet yields. We have developed methods of forming nearly pure A or B type films by thermal evaporation or drop-casting followed by thermal annealing. We have then utilized a large number of spectroscopic and structural probes to characterize the excited state kinetics and dynamics as a function of film morphology and intermolecular coupling. The transition of A- to B-type crystallinity is characterized by a change in the relative amplitudes of Franck-Condon envelopes of steady-state absorption and fluorescence, lower triplet yields, higher fluorescence quantum yields, and simpler fluorescence and transient absorption kinetics (Fig 2). The crystal structures reveal a slipped-stacking geometry of molecules that has been shown to be optimal for direct singlet fission,³ but a clear picture of which structural properties cause the variations in singlet fission yield is still evolving. Hypotheses currently under investigation include variations in excimer formation rates that may compete with singlet fission, changes in electronic delocalization influencing energy level alignment, or alterations in excitonic coupling (e.g., H- and J-type) affecting the matrix elements that determine the singlet fission rate.

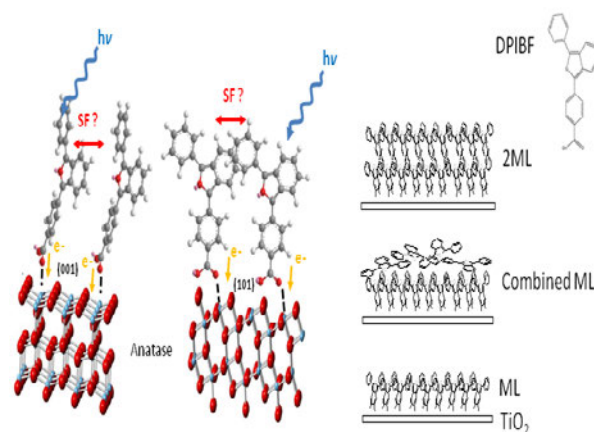


Fig 3. Possible DPIBF/ TiO_2 geometries leading to double charge injection after singlet fission.

3. Smith, M.; Michl, J.; *Chem. Rev.* **2010**, *110*, 6891.

DOE Sponsored Publications 2010-2013

1. Johnson, J.C.; et al. "Toward designed singlet fission: Solution photophysics of two indirectly coupled covalent dimers of 1,3-diphenylisobenzofuran." *J. Phys. Chem. B.* **2013**. Article ASAP DOI: 10.1021/jp310979q
2. Johnson, J.C.; Nozik, A.J.; Michl, J. "The role of chromophore coupling in singlet fission." *Acc. Chem. Res.* **2013**. Article ASAP. DOI: 10.1021/ar300193r
3. Grumstrup, E.; Johnson, J.C.; Damrauer, N.; "Enhanced Triplet Formation in Polycrystalline Tetracene Films by Femtosecond Optical-Pulse Shaping." *Phys. Rev. Lett.* **2010**, *105*, 257403.
4. Johnson, J. C.; Nozik, A. J.; Michl, J., High triplet yield from singlet fission in thin films of 1,3-diphenylisobenzofuran. *J. Amer. Chem. Soc.* **2010**, *132*, 16302.
5. Schwerin, A. F.; Johnson, J. C.; Smith, M. B.; Sreearunothai, P.; Popovic, D.; Cerny, J.; Havlas, Z.; Paci, I.; Akdag, A.; MacLeod, M. K.; Chen, X. D.; David, D. E.; Ratner, M. A.; Miller, J. R.; Nozik, A. J.; Michl, J. "Toward Designed Singlet Fission: Electronic States and Photophysics of 1,3-Diphenylisobenzofuran." *J. Phys. Chem. A* **2010**, *114* (3), 1457-1473.
6. Greyson, E. C.; Stepp, B. R.; Chen, X.; Schwerin, A. F.; Paci, I.; Smith, M. B.; Akdag, A.; Johnson, J. C.; Nozik, A. J.; Michl, J.; Ratner, M. "Singlet Exciton Fission for Solar Cell Applications: Energy Aspects of Interchromophore Coupling." *J. Phys. Chem. B* **2010**, *114*, 14223.
7. Smith, E.R.; Luther, J.M.; Johnson, J.C. "Ultrafast electronic delocalization in CdSe/CdS quantum rod heterostructures," *Nano Lett.* **2011**, *11*, 4923.
8. Ruddy, D.; Johnson, J.C.; Smith, E.R.; Neale, N.; "Size and bandgap control in the solution-phase synthesis of near-infrared-emitting germanium nanocrystals." *ACS Nano.* **2010**, *4*, 7459.
9. Rawls, M.; Johnson, J.C.; Gregg, B.A.; "Coupling one electron photoprocesses to multielectron catalysts: Towards a photoelectrocatalytic system." *J. Elec. Anal. Chem.* **2010**, *650*, 10.
10. Semonin, O.E.; Johnson, J.C.; Luther, J.M.; Midgett, A.G.; Nozik, A.J.; Beard, M.C.; "Absolute Photoluminescence Quantum Yields of IR-26 Dye, PbS, and PbSe Quantum Dots." *J. Phys. Chem. Lett.* **2010**, *1*, 2445.
11. Nozik, A. J.; Beard, M. C.; Luther, J. M.; Law, M.; Ellingson, R. J.; Johnson, J. C. "Semiconductor Quantum Dots and Quantum Dot Arrays and Applications of Multiple Exciton Generation to Third-Generation Photovoltaic Solar Cells." *Chem. Rev.* **2010**, *110*, 6873-6890.

Manuscripts in preparation:

- Ryerson, J.; Schrauben, J.; Nozik, A.; Michl, J.; Johnson, J. "Singlet fission in two solid thin film types of 1,3-diphenylisobenzofuran."
- Crisp, R.; Schrauben, J.; Luther, J.; Johnson, J.C.; "Coherent delocalization in strongly coupled CdSe quantum dots films."

Efficient Singlet Fission in Polycrystalline Perylene-3,9,10,16-tetracarboxylic Diimides and Related Rylene Dyes

Michael R. Wasielewski
Department of Chemistry
Northwestern University
Evanston, IL 60208-3113

Scope of the project. We are investigating molecular solids in which photogenerated singlet excitons fission to generate two triplet excitons, which in turn, efficiently charge separate to produce two electron-hole pairs. We are also developing self-ordering molecular assemblies (SOMAs) that produce segregated charge conduits that will be able to independently carry electrons and holes to either catalysts or electrodes. We are focusing on how these assemblies can be grown on solid supports and electrodes to utilize their light-harvesting and photodriven charge separation capabilities. Finally, we are investigating how SOMAs can be used to provide multiple electrons or holes to catalysts for solar fuels formation by designing structures to prevent unproductive competitive quenching of excited states by energy transfer, spin exchange, and unquenched angular momentum involving the nearby metal catalysts.

Recent Results. Singlet fission (SF) is the process by which a singlet exciton in a molecular material is energetically down-converted into two independent triplet excitons. Thermodynamic modeling predicts that using a SF material in a single-junction solar cell can theoretically increase the Shockley-Queisser limit for power conversion efficiency from 32% to 44%, assuming that SF results in the formation of two triplet excitons, each of which produce an electron-hole pair quantitatively. The SF rate is maximized if the sum of the energies of the two triplet excitons (T_1) is lower than that of the vibrationally-relaxed singlet state (S_1), i.e. $E(S_1) > 2E(T_1)$. This requirement is not easy to meet because in most common chromophores the $E(S_1) - E(T_1)$ gap is considerably smaller than the $E(T_1) - E(S_0)$ gap. In addition to the energetic requirements described above, it is clear that intermolecular electronic coupling and orientation are also critical for efficient SF. Theoretical work has shown that there is a delicate balance between molecular geometry, electronic coupling and SF efficiency. It has been suggested that a cofacial, π - π slip-stacked relationship between chromophores facilitates high SF efficiency.

Perylene-3,4,9,10-bis(dicarboximide) (PDI) and its derivatives have attracted a great deal of interest as visible chromophores for studies of energy and charge transport, especially with regard to their potential applications as visible light absorbing electron acceptors in organic photovoltaics. Not only are PDIs thermally and photochemically stable, they also exhibit a strong propensity to self-organize into ordered assemblies both in solution and in the solid phase by π - π

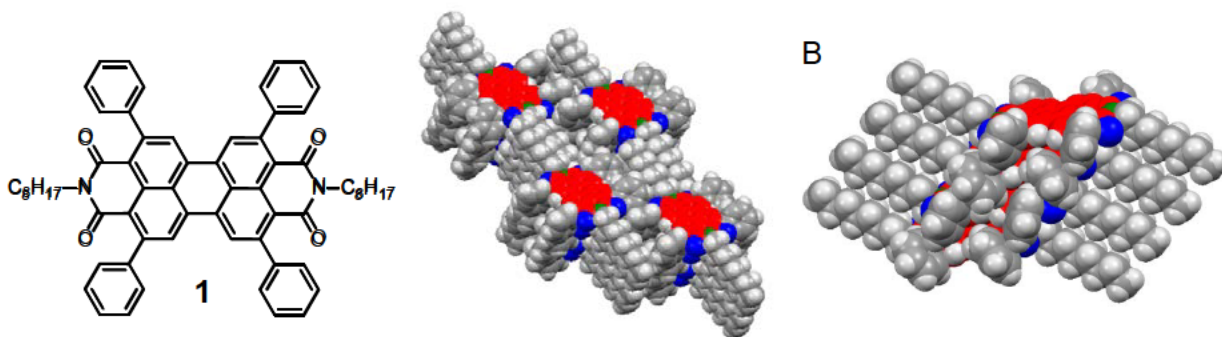


Figure 1. (A) Molecule 1. (B) and (C) Crystal structure of 1, space-filling packing diagrams.

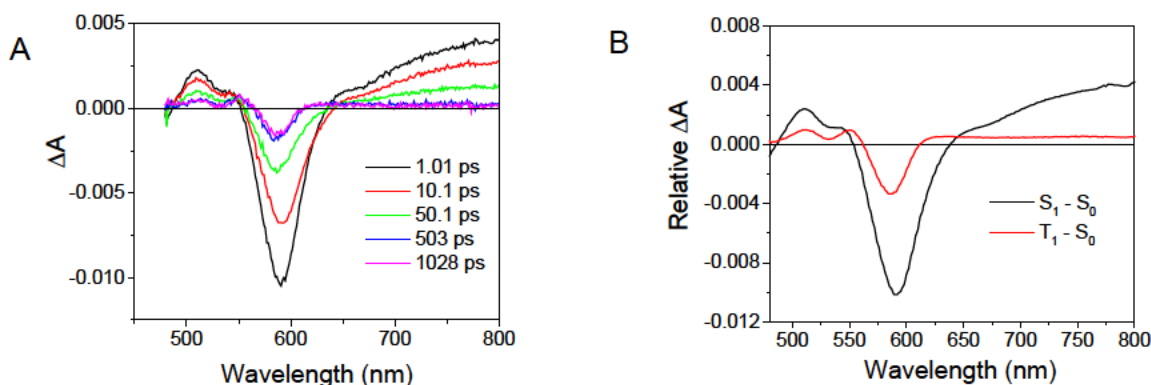


Figure 2. (A) Femtosecond transient absorption spectra of a 188 nm film of **1** at the indicated times following a 120 fs, 416 nm laser pulse having an excitation density of $7.1 \times 10^{18} \text{ cm}^{-3}$. (B) The species-associated spectra obtained from SVD analysis, global fitting, and target analysis of the data in (A).

stacking interactions, often aided by hydrogen bonding and nano- and micro-segregation. PDI comes close to satisfying the energy level requirements for SF: $E(T_2), E(S_1) > 2 E(T_1)$.

We will report on the photophysics of polycrystalline thin films of *N,N*-di-(*n*-octyl)-2,5,8,11-tetraphenyl-PDI, **1** and related rylene dyes. For example, the crystal structure of **1** obtained by x-ray diffraction reveals segregated, slip-stacked columns of **1** that are π - π stacked at a 3.5 Å interplanar distance. Femtosecond transient absorption spectroscopy on 188 nm thick vapor-deposited thin films of **1** demonstrates formation of $^3\text{*1}$ as a result of SF (Figure 2). SF occurs in $\tau = 180 \pm 10 \text{ ps}$ and competes with singlet-singlet annihilation at the laser fluences typical of the femtosecond experiments. At the lower fluences of nanosecond transient absorption spectroscopy, SF occurs exclusively to give a $170 \pm 10\%$ yield of triplet excitons (Figure 3A). The spectrum of $^3\text{*1}$ is similar to that of $^1\text{*1}$ (Figure 3B). These results illustrate a design strategy for producing PDI and related rylene derivatives that have the optimized inter-chromophore electronic interactions needed to undergo high-yield SF to enhance solar cell performance and charge separation in systems for artificial photosynthesis.

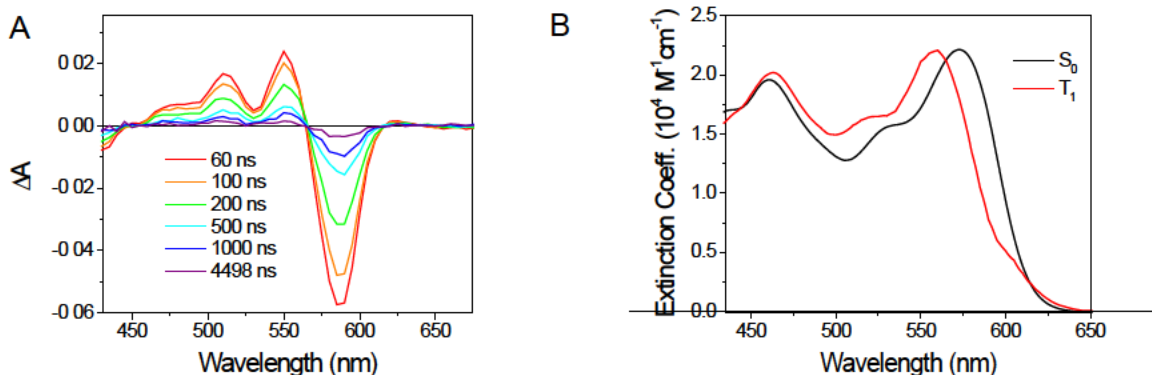


Figure 3. (A) Nanosecond transient absorption spectra of a 188 nm film of **1** excited with a 7 ns, 416 nm, 1.7 mJ, 1 cm diam. laser pulse (excitation density = $1.2 \times 10^{20} \text{ cm}^{-3}$). (B) S_0 and T_1 absorption spectra at 295 K of **1** in a 188 nm film.

Future Plans. Our overall plan and main goal is to understand the properties of photodriven redox systems well enough to produce integrated artificial photosynthetic systems that harvest light, separate charge and deliver that charge to catalysts for solar fuels formation.

DOE Sponsored Publications 2010-2013

1. Interrogating the Intramolecular Charge-Transfer State of a Julolidine-Anthracene Donor-Acceptor Molecule with Femtosecond Stimulated Raman Spectroscopy, J. V. Lockard, A. Butler Ricks, D. T. Co, and M. R. Wasielewski, *J. Phys. Chem. Lett.* **1**, 215-218 (2010).
2. Self-Assembly of a Hexagonal Supramolecular Light-Harvesting Array from Chlorophyll Trefoil Building Blocks, V. L. Gunderson, S. M. Mickley, and M. R. Wasielewski, *Chem. Commun.* **46**, 401-403 (2010).
3. Dynamics of Ultrafast Singlet and Triplet Charge Transfer in Anthraquinone-DNA Conjugates, F. D. Lewis, A. K. Thazhathveetil, T. A. Zeidan, J. Vura-Weis, and M. R. Wasielewski, *J. Am. Chem. Soc.* **132**, 444-445 (2010).
4. Photoinduced Electron Transfer from Rail to Rung within a Self-assembled Porphyrin Oligomeric Ladder, C. She, S.-J Lee, K.-T. Youm, K. L. Mulfort, J. E. McGarrah, O. K. Farha, J. Vura-Weis, M. R. Wasielewski, H. Chen, G. C. Schatz, M. A. Ratner and J. T. Hupp, *Chem. Commun.* **46**, 547-549 (2010).
5. Fluorescence Dynamics of Chlorophyll Trefoils in the Solid State Studied by Single Molecule Fluorescence Spectroscopy J.-E. Lee, J. Yang, V. L. Gunderson, M. R. Wasielewski, and D. Kim, *J. Phys. Chem. Lett.* **1**, 284-289 (2010).
6. Rapid Intramolecular Hole Hopping in *meso-meso* and *meta*-Phenylene-Linked Linear and Cyclic Multi-Porphyrin Arrays, T. M. Wilson, T. Hori, M.-C. Yoon, N. Aratani, A. Osuka, D. Kim, and M. R. Wasielewski, *J. Am. Chem. Soc.* **132**, 1383-1388 (2010).
7. Photophysics and Redox Properties of Rylene Imide and Bisimide Dyes Alkylated Ortho to the Imide Groups, J. E. Bullock, M. T. Vagnini, C. Ramanan, T. M. Wilson, T. J. Marks, and M. R. Wasielewski, *J. Phys. Chem. B* **114**, 1794-1802 (2010).
8. Comparing Spin-Selective Charge Transport through Oligomeric Aromatic Bridges in Donor-Bridge-Acceptor Molecules, A. M. Scott, A. Butler Ricks, M. T. Colvin, and M. R. Wasielewski, *Angew. Chem. Int. Ed.* **49**, 2904-2908 (2010).
9. Electron Spin Dynamics as a Controlling Factor for Spin-Selective Charge Recombination in Donor-Bridge-Acceptor Molecules, T. Miura, A. M. Scott, and M. R. Wasielewski, *J. Phys. Chem. C* **114**, 20370-20379 (2010).
10. Large Porphyrin Squares from Self-assembling of *meso*-Triazole-Appended L-shaped *meso-meso* Linked Zn(II) Triporphyrins: Synthesis and Efficient Energy Transfer, C. Maeda, P. Kim, S. Cho, J. K. Park, J. Min Lim, D. Kim, J. Vura-Weis, M. R. Wasielewski, H. Shinokubo, and A. Osuka, *Chem. Eur. J.* **16**, 5052-5061 (2010).

11. Time-resolved EPR Studies of Charge Recombination and Triplet State Formation within Donor-Bridge-Acceptor Molecules having Wire-like Oligofluorene Bridges, T. Miura, R. Carmieli, and M. R. Wasielewski, *J. Phys. Chem. A* **114**, 5769-5778 (2010).
12. Crossover from Single-Step Tunneling to Wire-like Multi-Step Hopping for Molecular Triplet Energy Transfer, J. Vura-Weis, S. H. Abdelwahed, R. Shukla, R. Rathore, M. A. Ratner, and M. R. Wasielewski, *Science* **328** 1547-1550 (2010).
13. Direct Measurement of the Dynamics of Hole Hopping in Extended DNA G-Tracts. An Unbiased Random Walk, S. M. Mickley Conron, A. K. Thazhathveetil, M. R. Wasielewski, A. L. Burin, and F. D. Lewis, *J. Am. Chem. Soc.* **132**, 14388-14390 (2010).
14. Controlling Electron Transfer in Donor-Bridge-Acceptor Molecules Using Cross-Conjugated Bridges. A. Butler Ricks, G. C. Solomon, M. T. Colvin, A. M. Scott, K. Chen, M. A. Ratner, and M. R. Wasielewski, *J. Am. Chem. Soc.* **132**, 15427-15434 (2010).
15. Magnetic Field-Induced Switching of the Radical-Pair Intersystem Crossing Mechanism in a Donor-Bridge-Acceptor Molecule for Artificial Photosynthesis, M. T. Colvin, A. Butler Ricks, A. M. Scott, A. L. Smeigh, R. Carmieli, T. Miura, and M. R. Wasielewski, *J. Am. Chem. Soc.* **133**, 1240-1243 (2011).
16. Temperature Dependence of Spin-Selective Charge Transfer Pathways in Donor-Bridge-Acceptor Molecules with Oligomeric Fluorenone and *p*-Phenylethynylene Bridges, A. M. Scott and M. R. Wasielewski, *J. Am. Chem. Soc.* **133**, 3005-3013 (2011).
17. Base Pair Sequence and Hole Transfer through DNA: Rational Design of Molecular Wires, J. Vura-Weis, F. D. Lewis, M. A. Ratner, M. R. Wasielewski, in "Charge and Exciton Transport in Molecular Wires", F. Grozema and L. Siebbeles, Eds. Wiley-VCH, Weinheim, 2011 pp. 133-156.
18. Photoinduced Singlet Charge Transfer in a Ruthenium(II) Perylene-3,4:9,10-bis(dicarboximide) Complex, V. L. Gunderson, E. Krieg, M. T. Vagnini, M. A. Iron, B. Rybtchinski, and M. R. Wasielewski, *J. Phys. Chem. B* **115**, 7533-7540 (2011).
19. Increasing the Speed Limit for Hole Transport in DNA, A. K. Thazhathveetil, A. Trifonov, M. R. Wasielewski, and F. D. Lewis, *J. Am. Chem. Soc.* **133**, 11485-11487 (2011).
20. Low-Temperature Frequency Domain Study of Excitation Energy Transfer in Ethynyl-Linked Chlorophyll-Trefoils and Aggregates, B. Neupane, N. C. Dang, R. F. Kelley, M. R. Wasielewski, and R. Jankowiak, *J. Phys. Chem. B* **115**, 10391-10399 (2011).
21. Belt-Shaped π -Systems: Relating Geometry to Electronic Structure in a Six-Porphyrin Nanoring, J. K. Sprafke, D. V. Kondratuk, M. Wykes, A. L. Thompson, M. Hoffmann, R. Drevinskas, W.-H. Chen, C. K. Yong, J. Kärnbratt, J. E. Bullock, M. Malfois, M. R.

- Wasielewski, B. Albinsson, L. M. Herz, D. Zigmantas, D. Beljonne, and H. L. Anderson, *J. Am. Chem. Soc.* **133**, 17262-17273 (2011).
22. Polymer Matrix Dependence of Conformational Dynamics within π -Stacked Perylenediimide Dimer and Trimer Revealed by Single Molecule Fluorescence Spectroscopy, H. Yoo, H. W. Bahng, M. R. Wasielewski, and D. Kim, *Phys. Chem. Chem. Phys.* **14**, 2001-2007 (2012).
 23. Intersystem Crossing Involving Strongly Spin Exchange-Coupled Radical Ion Pairs in Donor-Bridge-Acceptor Molecules, M. T. Colvin, A. Butler Ricks, A. M. Scott, D. T. Co, and M. R. Wasielewski, *J. Phys. Chem. A* **116**, 1923-1930 (2012).
 24. Role of Bridge Energetics on the Preference for Hole or Electron Transfer Leading to Charge Recombination in Donor-Bridge-Acceptor Molecules, M. T. Colvin, A. Butler Ricks, and M. R. Wasielewski, *J. Phys. Chem. A* **116**, 2184-2191 (2012).
 25. Exponential Distance Dependence of Photoinitiated Stepwise Electron Transfer in Donor-Bridge-Acceptor Molecules: Implications for Wire-like Behavior, A. Butler Ricks, D. T. Co, K. E. Brown, M. Wenninger, S. D. Karlen, Y. A. Berlin, and M. R. Wasielewski, *J. Am. Chem. Soc.* **134**, 4581-4588 (2012).
 26. Electron Transfer within Self-Assembling Cyclic Tetramers using Chlorophyll-Based Donor-Acceptor Building Blocks, V. L. Gunderson, A. L. Smeigh, C. H. Kim, D. T. Co, and M. R. Wasielewski, *J. Am. Chem. Soc.* **134**, 4363-4372 (2012).
 27. Structure and Dynamics of Photogenerated Triplet Radical Ion Pairs in DNA Hairpin Conjugates with Anthraquinone End Caps, R. Carmieli, A. L. Smeigh, S. M. Mickley Conron, A. K. Thazhathveetil, M. Fuki, Y. Kobori, F. D. Lewis, and M. R. Wasielewski, *J. Am. Chem. Soc.* **134**, 11251-11260 (2012).
 28. Supramolecular Chlorophyll Assemblies for Artificial Photosynthesis, V. L. Gunderson and M. R. Wasielewski, in "Handbook of Porphyrin Science", K. Kadish, K. M. Smith, and K. Guilard, Eds. World Scientific, Singapore, 2012, Vol. 20, pp. 45-105.
 29. Vibrational Dynamics of a Perylene-Perylenediimide Donor-Acceptor Dyad Probed with Femtosecond Stimulated Raman Spectroscopy, K. E. Brown, B. S. Veldkamp, D. T. Co, M. R. Wasielewski, *J. Phys. Chem. Lett.* **3**, 2362-2366 (2012).
 30. Dynamics and Efficiency of Hole Transport in LNA:DNA Hybrid Diblock Oligomers, A. Thazhathveetil, J. Vura-Weis, A. Trifonov, M. R. Wasielewski and F. D. Lewis, *J. Am. Chem. Soc.* **134**, 16434-16440 (2012).
 31. Excitonic Coupling between Linear and Trefoil Trimer Perylenediimide Molecules Probed by Single-Molecule Spectroscopy, H. Yoo, S. Furumaki, J. Yang; J.-E. Lee, H. Chung, T. Oba, H. Kobayashi, B. Rybtchinski, T. M. Wilson, M. R. Wasielewski, M. Vacha, and D. Kim, *J. Phys. Chem. B* **116**, 12878-12886 (2012).

32. Self-assembly of a Chlorophyll-based Cyclic Trimer: Structure and Intramolecular Energy Transfer, V. L. Gunderson and M. R. Wasielewski, *Chem. Phys. Lett.* **556**, 303-307 (2013).
33. Photoinitiated Electron Transfer in Zinc Porphyrin-Perylenediimide Cruciforms and their Self-assembled Oligomers, S. M. Mickley Conron, L. E. Shoer, A. L. Smeigh, A. Butler Ricks, and M. R. Wasielewski, *J. Phys. Chem. B* **117**, 2195-2204 (2013).
34. Dynamics and Efficiency of Photoinduced Charge Transport in DNA: Toward the Elusive Molecular Wire, F. D. Lewis and M. R. Wasielewski, *Pure Appl. Chem.* (submitted).
35. Photoinitiated Multi-step Charge Separation and Ultrafast Charge Transfer Induced Dissociation in a Pyridyl-Linked Photosensitizer-Cobaloxime Assembly, B. S. Veldkamp, W.-S. Han, S. M. Dyar, S. W. Eaton, M. A. Ratner, and M. R. Wasielewski, *Energy and Environ. Sci.* (submitted).

Session III

Coupled Donors and Acceptors

Tetrapyrrolic Architectures for Fundamental Studies of Light Harvesting and Energy Transduction

David F. Bocian,¹ Dewey Holten,² Christine Kirmaier,² and Jonathan S. Lindsey³

¹Department of Chemistry, University of California Riverside, Riverside, CA 92521

²Department of Chemistry, Washington University, St. Louis, MO 63130

³Department of Chemistry, North Carolina State University, Raleigh, NC 27695

A long-term goal of our program is to design, synthesize, and characterize molecular architectures that provide insights into principles for efficient solar-energy conversion. Efficient solar-energy conversion requires collection of solar light across the visible and near-infrared spectrum, excited-state charge separation, and movement of charge (hole, electron) to prevent charge recombination. Particularly noteworthy findings over the past three years are as follows:

Excited-state charge separation in molecular architectures has been widely explored, yet ground-state hole (or electron) transfer, particularly involving equivalent pigments, has been far less studied, and direct quantitation of the rate of transfer often has proved difficult. Prior studies of ground-state hole transfer between equivalent zinc porphyrins using electron paramagnetic resonance (EPR) techniques wherein ¹⁴N hyperfine interactions serve as clock give a lower limit of $\sim(50 \text{ ns})^{-1}$ on the rates. We also developed the use of site-specific ¹³C labeling of the meso or α -pyrrole carbons of the tetrapyrrole macrocycle. The rationale for incorporating the ¹³C labels is that the ¹³C hyperfine coupling is larger ($\sim 6.4 \text{ G}$ for meso ¹³C atoms) than the ¹⁴N hyperfine coupling ($\sim 1.6 \text{ G}$). The larger ¹³C hyperfine coupling affords a better opportunity of perform accurate spectral simulations to obtain exact hole-transfer rates. More recently, we have turned our focus to ²⁰³Tl/²⁰⁵Tl chelated macrocycles. The magnetogyric ratio(s) of ²⁰³Tl/²⁰⁵Tl is extremely large, $\sim 60\%$ of that of ¹H; accordingly, only very small spin density on the thallium metal center yields a significant hyperfine splitting (15-60 G). The thallium-hyperfine-clocking strategy has been utilized to examine hole transfer in the π -cation radicals of a several classes of tetrapyrrolic dyads and triads. Simulations of the EPR spectra of these cation radicals have been performed to extract exact hole-transfer rates and indicate that these rates fall in the 0.25 – 10 ns range (Fig. 1), consistent with the values obtained from the time-resolved optical studies. For all of the dyads and triads, the activation energies for hole transfer have been obtained from simulations of the spectra as a function of temperature. These studies indicate that hole transfer is governed by a complex interplay of mechanisms.

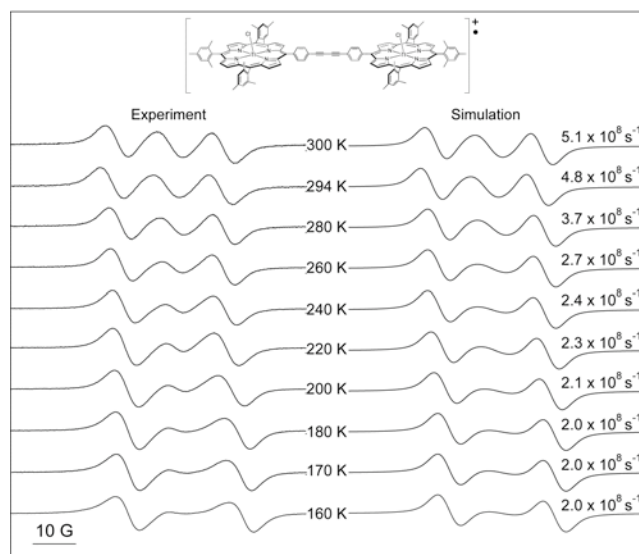


Fig. 1. Variable-temperature EPR spectra of a porphyrin dyad (left panel) and simulated spectra (right panel) with derived hole-transfer rates.

Panchromatic absorption is an ideal feature for light-harvesting architectures, yet molecular design approaches to achieve broad-band solar coverage have chiefly relied on a composite of narrow-banded absorbers in multipigment architectures. As an outgrowth of our studies on perylene-tetrapyrroles, an ethynyl-linked perylene-monoimide attached to a porphyrin afforded nearly panchromatic absorption across the visible region (Fig. 2). Despite the broad absorption, the porphyrin exhibited $\Phi_f = 0.40$ and $\tau_s = 6.5$ ns, indicating an excited singlet state with sufficient lifetime for coupling to downstream energy-transfer or charge-separation processes.

The vast majority of work over the years in artificial photosynthesis, including our own, has employed porphyrins as surrogates for the naturally occurring (bacterio)chlorophylls. The reliance on porphyrins stems from synthetic expediency despite the lack of red or near-infrared absorption that is characteristic of (bacterio)chlorins and is essential for effective solar-light harvesting. To remedy this deficiency we have developed de novo routes to synthetic chlorins and bacteriochlorins so as to be able to prepare simple analogues of the natural hydroporphyrins as well as arrange the synthetic hydroporphyrins in a variety of 3-dimensional architectures. Rational synthetic access is now available to diverse chlorins and bacteriochlorins. This set of hydroporphyrins provides strong absorption in the region 600 – 850 nm (Fig. 3).

Our present focus concerns the blending of several longstanding threads of our prior work, namely (1) the design, synthesis, and characterization of covalent and self-assembled arrays, and (2) the study of the fundamental (photophysical, redox, MO) properties of monomeric synthetic hydroporphyrins, (3) the development of synthetic methods for the preparation of hydroporphyrin building blocks, and (4) the attachment of tetrapyrrole macrocycles to surfaces. The resulting ensembles of synthetic (hydro)porphyrins will be the subject of future studies of energy and hole transfer that incorporate newly developed optical and EPR approaches. Collectively, these studies should aid the design of next-generation molecular architectures for studies of solar-energy conversion.

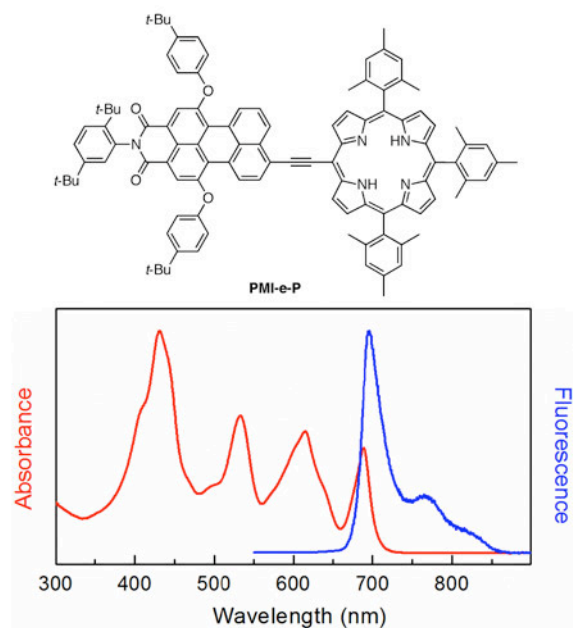


Fig. 2. Absorption and fluorescence spectra of PMI-e-P.

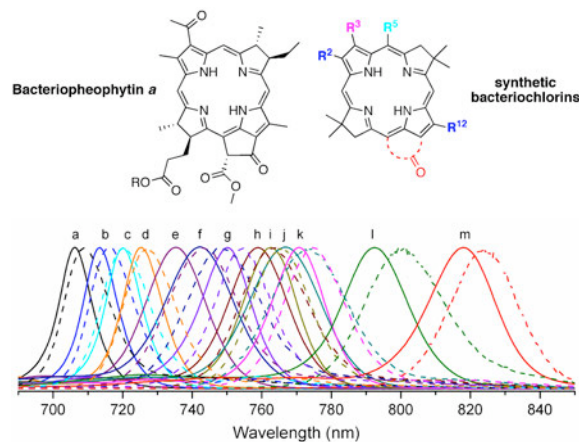


Fig. 3. Absorption (solid lines) and fluorescence (dashed lines) spectra of synthetic bacteriochlorins.

DOE Sponsored Publications 2010-2013

1. “Excited-State Photodynamics of Perylene–Porphyrin Dyads 5. Tuning Light-Harvesting Characteristics via Perylene Substituents, Connection Motif, and 3-Dimensional Architecture,” Kirmaier, C.; Song, H.-E.; Yang, E. K.; Schwartz, J. K.; Hindin, E.; Diers, J. R.; Loewe, R. S.; Tomizaki, K.-y.; Chevalier, F.; Ramos, L.; Birge, R. R.; Bocian, D. F.; Lindsey, J. S.; Holten, D. *J. Phys. Chem. B* **2010**, *114*, 14249–14264.
2. “Expanded Scope of Synthetic Bacteriochlorins via Improved Acid Catalysis Conditions and Diverse Dihydrodipyrin-Acetals,” Krayner, M.; Ptaszek, M.; Kim, H.-J.; Meneely, K. R.; Fan, D.; Secor, K.; Lindsey, J. S. *J. Org. Chem.* **2010**, *75*, 1016–1039. (*Selected as a Featured Article*)
3. “Stable Synthetic Bacteriochlorins Overcome the Resistance of Melanoma to Photodynamic Therapy,” Mroz, P.; Huang, Y.-Y.; Szokalska, A.; Zhiyentayev, T.; Janjua, S.; Nifli, A.-P.; Sherwood, M. E.; Ruzié, C.; Borbas, K. E.; Fan, D.; Krayner, M.; Balasubramanian, T.; Yang, E.; Kee, H. L.; Kirmaier, C.; Diers, J. R.; Bocian, D. F.; Holten, D.; Lindsey, J. S.; Hamblin, M. R. *FASEB J.* **2010**, *24*, 3160–3170.
4. “De Novo Synthesis of Long-Wavelength Absorbing Chlorin-13,15-Dicarboximides,” Ptaszek, M.; Lahaye, D.; Krayner, M.; Muthiah, C.; Lindsey, J. S. *J. Org. Chem.* **2010**, *75*, 1659–1673.
5. “In vitro Photodynamic Therapy and Quantitative Structure-Activity Relationship Studies with Stable Synthetic Near-Infrared-Absorbing Bacteriochlorin Photosensitizers,” Huang, Y.-Y.; Mroz, P.; Zhiyentayev, T.; Sharma, S. K.; Balasubramanian, T.; Ruzié, C.; Krayner, M.; Fan, D.; Borbas, K. E.; Yang, E.; Kee, H. L.; Kirmaier, C.; Diers, J. R.; Bocian, D. F.; Holten, D.; Lindsey, J. S.; Hamblin, M. R. *J. Med. Chem.* **2010**, *53*, 4018–4027.
6. “Stable Synthetic Cationic Bacteriochlorins as Selective Antimicrobial Photosensitizers,” Huang, L.; Huang, Y.-Y.; Mroz, P.; Tegos, G. P.; Zhiyentayev, T.; Sharma, S. K.; Lu, Z.; Balasubramanian, T.; Krayner, M.; Ruzié, C.; Yang, E.; Kee, H. L.; Kirmaier, C.; Diers, J. R.; Bocian, D. F.; Holten, D.; Lindsey, J. S.; Hamblin, M. R. *Antimicrob. Agents Chemother.* **2010**, *54*, 3834–3841.
7. “Structural Studies of Sparsely Substituted Chlorins and Phorbins Establish Benchmarks for Changes in the Ligand Core and Framework of Chlorophyll Macrocycles,” Taniguchi, M.; Mass, O.; Boyle, P. D.; Tang, Q.; Diers, J. R.; Bocian, D. F.; Holten, D.; Lindsey, J. S. *J. Mol. Structure* **2010**, *979*, 27–45.
8. “Probing the Rate of Hole Transfer in Oxidized Synthetic Chlorin Dyads via Site-Specific ¹³C-Labeling,” Nieves-Bernier, E. J.; Taniguchi, M.; Diers, J. R.; Holten, D.; Bocian, D. F.; Lindsey, J. S. *J. Org. Chem.* **2010**, *75*, 3193–3202. (*Selected as a Featured Article*)
9. “Synthesis of Oligo(*p*-Phenylene)-linked Dyads Containing Free Base, Zinc(II) or Thallium(III) Porphyrins for Studies in Artificial Photosynthesis,” Taniguchi, M.; Lindsey, J. S. *Tetrahedron* **2010**, *66*, 5549–5565.
10. “Probing the Rate of Hole Transfer in Oxidized Porphyrin Dyads Using Thallium Hyperfine Clocks,” Diers, J. R.; Taniguchi, M.; Holten, D.; Lindsey, J. S.; Bocian, D. F. *J. Am. Chem. Soc.* **2010**, *132*, 12121–12132.

11. “Structural Characteristics that Make Chlorophylls Green: Interplay of Hydrocarbon Skeleton and Substituents,” Mass, O.; Taniguchi, M.; Ptaszek, M.; Springer, J. W.; Faries, K. M.; Diers, J. R.; Bocian, D. F.; Holten, D.; Lindsey, J. S. *New J. Chem.* **2011**, *35*, 76–88.
12. “De Novo Synthesis and Photophysical Characterization of Annulated Bacteriochlorins. Mimicking and Extending the Properties of Bacteriochlorophylls,” Krayner, M.; Yang, E.; Diers, J. R.; Bocian, D. F.; Holten, D.; Lindsey, J. S. *New J. Chem.* **2011**, *35*, 587–601.
13. “Tapping the Near-Infrared Spectral Region with Bacteriochlorin Arrays,” Lindsey, J. S.; Mass, O.; Chen, C.-Y. *New J. Chem.* **2011**, *35*, 511–516.
14. “Facile Synthesis of a B,D-Tetradehydrocorrin and Rearrangement to Bacteriochlorins,” Aravindu, K.; Krayner, M.; Kim, H.-J.; Lindsey, J. S. *New J. Chem.* **2011**, *35*, 1376–1384.
15. “Synthesis and Photochemical Characterization of Stable Indium Bacteriochlorins,” Krayner, M.; Yang, E.; Kim, H.-J.; Kee, H. L.; Deans, R. M.; Sluder, C. E.; Diers, J. R.; Kirmaier, C.; Bocian, D. F.; Holten, D.; Lindsey, J. S. *Inorg. Chem.* **2011**, *50*, 4607–4618.
16. “Photophysical Properties and Electronic Structure of Stable, Tunable Synthetic Bacteriochlorins: Extending the Features of Native Photosynthetic Pigments,” Yang, E.; Kirmaier, C.; Krayner, M.; Taniguchi, M.; Kim, H.-J.; Diers, J. R.; Bocian, D. F.; Lindsey, J. S.; Holten, D. *J. Phys. Chem. B* **2011**, *115*, 10801–10816.
17. “A *trans*-AB-Bacteriochlorin Building Block,” Mass, O.; Lindsey, J. S. *J. Org. Chem.* **2011**, *76*, 9478–9487.
18. “Effects of Substituents on Synthetic Analogs of Chlorophylls. Part 3: The Distinctive Impact of Auxochromes at the 7- versus 3-Positions,” Springer, J. W.; Faries, K. M.; Kee, H. L.; Diers, J. R.; Muthiah, C.; Mass, O.; Kirmaier, C.; Lindsey, J. S.; Bocian, D. F.; Holten, D. *Photochem. Photobiol.* **2012**, *88*, 651–674.
19. “Synthesis and Physicochemical Properties of Metallobacteriochlorins,” Chen, C.-Y.; Sun, E.; Fan, D.; Taniguchi, M.; McDowell, B. E.; Yang, E.; Diers, J. R.; Bocian, D. F.; Holten, D.; Lindsey, J. S. *Inorg. Chem.* **2012**, *51*, 9443–9464.
20. “Stable Synthetic Bacteriochlorins for Photodynamic Therapy: Role of Dicyano Peripheral Groups, Central Metal Substitution (2H, Zn, Pd), and Cremophor EL Delivery,” Huang, Y.-Y.; Balasubramanian, T.; Yang, E.; Diers, J. R.; Bocian, D. F.; Lindsey, J. S.; Holten, D.; Hamblin, M. R. *ChemMedChem* **2012**, *7*, 2155–2167.
21. “Effects of Linker Torsional Constraints on the Rate of Ground-State Hole Transfer in Porphyrin Dyads,” Hondros, C. J.; Aravindu, K.; Diers, J. R.; Holten, D.; Lindsey, J. S.; Bocian, D. F. *Inorg. Chem.* **2012**, *51*, 11076–11086.
22. “Synthesis and Characterization of Lipophilic, Near-Infrared Absorbing Metallobacteriochlorins,” Sun, E.; Chen, C.-Y.; Lindsey, J. S. *Chem. J. Chin. Univ.* **2013**, *in press*.
23. “Photophysical Properties and Electronic Structure of Bacteriochlorin–Chalcones with Extended Near-Infrared Absorption,” Yang, E.; Ruzié, C.; Krayner, M.; Diers, J. R.; Niedzwiedzki, D. M.; Lindsey, J. S.; Bocian, D. F.; Holten, D. *Photochem. Photobiol.* **2013**, *89*, DOI: 10.1111/php.12053.

I. Use of time resolved infrared to evaluate charge transfer excited states and intramolecular electron transfer in Re(I) dimethylaminobenzonitrile complexes.
II. Triplet states and photoreactions of Sn(IV) N[^]N[^]O Schiff base complexes.

Tod Grusenmeyer, Yunkai Yue^{*}, Joel Mague, James Donahue, Igor Rubtsov^{*}, Peng Zhang[‡],
 Zheng Ma[‡], David Beretan[‡] and Russell Schmehl

Department of Chemistry
 Tulane University
 New Orleans LA, 70118
[‡] Department of Chemistry
 Duke University
 Durham, NC, 22708

I. Electron density changes in chromophores following absorption of light can, in certain circumstances, be followed by time resolved infrared spectroscopic analysis. Metal carbonyl complexes are particularly useful in this regard because of the isolated CO stretching modes in the mid-infrared. We are currently exploring the evolution of excited states in a series of [Re^I(bpy)(CO)₃L] compounds where L is benzonitrile (ReBN), 4-dimethylaminobenzonitrile (Re(4-DMABN)), and 3-dimethylaminobenzonitrile (Re(3-DMABN)). The dimethylamino complexes present the possibility of intramolecular electron transfer from the amine to the photoexcited metal-to-ligand charge transfer (MLCT) state of the Re chromophore; the behavior varies from polar to nonpolar solvent. The Re(BN) complex exhibits strong luminescence with a yield and lifetime that is relatively independent of solvent. The time resolved infrared (TRIR) reveals instantaneous formation of an excited state with MLCT character (figure 1) as evidenced by the increase in frequency of the CO stretching modes; little change is observed in the nitrile stretch at 2250 cm⁻¹.

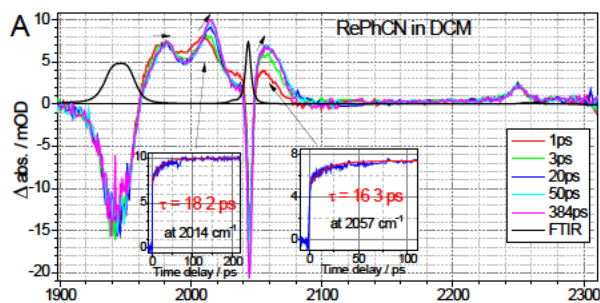


Figure 1: TRIR of Re(BN) in dichloromethane

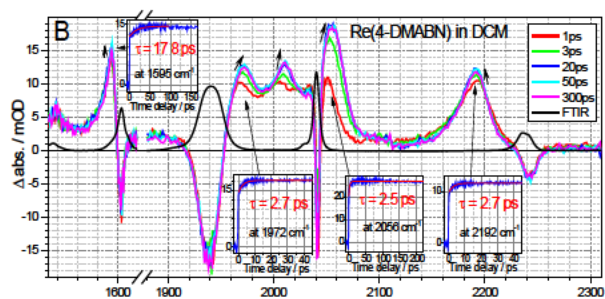


Figure 2: TRIR of Re(4DMABN) in DCM

Excitation of the Re(4DMABN) complex results in strong luminescence in dichloromethane (DCM), but nearly complete quenching in mixed DCM/MeOH; the excited state lifetime decreases by more than a factor of 100 following the solvent change. TRIR reveals a mixed MLCT and interligand charge transfer state (LLCT) (fig. 2); the LLCT contribution is revealed by a large shift in the CN stretch to lower frequency. DFT

^{*} Yue and Rubtsov obtained all time resolved IR data in this work. Synthesis, characterization, uv-vis absorption and luminescence and transient absorption was done by Grusenmeyer and Schmehl. DFT calculations were performed by Zheng and Ma under the direction of Beretan. Crystal structures were obtained by Mague and Donahue.

and TDDFT calculations indicate a significant increase in the Mulliken charge of the nitrile ligand relative to the ground state, but also an increase in charge of the Re center; the dimethylamine partial cation formation has the effect of inducing a decrease in the CN stretching frequency. The Re(3DMABN) complex exhibits increases in the CO stretching frequencies in the TRIR immediately following excitation (fig. 3); this is followed by disappearance of these bands and appearance of new bands at lower frequencies over 60-80 ps. These changes are accompanied by a very large shift to lower frequency of the CN modes. The results are consistent with evolution of the initially formed MLCT state to a LLCT state in which the Re center has decreased charge, resulting in the CO modes shifting to lower frequency.

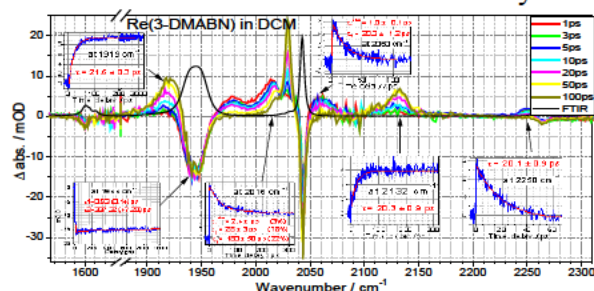


Figure 3: TRIR of Re(3DMABN) in DCM

Significant differences are observed in the behavior in mixed DCM/MeOH, especially for the Re(3DMABN) complex where the initially formed MLCT state does not appear to evolve to the fully charge separated state. DFT geometry optimization of the lowest energy triplet state of the complex suggests that, in DCM, the excited state is actually a triplet localized on the 3DMABN ligand; the TRIR results are consistent with this interpretation and also with the observation of the very long excited state lifetime in DCM (~25 μ s). The results indicate that luminescence spectral and lifetime results alone can provide a misleading picture of intramolecular excited state electron density changes and reactivity.

II. We have begun a search for new chromophores containing earth abundant metals that have visible absorption, form long lived excited states and are capable of photoredox reactivity from the long lived excited states. In this regard we began investigation of Sn(IV) schiff base complexes, in part because reported complexes absorb in the visible and Sn has a very high spin-orbit coupling matrix element. The complexes and ligands (aminoquinoline and naphthol carboxaldehyde Schiff base) are straightforward to synthesize. The complexes exhibit fluorescence with reasonably high yields, but also have long lived triplets that are readily observed by ns transient

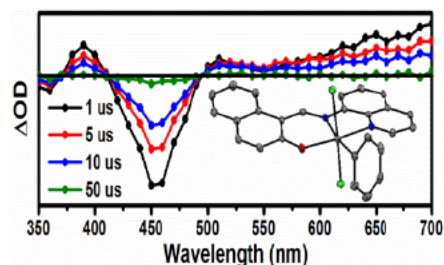


Figure 4: ns TA spectrum of [(N^NO)SnCl₂(Ph)] in AN

absorption spectroscopy (fig. 4). The complexes are quenched by electron donors and, with 10-methylphenothiazine, back electron transfer occurs with little decomposition. Efforts in the lab are focused on making complexes that absorb further into the visible, have higher intersystem crossing yields and exhibit reversible electrochemistry in the ground state.

DOE Sponsored Publications 2010-2013

1. Jing Gu, Jin Chen, Russell H. Schmehl “Using Intramolecular Energy Transfer to Transform non-Photoactive, Visible-Light-Absorbing Chromophores into Sensitizers for Photoredox Reactions” *J. Am. Chem. Soc.*, **2010**, *132*, 7338 – 46.
2. Kurtz, J. P.; Grusenmeyer, T.; Tong, L.; Kosgei, G.; Schmehl, R. H.; Mague, J. T.; Pascal, R. A., Jr. “Highly luminescent, polyaryl mesobenzanthrones.” *Tetrahedron*, **2011**, *67*, 7211-7216.
3. Grusenmeyer, Tod A.; Chen; Jin, Jin, Yuhuan; Nguyen, Jonathan; Rack, Jeffrey J. ; Schmehl, Russell H. “pH Control of Intramolecular Energy Transfer and Oxygen Quenching in Ru(II) Complexes Having Coupled Electronic Excited States” *J. Am. Chem. Soc.*, 2012, *134*, 7497–7506.
4. Shan, Bing; Baine, T; Ma, X.A. N.; Zhao, X; Schmehl, Russell “Mechanistic Details for Cobalt Catalyzed Photochemical Hydrogen Production in Aqueous Solution: Efficiencies of the Non-Photochemical Steps” *Inorg. Chem.*, in revision.
5. Yue, Yuankai; Grusenmeyer, Tod; Zhang, Peng; Ma, Zheng; Schmehl, Russell, Beretan, David N.; Rubtsov, Igor V. “Evaluation of charge transfer extent in excited rhenium(I) complexes using time-resolved vibrational spectroscopy”, manuscript in preparation.
6. J. Draggich, A. Neuberger, R. H. Schmehl “Excited State Electron Transfer of [Pt(II)(N[^]C[^]N)Cl] complexes: Direct Observation of Pt(III) Species”, in preparation.
7. A. Neuberger, J. Adams, D. Roddick and R. H. Schmehl “Photophysical Behavior of Re(II) Phosphine Complexes in Solution”, in preparation.
8. G. Kosgei and R. H. Schmehl “RAFT Polymerization of Ru(II) Diimine Complexes and Photoredox Reactivity in Solution” , in preparation.

Session IV

Solar Photoconversion with Quantum Dots

Strongly Coupled Quantum Dot-Ligand Systems

Matthew T. Frederick, Victor A. Amin, Laura C. Cass, Rachel Harris, and Emily A. Weiss
Department of Chemistry
Northwestern University
Evanston, IL 60208-3113

This talk describes the mechanisms by which organic surfactants – in particular phenyldithiocarbamates (PTC), **Figure 1** – couple electronically to the delocalized states of semiconductor quantum dots (QDs).

Coordination of phenyldithiocarbamate (X = H in **Figure 1**) ligands to colloidal CdSe, CdS, and PbS QDs decreases the optical bandgaps, E_g , of the QDs by up to 970 meV. These values of ΔE_g are the largest shifts achieved by chemical modification of the surfaces of solution-phase CdSe QDs, and are—by more than an order of magnitude in energy—the largest bathochromic shifts achieved for QDs in either the solution or solid phases. Measured values of ΔE_g upon coordination to PTC correspond to an apparent increase in the excitonic radius (ΔR) of up to 0.3 nm for CdSe, 0.9 nm for CdS, and 0.15 nm for PbS, **Figure 2**. Electronic structure calculations indicate that the highest occupied molecular orbital of PTC is near resonant with a high density of states portion of the QD valence band, and that the two have correct symmetry to exchange electron density (PTC is a π -donor and the photoexcited QD is a π -acceptor). These results indicate that the relaxation of exciton confinement occurs through delocalization of the photoexcited hole of the QD into the ligand shell.

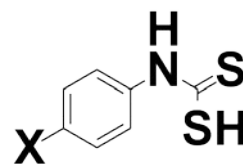


Fig.1 Chemical structure of a *para*-substituted phenyldithiocarbamate (PTC)

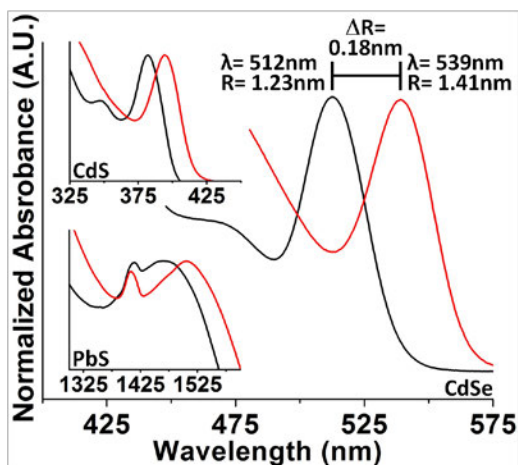


Fig. 2. Absorption spectra of CdS, CdSe, and PbS QDs before (black) and after (red) adsorption of PTC. We calculate ΔR by subtracting the apparent radius before PTC exchange from the radius after PTC exchange.

Control of the quantum confinement, and therefore the energy, of excitonic holes in CdSe QDs is achievable through adsorption of PTC with various electron-donating and electron-withdrawing groups *para*- (**Figure 3**) and *meta*-substituents on the phenyl ring. These substitutions control hole delocalization in the QDs through the energetic alignment of the highest occupied orbitals of PTC with the highest density-of-states region of the CdSe valence band, to which PTC couples selectively.

For a given QD material and physical radius, R , the magnitude of the increase in apparent excitonic radius (ΔR) upon delocalization by PTC directly reflects the degree of quantum confinement of one or both charge carriers, **Figure 4**. The plots of ΔR vs. R for CdSe

and CdS show that exciton delocalization by PTC occurs specifically through the excitonic hole, which has a dependence of confinement energy on R that distinguishes it from the electron. Furthermore, the plot for CdSe, which spans a range of R over multiple confinement regimes for the hole, identifies the radius ($R \sim 1.9$ nm) at which the hole transitions between regimes of strong and intermediate confinement. This demonstration of ligand-induced delocalization of a *specific* charge carrier is a first step toward eliminating current-limiting resistive interfaces at organic-inorganic junctions within solid-state hybrid devices.

Currently, we are utilizing Fourier-transform Infrared (FTIR) spectroscopy on dispersions of PTC-substituted QDs to determine the range of adsorption modes of PTC as a function of their added concentration and the surface chemistry of the QDs. Ongoing NMR studies are aimed at quantifying the surface coverage of PTC on the QDs and determining the extent of intermolecular (PTC-PTC) interactions, and whether they contribute to the QDs optical response to PTC. We are also doing a computational screen to identify other ligands that have to the potential to couple strongly to delocalized states of the QD core.

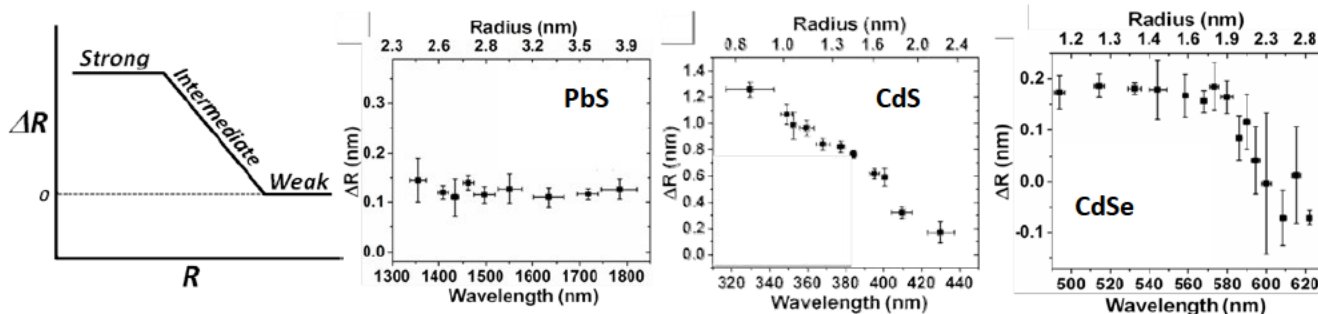


Figure 4. Left: Predicted trend of ΔR vs. R for a single carrier that experiences all three confinement regimes over the range of R that is studied. In the intermediate confinement regime, ΔR is a decreasing (although not necessarily linearly decreasing) function of R . Right: Plots of ΔR vs. R for three different types of QDs. The affected carrier in PbS is strongly confined throughout the range of R (this is characteristic of both electron and hole). The affected carrier in CdS is in the intermediate confinement regime throughout the range of R (this is characteristic of the hole only). The affected carrier in CdSe is in the strong confinement regime at small R , and the intermediate confinement regime at larger R (this is characteristic of the hole only).

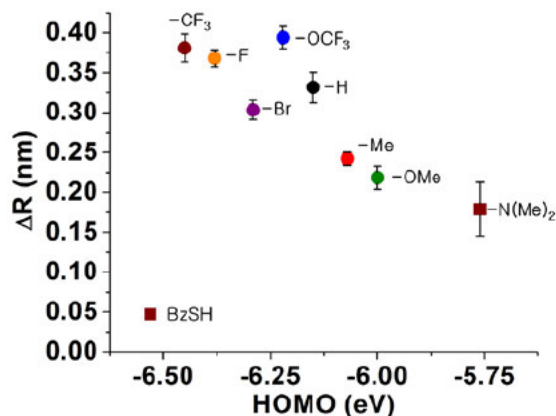


Fig. 3. Plot of ΔR for CdSe QDs upon adsorption of *para*-substituted X-PTC, as a function of the HOMO of X-PTC, and for CdSe QDs functionalized with benzylmercaptan (BzSH), for reference. The more electron-withdrawing the substituent, the more energetically stabilized the HOMO. As the HOMO of X-PTC decreases in energy, it becomes more energetically resonant with the highest density of states region of the CdSe valence band, and effects a larger delocalization radius, ΔR , for the excitonic hole.

DOE Solar Photochemistry-Sponsored Publications 2010-2013

1. Frederick, M.T.; Amin, V.A.; **Weiss, E.A.** The Optical Properties of Strongly Coupled Quantum Dot-Ligand Systems, *J. Phys. Chem. Lett.*, 4, 634-640 (2013).
2. Frederick, M.T.; Amin, V.A. Swenson, N.K.; Ho, A.Y.; **Weiss, E.A.** Control of Exciton Confinement in Quantum Dot-Organic Complexes through Modulation of the Energetic Alignment of Interfacial Orbitals, *Nano Lett.*, 13, 287-292 (2013).
3. Morris-Cohen, A.J.; Peterson, M.D.; Kamm, J.; Frederick, M.T.; **Weiss, E.A.** Evidence for a van der Waals Path for Electron Transfer from Quantum Dots to Carboxylate-Functionalized Viologens, *J. Phys. Chem. Lett.*, 3, 2840-2844 (2012).
4. Morris-Cohen, A.J.; Vasilenko, V.; Amin, V.A.; Reuter, M.; **Weiss, E.A.** A Model for Binding of Ligands to Colloidal Quantum Dots with Concentration-Dependent Surface Structure, *ACS Nano*, 6, 557-565 (2012).
5. Knowles, K.E.; Frederick, M.T.; Tice, D.B.; Morris-Cohen, A.J., **Weiss, E.A.** Colloidal Quantum Dots: Think Outside the (Particle-in-a-)Box. *J. Phys. Chem. Lett.*, 3, 18-26 (2012).
6. Frederick, M.T.; Cass, L.C.; Amin, V.A.; **Weiss, E.A.** A Molecule to Detect and Perturb the Confinement of Charge Carriers in Quantum Dots, *Nano Lett.*, 11, 5455-5460 (2011).
7. Morris-Cohen, A.J.; Frederick, M.T.; Cass, L.C.; **Weiss, E.A.** Simultaneous Determination of the Adsorption Constant and the Photoinduced Electron Transfer Rate for a CdS Quantum Dot-Viologen Complex with Transient Absorption Spectroscopy, *J. Am. Chem. Soc.*, 133, 10146–10154 (2011).
8. Peterson, M.D.; Hayes, P.L; Martinez, I.S.; Cass, L.C.; Achtyl, J.L.; **Weiss, E.A.**; Geiger, F.M., Second Harmonic Generation Imaging with a kHz Amplifier, *Optics Mater. Expr.*, 1, 57-66 (2011).
9. Frederick, M.T.; Achtyl, J.L.; Knowles, K.E.; **Weiss, E.A.**; Geiger, F.M. Surface-Amplified Ligand Disorder in CdSe Quantum Dots Determined by Electron and Coherent Vibrational Spectroscopies, *J. Am. Chem. Soc.*, 133, 7476-7481 (2011).

Dependence of Size, Composition, and Doping on the Multiple Exciton Generation Efficiency in Quantum Dots

Barbara K. Hughes, Aaron G. Midgett, Arthur J. Nozik, Jeffery L. Blackburn, Justin C. Johnson,
Sagar Dodderi and Matthew C. Beard
Chemical and Material Sciences Department
National Renewable Energy Laboratory
Golden, Co 83401

In this program we are interested in understanding the exciton relaxation dynamics in quantum-confined semiconductors. In recent years we have discovered and studied multiple exciton generation (MEG) as a novel phenomenon that can boost the primary energy conversion step of hot-excitons into usable charge-carriers. While a similar process, impact ionization, occurs in bulk semiconductors, MEG is enhanced in semiconductor nanostructures due to increased Coulomb interactions and reduced momentum conservation that relaxes selection rules and increases the number of final states that can be coupled to the initially excited state. Key questions that we are focusing on are measuring and understanding the size-dependence of the MEG process. How do the surfaces and stoichiometry impact MEG? Do electronically doped QDs exhibit a reduced MEG efficiency? How does composition affect the MEG efficiency? In this discussion we present our recent results addressing these important questions.

Using ultrafast transient absorption and time-resolved photoluminescence spectroscopies, we studied MEG in quantum dots (QDs) consisting of either PbSe, PbS, or a $\text{PbS}_x\text{Se}_{1-x}$ alloy for various QD diameters with corresponding bandgaps ranging from 0.6 to 1 eV. For each QD sample we determine the MEG efficiency, η_{MEG} , defined in terms of the electron-hole pair creation energy (ϵ_{eh}) such that $\eta_{\text{MEG}} = E_g/\epsilon_{eh}$. In previous reports, we found that η_{MEG} is about two times greater in PbSe QDs compared to bulk PbSe, however, little could be said about the QD-size dependence of MEG. In this study, we find for both PbS and $\text{PbS}_x\text{Se}_{1-x}$ alloyed QDs that η_{MEG} decreases lineally with increasing QD diameter within the strong confinement regime. When the QD radius is normalized by a material-dependent characteristic radius, defined as the radius at which the electron-hole

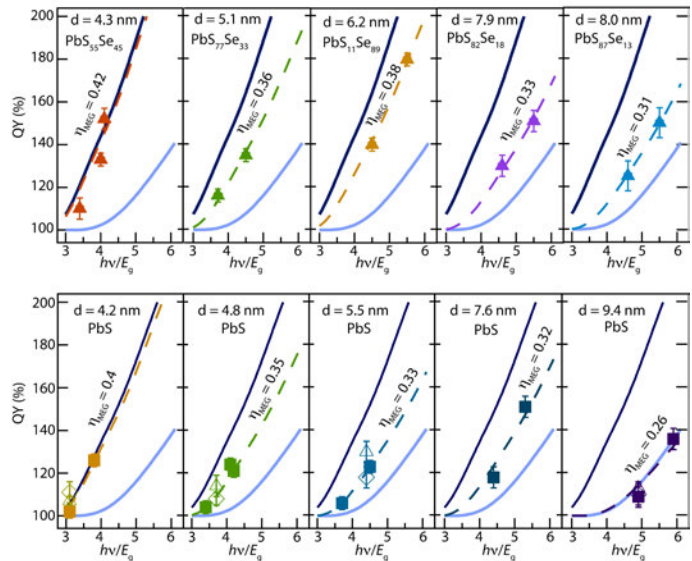


Figure 1. Top row: Photon-to-exciton QYs for various sizes of $\text{PbS}_x\text{Se}_{1-x}$ alloy QDs. Bottom row: QYs for a variety of PbS QD sizes. The solid dark blue line represents η_{MEG} determined from PbSe QDs while the light blue lines are for bulk PbS. The dotted lines are η_{MEG} determined from a linear least squares best-fit to the data. Note that for each size the QY was also determined at $h\nu/E_g$ less than 2 (but not shown).

Coulomb and confinement energies are equivalent, PbSe, PbS, and $\text{PbS}_x\text{Se}_{1-x}$ exhibit similar MEG behaviors. Our results suggest that MEG increases with quantum confinement, and we discuss the interplay between a size-dependent MEG rate vs. hot exciton cooling.

We have developed synthetic strategies for tuning the stoichiometry of PbSe QDs, as-prepared QDs are Pb-rich (figure 2). We have synthesized alkylselenide reagents to replace the native oleate ligand on PbSe QDs in order to investigate the effect of surface modification on their stoichiometry, photophysics, and air stability. The alkylselenide reagent removes all of the oleate on the QD surface and results in Se addition; however, complete Se-enrichment does not occur, achieving a 53% decrease in the amount of excess Pb for 2 nm diameter QDs and a 23% decrease for 10 nm QDs. Our analysis suggests that the Se-ligand preferentially binds to the {111} faces, which are more prevalent in smaller QDs. We find that attachment of the alkylselenide ligand to the QD surface enhances oxidative resistance, likely resulting from a more stable bond between surface Pb atoms and the alkylselenide ligand compared to Pb-oleate.

We are developing strategies to dope PbSe and PbS QDs either n or p-type by diffusion of impurity atoms. We find the ability to dope the QDs with Ag is size-dependent. For those sizes where Ag dopes the QDs, we find a bleach of the 1st exciton transition accompanied by an intraband absorption in the infrared (see Figure 3). We compare the exciton dynamics of a sample of PbSe QDs with ~ 10% Ag doping and to that of as-prepared QDs. Finally, we studied the MEG efficiency in the doped QDs and compare that to as-prepared QDs.

Finally, we are investigating MEG in colloidal Si QDs and find that for QD size of less 4 nm the MEG efficiency is very high, approaching the energy conservation limit.

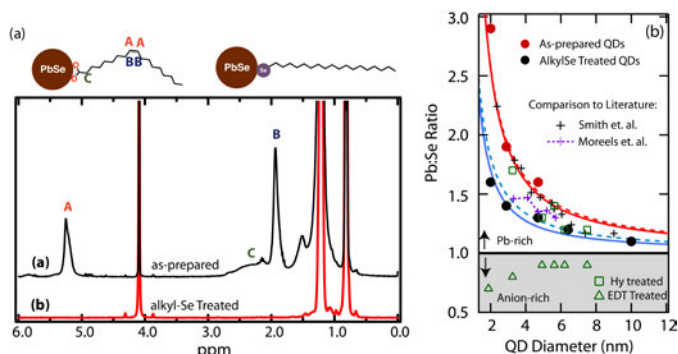


Figure 2. (a) NMR analysis showing that the alkyl-Se ligand replaces the OA ligand on the QD surface and (b) ICP analysis showing that addition of the alkyl-Se ligand decreases the Pb content in the QDs.

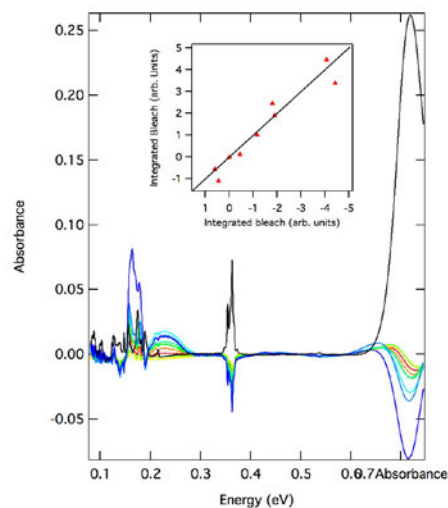


Figure 3. Change in absorbance for Ag-doped PbSe QDs. The 1st exciton is bleached while an intraband absorbance grows in.

DOE Solar Photochemistry Sponsored Publications 2010-2013

1. A.G. Midgett, J.M. Luther, J.T. Stewart, D.K. Smith, L.A. Padilha, V.I. Klimov, A.J. Nozik, M.C. Beard, "Size and Composition Dependent Multiple Exciton Generation Efficiency in PbS, PbSe and PbSSe Alloyed Quantum Dots", *Nano Letters*, **2013**, Submitted
2. O.E. Semonin, J. M. Luther, M.C. Beard, "Quantum Dots For Next-Generation Photovoltaics", *Materials Today*, **2012**, 15, 508
3. M.C. Beard, Joseph M. Luther, Octavi E. Semonin, A.J. Nozik, "Third Generation Photovoltaics based on Multiple Exciton Generation in Quantum Confined Semiconductors", *ACR*, **2013**, ASAP, doi:10.1021/ar3001958
4. B.K. Hughes, J.M. Luther, M.C. Beard, "The Subtle Chemistry of Colloidal, Quantum-Confined Semiconductor Nanostructures", *ACS Nano*, **2012**, 6, 4573, doi:10.1021/nn302286w
5. .K. Hughes, D.A. Ruddy, J.L. Blackburn, D.K. Smith, M.R. Bergren, A.J. Nozik, J.C. Johnson, M.C. Beard, "Control of PbSe Quantum Dot Surface Chemistry and Photophysics Using an Alkylselenide Ligand", *ACS Nano.*, **2012**, 6, 5498, doi: 10.1021/nn301405j
6. J.T. Stewart, L.A. Padilha, M.M. Qazilbash, J.M. Pietryga, A.G. Midgett, J.M. Luther, M.C. Beard, A.J. Nozik, V.I. Klimov, "Comparison of Carrier Multiplication Yields in PbS and PbSe Nanocrystals: The Role of Competing Energy-Loss Processes", *Nano Lett*, 12, 622, **2012**, doi:10.1021/nl203367m
7. B Heshmat, H Pahlevaninezhad, M.C. Beard, C. Papadopoulos, TE Darcie, "Single-walled carbon nanotubes as base materials for THz photoconductive switching: a theoretical study from input power to output THz emission", *Optics Express*, 19, 15077, **2011**, doi:10.1364/OE.19.015077
8. M.C. Beard, "Multiple Exciton Generation in Semiconductor Quantum Dots", *JPCL*, 2(11), 1282, **2011**, doi: 10.1021/jz200166y
9. M.T. Trinh, L. Polak, J.M. Schins, A.J. Houtepen, R. Vaxenburg, G.I. Maikov, G. Grinbom, A. G. Midgett, J.M. Luther, M.C. Beard, A.J. Nozik, M. Bonn, E. Lifshitz, and L.D.A. Siebbeles, "Anomalous Independence of Multiple Exciton Generation on Different Group IV-VI Quantum Dot Architectures", *Nano. Lett.*, 11, 1623, **2011**, doi: 10.1021/nl200014g
10. H.E. Chappell, B.K. Hughes, M.C. Beard, A.J. Nozik, and J.C. Johnson, "Emission Quenching in PbSe Quantum Dot Arrays by Short-Term Air Exposure", *JPCL*, 2, 889, **2011**, doi: 10.1021/jz2001979
11. A.J. Nozik, M.C. Beard, J.M. Luther, M. Law, R.J. Ellingson, J.C. Johnson, "Semiconductor Quantum Dots and Quantum Dot Arrays and Applications of Multiple Exciton Generation to Third-Generation Photovoltaic Solar Cells", *Chemical Reviews*, 110, 6873, **2010**, doi: 10.1021/cr900289f

12. A.G. Midgett, H.W. Hillhouse, B.K. Hughes, A.J. Nozik, M.C. Beard, “Flowing versus Static conditions for measuring multiple exciton generation in PbSe quantum dots”, *JPCA*, 114 (11),6873, **2010**
13. O.E. Semonin, J.C. Johnson, J.M. Luther, A.G. Midgett, A.J. Nozik, M.C. Beard, “Absolute photoluminescence quantum yields of IR-26 Dye, PbS, and PbSe quantum dots”, *JPCL*, 1, 2445, 2010
14. M.C. Beard, A.G. Midgett, M.C. Hanna, J.M. Luther, B.K. Hughes, A.J. Nozik, “Comparing Multiple Exciton generation in Quantum Dots to impact ionization in Bulk Semiconductors: Implications for Enhancement of Solar Energy Conversion”, *Nano Letters*, 10, 8, 3019, **2010**, doi: 10.1021/nl101490z

Modulation of Light Harvesting Properties of Semiconductor Quantum Dot Assemblies

Prashant V. Kamat
Radiation Laboratory, Department of Chemistry and Biochemistry
University of Notre Dame
Notre Dame, IN 46556

Using semiconductor nanocrystals as the building blocks we have succeeded in improving the photon capture and achieving better charge separation in light energy harvesting assemblies. The major focus of our research effort is to elucidate the photoinduced electron transfer processes in quantum dot sensitized solar cells (QDSC) and identify strategies to overcome the limitations of various interfacial electron transfer processes.

Electron transfer from quantum dots to metal oxide nanoparticles A comprehensive examination of electron transfer at QD-metal oxide junctions has been carried out using a series of CdSe quantum dot donors (sizes 2.8, 3.3, 4.0, and 4.2 nm) and metal oxide nanoparticle acceptors (SnO₂, TiO₂, and ZnO). Utilizing ultrafast transient absorption spectroscopy, we measured electron transfer rates from four different sizes of CdSe quantum dots to three unique metal oxide species. Apparent electron transfer rate constants which ranged from $1.9 \times 10^{10} \text{ s}^{-1}$ to $4.6 \times 10^{11} \text{ s}^{-1}$ showed strong dependence on system free energy, exhibiting a sharp rise at small driving forces followed by a modest rise further away from the characteristic reorganization energy (Figure 1). The observed trend mimics the predicted behavior of electron transfer from a single quantum state to a continuum of electron accepting states, such as those present in the conduction band of a metal oxide nanoparticle, and agreed with Marcus theory. We have also probed the effect of linker molecule binding on the electron transfer rate. Since the mechanism of electron transfer in the case of CdSe QDs on TiO₂ nanoparticles involves tunneling through the QD-metal oxide junction, we observe the transfer rate in the case of directly adsorbed QDs to be greater than that of those attached with a linker molecule.

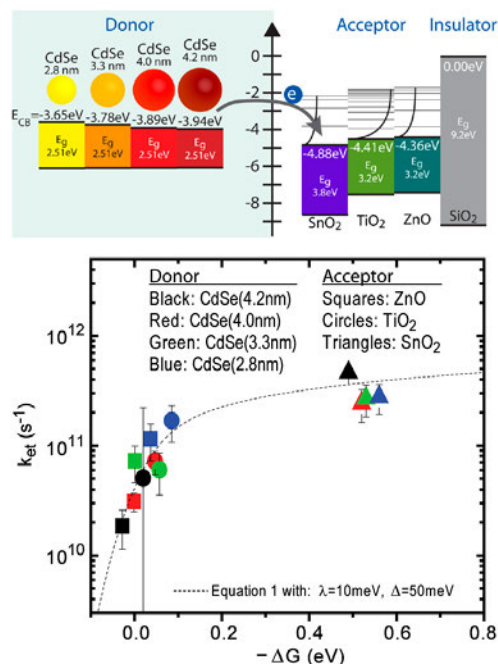


Figure 1 Relative electronic energy differences between CdSe donating species and MO accepting species (top) and Global plot of all CdSe (donor) to MO (acceptor) rate constants. Electron transfer data and trace fitted to Marcus Many-State model. (From reference 17)

Photoinduced charge transfer processes in semiconductor quantum dots coupled with IR dyes Energy and electron transfer processes in quantum dot-dye-metal oxide junctions are being investigated for efficient conversion of solar energy with a good spectral match between sensitizer absorption and incident solar radiation. Semiconductor quantum dots such as CdS and CdSe absorb only in the visible. In order to maximize the absorption range of incident photons we have coupled the short-band gap semiconductor with an red-infrared absorbing dye molecule. For example, CdS nanoparticles anchored on mesoscopic TiO₂ films obtained by successive

ionic layer adsorption and reaction (SILAR) exhibit absorption below 500 nm with a net power conversion efficiency of $\sim 1\%$ when employed as a photoanode in QDSC. When linked to TiO_2 through a SQSH linker dye, CdSe QDs participate in an energy transfer process (Figure 2). The hybrid solar cells prepared with squaraine dye as a linker between CdSe QD and TiO_2 exhibited power conversion efficiency of 3.65% and good stability during illumination with global AM 1.5 solar illumination. The synergy of combining semiconductor quantum dots and NIR absorbing dyes provides new opportunities to harvest photons from different regions of the solar spectrum.

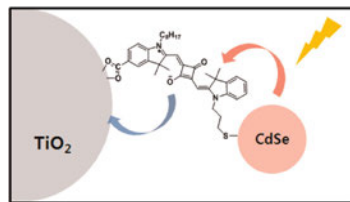


Figure 2. Linking CdSe QD to TiO_2 with a squaraine dye linker enables synchronized energy and electron transfer processes in QDSC. (From reference 33)

Tandem layered quantum dot solar cells One of the possibilities to engineer the light harvesting features over a broader region and utilize the photons more effectively is to develop a tandem layers of semiconductor QDs such that the absorption of photons within the film is carried out in a systematic and gradient fashion.

We have now succeeded in assembling highly luminescent 4.5 nm CdSeS quantum dots with a gradient structure within the mesoscopic film of TiO_2 . The electrophoretic deposition of these QDs enabled us to design tandem layers of CdSeS of varying bandgap within the mesoscopic TiO_2 film. The photoactive anode exhibited an increased power conversion efficiency of 3.2 - 3.0% in a two- and three-layered tandem QDSC as compared to 1.97% - 2.81% with single-layered CdSeS (Fig. 3). The alignment of band energies between different layers of quantum dots will facilitate an energy and/or electron transfer cascade from larger bandgap QDs to smaller bandgap QDs, thus facilitating the accumulation of electrons in the later. For the first time we were able to establish the synergy of ordered assembly of quantum dots within the mesoscopic TiO_2 film.

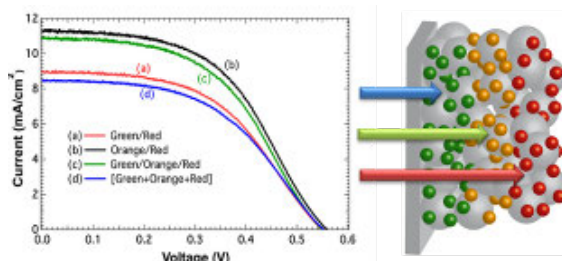


Figure 3 J - V characteristics of QDSCs with working electrodes containing (a) green, (b) orange, and (c) red CdSeS QDs under AM 1.5 irradiation. A $\text{Cu}_2\text{S}/\text{RGO}$ composite counter electrode was used, and aqueous 2 M $\text{Na}_2\text{S}/2$ M S served as the electrolyte. (From reference 43)

Future Work will focus on tuning the optical response of ternary metal chalcogenides (CdSeS and CuInS_2) and elucidate the excited state dynamics and the electron transfer in heterogeneous assemblies. We will investigate the energy gap dependence of electron transfer rate between the ternary chalcogenide QDs and the semiconductor oxide. Of particular interest will be the surface modification of CdSeS and CuInS_2 , specifically the role of ligands in modifying the excited state dynamics and facilitating charge transfer across the interface. The mechanism of energy and electron transfer between two different size semiconductor QDs assembled in Tandem layer will be elucidated. A better understanding of photon management of tandem layer QD solar cell will enable us to capture the incident visible-infrared photons in an efficient way.

DOE Sponsored Publications 2010-2013

1. Zhang, J.; Bang, J. H.; Tang, C.; Kamat, P. V. Tailored TiO₂-SrTiO₃ Heterostructure Nano tube Arrays for Improved Photoelectrochemical Performance. *ACS Nano* **2010**, *4*, 387-395.
2. Ohtani, M.; Kamat, P. V.; Fukuzumi, S. Supramolecular Donor-Acceptor Assemblies Composed of Carbon Nanodiamond and Porphyrin for Photoinduced Electron Transfer and Photocurrent Generation. *J. Mater. Chem.* **2010**, *20*, 582-587.
3. Lightcap, I. V.; Kosel, T. H.; Kamat, P. V. Anchoring Semiconductor and Metal Nanoparticles on a 2-Dimensional Catalyst Mat. Storing and Shuttling Electrons with Reduced Graphene Oxide. *Nano Lett.* **2010**, *10*, 577-583. (*Perspective article*)
4. Yu, Y.; Kamat, P. V.; Kuno, M. A CdSe Nanowire/Quantum Dot Hybrid Architecture for Improving Solar Cell Performance. *Adv. Funct. Mater.* **2010**, *20*, 1464-1472.
5. Chakrapani, V.; Tvrdy, K.; Kamat, P. V. Modulation of Electron Injection in CdSe-TiO₂ System through Medium Alkalinity. *J. Am. Chem. Soc.* **2010**, *132*, 1228-1229.
6. Kamat, P. V. Graphene based Nanoarchitectures. Anchoring Semiconductor and Metal Nanoparticles on a 2-Dimensional Carbon Support. *J. Phys. Chem. Lett.* **2010**, *1*, 520-527.
7. Bang, J. H.; Kamat, P. V. Solar Cell by Design. Photoelectrochemistry of TiO₂ Nanorod Arrays Decorated with CdSe. *Adv. Funct. Mater.* **2010**, *20*, 1970-1976.
8. Wojcik, A.; Nicolaescu, R.; Kamat, P. V.; Patil, S. Photochemistry of Far Red Responsive Tetrahydroquinoxaline-Based Squaraine Dyes. *J. Phys. Chem. A* **2010**, *114*, 2744-2750.
9. Baker, D. R.; Kamat, P. V. Tuning the Emission of CdSe Quantum Dots by Controlled Trap Enhancement. *Langmuir* **2010**, *26*, 11272-11276.
10. Vinodgopal, K.; Neppolian, B.; Lightcap, I. V.; Grieser, F.; Ashokkumar, M.; Kamat, P. V. Sonolytic Design of Graphene Au Nanocomposites. Simultaneous and Sequential Reduction of Graphene Oxide and Au(III). *J. Phys. Chem. Lett.* **2010**, *1*, 1987-1993.
11. Ng, Y. H.; Lightcap, I. V.; Goodwin, K.; Matsumura, M.; Kamat, P. V. To What Extent Do Graphene Scaffolds Improve the Photovoltaic and Photocatalytic Response of TiO₂ Nanostructured Films? *J. Phys. Chem. Lett.* **2010**, *1*, 2222-2227.
12. Kamat, P. V.; Tvrdy, K.; Baker, D. R.; Radich, J. G. Beyond Photovoltaics: Semiconductor Nanoarchitectures for Liquid Junction Solar Cells. *Chem. Rev.* **2010**, *110*, 6664-6688. (*Review article*)
13. Kamat, P. V. Capturing Hot Electrons. *Nature Chemistry* **2010**, *2*, 809-810. (*Commentary*)
14. Wojcik, A.; Kamat, P. V. Reduced Graphene Oxide and Porphyrin. An Interactive Affair in 2-D. *ACS Nano* **2010**, *4*, 6697-6706.
15. Harris, C.; Kamat, P. V. Photocatalytic Events of CdSe Quantum Dots in Confined Media. Electrode Behavior of Coupled Platinum Nanoparticles. *ACS Nano* **2010**, *4*, 7321-7330.
16. Gassensmith, J. J.; Matthys, S.; Wojcik, A.; Kamat, P. V.; Smith, B. D. Squaraine Rotaxane as Optical Chloride Sensor. *Chemistry, European J.* **2010**, *16*, 2916-2921.
17. Tvrdy, K.; Frantszov, P.; Kamat, P. V. Photoinduced Electron Transfer from Semiconductor Quantum Dots to Metal Oxide Nanoparticles. *Proc. Nat. Acad. Sci. USA* **2011**, *108*, 29-34.
18. Kamat, P. V. Graphene-based Nanoassemblies for Energy Conversion. *J. Phys. Chem. Lett.* **2011**, *2*, 242-251. (*Perspective article*)

19. Krishnamurthy, S.; Lightcap, I. V.; Kamat, P. V. Electron Transfer between Methyl Viologen Radicals and Graphene Oxide: Reduction, Electron Storage and Discharge *J. Photochem. Photobiol. A: Chem.* **2011**, *221*, 214-219.
20. Pernik, D.; Tvrđy, K.; Radich, J. G.; Kamat, P. V. Tracking the Adsorption and Electron Injection Rates of CdSe Quantum Dots on TiO₂: Linked Versus Direct Attachment. *J. Phys. Chem. C* **2011**, *115*, 13511–13519.
21. Chakrapani, V.; Baker, D.; Kamat, P. V. Understanding the Role of the Sulfide Redox Couple (S²⁻/S_n²⁻) in Quantum Dot Sensitized Solar Cells. *J. Am. Chem. Soc.* **2011**, *133*, 9607–9615.
22. Hayashi, H.; Lightcap, I. V.; Tsujimoto, M.; Takano, M.; Umeyama, T.; Kamat, P. V.; Imahori, H. Electron Transfer Cascade by Organic/Inorganic Ternary Composites of Porphyrin, Zinc Oxide Nanoparticles, and Reduced Graphene Oxide on a Tin Oxide Electrode that Exhibits Efficient Photocurrent Generation. *J. Am. Chem. Soc.* **2011**, *133*, 7684–7687.
23. Bang, J. H.; Kamat, P. V. CdSe Quantum Dot-Fullerene Hybrid Nanocomposite for Solar Energy Conversion: Electron Transfer and Photoelectrochemistry. *ACS Nano* **2011**, *5*, 9421-9427.
24. Murphy, S.; Huang, L.; Kamat, P. V. Charge-Transfer Complexation and Excited State Interactions in Porphyrin-Silver Nanoparticle Hybrid Nanostructures". *J. Phys. Chem. C* **2011**, *115*, 22761–22769.
25. Takai, A.; Kamat, P. V. Capture, Store and Discharge. Shuttling Photogenerated Electrons Across TiO₂-Silver Interface. *ACS Nano* **2011**, *4*, 7369–7376.
26. Meekins, B. H.; Kamat, P. V. Role of Water Oxidation Catalyst, IrO₂ in Shuttling Photogenerated Holes Across TiO₂ Interface. *J. Phys. Chem. Lett.* **2011**, *2*, 2304-2310.
27. Radich, J. G.; Dwyer, R.; Kamat, P. V. Cu₂S -Reduced Graphene Oxide Composite for High Efficiency Quantum Dot Solar Cells . Overcoming the Redox Limitations of S²⁻/S_n²⁻ at the Counter Electrode. *J. Phys. Chem. Lett.* **2011**, *2*, 2453–2460.
28. Choi, H.; Nicolaescu, R.; Paek, S.; Ko, J.; Kamat, P. V. Supersensitization of CdS Quantum Dots with NIR Organic Dye: Towards the Design of Panchromatic Hybrid-Sensitized Solar Cells. *ACS Nano* **2011**, *5*, 9238–9245.
29. Genovese, M. P.; Lightcap, I. V.; Kamat, P. V. Sun-Believable Solar Paint. A Transformative One-Step Approach for Designing Nanocrystalline Solar Cells. *ACS Nano* **2012**, *6*, 865–872.
30. Santra, P. K.; Kamat, P. V. Mn-Doped Quantum Dot Sensitized Solar Cells. A Strategy to Boost Efficiency over 5% *J. Am. Chem. Soc.* **2012**, *134*, 2508–2511.
31. Kamat, P. V. Manipulation of Charge Transfer Across Semiconductor Interface. A Criterion that Cannot be Ignored in Photocatalyst Design. *J. Phys. Chem. Lett.* **2012**, *3*, 663-672. (Perspective article)
32. Kamat, P. V. Boosting the Efficiency of Quantum Dot Sensitized Solar Cells Through Modulation of Interfacial Charge Transfer. *Acc. Chem. Res.* **2012**, *45*, 1906–1915. (Review article)

33. Choi, H.; Santra, P. K.; Kamat, P. V. Synchronized Energy and Electron Transfer Processes in Covalently Linked CdSe-Squaraine Dye-TiO₂ Light Harvesting Assembly. *ACS Nano* **2012**, *6*, 5718–5726.
34. Lightcap, I. V.; Kamat, P. V. Fortification of CdSe Quantum Dots with Graphene Oxide. Excited State Interactions and Light Energy Conversion. *J. Am. Chem. Soc.* **2012**, *134*, 7109–7116.
35. Lightcap, I. V.; Murphy, S.; Schumer, T.; Kamat, P. V. Electron Hopping Through Single-to-Few Layer Graphene Oxide Films. Photocatalytically Activated Metal Nanoparticle Deposition. *J. Phys. Chem. Lett.* **2012**, *3*, 1453–1458.
36. Choi, H.; Chena, W. T.; Kamat, P. V. Know Thy Nano Neighbor. Plasmonic *versus* Electron Charging Effects of Gold Nanoparticles in Dye Sensitized Solar Cells. *ACS Nano* **2012**, *6*, 4418–4427.
37. Hines, D. A.; Becker, M. A.; Kamat, P. V. Photoinduced Surface Oxidation and Its Effect on the Exciton Dynamics of CdSe Quantum Dots. *J. Phys. Chem. C* **2012**, *116*, 13452–13457.
38. Vinodgopal, K.; Neppolian, B.; Salleh, N.; Lightcap, I. V.; Grieser, F.; Ashokkumar, M.; Ding, T. T.; Kamat, P. V. Dual-Frequency Ultrasound for Designing Two Dimensional Catalyst Surface: Reduced Graphene Oxide-Pt Composite. *Coll. Surf. A* **2012**, *409*, 81–87.
39. Chen, W.-T.; Hsu, Y.-J.; Kamat, P. V. Realizing Visible Photoactivity of Metal Nanoparticles. Excited State Behavior and Electron Transfer Properties of Silver (Ag₈) Clusters *J. Phys. Chem. Lett.* **2012**, *3*, 2493–2499.
40. Yokomizo, Y.; Krishnamurthy, S.; Kamat, P. V. Photoinduced Electron Charge and Discharge of Graphene-ZnO Nanoparticle Assembly. *Catal. Today* **2013**, *199*, 36–41.
41. Lightcap, I. V.; Kamat, P. V. Graphitic Design: Prospects of Graphene-Based Nanocomposites for Solar Energy Conversion, Storage, and Sensing. *Acc. Chem. Res.* **2013**, DOI:10.1021/ar300248f. (*Review article*)
42. Krishnamurthy, S.; Kamat, P. V. Galvanic Exchange on Reduced Graphene Oxide. Designing a Multifunctional Two-Dimensional Catalyst Assembly. *J. Phys. Chem. C* **2013**, *117*, 571–577.
43. Santra, P.; Kamat, P. V. Tandem Layered Quantum Dot Solar Cells. Tuning the Photovoltaic Response with Luminescent Ternary Cadmium Chalcogenides. *J. Am. Chem. Soc.* **2013**, *135*, 877–885.
44. Murphy, S.; Huang, L.; Kamat, P. V. Reduced Graphene Oxide-Silver Nanoparticle Composite as an Active SERS Material. *J. Phys. Chem. C* **2013**, *117*, 4740–4747.
45. Choi, H.; Kuno, M.; Hartland, G. V.; Kamat, P. V. CdSe Nanowire Solar Cells using a Carbazole as Surface Modifier. *J. Mater. Chem. A* **2013**, *3*, DOI: 10.1039/C3TA10387K.
46. Kamat, P. V. Quantum Dot Solar Cells. *The Next Big Thing in Photovoltaics*. *J. Phys. Chem. Lett.* **2013**, *4*, 908–918. (*Perspective article*)
47. Santra, P. K.; Nair, P. V.; Thomas, K. G.; Kamat, P. V. CuInS₂ Sensitized Quantum Dot Solar Cell. Electrophoretic Deposition, Excited State Dynamics and Photovoltaic Performance. *J. Phys. Chem. Lett.* **2013**, *4*, 722–729.

Session V

Mostly Carbon

Interfacial Exciton Dissociation in Organic Heterojunction Blends with Highly Enriched Semiconducting Single-Walled Carbon Nanotubes

Jeff Blackburn, Kevin Mistry, Josh Holt, Andrew Ferguson, Nikos Kopidakis, Dominick Bindl, Michael Arnold, Garry Rumbles

Chemical and Materials Science Center, National Renewable Energy Laboratory - Golden, CO, 80401.

Single-walled carbon nanotubes (SWCNTs) are dimensionally confined quantum wires that have the potential to impact a variety of solar photochemical applications. The ability to incorporate SWCNTs into solar conversion schemes requires an understanding of how SWCNT electronic structure affects excited state charge transfer.

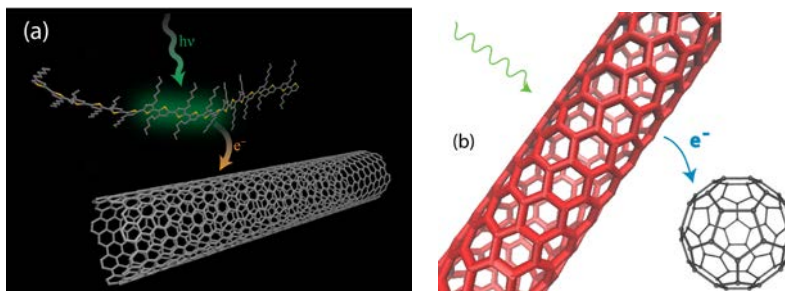


Figure 1. Schematics of SWCNT solar conversion interfaces. (a) SWCNTs accept electrons from photoexcited polymers. (b) Photoexcited SWCNT excitons are dissociated at SWCNT:C₆₀ interface.

One important consideration for SWCNT heterojunction blends is the high degree of electronic poly-dispersity present in as-synthesized SWCNT samples. This poly-dispersity implies the presence of potentially deleterious SWCNT species (zero-gap metallic SWCNTs), as well as a wide variation in the diameter-dependent absorption energies, electron affinities, and ionization potentials for the semiconducting species present. To surmount this poly-dispersity problem, there is a clear need for efficient methods of separating SWCNTs by electronic structure and diameter, and the characterization of exciton dissociation at interfaces formed with the desired SWCNT species.

This presentation focuses on our recent studies aimed at rationally constructing and characterizing SWCNT interfaces with the correct electronic structure to promote photo-induced exciton dissociation and long-lived charge separation (Figure 1). I will first discuss blends of SWCNTs with the semiconducting polymer poly(3-hexylthiophene) (P3HT), where SWCNTs act as electron acceptors for the photoexcited P3HT (Figure 1a). Time-resolved microwave conductivity (TRMC) was used to study the dissociation of excitons at the interface between P3HT and SWCNTs. Excitation of the polymer at 2.3 eV results in a dramatic increase in charge carrier generation relative to a film of P3HT with no SWCNTs, along with a significant lengthening of the lifetime of free charges relative to charges created in isolated P3HT (Figure 2). These observations indicate efficient exciton dissociation at the

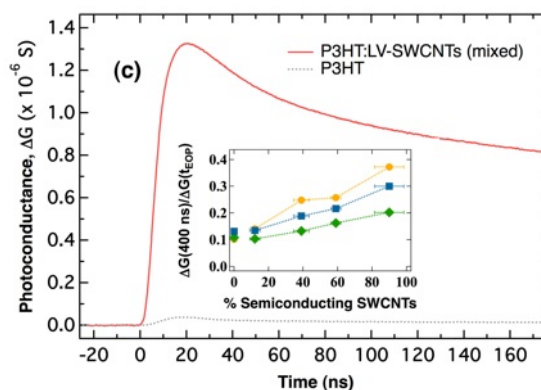


Figure 2. Microwave absorbance transients following 2.3 eV photoexcitation of P3HT, either with or without SWCNTs. Inset shows relative measure of the percentage of long-lived carriers as a function of the percentage of s-SWNT content. The three lines represent different photon fluences, ranging from low (squares) to high (triangles).

SWCNT:P3HT interface. We have also studied blends of P3HT with SWCNTs separated by electronic structure into type-pure metallic and semiconducting SWCNTs. We find that both the yield and lifetime of the photo-induced charge-separated state is dramatically increased as the percentage of semiconducting SWCNTs within the blend is increased (Figure 2, inset). This is the first experimental demonstration of the prevailing theoretical hypothesis that metallic SWCNTs should act as efficient recombination centers in such SWCNT blends.

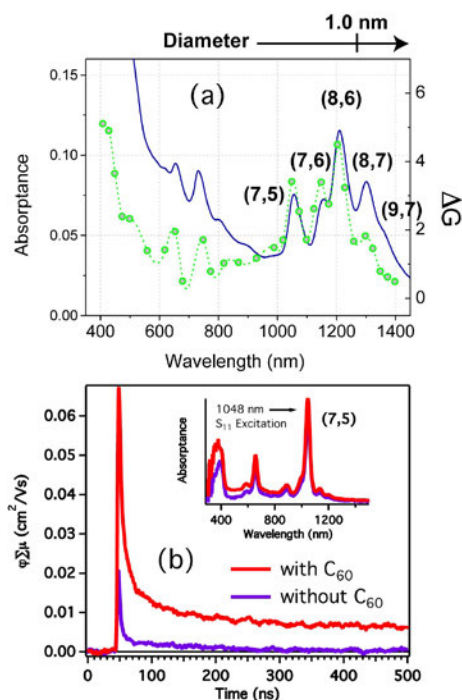


Figure 3. (a) Comparison of absorbance spectrum (blue) to TRMC action spectrum (green) for a SWCNT:C60 blend containing five semiconducting SWCNT species. (b) Microwave absorbance transients for SWCNT films consisting of one dominant SWCNT species, the (7,5) SWCNT, with or without C₆₀. Absorbance spectrum shown in inset.

microseconds. I will then discuss samples with only one dominant small-diameter semiconducting species (Figure 3b), which allow us to explore the role of energetic dispersion on exciton transport/dissociation, and charge transport/recombination following exciton dissociation.

Our future plans include ongoing efforts aimed at quantitatively understanding the free charge carrier yield and mobility. We are concerned with several important effects: SWCNT length, diameter, diameter distribution, and degree of communication (isolated SWCNTs versus coupled films). One method by which we plan to study these effects is the injection of known amounts of dark carriers into SWCNTs, so that electron and hole mobilities can be obtained at known carrier densities. Finally, we plan to couple SWCNT films containing one semiconducting species to acceptors with tunable electron affinities, so that exciton dissociation yield can be measured as a function of well-characterized energetic driving forces.

In the second discussion, I will examine exciton dissociation in systems where the photoexcited SWCNTs act as the electron donors. In these systems, photoexcited SWCNT excitons are dissociated at the interface between the SWCNTs and fullerenes (Figure 1b). Polyfluorene (PFO) polymers are used to selectively extract semiconducting SWCNTs, so that metallic SWCNTs are quantitatively excluded from the SWCNT:fullerene blends. By varying the combination of the PFO polymer and the SWCNT starting material, we can achieve a wide variation of semiconducting SWCNT average diameter and diameter distribution, allowing us to produce blends with one dominant semiconducting SWCNT species or blends with several semiconducting species. This variation allows us to explore the influence of energetic dispersion on exciton transport to the interface, exciton dissociation efficiency, and interfacial charge recombination.

In samples with several different semiconducting SWCNT species, we observe an exciton dissociation yield that depends on SWCNT diameter. Above a SWCNT diameter of ~ 1.0 nm, the exciton dissociation yield decreases significantly, in agreement with previous EQE measurements on devices made with the same blends (Figure 3a). This drop-off in exciton dissociation yield indicates a low energetic driving force for electron transfer from the larger diameter SWCNTs to C₆₀. The lifetime of free charges produced by exciton dissociation of photoexcited small-diameter SWCNTs is on the order of

DOE Sponsored Solar Photochemistry Publications 2010 – 2013:

1. Arnold, M.S., Blackburn, J.L., Crochet, J.J., Doorn, S.K., Duque, J.G., Mohite, A., Telg, H. Recent Developments in the Photophysics of Single-Wall Carbon Nanotubes for Active and Passive Material Elements in Thin Film Photovoltaics. *Energy Environ. Sci.*, **2013**, In Press.
2. Mistry, K.S., Larsen, B.A., Blackburn, J.L. High-Yield Dispersions of Large-Diameter Semiconducting Single-Walled Carbon Nanotubes with Tunable Narrow Chirality Distributions. *ACS Nano*, **2013**, *7*, 2231.
3. Ferguson, A.J., Blackburn, J.L., Kopidakis, N. Fullerenes and Carbon Nanotubes as Acceptor Materials in Organic Photovoltaics. *Materials Letters*, **2012**, *90*, 115.
4. Larsen, B.A., Dheria, P., Heben, M.J., Therein, M., Blackburn, J.L. Solvatochromic Shifts in Single-walled Carbon Nanotube Dispersions with Widely Varying Dielectric Properties. *J. Amer. Chem. Soc.*, **2012**, *134*, 12485.
5. Hughes, B.K., Ruddy, D.A., Blackburn, J.L., Smith, D.K., Bergren, M.R., Nozik, A.J., Johnson, J.C., Beard, M.C. Control of PbSe Quantum Dot Surface Chemistry and Photophysics Using an Alkylselenide Ligand. *ACS Nano*, **2012**, *6*, 5498.
6. Engtrakul, C., Irurzun, V.M., Gjersing, E.L., Holt, J.M., Larsen, B.A., Resasco, D.E., Blackburn, J.L. Unraveling the ^{13}C NMR Chemical Shifts in Single-walled Carbon Nanotubes: Dependence on Diameter and Electronic Structure. *J. Amer. Chem. Soc.*, **2012**, *134*, 4850.
7. Blackburn, J.L., Holt, J.M., Irurzun, V.M., Resasco, D.E., Rumbles, G. Confirmation of K-Momentum Dark Exciton Vibronic Sidebands Using ^{13}C -labeled, Highly Enriched (6,5) Single-walled Carbon Nanotubes. *Nano Letters*, **2012**, *12*, 1398.
8. Fagan, J.A., Huh, J.Y., Simpson, J.R., Blackburn, J.L., Holt, J.M., Larsen, B.A., Hight Walker, A.R. Separation of Empty and Water-Filled Single-Wall Carbon Nanotubes. *ACS Nano*, **2011**, *5*, 3943.
9. Mistry, K., Larsen, B.A., Teeter, G., Bergeson, J., Barnes, T., Blackburn, J.L. n-Type Transparent Conducting Films of Small Molecule and Polymer Amine Doped Single-Walled Carbon Nanotubes. *ACS Nano*, **2011**, *5*, 3714.
10. Blackburn, J.L., Chappell, H., Luther, J.M., Nozik, A.J., Johnson, J.C. Correlation between Photooxidation and the Appearance of Raman Scattering Bands in Lead Chalcogenide Quantum Dots. *J. Phys. Chem. Lett.*, **2011**, *2*, 599.
11. Svedruzic, D., Blackburn, J.L., Tenent, R.C., Rocha, J.R., Vinzant, T.B., Heben, M.J., King, P.W. High Performance Hydrogen Production and Oxidation Electrodes with Hydrogenase on Single-walled Carbon Nanotube Networks with High Metallic Tube Content. *J. Am. Chem. Soc.*, **2011**, *133*, 4299.
12. Holt, J.M., Ferguson, A.J., Kopidakis, N., Rumbles, G., Blackburn, J.L. Prolonging Charge Separation in P3HT Composites Using Highly Enriched Semiconducting SWNTs. *Nano Letters*, **2010**, *10*, 4627.
13. Engtrakul, C., Davis, M.F., Mistry, K., Larsen, B.A., Dillon, A.C., Heben, M.J., Blackburn, J.L. Solid-State ^{13}C NMR Assignment of Carbon Resonances on Metallic and Semiconducting Single-walled Carbon Nanotubes. *J. Am. Chem. Soc.*, **2010**, *132*, 9956.
14. Ferguson, A.J., Blackburn, J.L., Holt, J.M., Kopidakis, N., Tenent, R.C., Barnes, T.M., Heben, M.J., Rumbles, G. Photo-induced Energy and Charge Transfer in P3HT:SWNT Composites. *J. Phys. Chem. Lett.*, **2010**, *1*, 2406.

Ultrafast Optical Microscopy of Multi-scale Energy Flow

Libai Huang

Notre Dame Radiation Laboratory
Notre Dame, IN and 46556

Novel nanoscale structures and materials with unique physical properties are highly promising for applications in the next generation of solar energy conversion devices. The frontier in solar energy conversion utilizing nanoscale materials now lies in learning how to integrate functional entities across multiple length scales to create optimal devices. To address this new frontier, this research program focuses on elucidating multi-scale energy transfer, migration, and dissipation processes with simultaneous femtosecond temporal resolution and nanometer spatial resolution. We have combined/correlated ultrafast spectroscopy with high spatial resolution techniques such as optical microscopy and X-ray crystallography to achieve high-resolution spatial mapping of charge carrier dynamics in solar energy harvesting systems.

Environmental effect on charge and exciton dynamics of low-dimensional nanostructures

We have applied transient absorption microscopy (TAM) to probe environmentally-dependent energy relaxation pathways in single-walled carbon nanotubes and graphene. Figure 1 shows an example of TAM experiments performed on suspended and substrate-supported graphene on SiO₂. We observed that the hot phonon effect occurs at much lower excitation



Figure 1 Correlated AFM and TAM images for suspended graphene at two different delay times. Scale bars: 2 μm

intensity for suspended graphene compared to substrate-supported graphene. These results show the importance of the environment in controlling the properties of graphene. We have successfully demonstrated structure-specific transient absorption imaging of single-walled carbon nanotubes as a way to investigate intrinsic relaxation pathways in these important materials.

We have also initiated an investigation into exciton dynamics in novel 2D atomically thin crystals. Femtosecond transient absorption spectroscopy and microscopy were employed to study exciton dynamics in suspended and Si₃N₄ substrate-supported monolayer and few-layer MoS₂ 2D crystals. Exciton dynamics for the monolayer and few-layer structures were found to be remarkably different from those of the bulk. Fast trapping of excitons by surface trap states was observed in monolayer and few-layer structures, pointing to the importance of controlling surface properties in atomically thin crystals such as MoS₂ in addition to controlling their dimensions.

Morphology dependent charge dynamics in organic photovoltaics Transient absorption microscopy experiments have been performed on thermally annealed poly(3-hexylthiophene) (P3HT) and [6,6]-phenyl-C₆₁-butyric acid methyl ester (PCBM) blends. By directly comparing spatially resolved charge dynamics to ensemble dynamics, the results summarized in Figure 2 demonstrate that the apparent lifetimes obtained by ensemble measurements can be misleading

due to averaging over microscopically disparate areas. In these proof-of-concept experiments the spatial resolution is ~ 400 nm, much larger than the optimal domain size of ~ 20 nm. Near-field TAM with sub-diffraction spatial resolution of ~ 50 nm, approaching optimal domain size, is highly desirable for further investigation on the morphology-dependent charge generation and recombination. Construction of a near-field TAM apparatus is currently underway.

Cofactor-specific function mapping in single photosynthetic reaction center crystals

High-resolution mapping of cofactor-specific photo-chemistry in photosynthetic reaction centers (RCs) from *Rhodobacter sphaeroides* was achieved by polarization selective ultrafast spectroscopy in single crystals at cryogenic temperatures. By exploiting the fixed orientation of cofactors within crystals, we isolated a single transition within the multi-cofactor manifold, and elucidated the site-specific photochemical functions of the cofactors associated with the symmetry-related active A and inactive B branches (Figure 3). Transient spectra associated with the initial excited states were found to involve a set of cofactors that differ depending upon whether the monomeric bacteriochlorophylls, BChl_A, BChl_B, or the special pair bacteriochlorophyll

dimer (P) was chosen for excitation. Proceeding from these initial excited states, characteristic photochemical functions were resolved. These experiments demonstrate the opportunity to resolve the photochemical function of individual cofactors within the multi-cofactor RC complexes using single crystal spectroscopy.

Future direction:

Future research will focus on understanding the interactions between nanostructured functional components to provide guidelines for designing functional materials for efficient energy and charge transport. Further improvement on spatial resolution will be achieved by a near-field geometry using sub-diffraction optical probes.

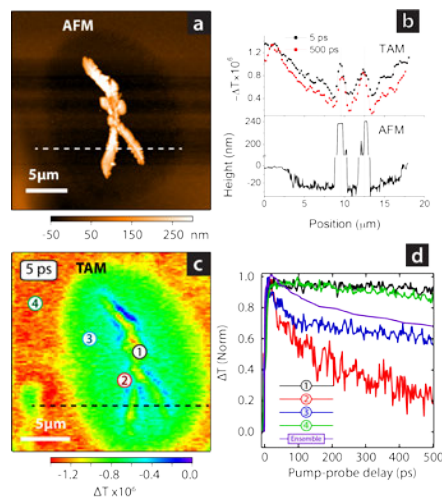


Figure 2 Atomic force microscopy (AFM) height image of a P3HT:PCBM blend (a) and transient absorption microscopy (TAM) image of the same sample area taken at times of 5 ps (c). (b) shows line section of AFM and TAM. (d) shows the decay curves taken with different positions along with the ensemble kinetics. The positions where the decay curves are obtained are labeled in (c).

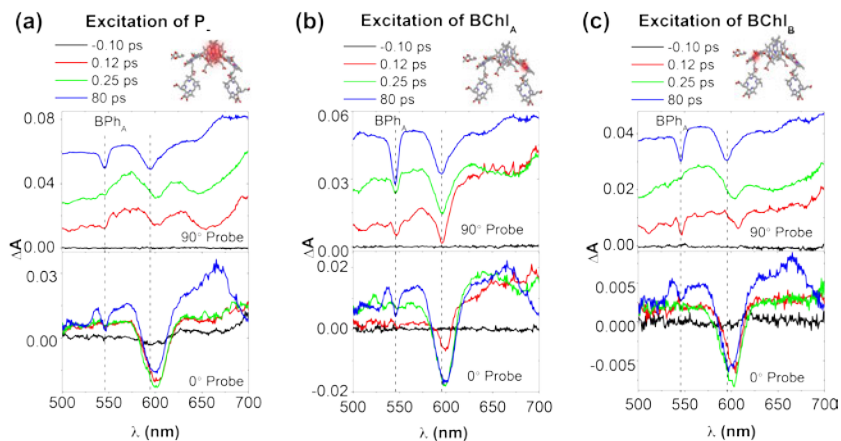


Figure 3 Pump wavelength-dependent patterns of transient optical absorption changes in a single *Rb. Sphaeroides* wild-type crystal at 100K. The pump is adjusted to 900 nm (90°), 790 nm (90°), and 824 nm (0°), in panels a, b, and c, to selectively pump Q_y optical transitions of P., BChl_A and BChl_B, respectively. The top spectra are for probing at 90° with respect to the crystal c axis and the spectra are offset for clarity. The bottom spectra are the spectra for probing at

DOE Sponsored Publications 2010-2013

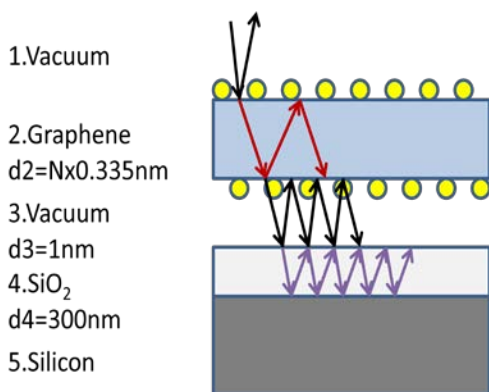
1. Shun Shang Lo, Hongyan Shi, Libai Huang, and Greg Hartland, "Imaging the Extent of Plasmon Excitation in Au Nanowires Using Pump-Probe Microscopy", *Optics Letters*, **38**, 1265, 2013.
2. Sean Murphy, Libai Huang, and Prahsant Kamat, "Reduced Graphene Oxide-Silver Nanoparticle Composite as an Active SERS Material", *Journal of Physical Chemistry C*, **117**, 4740, 2013.
3. Sean Murphy and Libai Huang, "Transient Absorption Microscopy Studies of Energy Relaxation in Graphene Oxide Thin Film", *Journal of Physics: Condensed Matters*, **25**, 144203, 2013.
4. Hongyan Shi, Rusen Yan, Simone Bertolazzi, Bo Gao, Andras Kis, Debdeep Jena, Huili (Grace) Xing, and Libai Huang, "Exciton Dynamics in Suspended Monolayer and Few-Layer MoS₂ 2D Crystals", *ACS Nano*, **7**, 1073, 2013
5. Hongwei Geng, Caleb M. Hill, Shilei Zhu, Daniel A. Clayton, Haiying Liu, Libai Huang, Shanlin Pan, "Photoelectrochemical Properties and Interfacial Charge Transfer Kinetics of BODIPY-sensitized TiO₂ electrode", *RSC Advances*, **3**, 2306-2312, 2013.
6. Hongwei Geng, Caleb M. Hill, Daniel A. Clayton, Shanlin Pan and Libai Huang "Interfacial Charge Transfer Dynamics of Poly (3-hexylthiophene-2, 5-diyl) (P3HT)-Monodisperse TiO₂ Nanoparticle Thin Film", *Phys. Chem. Chem. Phys.*, **15**, 3504-3509, 2013.
7. Libai Huang and Ji-Xin Cheng, "Nonlinear Optical Microscopy of Single Nanostructures", Invited Review, *Annual Review of Materials Research*, in press, 2013.
8. Bo Gao, Gregory V. Hartland, and Libai Huang, "Transient Absorption Microscopy Studies of Individual Chirality Assigned Single-Walled Carbon Nanotubes", *ACS Nano*, **6**, 5083, 2012.
9. Shun Shang Lo, Todd A. Major, Nattasamon Petchsang, Libai Huang, Masaru K. Kuno, and Gregory V. Hartland, "Charge Carrier Trapping and Acoustic Phonon Modes in Single CdTe Nanowires", *ACS Nano*, **6**, 5274, 2012.
10. Chris Wong, Shun S. Lo, and Libai Huang, "Ultrafast Spatial Imaging of Charge Dynamics in Heterogeneous Polymer Blends", *Journal of Physical Chemistry Letters*, **3**, 879, 2012.
11. Libai Huang, Nina Ponomarenko, Gary P. Wiederrecht, David M. Tiede, "Cofactor-specific Photochemical Function Resolved by Ultrafast Spectroscopy in Photosynthetic Reaction Center Crystals", *Proceedings of the National Academy of Sciences*, **109**, 4851, 2012.
12. Lisa J. Nogaj, Libai Huang and Todd D. Krauss, "Semiconductor Carbon Nanotube Optics", in *Handbook of Carbon Nano Materials* (Editors: Francis D'Souza and Karl M. Kadish), World Scientific Series on Carbon Nanoscience, 2012.

13. Sean Murphy, Libai Huang, and Prashant Kamat, “Charge-Transfer Complexation and Excited State Interactions in Porphyrin-Silver Nanoparticle Hybrid Nanostructures”, *Journal of Physical Chemistry C*, **115**, 22761, 2011.
14. Bo Gao, Gregory Hartland, Tian Fang, Michelle Kelly, Debdeep Jena, Huili (Grace) Xing, and Libai Huang, “Studies of Intrinsic Hot Phonon Dynamics in Suspended Graphene by Transient Absorption Microscopy”, *Nano Letters*, **11** 3184, 2011.
15. Iltai Kim, Shana L. Bender, Jasmina Hranisavljevic, Lisa M. Utschig, Libai Huang, Gary P. Wiederrecht, and David M. Tiede, Metal Nanoparticle Plasmon-Enhanced Light-Harvesting in a Photosystem I Thin Film, *Nano Letters*, **11** 3091, 2011.
16. Libai Huang, Bo Gao, Gregory Hartland, Michelle Kelly, HuiLi Xing, “Ultrafast relaxation of hot optical phonons in monolayer and multilayer graphene on different substrates”, *Surface Science*, **605**, 1657, 2011.
17. Claire Deeb, Renaud Bachelot, Jerome Plain, Anne-Laure Baudrion, Safi Jradi, Alexandre Bouhelier, Olivier Soppera, Prashant K. Jain, Libai Huang, Carole Ecoffet, Lavinia Balan and Pascal Royer, “Quantitative Analysis of Localized Surface Plasmons Based on Molecular Probing”, *ACS Nano* **4**, 4579, 2010.
18. Libai Huang, Gregory V. Hartland, Li-Qiang Chu, Luxmi, Randall M. Feenstra, Chuanxin Lian, Kristof Tahy and Huili Xing, “Ultrafast Transient Absorption Microscopy Studies of Carrier Dynamics in Epitaxial Graphene”, *Nano Letters*, **10**, 1308, 2010.

Graphene: Charge Transfer, Spectroscopy and “Hot” Electrons

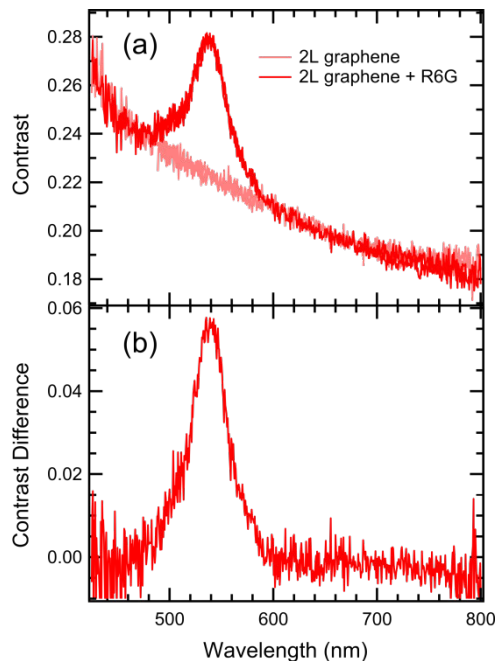
Zheyuan Chen, Elizabeth Thrall, Andrew Crowther, Louis Brus
Chemistry Department, Columbia University, New York, NY, 10027

Our DOE experimental solar energy research focuses on the special electronic and optical properties of graphene. Graphene makes an excellent substrate for current collection in nanostructured photovoltaic designs. Graphene is only one atom thick, yet is extremely durable as it has strongest chemical bonding of any substance. Graphene is also almost optically transparent, and can be used as a solar cell window. It has no intrinsic surface states, and thus current is efficiently transported over long distances. Progress in graphene synthesis indicates that there will soon be practical methods for making large pieces of graphene for devices. We describe our efforts to understand exactly what happens to both ground state and electronically excited molecules and Qdots near graphene. We also describe how molecular adsorption on graphene can substantially shift the Fermi level, allowing such modified graphenes to act as both anodes and cathodes. We describe how Br₂ molecular charge transfer onto graphene varies with surface coverage. We also describe how graphene modifies the local electromagnetic field for incident light; this effect makes graphene an excellent substrate for molecular Raman Spectroscopy. Finally we describe how strong electron correlation the two-dimensional graphene “pi” system enhances “hot” electron process and multiple exciton generation.



Normally Raman spectra are too weak to allow detection of a monolayer. We show through accurate Fresnel calculations that a multilayer graphene film acts internally as a modest optical cavity for both laser and Raman light; for example G band Raman light generated inside graphene has a 36% back reflection probability at the graphene:air interface for normal incidence. An additional reason we can detect Raman signals from adsorbed species with high sensitivity is that the graphene quenches any interfering luminescence.

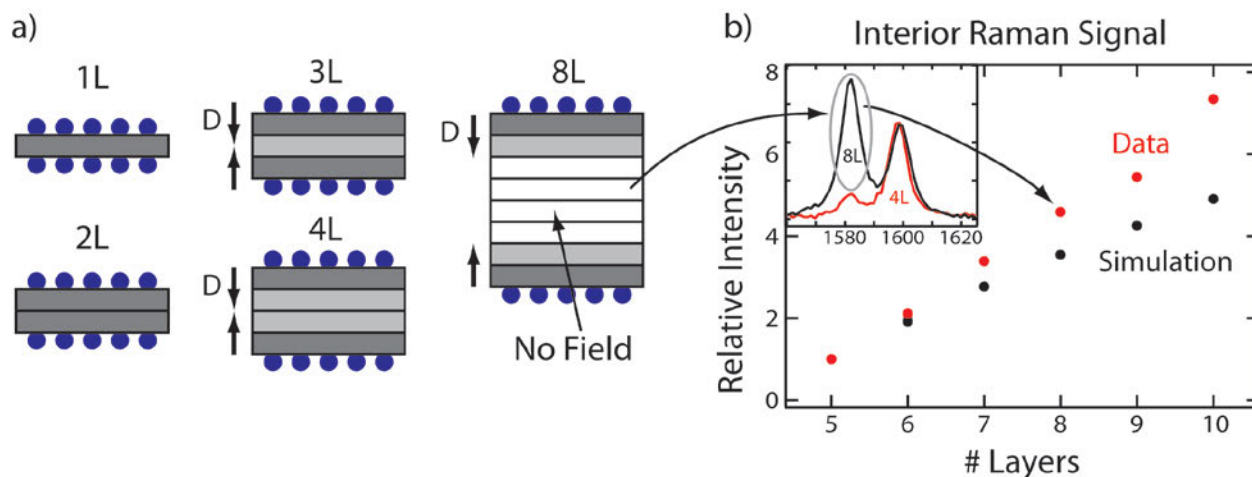
These ideas are further developed in a study of the question of possible Surface Enhanced Raman spectroscopy from molecular Charge Transfer onto Graphene substrates. In order to carefully investigate the question of possible chemical SERS, we studied Rhodamine 6G dye (R6G) on graphene, as R6G is the standard, well characterized molecule for high Raman cross section SERS with Ag particles. By comparing the optical contrast visible spectrum, and the Raman spectrum, we were able to determine the absolute Raman cross section for R6G on the graphene surface. On the next page we show the contrast spectrum, with in (a) shows the strong visible R6G absorption on top of the broad graphene continuum absorption. (b) shows the



subtracted R6G spectrum. We find that the R6G section is perhaps a factor of 3 less on the graphene surface, apparently because the R6G absorption is red-shifted away from the laser line. In this system there is no evidence for field enhancement or chemical SERS. Nevertheless, the R6G Raman shows high signal to noise, as interfering dye luminescence, present for example in solution, is strongly quenched by the metallic graphene. In addition, luminescence from the graphene itself is negligible despite 2% optical absorption of the laser. As a net result, graphene makes an excellent substrate for Raman scattering by adsorbed molecular species.

We also use resonance Raman and optical reflection contrast methods to study charge transfer in 1-10 layer (1L – 10L) thick graphene samples on which strongly electronegative NO_2 has been adsorbed. Electrons transfer from the graphene to NO_2 , leaving the

graphene layers doped with mobile delocalized holes. Raman and optical contrast spectra provide independent, self-consistent measures of the hole density and distribution as a function of the number of layers (N). As the doping induced Fermi level shift E_F reaches half the laser photon energy, an intensity resonance in the graphene G mode Raman intensity is observed. We observe a decrease of graphene optical band-to-band absorption in the near-IR that is due to hole doping. Highly doped samples are more transparent, and they are expected to have high metallic conductivity. In thicker samples holes are effectively confined near the surface as shown below; the interior graphene layers show an essentially pristine Raman signal. In these multilayer samples, recent theory suggests that a small band gap opens near the surface due to asymmetric doping. These few layer graphene samples with chemical intercalation and adsorption promise to be a new class of electronic materials.



In this DOE solar energy program I also work closely with R. Friesner on theoretical DFT studies of extra electrons in titanium dioxide nanoparticles, in situations relevant to the Gratzel Cell.

DOE Sponsored Publications 2010-2013

- 1) E. Thrall, A. Crowther, Z. Yu, L. Brus, "R6G on Graphene: High Raman Detection Sensitivity, Yet Decreased Raman Cross-Section", *Nano Letters* (2012), 12, 1571-1577.
- 2) Crowther, A. Ghassaei, N. Jung, L. Brus, "Strong Charge-Transfer Doping of 1 to 10 Layer Graphene by NO₂", *ACS Nano* (2012), 6, 1865-1875.
- 3) Zheyuan Chen, Andrew Crowther, Louis Brus "Adsorption Isotherm and Charge Transfer as a Function of Coverage for Br₂ adsorbed on Graphene", in preparation.
- 4) Jing Zhang, Thomas F. Hughes, Michael Steigerwald, Louis Brus, and Richard A. Friesner "Realistic Cluster Modeling of Electron Transport and Trapping in Solvated TiO₂ Nanoparticles", *J. Am. Chem. Soc.* (2012), 134, pp. 12028-12042.

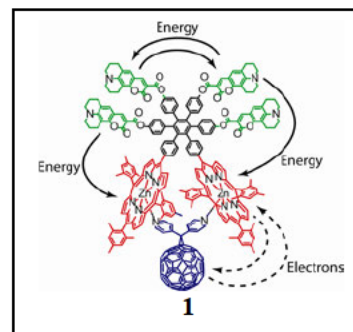
Session VI

Photosynthetic Systems – Artificial and Real

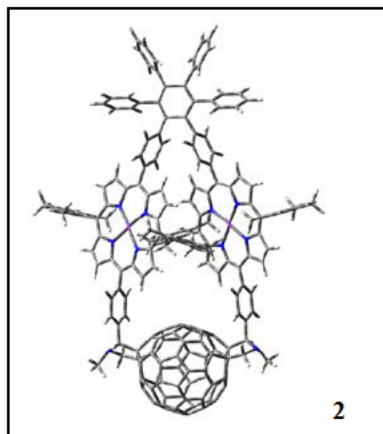
Interchromophore Interactions in Artificial Photosynthesis

Ana L. Moore, Thomas A. Moore, Devens Gust, Vikas Garg, Paul A. Liddell, Yuichi Terazono, Gerdenis Kodis, Smitha Pillai, Antaeres Antoniuk-Pablant, Benjamin D. Sherman, Katie Wong
Department of Chemistry and Biochemistry, Arizona State University, Tempe, AZ 85287

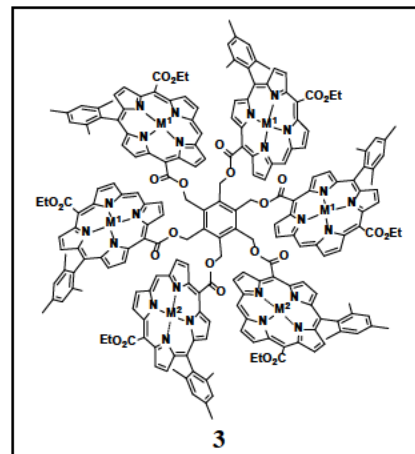
Artificial Photosynthetic Antennas and Reaction Centers. The rates and efficiencies of both singlet energy transfer and electron transfer are functions of the electronic interactions between chromophores, and therefore of interchromophore separation and orientation. As a result, photosynthetic antennas and reaction centers precisely control these parameters, and artificial analogs must do the same. For the case of artificial systems where the chromophores are connected by covalent bonds or via self assembly, a promising approach is to employ a relatively rigid framework to organize the components. In molecule **1**, for example, the rigid hexaphenylbenzene core organizes four coumarin 343 antennas and two zinc porphyrins.¹³ The coumarins, which absorb in spectral regions similar to those where natural carotenoid antennas absorb, transfer singlet excitation to the porphyrins with time constants < 10ps and a quantum yield of essentially 1.0. Self assembly of the fullerene electron acceptor creates an antenna-reaction center. The porphyrin excited states transfer electrons to the fullerene with a time constant of 3 ps to generate a charge-separated state, which has a lifetime of 230 ps.



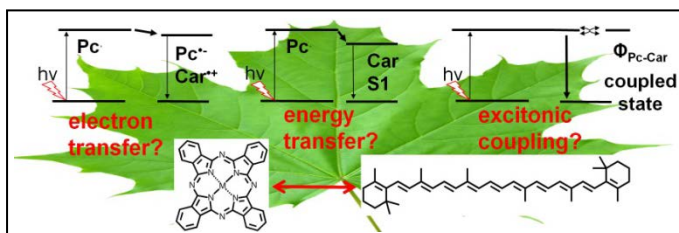
Artificial reaction center **2**, which was synthesized via an unusual cyclization process, is an extremely strained, rigid structure which allows very little motion of the porphyrin donor and fullerene acceptor moieties.⁴ Photoinduced electron transfer in **2** occurs with a time constant of only 1.1 ps, but the lifetime of the charge separated state is 2.7 ns. The ratio of the rates of charge separation to charge recombination is over 2000 as a result of the rigid geometry.



Artificial antenna system **3** features six porphyrins with very short linkages to the central benzene ring, which brings the chromophores into close proximity. The interactions are strong enough to cause significant excitonic coupling between the chromophores, and to lead to extremely rapid singlet energy transfer among the porphyrins. These molecules will be investigated collaboratively for the possibility of quantum coherence during energy transfer. Quantum coherence has been observed in natural photosynthetic antenna systems, and may play a role in achieving the ultrafast energy transfer in some large photosynthetic antennas that is necessary in order to attain high quantum yields.



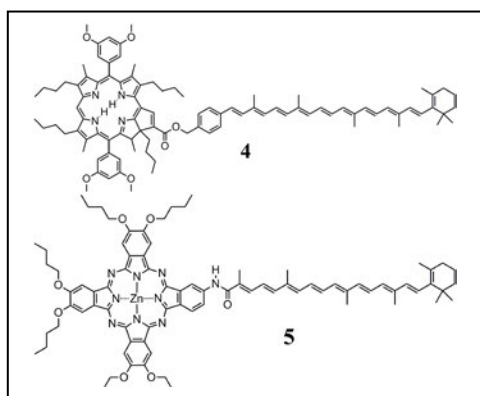
Photoregulation by Carotenoids in Artificial Antennas. Regulatory mechanisms exist in photosynthetic organisms to prevent oxidative damage under high light conditions when non-photochemical metabolic processes cannot keep up with the rates of the photochemical steps of photosynthesis. Such regulatory mechanisms contribute to a large extent to the low yield of photosynthesis; regulatory processes have clear implications for agricultural productivity. It is well accepted that the regulatory mechanisms are located in the antennas of photosynthetic organisms and that carotenoids are involved in the process by quenching the singlet excited state of chlorophylls. Based on accumulated work on various carotenophthalocyanine dyads (Car–Pc), we have identified the three mechanisms shown below whereby tetrapyrrole singlet excited states



can be quenched by carotenoids: (i) Car–Pc electron transfer followed by charge recombination; (ii) ^1Pc to Car S_1 energy transfer and fast internal conversion to the Car ground state; (iii) excitonic coupling between ^1Pc and Car S_1 and ensuing internal conversion to the

ground states of both pigments.^{2,3,5} The dominant mechanism depends upon energy levels, details of the molecular architecture controlling the coupling, and solvent environment. These synthetic systems have provided a deeper understanding of the structural and environmental effects on the interactions between carotenoids and tetrapyrroles and thereby better defined their role in controlling photosynthetic systems.^{7,11,14}

Triplet State Interchromophore Interactions in Photosynthesis and Artificial Photosynthesis. Photoprotection from the deleterious effects of singlet oxygen is ubiquitous in oxygenic photosynthesis. Carotenoid pigments are found in all such photosynthetic membranes where they serve to both quench triplet chlorophylls at a rate sufficient to preclude singlet oxygen sensitization and quench singlet oxygen itself. Carotenoids are found in the chlorophyll binding proteins of both oxygenic and anaerobic organisms, but the triplet – triplet energy transfer times are much faster in the former. Recently, the very fast transfer times found in chlorophyll/carotenoid antenna proteins from oxygenic organisms were found to correlate with



(i) observations in the IR of chlorophyll features in the carotenoid triplet spectrum, (ii) features of the Raman triplet carotenoid, particularly the ν_1 C=C stretch mode, that are significantly shifted to higher frequency than observed for an unperturbed carotenoid triplet, and (iii) a perturbation of the chlorophyll Qy band having the dynamics of the carotenoid triplet species. Changing the coupling and therefore the T-T transfer time in dyads **4** (weaker coupling, slow transfer) and **5** (stronger coupling, fast transfer) led to the observation of similar effects. These data are interpreted as evidence that in oxygenic systems selective photoprotective pressure increased the

coupling to the point that a complete quantum mechanical description of the pigment system must include terms in which the triplet state is to some extent delocalized. Charge transfer interactions provide one possible delocalization mechanism and perhaps result in a CT triplet that is below singlet oxygen and therefore not competent at singlet oxygen sensitization.

DOE Sponsored Publications 2010-2013

1. "A photo- and electrochemically-active porphyrin-fullerene dyad electropolymer," Gervaldo, M.; Liddell, P. A.; Kodis, G.; Brennan, B. J.; Johnson, C. R.; Bridgewater, J. W.; Moore, A. L.; Moore, T. A.; Gust, D. *Photochem. Photobiol. Sci.* **2010**, *9*, 890-900. DOI: 10.1039/c0pp00013b
2. "Two-photon study on the electronic interactions between the first excited singlet states in carotenoid-tetrapyrrole dyads," Liao, P. N. Pillai, S.; Gust, D.; Moore, T. A.; Moore, A. L.; Walla, P. J. *J. Phys. Chem. A* **2011**, *115*, 4082-4091. DOI: 10.1021/jp1122486
3. "Carotenoid photoprotection in artificial photosynthetic antennas," Kloz, M.; Pillai, S.; Kodis, G.; Gust, D.; Moore, T. A.; Moore, A. L.; van Grondelle, R.; Kennis, J. T. M., *J. Am. Chem. Soc.* **2011**, *133*, 7007-7015. DOI: 10.1021/ja1103553
4. "Conformationally constrained macrocyclic diporphyrin-fullerene artificial photosynthetic reaction center," Garg, V.; Kodis, G.; Chachisvilis, M.; Hambourger, M.; Moore, A. L.; Moore, T. A.; Gust, D. *J. Am. Chem. Soc.* **2011**, *133*, 2944-2954. DOI: 10.1021/ja1083078
5. "On the role of excitonic interactions in carotenoid-phthalocyanine dyads and implications for photosynthetic regulation," Liao, P. N.; Pillai, S.; Kloz, M.; Gust, D.; Moore, A. L.; Moore, T. A.; Kennis, J. T. M.; van Grondelle, R.; Walla, P. J. *Photosynth. Res.* **2011**, *111*, 237-243. DOI 10.1007/s11120-011-9687-4.
6. "Oxidative coupling of porphyrins using copper(II) salts," Brennan, B. J.; Kenney, M. J.; Liddell, P. A.; Cherry, B. R.; Li, J.; Moore, A. L.; Moore, T. A.; Gust, D. *Chem. Commun.* **2011**, *47*, 10034-10036. DOI: 10.1039/c1cc13596a
7. "New light-harvesting roles of hot and forbidden carotenoid states in artificial photosynthetic constructs," Kloz, M.; Pillai, S.; Kodis, G.; Gust, D.; Moore, T. A.; Moore, A. L.; van Grondelle, R.; Kennis, J. T. M. *Chem. Sci.*, **2012**, *3*, 2052-2061. DOI: 10.1039/c2sc01023b.
8. "Porphyrins as ITO photosensitizers: Substituents control photo-induced electron transfer direction," Furmansky, Y.; Sasson, H.; Liddell, P.; Gust, D.; Ashkenasy, N.; Visoly-Fisher, I. *J. Mater. Chem.* **2012**, *22*, 20334-20341. DOI: 10.1039/c2jm34118b
9. "Hole mobility in porphyrin- and porphyrin-fullerene electropolymers," Brennan, B. J.; Liddell, P. A.; Moore, T. A.; Moore, A. L.; Gust, D. *J. Phys. Chem. B*, **2013**, *117*, 426-432. DOI: 10.1021/jp3099945
10. "Evolution of reaction center mimics to systems capable of generating solar fuel," Sherman, B. D.; Vaughn, M. D.; Bergkamp, J. J.; Gust, D.; Moore, A. L.; Moore, T. A. *Photosyn. Res.* **2013**, DOI 10.1007/s11120-013-9795-4.
11. "Carotenoids as electron or excited-state energy donors in artificial photosynthesis: an ultrafast investigation of a carotenoporphyrin and a carotenofullerene dyad," S. Pillai, J. Ravensbergen, A. Antoniuk-Pablant, B. D. Sherman, R. van Grondelle, R. N. Frese, T. A. Moore, D. Gust, A. L. Moore and J. T. M. Kennis, *Phys. Chem. Chem. Phys.* **2013** in press.

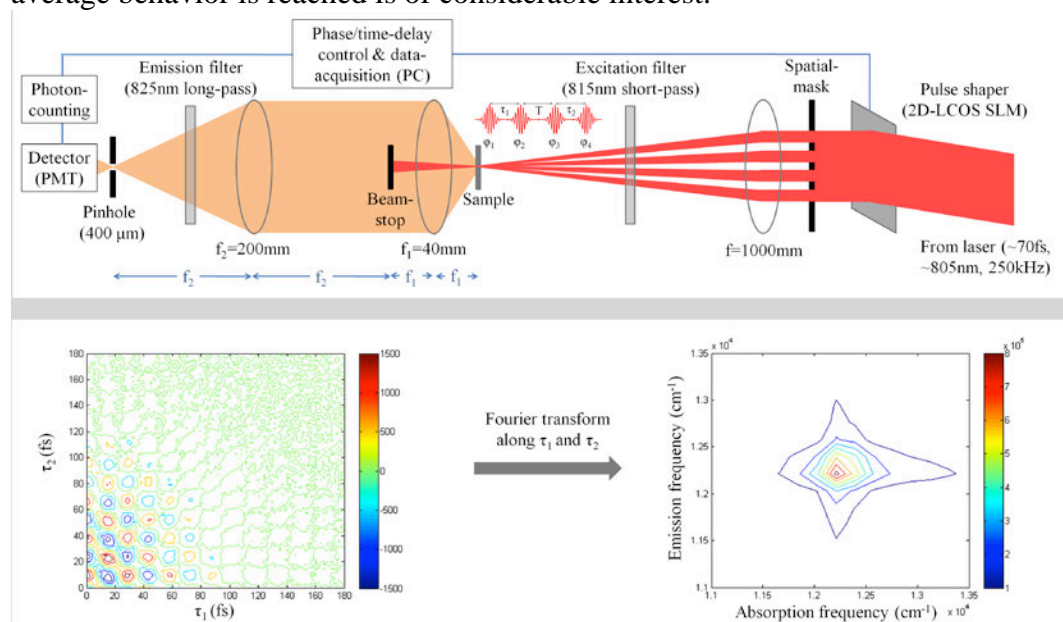
12. "Selective oxidative synthesis of *meso*-beta fused porphyrin dimers," Brennan, B. J.; Arero, J.; Liddell, P. A.; Moore, T. A.; Moore, A. L.; Gust, D. *J. Porphyrins Phthalocyanines* **2013**, in press.
13. "Artificial photosynthetic reaction center with a coumarin-based antenna system," Garg, V.; Kodis, G.; Liddell, P. A.; Terazono, Y.; Moore, T. A.; Moore, A. L.; Gust, D. *J. Phys. Chem. B* **2013**, in press.
14. "Ultrafast energy transfer and excited state coupling in an artificial photosynthetic antenna," Maiuri, M.; Snellenburg, J. J.; van Stokkum, I. H. M.; Pillai, S.; Gust, D.; Moore, T. A.; Moore, A. L.; van Grondelle, R.; Cerullo, G.; Polli, D. *J. Phys. Chem. B*, **2013** in revision.
15. "Comparison of silatrane, phosphonic acid, and carboxylic acid functional groups for attachment of porphyrin sensitizers to TiO₂ in photoelectrochemical cells," Brennan, B. J.; Llansola Portolés, M. J.; Liddell, P. A.; Moore, T. A.; Moore, A. L.; Gust, D. **2013** submitted for publication.

Light Harvesting Dynamics

Graham R. Fleming, Hui Dong, Arijit De, Doran Bennett, Kapil Amarnath
Physical Biosciences Division
Lawrence Berkeley National Laboratory
Berkeley, CA 94720

This project aims to determine the design principles used by natural photosynthesis to harvest solar energy. Understanding the origin of the decay of electronic coherence observed in multiple light harvesting systems and reaction centers appears to be essential for understanding the role of coherence under incoherent excitation (e.g., sunlight), and to understand at a more microscopic level the nature of the system-environment interactions that lead to energy transfer and coherence decay. Such understanding, in our view, is critical for improved design strategies for synthetic light harvesting, as well as greater clarity on the design principles used by nature. We have approached this issue via the question: Is the observed coherence decay true loss of “quantum mechanicalness” (true decoherence) or is it the result of destructive interference at the ensemble level (fake decoherence)? We have attempted to approach this question from both the theoretical and experimental perspectives.

We have developed a theory of single molecule photon echo spectroscopy based on the coherent states representation from quantum optics. A new phase term appears in the signal that describes the thermal fluctuations of the initial state of the environment. These initial states are uncontrollable and, if the signal is collected by incrementing delays in steps each new point on the echo decay will have a different initial state sampled from the thermal distribution. Thus an analysis of the fluctuations in the signal will be very informative on the nature of the individual spectral density. A further point is that there is no concept of phase matching at the single molecule level. Phase cycling methods will be necessary in order to extract the desired signals. Importantly, we have shown that our new formulation reduces to the conventional ensemble expressions as the number of molecules becomes large; however the way in which the ensemble average behavior is reached is of considerable interest.

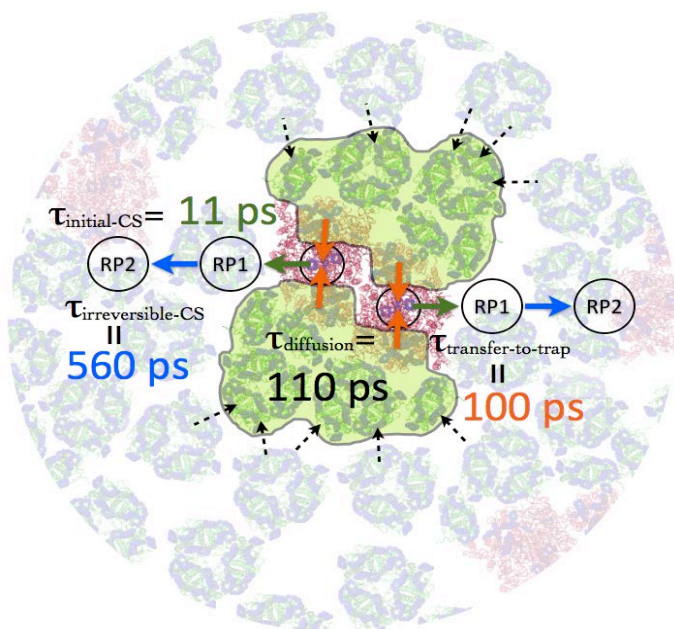


Caption for Fig. 1:
Experimental set-up (top) and results (bottom) of fluorescence-detected two-dimensional spectroscopy of a dye using regular non-collinear beam geometry.

Almost all single molecule experiments utilize fluorescence detection, and we have constructed a fluorescence detected four-pulse two-dimensional spectrometer with the ability to manipulate the phase of all four pulses. This is an equivalent of a 2-D echo experiment with fluorescence detection. It is a development of a technique introduced by us using two phase-controlled pulses. We have demonstrated 8-step phase cycling at low concentration. Such elaborate signal processing clearly places great demands on sample stability, which, as we move towards the single complex limit, will be even more important.

Our future plans include development of the coherent states representation to more complex electronic structures than the single two state system for which we derived the initial results. We also need to explore the evaluation of the ensemble average (is the system ergodic?) and the evaluation of phase matching. Experimentally we will implement a new modulator to allow fully collinear excitation and detection, which will improve sensitivity in the four pulse fluorescence experiment shown in Fig. 1. We plan to extend the energy transfer modeling to Photosystem II grana membranes by extending our domain approach to include the different supercomplexes and LHCII complexes. We plan to use a model of the spatial organization of the membrane developed by Geissler and Schneider (U. C. Berkeley).

We constructed what we believe to be the first structure-based model of energy transfer in photosystem II (PSII) supercomplexes. In order to model the large number of pigment molecules present in a supercomplex (as many as 324), it is useful to decrease the computational intensity of the energy transfer calculations. We have developed a new metric for clustering chlorophylls into groups (called domains) that increases the separation of timescales between inter- and intra-domain transfer. This has allowed us to coarse-grain the overall dynamics at the domain level by assuming infinitely fast intra-domain thermalization. We combined the energy transfer rates between domains with a minimal phenomenological model of charge separation at the reaction center (RC) to build a 3-parameter simultaneous fit to fluorescence decay spectra measured for a range of different size PSII supercomplexes.



Caption for Fig. 2: *The timescales for light harvesting in PSII supercomplexes are shown in the figure: the timescale for diffusion from the periphery to the core is 110 ps, for transfer from the core antenna to the reaction center (RC) is 100 ps, initial charge separation at the RC is 11 ps, and irreversible charge separation is 560 ps. This means light harvesting should not be considered either trap or transfer-to-trap limited.*

We showed that the average timescale of excitation energy capture is linearly dependent on the distance of the excitation from the nearest reaction center.

Understanding the energy flow and structure/function relationships in light harvesting at the system level requires incorporating the kind of microscopic information on energy transfer we have been developing with this FWP into a model that incorporates the spatial and energetic landscapes of the appropriate complexes.

DOE Sponsored Publications 2010 - 2013

1. Quantum Coherence and its Interplay with Protein Environments in Photosynthetic Electronic Energy Transfer, A. Ishizaki, T. Calhoun, G. Schlau-Cohen, and G. Fleming, *Phys Chem Chem Phys*, 27, 7319-7337 (2010)
2. Spectroscopic Elucidation of Uncoupled Transition Energies in the Major Photosynthetic Light Harvesting Complex, LHCII, G.Schlau-Cohen, T.Calhoun, N.Ginsberg, M.Ballottari, R.Bassi, and G. Fleming, *PNAS*, 107, (30), 13276-13281, (2010).
3. Quantum Superposition in Photosynthetic Light Harvesting: Delocalization and Entanglement, A. Ishizaki and G. Fleming, *New J Phys*, 12, #055004 (2010)
4. Quantum Entanglement in Photosynthetic Light Harvesting Complexes, M. Sarovar, A. Ishizaki, G. Fleming and K.B. Whaley, *Nature Physics*, 6, 462-467 (2010)
5. Solving Structure in the CP29 Light Harvesting Complex with Polarization Phased 2D Electronic Spectroscopy, N. Ginsberg, J. Davis, M. Ballottari, Y-C Cheng, R. Bassi, and G. Fleming, *PNAS*, 108, 3848-3858 (2011)
6. Comparing Photosynthetic and Photovoltaic Efficiencies and Recognizing the Potential for Improvement, Robert E. Blankenship, David M. Tiede, James Barber, Gary W. Brudvig, Graham Fleming, Maria Ghirardi, M. R. Gunner, Wolfgang Junge, David M. Kramer, Anastasios Melis, Thomas A. Moore, Christopher C. Moser, Daniel G. Nocera, Arthur J. Nozik, Donald R. Ort, William W. Parson, Roger C. Prince, Richard T. Sayre, *Science*, 332, 805 (2011)
7. Quantum Effects in Biology, Graham R. Fleming, Gregory D. Scholes, and Yuan-Chung Cheng, *Proceedings of 22nd Solvay Conference on Chemistry*, Elsevier Press, 3, 37-58 (2011)
8. Are Reduced Density Matrices Enough? – On the Interpretation of Two-Dimensional Electronic Spectra of Photosynthetic Light Harvesting Complexes, Akihito Ishizaki and Graham R. Fleming, *The Journal of Physical Chemistry*, (J Phys Chem B. 2011 May 19;115(19):6227-33. doi: 10.1021/jp112406h. Epub Apr 13 (2011))
9. Are Reduced Density Matrices Enough? – On the Interpretation of Two-Dimensional Electronic Spectra of Photosynthetic Light Harvesting Complexes, Akihito Ishizaki and Graham R. Fleming, *The Journal of Physical Chemistry*, (J Phys Chem B. 2011 May 19;115(19):6227-33. doi: 10.1021/jp112406h. Epub Apr 13 (2011))
10. Elucidation of Electronic Structure and Quantum Coherence in LHCII with Polarized 2-D Spectroscopy, Gabriela S. Schlau-Cohen, Tessa R. Calhoun, Naomi S. Ginsberg, Matteo Ballottari, Roberto Bassi, Graham R. Fleming, *Ultrafast Phenomena XVII* (Springer Series in Chemical Physics), (Ultrafast Phenomena XVII (Springer Series in Chemical Physics), 610 (2011))
11. Determining Chlorophyll Orientation in the CP29 Light Harvesting Complex with Arithmetic Polarized 2-D Electronic Spectroscopy, Naomi S. Ginsberg, Jeffrey A. Davis, Matteo Ballottari, Yuan-Chung Cheng, Roberto Bassi, Graham R. Fleming, *Ultrafast Phenomena XVII* (Springer Series in Chemical Physics), (63 (2011))
12. Quantum Coherence in Photosynthetic Complexes, Tessa Calhoun and Graham R. Fleming, (*Physical Status Solidi*, 248, 833-838 (2011))
13. Ultrafast Multidimensional Spectroscopy: Principles and Applications to Photosynthetic Systems, Gabriela Schlau-Cohen, Jahan M. Dawlaty, and Graham R. Fleming, *IEEE J. Sel. Top. Quantum Electron*, 99, 1-13 (2011)

14. Iterative Path-Integral Algorithm versus Cumulant Time-Nonlocal Master Equation Approach for the Dissipative Biomolecular Exciton Transport, Peter Nalbach, Akihito Ishizaki, Graham Fleming, and Michael Thorwart, *New Journal of Physics*, 13, 063040 (2011)
15. On the Interpretation of Two-Dimensional Electronic Spectra of Photosynthetic Light Harvesting Complexes, Akihito Ishizaki and Graham R. Fleming (*The Journal of Physical Chemistry B*, 115 (19), 6227-6233 (2011))
16. Two-Dimensional Electronic Spectroscopy and Photosynthesis: Fundamentals and Applications to Photosynthetic Light-Harvesting (Perspective), Gabriela Schlau-Cohen, Akihito Ishizaki and Graham R. Fleming, (*Chemical Physics*, 386, 1-3, 1-22 (2011))
17. Lessons from nature about solar light harvesting, Gregory D. Scholes, Graham R. Fleming, Alexandra Olaya-Castro, and Rienk van Grondelle, *Nature Chemistry*, 3, 763-774 (2011)
18. Focus on quantum effects and noise in biomolecules, Graham Fleming, Susana Huelga and Martin Plenio, Editorial, (*New Journal of Physics*, 13, 115002 (2011))
19. Quantum Coherence in Photosynthetic Light Harvesting, Akihito Ishizaki and Graham R. Fleming, (*Annual Review Condensed Matter Physics*, 3, 333-361(2012))
20. Microscopic Quantum Coherence in Photosynthetic Light Harvesting Antenna, Jahan, M. Dawlaty, Akihito Ishizaki, Arijit K. De and Graham R. Fleming, *Philosophical Transactions of Royal Society A* (370, 3672–3691 (2012))
21. Elucidation of Timescales and Origins of Quantum Electronic coherence in LHCII, Gabriela Schlau-Cohen, Akihito Ishizaki, Tessa Calhoun, Naomi Ginsberg, Mateo Ballottari, Roberto Bassi, and Graham R. Fleming, *Nature Chemistry*, (doi: 10.1038/NCHEM.1303, 4, 389 (2012))
22. Determination of Excited-State Energies and Dynamics in the B Band of the Bacterial Reaction Center with 2D Electronic Spectroscopy, Gabriela Schlau-Cohen, Eleonora De Re, Richard Cogdell and Graham Fleming (*Journal of Physical Chemistry Letters*, 3, 17, 2487-2492 (2012))
23. Structure, Dynamics, and Function in the Major Light Harvesting Complex of Photosystem II, Gabriela S. Schlau-Cohen and Graham R. Fleming, (*Australian Journal of Chemistry*, 65, 583-590 (2012))
24. Quantum-coherent energy transfer: implications for biology and new energy technologies, Alexandra Olaya-Castro, Ashan Nazir, Graham Fleming (Philosophical Transactions of the Royal Society A, 370, 1972, 3613-3617 (2012))
25. Dedication Robert Silbey 1940 – 2011, Robert Harris and Graham Fleming (Philosophical Transactions of the Royal Society A, 370, 1972, 3618-3619 (2012))
26. Three pulse photon echo of finite numbers of molecules: single molecule traces, Hui Dong and Graham Fleming (*Journal of Physical Chemistry*, (submitted))
27. A Structure-Based Model of Energy Transfer Reveals the Principles of Light Harvesting in Photosystem II Supercomplexes, Doran Bennett, Kapil Amarnath, Graham R. Fleming, (*Journal of American Chemical Society* (submitted))

Session VII

Inorganic Homogeneous Photocatalysis

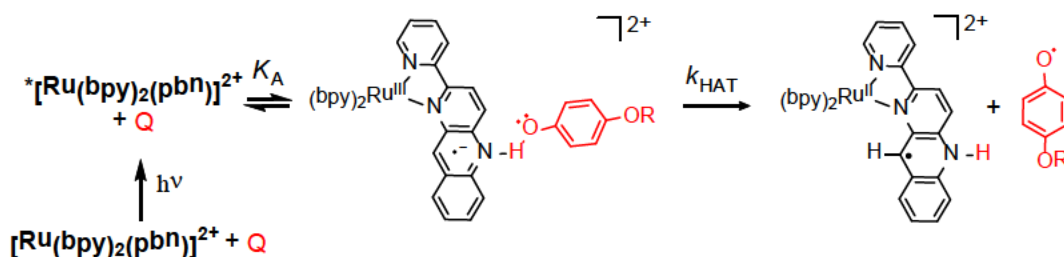
Mechanistic Understanding of Proton-Coupled Electron Transfer In Artificial Photosynthesis

Dmitry E. Polyansky, James T. Muckerman and Etsuko Fujita
Department of Chemistry, Brookhaven National Laboratory
Upton, New York 11973-5000

Artificial photosynthetic systems exploit a variety of photochemical transformations with the ultimate result of efficient conversion of the energy of photons into chemical bonds. The efficiency of these transformations strongly depends on how successfully PCET processes are implemented. In this part of our program we focus on mechanistic understanding of the role of PCET in reactions such as: (1) photochemical formation and reactivity of NADPH-like transition metal complexes; (2) hydrogen atom transfer (HAT) in the excited states of transition metal systems; and (3) light-driven water oxidation catalyzed by transition metal complexes.

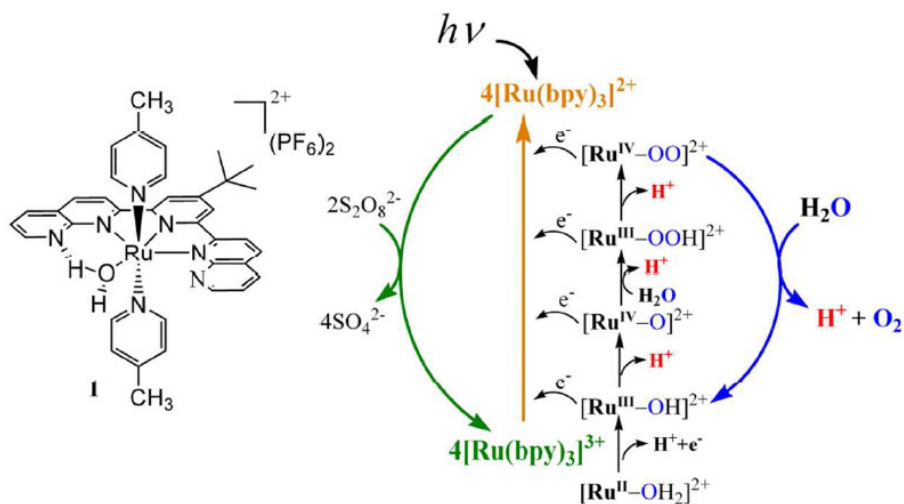
Understanding the ability of NADPH model compounds to shuttle charge in a manner that is coupled to the proton movement in reactions such as HAT or hydride ion transfer is crucial for development of efficient systems involving light-induced charge separation, charge transfer and catalytic systems. In our early work, we found that the renewable hydride donor $[\text{Ru}(\text{bpy})_2(\text{pbnHH})]^{2+}$ (bpy = 2,2'-bipyridine, pbn = 2-(2-pyridyl)benzo[*b*]-1,5-naphthyridine) can be generated photochemically in high yields (quantum yield ca. 21% at 355 nm and quantitative chemical yield) and its formation in the low pH region is mainly achieved through disproportionation of a π -stacking dimer via an intermolecular PCET reaction [6,8]. The net hydride ion transfer reaction from photo-generated hydride donors was found to be controlled by steric factors around the hydride donor sites [19]. The hydride donor ability of the produced organic hydrides was not sufficient to reduce uncoordinated CO_2 , however the further photogenerated one-electron reduced form shows reactivity towards $[\text{CpRe}^{\text{I}}(\text{NO})(\text{CO})_2]^+$ (CO and CH_4 products were observed) [27].

Implementing a series of NAD^+ -type ligands into coordination complexes allowed us to systematically study the influence of factors such as the pK_a of donors, the steric bulk of acceptors, solvent effects and the thermodynamic driving force on light-driven HAT reactions. Mechanistic insights into reactions between a series of NAD^+ model compounds such as $[\text{Ru}(\text{bpy})_2(\text{pbn})]^{2+}$, $[\text{Ru}(\text{bpz})_3]^{2+}$ (bpz = 2,2'-bipyrazine), $[\text{Ru}(\text{bpy})_2(\text{bpz})]^{2+}$ and hydrogen atom donors such as substituted hydroquinones and para-substituted phenols have been studied. A number of factors such as substantial kinetic isotope effects (KIEs), steric control, etc. indicates that a concerted HAT takes place.



Our findings point toward a substantial kinetic solvent effect for HAT in high donor number solvents such as acetonitrile. The decrease in KIE with an increase in the electron withdrawing ability of *para*-substituents of phenols might be associated with a decreased tunneling distance for hydrogen atom transfer.

Another aspect of our work is related to studies of light-induced catalytic reactions. A system in which a water oxidation catalyst interacts directly in uni- or bi-molecular fashion with photoinduced charges can provide valuable mechanistic insights. In our recent work, we have demonstrated that the mononuclear ruthenium catalyst $[\text{Ru}(\text{NPM})(\text{pic})_2]^{2+}$ (**1**) (NPM = 4-*t*-butyl-2,6-di-1',8'-(naphthyrid-2'-yl)-pyridine, pic = 4-picoline) can promote light-driven water oxidation with 9 % quantum efficiency in homogeneous aqueous solution in the presence of $[\text{Ru}(\text{bpy})_3]^{2+}$ and $[\text{S}_2\text{O}_8]^{2-}$ [40]. With complex **1**, we were able to reach a TON and TOF of > 103 and 0.12 s^{-1} , respectively. These values render catalyst **1** to be one of the most active mononuclear ruthenium-based catalysts for light-driven water oxidation in a homogeneous system. According to the previously proposed mechanism for water oxidation catalyzed by **1**, a low-energy pathway for O–O bond formation via the $[\text{Ru}^{\text{IV}}=\text{O}]^{2+}$ intermediate can be achieved at neutral pH [16], thus enabling the use of a mild oxidant such as photogenerated (1.26 V vs NHE) $[\text{Ru}(\text{bpy})_3]^{3+}$. Our work demonstrates that catalytic pathways for complex **1** can be tuned by a simple change of proton concentration, and that the more efficient low energy “direct pathway” enables photochemical water oxidation using $[\text{Ru}(\text{bpy})_3]^{2+}$ with persulfate. In addition, we have established a comprehensive model for the accurate description of similar reactions involving catalyst/sensitizer/quencher systems [44]. We are planning to extend this work to other catalytic systems in order to explore their advantages and limitations under photochemical conditions.



Acknowledgements: We thank our coworkers Jacob Schneider, Anna Lewandowska-Andralojc, Y. Badiel, P. Achord and B. W. Cohen for their assistance, and C. Creutz, D. C. Grills and N. Sutin for helpful discussions. We also thank our collaborators R. P. Thummel and K. Tanaka.

DOE Sponsored Publications 2010-2013

1. Boyer, J. L.; Rochford, J.; Tsai, M.-K.; Muckerman, J. T.; Fujita, E., "Ruthenium Complexes with Non-innocent Ligands: Electron Distribution and Implications for Catalysis," *Coord. Chem. Rev.* **2010**, *254*, 309-330.
2. Grills, D.C.; Cook, A. R.; Fujita, E.; George, M. W.; Miller, J. R.; Preses, J. M.; Wishart, J. F. "Application of External-Cavity Quantum Cascade Infrared Lasers to Nanosecond Time-Resolved Infrared Spectroscopy of Condensed-Phase Samples Following Pulse Radiolysis," *Appl. Spec.* **2010**, *64*, 563-570.
3. Rochford, J.; Tsai, M.-K.; Szalda, D. J.; Boyer, J. L.; Muckerman, J. T.; Fujita, E., "Oxidation State Characterization of Ruthenium 2-Iminoquinone Complexes through Experimental and Theoretical Studies," *Inorg. Chem.* **2010**, *49*, 860-869.
4. Chen, H.; Wang, L.; Bai, J.; Hanson, J. C.; Warren, J. B.; Muckerman, J. T.; Fujita, E.; Rodriguez, J. A. "In Situ XRD Studies of ZnO/GaN Mixtures at High Pressure and High Temperature: Synthesis of Zn-Rich (Ga_{1-x}Zn_x)(N_{1-x}O_x) Photocatalysts," *J. Phys. Chem. C* **2010**, *114*, 1809-1814.
5. Concepcion, J. J.; Tsai, M.-K.; Muckerman, J. T.; Meyer, T. J. "Mechanism of Water Oxidation by Single-Site Ruthenium Complex Catalysts," *J. Am. Chem. Soc.* **2010**, *132*, 1545-1557.
6. Doherty, M. D.; Grills, D. C.; Muckerman, J. T.; Polyansky, D. E.; Fujita, E. "Toward More Efficient Photochemical CO₂ Reduction: Use of scCO₂ or Photogenerated Hydrides," *Coord. Chem. Rev.* **2010**, *254*, 2472-2482.
7. Grills, D. C.; Fujita, E. "New Directions for the Photocatalytic Reduction of CO₂: Supramolecular, scCO₂ or Biphasic Ionic Liquid-scCO₂ Systems," *J. Phys. Chem. Lett.* **2010**, *1*, 2709-2718.
8. Cohen, B. W.; Polyansky, D. E.; Zong, R.; Zhou, H.; Ouk, T.; Cabelli, D.; Thummel, R. P.; Fujita, E. "Differences of pH-Dependent Mechanisms on Generation of Hydride Donors using Ru(II) Complexes Containing Geometric Isomers of NAD⁺ Model Ligands: NMR and Radiolysis Studies in Aqueous Solution," *Inorg. Chem.* **2010**, *49*, 8034-8044.
9. Shen, X.; Small, Y. A.; Wang, J.; Allen, P. B.; Fernandez-Serra, M. V.; Hybertsen, M. S.; Muckerman, J. T. "Photocatalytic Water Oxidation at the GaN (1010) – Water Interface," *J. Phys. Chem. C* **2010**, *114*, 13695-13704.
10. Chen, J.; Szalda, D. J.; Fujita, E.; Creutz, C. "Iron(II) and Ruthenium(II) Complexes Containing P, N, and H Ligands: Structure, Spectroscopy, Electrochemistry and Reactivity," *Inorg. Chem.* **2010**, *49*, 9380-9391.
11. Creutz, C.; Chou, M. H.; Hou, H.; Muckerman, J. T. "Hydride Ion Transfer from Ruthenium(II) Complexes in Water: Kinetics and Mechanism," *Inorg. Chem.* **2010**, *49*, 9809-9822.
12. Fujita, E.; Muckerman, J. T.; Domen, K. "A Current Perspective on Photocatalysis," *ChemSusChem.* **2011**, *4*, 155-157.
13. Wada, T.; Muckerman, J. T.; Fujita, E.; Tanaka, K. "Substituents Dependent Capability of

- Bis(ruthenium-dioxolene-terpyridine) Complexes Toward Water Oxidation,” *Dalton Trans.* **2011**, 40, 2225-2233.
14. Small, Y. A.; DuBois, D. L.; Fujita, E.; Muckerman, J. T. “Proton Management as a Design Principle for Hydrogenase-Inspired Catalysts,” *Energy Environ. Sci.* **2011**, 4, 3008-3020.
 15. Li, L.; Muckerman, J. T.; Hybertsen, M. S.; Allen, P. B. “Phase Diagram, Structure and Electronic Properties of $(\text{Ga}_{1-x}\text{Zn}_x)(\text{N}_{1-x}\text{O}_x)$ Solid Solution from DFT-Based Simulations,” *Phys. Rev. B* **2011**, 83, 134202.
 16. Polyansky, D. E.; Muckerman, J. T.; Rochford, J.; Zong, R.; Thummel, R. P.; Fujita, E. “Water Oxidation by a Mononuclear Ruthenium Catalyst: Characterization of the Intermediates,” *J. Am. Chem. Soc.* **2011**, 133, 14649-14665.
 17. Boyer, J. L.; Polyansky, D. E.; Szalda, D. J.; Zong, R.; Thummel, R. P.; Fujita, E. “Effects of a Proximal Base on Water Oxidation and Proton Reduction Catalyzed by Geometric Isomers of $[\text{Ru}(\text{tpy})(\text{pynap})(\text{OH}_2)]^{2+}$,” *Angew. Chem. Int. Ed.* **2011**, 50, 12600-12604.
 18. Muckerman, J. T.; Fujita, E. “Theoretical Studies of the Mechanism of Catalytic Hydrogen Production by a Cobaloxime,” *Chem. Commun.* **2011**, 47, 12456-12458.
 19. Cohen, B. W.; Polyansky, D. E.; Achord, A.; Cabelli, D.; Muckerman, J. T.; Tanaka, K.; Thummel, R. P.; Zong, R.; Fujita, E. “Steric Effect for Proton, Hydrogen-Atom, and Hydride Transfer Reactions with Geometric Isomers of NADH-Model Ruthenium Complexes,” *Faraday Discuss.* **2012**, 155, 129-144.
 20. Schneider, J.; Jia, H.; Muckerman, J. T.; Fujita, E. “Thermodynamics and Kinetics of CO_2 , CO and H^+ Binding to a Metal Centre of CO_2 Reduction Catalysts,” *Chem. Soc. Rev.* **2012**, 41, 2036-2051.
 21. Hull, J. F.; Himeda, Y.; Wang, W.-H.; Hashiguchi, B.; Periana, R.; Szalda, D. J.; Muckerman, J. T.; Fujita, E. “Reversible Hydrogen Storage using CO_2 and a Proton-Switchable Iridium Catalyst in Aqueous Media under Mild Temperatures and Pressures,” *Nat. Chem.* **2012**, 4, 383-388.
 22. Agarwal, J.; Fujita, E.; Schaefer, H. F. III; Muckerman, J. T. “Mechanisms for CO Production from CO_2 Using Reduced Rhenium Tricarbonyl Catalysts,” *J. Am. Chem. Soc.* **2012**, 134, 5180-5186.
 23. Agarwal, J.; Sanders, B. C.; Fujita, E.; Schaefer III, H. F.; Harrop, T. C.; Muckerman, J. T. “Exploring the Intermediates of Photochemical CO_2 Reduction: Reaction of $\text{Re}(\text{dmb})(\text{CO})_3\text{COOH}$ with CO_2 ,” *Chem. Commun.* **2012**, 48, 6797-6799.
 24. Wang, W.-H.; Hull, J. F.; Muckerman, J. T.; Fujita, E.; Hirose, T.; Himeda, Y. “Highly Efficient D_2 Generation by Dehydrogenation of Formic Acid in D_2O via H^+/D^+ Exchange on Iridium Catalyst. Application to Synthesis of Deuterated Compounds by Transfer Deuterogenation,” *Chem. Eur. J.* **2012**, 18, 9397-9404.
 25. Wang, W.-H.; Hull, J. F.; Muckerman, J. T.; Fujita, E.; Himeda, Y. “Combined Ligand Effects Enhance Iridium(III)-Catalyzed Homogeneous Hydrogenation of Carbon Dioxide in Water near Ambient Temperature and Pressure,” *Energy Environ. Sci.* **2012**, 5, 7923-7926.
 26. Polyansky, D. E. “Electrocatalysts for Carbon Dioxide Reduction,” in *Encyclopedia of*

Applied Electrochemistry, Eds. R. Adzic and N. Marinkovic, Springer, in press.

27. Muckerman, J. T.; Achord, P.; Creutz, C. A.; Polyansky, D. E.; Fujita, E. "Calculation of Thermodynamic Hydricities and the Design of Hydride Donors for CO₂ Reduction," *Proc. Nat. Acad. Sci. USA* **2012**, *109*, 15657-15662.
28. Kundu, S.; Ciston, J.; Senanayake, S. D.; Arena, D.; Fujita, E.; Stacchiola, D.; Rodriguez, J. A. "Exploring the Structural and Electronic Properties of Pt/Ceria-Modified TiO₂ and its Photo-Catalytic Activity for Water Splitting under Visible Light," *J. Phys. Chem. C* **2012**, *116*, 14062-14070.
29. Matsubara, Y.; Fujita, E.; Doherty, M. D.; Muckerman, J. T.; Creutz, C. "Thermodynamic and Kinetic Hydricity of Ruthenium(II) Hydride Complexes," *J. Am. Chem. Soc.* **2012**, *134*, 15743-15757.
30. Schneider, J.; Jia, H.; Kobiro, K.; Cabelli, D.; Muckerman, J. T.; Fujita, E. "Nickel(II) Macrocycles: Highly Efficient Electrocatalysts for the Selective Reduction of CO₂ to CO," *Energy Environ. Sci.* **2012**, *5*, 9502-9510.
31. Doherty, M. D.; Grills, D. C.; Huang, K.-W.; Muckerman, J. T.; Polyansky, D.; Fujita, E. "Kinetics and Thermodynamics of Small Molecule Binding to Pincer-PCP Rhodium(I) Complexes," *Inorg. Chem.*, ASAP, DOI: 10.1021/ic300067g.
32. Hayashi, Y.; Szalda, D. J.; Grills, D. C.; Hanson, J.; Huang, K. -W.; Muckerman, J. T.; Fujita, E. "Isolation and X-ray Structures of Four Rh(PCP) Complexes Including a Rh(I) Dioxygen Complex with a Short O–O Bond," *Polyhedron* (Michelle Millar Special Issue), accepted, DOI: 10.1016/j.poly.2012.10.006
33. Fujita, E.; Muckerman, J. T.; Himeda, Y. "Interconversion of CO₂ and Formic Acid by Bio-Inspired Ir Complexes with Pendent Bases," *Biochim. Biophys. Acta - Bioenergetics*, ASAP, DOI:10.1016/j.bbabbio.2012.11.004.
34. Muckerman, J. T.; Skone, J. H.; Ning, M.; Wasada-Tsutsui, Y. "Toward the Accurate Calculation of pK_a Values in Water and Acetonitrile," *Biochim. Biophys. Acta - Bioenergetics*, accepted.
35. Appel, A. M.; Bocarsly, A. B.; Bercaw, J. E.; Dobbek, H.; Dupuis, M.; DuBois, D. L.; Ferry, J. G.; Fujita, E.; Hille, R.; Kenis, P. J. A.; Kerfeld, C. A.; Morris, R. H.; Peden, C.; Portis, A.; Ragsdale, S.; Rauchfuss, T. B.; Reek, J. N. H.; Seefeldt, L. C.; Spitler, M.; Stack, R. J.; Thauer, R. K.; Waldrop, G. L. "Frontiers, Opportunities, and Challenges in Biochemical and Chemical Catalysis of CO₂", *Chem. Rev.* in revision
36. Wang, W.-H.; Hull, J. F.; Muckerman, J. T.; Fujita, E.; Himeda, Y. "Hydroxy-substituted aromatic N-heterocycles: Versatile ligands in organometallic catalysis" *New J. Chem.*, ASAP, DOI: 10.1039/c3nj41146.
37. Wang, W.-H.; Muckerman, J. T.; Fujita, E.; Himeda, Y. "Mechanistic insight through factors controlling effective hydrogenation of CO₂ catalyzed by bio-inspired proton-responsive iridium(III) complexes", *ACS Catalysis*, ASAP, DOI: 10.1021/cs400172j.
38. Chen, W. -F.; Iyer, S.; Iyer, S.; Sasaki, K., Wang, C. -H.; Zhu, Y.; Muckerman, J. T.; Fujita, E. "Noble-Metal-Like Electrocatalyst Made from Soybeans and Molybdenum for

Critical Steps in Water Oxidation by Ru Blue Dimer Catalysts: Insights into the Electronic Requirements of Water Activation for Artificial Photosynthesis

Y. Pushkar, D. Moonshiram, I. Alperovich, J. Concepcion, T.J. Meyer

Department of Physics
Purdue University
West Lafayette, Indiana, 47907

The light driven water splitting process accomplished by Photosystem II (PS II) provides a blueprint for future energy solutions based on artificial photosynthesis. The main challenge is the development of economically feasible catalysts for water splitting. Design of such optimal catalysts is pending the understanding of the mechanistic aspects of water activation by metal-oxo catalysts. PS II accomplishes the water splitting cycle ($2\text{H}_2\text{O} + 4h\nu = \text{O}_2 + 4\text{H}^+ + 4\text{e}^-$) within a few milliseconds. The fast kinetic and complex protein environment of the PS II oxygen evolving complex (OEC) has so far prevented identification of the molecular and electronic structure of the S-state (presumably S_4) that is reactive to the water molecule. To address this gap in fundamental knowledge, we have chosen to study a Ru based water oxidation catalyst – the blue dimer (BD) (see Figure 1). This is the first molecular catalysts reported for water splitting. The rationale behind this choice is twofold: i) the relatively simple molecular structure accessible via multiple spectroscopic techniques; ii) the kinetics in the seconds time frame, yielding the freeze quench approach viable for trapping of the reactive intermediates.

X-ray spectroscopy (XAS) at the Ru K- and L-edges was selected as a key tool for analysis of the structure and electronic configurations of BD's reactive intermediates and indeed its application proved to be critical to clarify the outstanding issues and deliver new insights about the catalysis mechanism. There is a general tendency (regardless of whether water oxidation, hydrogen production or CO_2 reduction catalysts are analyzed) to guess the oxidation states of the metal catalytic centers based on UV-vis kinetic measurements. In most cases UV-vis provides no insight about the oxidation states and such overinterpretation of data can be detrimental for the development of catalytic systems.

In spite of the high information content, XAS alone is not sufficient for analysis of the catalytic mechanism. The following measurements were therefore routinely performed in parallel during the analysis of the water oxidation reaction: O_2 evolution, UV-vis stopped-flow kinetic measurements (provides guidance on the time window for trapping of kinetic intermediates), EPR, Ru K-edge and $\text{L}_{2,3}$ -edges XANES, Ru K-edge EXAFS and resonance Raman (RR). The measurements were done on freeze-quenched samples (a few ms to a few seconds time) of reaction mixtures generated in several acidic media (1M and

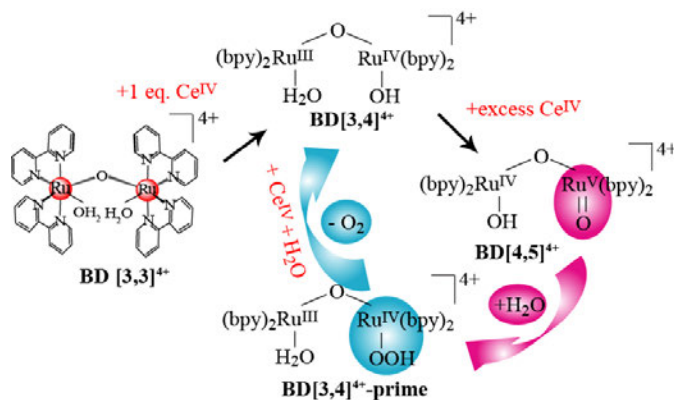


Figure 1. Key intermediates in the water oxidation catalytic cycle of the blue dimer were characterized under this proposal. Optimization of the reactivity towards water (purple arrow) as well as oxidation of the resulting peroxo-intermediate (blue arrow) are needed for improved activity.

0.1M HNO₃ and CF₃SO₃H with H₂O as well as D₂O) using Ce(IV) or Co(III) oxidants. The spectroscopic results were supplemented by relativistic DFT calculations for analysis of the molecular geometries (experimentally determined by EXAFS), spin densities and g-tensors (EPR) as well as the electronic structure (by Ru L-edge XAS).

Both BD and PS II OEC are activated by proton-coupled electron transfer to reach a higher oxidation state. The highest oxidation state of the PS II OEC is not known with certainty, but for BD we have experimentally shown that the highest detectable oxidation state corresponds to BD [4,5] (one Ru center in oxidation state 4+ and one with 5+) (XAS, EPR data). This result has a significant impact on the modeling of the water oxidation by this catalyst. All past DFT analyses implied BD [5,5] as a species activating the water molecule for formation of the O-O bond. However, our data show that BD[4,5] containing one Ru^V center is sufficient. This is not surprising, given that a large number of monomeric Ru complexes have been established for catalytic water splitting. These can maximum achieve a single Ru^V site.

Both PS II OEC and BD have terminal water molecules coordinated to the metal center as well as μ -oxo-bridges. For BD we showed that the oxygen of the Ru-O-Ru μ -oxo-bridge remains intact (inactive) in the water oxidation (EXAFS, RR and ¹⁶O/¹⁸O data). The main action happens at the terminal Ru-H₂O water molecule which is converted to Ru^V=O. We determined Ru^V=O 1.7Å distance by EXAFS and confirmed this bond via 816 cm⁻¹ vibrations frequency (¹⁶O/¹⁸O isotope shift 35 cm⁻¹).

Our main findings include mapping of the spin density over this reactive Ru^V=O moiety. We successfully introduced the ¹⁷O isotope as a tool to determine the spin density on the Ru^V=¹⁷O oxygen and recorded the ¹⁷O hyperfine splitting in EPR: $|A_{xx}|=60$ G, A_{yy} and A_{zz} estimated at 25G (upper limit) from EPR modeling. The Ru^V=O unit is the first to demonstrate large radicaloid character and an associated large ¹⁷O hfs. We call this a new type of radical based on localized ligand orbitals (see Figure 2). More radicals of this type will likely be discovered in the future by analysis of highly reactive M=O units with different metal ions exhibiting electronic configurations similar to Ru^V=O.

Contrary to the general assumption that the reaction of Ru^V=O with water is slow (making it a rate-limiting step) and that Ru^V=O intermediates, thus, should build up in the reaction mixtures, BD [4,5] is short lived (a few seconds). We have never observed Ru^V=O (which has distinct EPR, Raman and XAS) build up, neither for BD nor for a variety of single site Ru catalysts. However, we observed other species with longer life times resulting from BD [4,5] (or single site Ru catalysts) reactivity with water - presumably peroxides. Thus, in optimizing water oxidation catalysts, attention must be paid to both steps: enhancing the reactivity of the Ru=O towards O-O bond formation (by designing strong radicaloid character) as well as ensuring efficient decomposition/oxidation of the resulting peroxides (Figure 1) if these happen to have long life times and build up in the reaction mixtures.

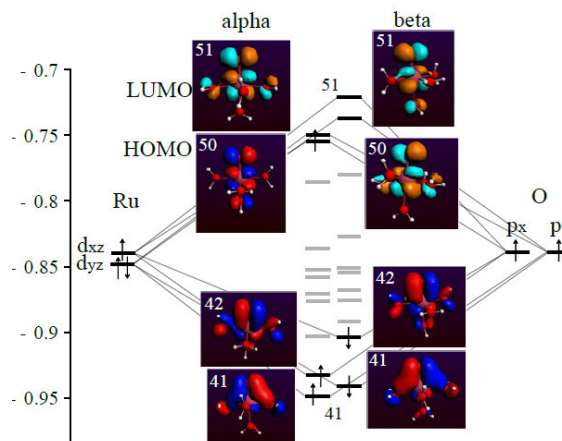


Figure 2. Schematic MO diagram of the [RuO(H₂O)₅]³⁺ model. The energies of MOs are in Hartree. An unpaired electron on the HOMO orbital (anti-bonding for Ru^V=O) is distributed between oxygen and Ru resulting in considerable spin density on the oxygen in the Ru^V=O.

DOE Sponsored Publications 2010-2013

1. "Experimental Demonstration of Radicaloid Character in a $\text{Ru}^{\text{V}}=\text{O}$ Intermediate in Catalytic Water Oxidation" D. Moonshiram, I. Alperovich, J. Concepcion, T. Meyer, Y. Pushkar, **PNAS**, 2013, 110 (10), pp 3765-3770.
2. "Mechanism of Catalytic Water Oxidation by Ruthenium Blue dimer catalyst: comparative study in D_2O versus H_2O " D. Moonshiram, V. Purohit, J. Concepcion, T. Meyer, Y. Pushkar, **Materials**, 2013, 6 (2), pp 392-409.
3. "Ru $L_{2,3}$ XANES theoretical simulation with DFT: a test of the core-hole treatment" I. Alperovich, D. Moonshiram, A. Soldatov, Y. Pushkar, **Solid State Communications**, 2012, V.152, 1880-1884.
4. "Theoretical modelling of $L_{2,3}$ -edges XANES using DFT" I. Alperovich, A. Soldatov, D. Moonshiram, Y. Pushkar, **Journal of Experimental and Theoretical Physics Letters**, 2012, 95 (10), pp 504-510.
5. "Structure and Electronic Configurations of the Intermediates of Water Oxidation in Blue Ruthenium Dimer Catalysis" D. Moonshiram, J. Jurss, J. Concepcion, T. Zakharova, I. Alperovich, T. Meyer, Y. Pushkar, **Journal of American Chemical Society**, 2012, 134, 4625-4636.
6. "Understanding the Electronic Structure of 4d Metal Complexes: From Molecular Spinors to L-edge Spectra of a di-Ru Catalyst" I. Alperovich, G. Smolentsev, D. Moonshiram, J. W. Jurss, J. J. Concepcion, T. Meyer, A. Soldatov, Y. Pushkar, **Journal of American Chemical Society**, 2011, 133 (39), p 15786–15794.
7. "A Mononuclear Nonheme Manganese(IV)-Oxo Complex Binding Redox-Inactive Metal Ions." J. Chen, Y.-M. Lee, K. Davis, X. Wu, M. S. Seo, K.B. Cho, H. Yoon, Y. J. Park, S. Fukuzumi, Y. Pushkar, W. Nam. **Journal of the American Chemical Society**, 2013, published on-line.
8. "A Highly Reactive Mononuclear Nonheme Manganese(IV)-Oxo Complex That Can Activate the Strong C-H Bonds of Alkanes" X. Wu, M. S. Seo, K. Davis, Y. Lee, J. Chen, K.-B. Cho, Y. Pushkar, W. Nam, **Journal of American Chemical Society**, 2011, 133 (50), pp 20088–20091.

Electrochemical Water Oxidation by Homogenous Co Catalyst

Laleh Tahsini¹, Sarah E. Specht¹, James A. Golen², Arnold L. Rheingold², and Linda H. Doerrer¹

¹Department of Chemistry, Boston University, Boston, MA 02215,

²Department of Chemistry and Biochemistry, University of California San Diego, La Jolla, CA 92093-0358

The catalytic separation of water into its elements using solar energy followed by their recombination provides a way to recover the photochemical energy stored in the O-H chemical bond. Heterogeneous water oxidation catalysts (WOC) can efficiently oxidize water but are intractable to many analytical techniques. In contrast, homogenous catalysts can bring molecular-level clarity to our understanding of the water oxidation reaction.

The susceptibility of C-H bonds to strong oxidants led us to use highly fluorinated ligands. Prior to these studies some work had been done with the perfluorinated pinacolate ligand, which we have considerably enhanced. Transition metal complexes of the bidentate ligand H₂ddfp = dodecafluoropinacol can be soluble and hydrolytically stable in water. The mononuclear M(II) complexes, (A)₂[M(ddfp)₂] with A = K⁺, Me₄N⁺, or nBu₄N⁺ and M = Co, Ni, Cu, and Zn have been prepared in air. The Co(II) and Ni(II) species are high spin, and the Ni(II) and Cu(II) species are square planar, regardless of cation. The Co(II) species can be forced into a square planar structure with K⁺ chelation between two ddfp ligands, whereas the Zn anion is distorted tetrahedral. The absorption bands in non-coordinating solvents (λ_{\max} = 388 nm (CH₂Cl₂)) are quite different from those in coordinating solvents (λ_{\max} ~ 560 nm (CH₃CN, H₂O)), which acetone and THF showing intermediate behavior, all of which indicate solvent Lewis base coordination.

Single crystal X-ray diffraction data have been obtained for the square pyramidal [Co(OH₂)(ddfp)₂]²⁻ anion from wet toluene (K(18C6)⁺) and from water (mixed Me₄N⁺/Mg(aq)²⁺ cations). Diffraction data do not distinguish definitively between a bound water in [Co(OH₂)(ddfp)₂]²⁻ or a bound hydroxide with a partially protonated ddfp in [Co(OH)(Hddfp)(ddfp)]²⁻, though some asymmetry exists in the Co-O_{ddfp} distances. The protonation constant for this anion is $3.63 \times 10^2 \pm 10\%$ and therefore its pK_a is 11.4. The pH titration studies and complementary UV-vis spectroscopy revealed [Co(OH₂)(ddfp)₂]²⁻ to be stable over a wide pH range (4 - 11), suggesting that the coordinated ddfp ligand can serve as an internal buffer. Complex degradation is not observed at low pH until more than three equivalents of H⁺ per Co have been added.

In water, the cyclic voltammetry of [Co(ddfp)₂(OH₂)]²⁻ exhibits an oxidation catalytic wave at 1.20 V versus Ag/AgCl in potassium nitrate (KNO₃) electrolyte. At higher scan rates, a quasi-reversible couple is also obtained at 0.88 V, likely due to the higher oxidation states of the complex. The same strong oxidation wave was also obtained in other electrolytes including sodium fluoride (NaF), sodium acetate (NaOAc) and sodium phosphate (NaH₂PO₄). Gas bubbles was observed on the electrode surface over several scans, consistent with O₂ formation. Comparative study of the [Zn(ddfp)₂]²⁻ derivative confirmed that the observed features in cyclic voltammograms with [Co(ddfp)₂(OH₂)]²⁻ are metal, not ligand, based. The following data obtained in control reactions support the present system as a new homogeneous catalytic water oxidation system: (i) neither discoloration of the electrode during CV measurements nor any

deposition on the electrode surface is observed, (ii) no catalytic wave due to water oxidation was observed using an unpolished carbon electrode from multiple CV scans cycled in a fresh cobalt-free KNO_3 electrolyte at pH 10.0 (Figure 1b), (iii) The observed activity for $[\text{Co}(\text{ddfp})_2]^{2-}$ complex is independent of weakly coordinating electrolytes, and (iv) the electronic spectra of $[\text{Co}(\text{ddfp})_2(\text{OH}_2)]^{2-}$ in the presence of all electrolytes, except NaH_2PO_4 clearly show no difference from the spectra of $[\text{Co}(\text{ddfp})_2(\text{OH}_2)]^{2-}$ in water without other electrolytes.

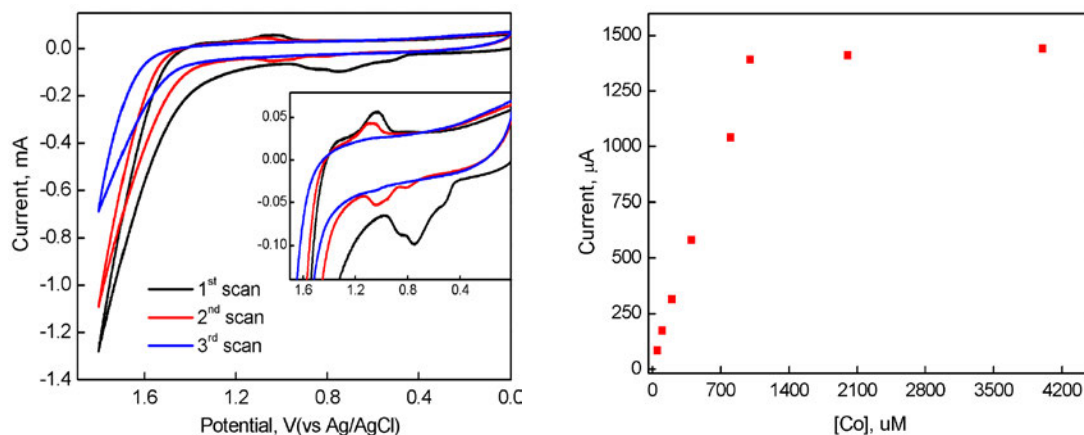


Figure 1. (a) Cyclic voltammetry of $(\text{Me}_4\text{N})_2[\text{Co}(\text{OH}_2)(\text{ddfp})_2]$ (1.0mM) in KNO_3 (0.1M) with the scan rate = 1.0 V s^{-1} and (b) catalytic current obtained at 1.20 V (vs Ag/AgCl) as a function of time.

Bulk electrolysis experiments show the catalytic current is proportional to the concentration of cobalt complex, up to a concentration of 1.0 mM. The chromophore observed during electrolysis is the same as observed in the pH titration studies at high pH values. In the absence of an external buffer, the pH decreases during electrolysis and after 1200 - 1400 seconds, the current begins to decrease and the solution loses its color. If the pH is adjusted back to 10, both the catalytic current and the chromophore are regenerated. The best values to date are 10 for the TON and 30 h^{-1} for the TOF, and the overpotential is 0.76 V. The evolution of O_2 gas during bulk electrolysis has been confirmed qualitatively with a fluorescence-quench O_2 probe.

Acetonitrile solutions of $[\text{Co}(\text{ddfp})_2]^{2-}$ exposed to air for days gradually form a tetrahedral Co(II) species with four equivalents of the hexafluoropropanediol, H_2hfpd , in monodeprotonated form $[\text{Co}\{\text{OC}(\text{CF}_3)_2(\text{OH})\}_4]^{2-}$. This oxidative C-C bond cleavage and net transfer of two hydroxide groups to a pinacolate ligand occurs only in organic solvents. When H_2O_2 was reacted with the cobalt complex in acidic aqueous solutions (pH = 2.5 – 3.5), the ESI-MS data confirm the formation of $[\text{Co}(\text{III})(\text{ddfp})_2]$. Only in organic solvents does this species decay slowly to the gem diolate product.

DOE Sponsored Publications 2012-2013

- [1] Cantalupo, S. A.; Fiedler, S. R.; Shores, M. P.; Rheingold, A. L., Doerr, L. H. *Angew. Chem. Int. Ed.* **2011**, *50*, 1-7.
- [2] Tahsini, L., Specht, E. S., Lum, J. S., Long, A., Rheingold, A. L., Golen, J. A., Doerr, L. H., "Late Transition Metal Complexes with the Perfluoropinacolate Ligand", *Manuscript in prep.*
- [3] Tahsini, L., Specht, E. S., Doerr, L. H., *Manuscript in prep.*

Session VIII

*Solar Photoconversion at Semiconductor Surfaces-
Computational and Model Interfaces*

Quantum Chemical Modeling of Systems for Solar Energy Conversion

Richard A. Friesner, Louis Brus, Mike Steigerwald, Jing Zhang, Thomas Hughes
Department of Chemistry
Columbia University
New York, NY 10025

Over the past 3 years, the present project has focused on two principal objectives: (1) development of an improved density functional theory (DFT) electronic structure methodology, which is capable of achieving high accuracy for a range of important chemical and electrical properties, particularly for transition metal containing systems; (2) application of DFT to systems relevant to solar energy conversion. In what follows, progress in the theoretical methodology development and two applications projects will be described.

Our approach to improving DFT methods is to augment standard DFT functionals (of which the B3LYP functional has proven to be the most suitable) with localized orbital corrections (LOCs), which represent the error made by the DFT methodology in treating a particular type of electron pair. For systems composed of second and third row elements, correction terms for atomic hybridization states, various types of chemical bonds, radical species, and the local environment are the most important terms; a 22 parameter model appended to B3LYP, the B3LYP-LOC model, yields a mean unsigned error (MUE) of 0.8 kcal/mole using the G3 atomization energy data set of Pople and coworkers. Subsequent work has developed the B3LYP-LOC model for ionization potentials, electron affinities, activation barriers, and reaction energies; the MUE is in all cases on the order of 1 kcal/mole, which is close to chemical accuracy and comparable to what is obtained with CCSD(T) based methods such as G3 theory.

Over the past several years, we have worked to extend the methodology to transition metal containing species. Our initial focus has been on the first transition metal series, displays larger errors in DFT calculations than the subsequent series, and furthermore is of increasing importance in energy conversion efforts due to the earth abundance of these metals. For spin splittings, we developed a novel data set, containing 57 diverse octahedral complexes, based on spin forbidden shoulders in optical spectra; B3LYP-LOC reduces the errors in B3LYP calculations from a MUE of 10.1 kcal/mole to a MUE of 2.0 kcal/mole [5]. Similarly, for redox potentials, a data set of 105 diverse complexes was extracted from the literature, and the MUE was reduced from 0.4 eV (with outliers as large as 1V) to 0.1eV, close to the accuracy of the experimental data [2]. Finally, for metal-ligand bond energies, DBLOC corrections reduce the MUE from 3.7 kcal/mole per ligand to 0.94 kcal/mole, using a set of gas phase ligand removal energies curated by Johnson and Becke from the NIST archive [3].

Our first application of DFT methods to systems of interest in solar energy conversion involves an analysis of the catalytic cycle of a ruthenium based catalyst discovered by Meyer and coworkers [4]. These workers proposed reaction mechanisms for the various steps in the cycle, which accomplishes oxygen evolution via the use of a sacrificial Ce^{4+} acceptor, oxidizing the Ru catalyst to an Ru(V) electronic state which is then capable of carrying out the water splitting chemistry. We first showed that continuum solvent based thermodynamic cycle calculation of the redox potentials of the relevant Ru species in the cycle, as well as various other Ru complexes reported in the literature, is in good agreement with experiment, on the order of

0.1eV. This observation is in line with the comment above to the effect that DFT errors for the second transition metal series and beyond are typically more moderate than they are for the first transition metal series. We then compute the energies and activation barriers for all intermediates and transition states in the cycle, and compare the two rate limiting steps with experiment. The predicted barrier of ~ 20 kcal/mole for both of the key rate limiting steps is within a few kcal/mole of the experimental measurements. A crucial correction for the entropic loss associated with binding a water molecule to the complex (the “cratic” entropy, on the order of 7 kcal/mole) was necessary to obtain results in agreement with experiment for these barrier heights. The reported agreement is superior to that presented in other papers in the literature for the same set of reactions. These results confirm the mechanistic details of the catalytic cycle proposed by Meyer and coworkers, and provide atomic level predictions of the structures and energetics of the intermediates and transition states.

Our second application is an analysis of electron transport and trapping in the TiO_2 nanoparticles of the Gratzel cell [1]. A basic picture of Gratzel cell functioning has been available for many years: an electron in a dye molecule attached to the nanoparticle is excited by light, and then is injected from the excited state of the dye into the nanoparticle. However, transport in the nanoparticle is not bandlike (as it would be in crystalline silicon) but rather appears to be based on hopping conduction and displays a temperature dependence from which a distribution of hopping barriers can be extracted. The question then arises as to the atomic level structure of the states involved in the initial trapping of the electron and in subsequent electron transport to the electrode. These states must be localized, have an appropriate energy relative to the conduction band, and enable hopping with barriers consistent with the experimental data.

Several years ago, Frank and coworkers proposed that transport in the Gratzel cell takes place via ambipolar diffusion, in which small cations (ordinarily lithium) hop from site to site along with the injected electron. This suggests that the trapping site is assembled simply by bringing a Li^+ cation near a Ti atom which contains an excess electron. DFT calculations of such structures using a cluster model and continuum solvent demonstrate that states of this type have an energy in agreement with the experimental energy relative to the conduction band, and yield an open circuit voltage $\sim 0.1\text{eV}$ agreement with experiment. In order to achieve this agreement, the redox corrections of ref. [2], which are $\sim 0.5\text{eV}$ for the open circuit voltage calculations, were used without any parameter adjustment. The hopping conduction is driven by moving an Li from one Ti site to another; the barriers to this process are in good agreement with the experimental barrier heights extracted from analysis of the temperature dependence of the conduction. Overall, the agreement between theory and experiment for the model is quite good for multiple points of contact, establishing the methodology as reasonable and the ambipolar diffusion hypothesis as a promising model for conduction in the Gratzel cell.

Moving forward, we are continuing to work on applications, as well as advancing the LOC methodology. Currently we are applying the LOC model to computation of the pKa's of hexaaquo complexes of metals in the first transition series. This is a surprisingly complex and difficult problem, with B3LYP yielding errors as large as 10 pKa units and an average MUE of ~ 6 pKa units; when the B3LYP-LOC methodology is used without any further parameter adjustment, the MUE is reduced to 1.7 pKa units and the maximum error to 2.3 units. Finally, we are implementing the LOC methodology in Jaguar where it will be distributed to interested users in robust commercial form.

DOE Sponsored Publications 2010-2013:

1. Zhang, Jing, Thomas F. Hughes, Michael Steigerwald, Louis Brus, Richard A. Friesner, Realistic Cluster Modeling of Electron Transport and Trapping in Solvated TiO₂ Nanoparticles, *J. Am. Chem. Soc.*, 134, 29, 12028 – 12042 (2012).
2. Hughes, Thomas F. and Richard A. Friesner, Development of Accurate DFT Methods for Computing Redox Potentials of Transition Metal Complexes: Results for Model Complexes and Application to Cytochrome P450, *J. Chem. Theor. Comput.*, 8, 2, 442 – 459 (2012).
3. Hughes, Thomas F., Jeremy N. Harvey and Richard A. Friesner, A B3LYP-DBLOC empirical correction scheme for ligand removal enthalpies of transition metal complexes: parameterization against experimental and CCSD(T)-F12 heats of formation, *Phys. Chem. Chem. Phys.*, 14, 21, 7724 – 7738 (2012).
4. Hughes, Thomas F., and Richard A. Friesner, Systematic Investigation of the Catalytic Cycle of a Single Site Ruthenium Oxygen Evolving Complex Using Density Functional Theory, *J. Phys. Chem. B*, 1, 115, 9280 - 9289 (2011).
5. Hughes, Thomas F. and Richard A. Friesner, Correcting Systematic Errors in DFT Spin-Splitting Energetics for Transition Metal Complexes, *J. Chem. Theor. Comput.*, 7, 1, 19 - 32 (2011).
6. Schneebeli, Severin, T., M. Kamenetska, Z. Cheng, R. Skouta, R. Friesner, L. Venkataraman, R. Breslow, Single-molecule conductance through multiple π - π stacked benzene rings determined with direct electrode-to-benzene ring connections, *J. Am. Chem. Soc.*, 133, 7, 2136-2139. (2011).
7. Hall, Michelle Lynn, Jing Zhang, and Richard A. Friesner, Continuous Localized Orbital Corrections to Density Functional Theory: B3LYP - CLOC, *J. Chem. Theo. Comput.*, 6, 3647 (2010).

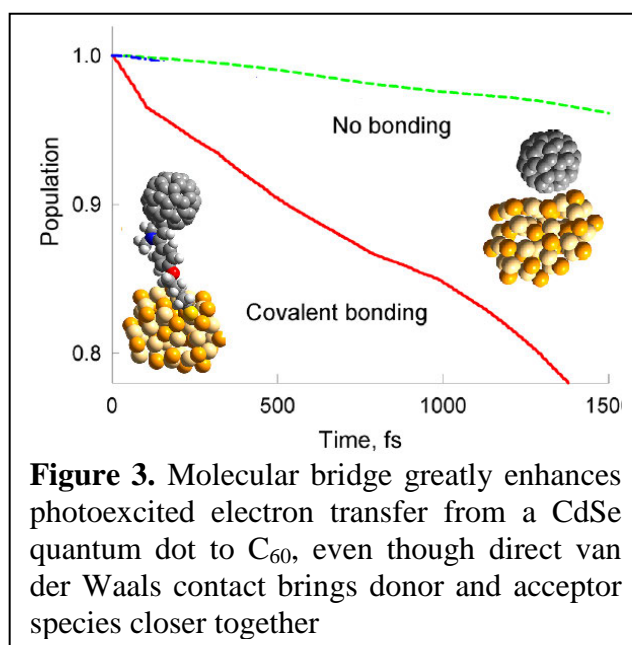
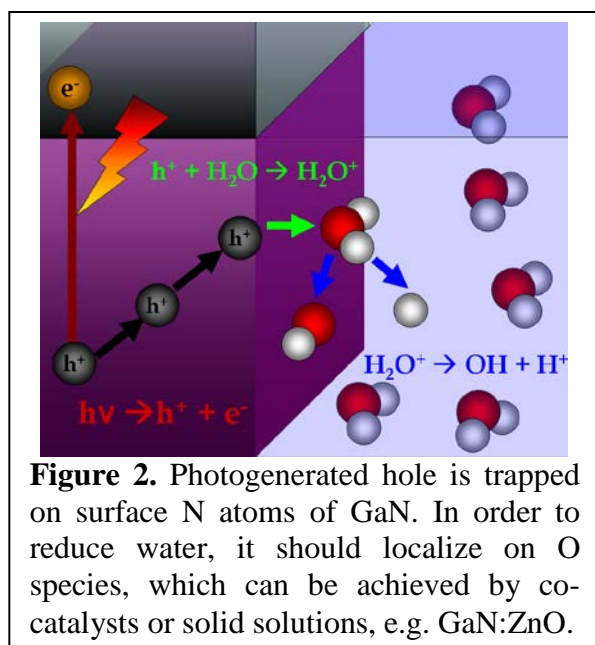
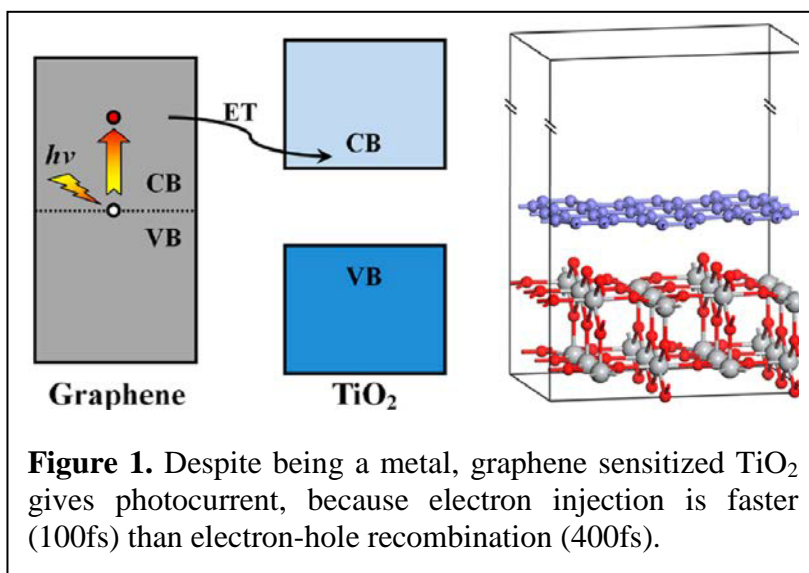
Time-Domain Ab Initio Studies of Light-Harvesting and Charge Transfer in Nanoscale Systems for Solar Photoconversion

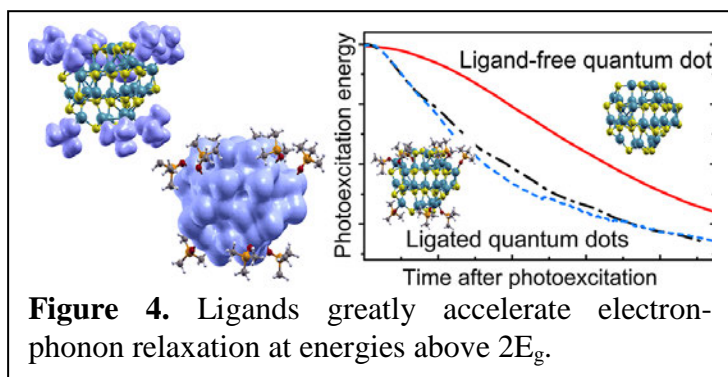
Oleg Prezhdo

Department of Chemistry
University of Rochester
Rochester, NY 14534

Solar energy applications require understanding of dynamical response of novel materials on nanometer scale. Our state-of-the-art non-adiabatic molecular dynamics techniques, implemented within time-dependent density functional theory, allow us to model such response at the atomistic level and in real time.

The talk will focus on photoinitiated charge transfer at the interfaces of bulk semiconductors with a variety of systems, including organic chromophores, monolayer and bulk water, semiconductor quantum dots, and graphene. Theoretical description of these processes meets multiple challenges due to stark differences in the properties of the individual components forming the interface.

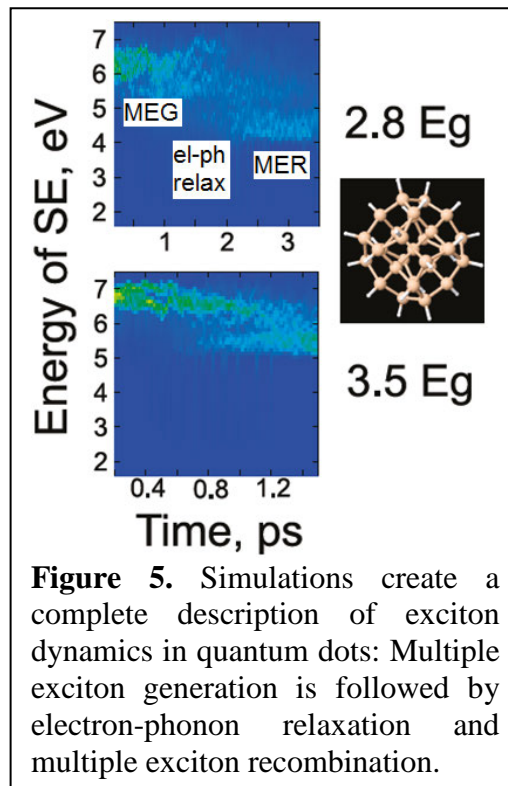




Efficiencies of dye-sensitized semiconductor solar cells rely on rapid electron transfer from a dye molecule into a semiconductor substrate, electron transport from surface to bulk to electrode, and limited charge trapping and recombination at the interface. Photocatalytic water splitting requires migration of a hole, generated in a bulk semiconductor, to the semiconductor surface, and hole transfer onto oxygens of hydroxyl group and water molecules. Quantum dots are quasi-zero dimensional structures with a unique combination of molecular and bulk properties. Used in

place of molecular chromophores, they can increase solar cell efficiencies due to new physical phenomena, such as phonon bottleneck and multiple exciton generation. An excellent conductor, graphene has been used to sensitize inorganic semiconductors and to achieve a photovoltaic effect. At the same time, it has zero band-gap, and photoexcited electrons and holes can rapidly lose all energy by coupling to phonons, resulting in complete photovoltaic efficiency loss.

We are able to characterize the rates, mechanisms and branching ratios of the competing steps involved in the photovoltaic and photocatalytic processes in nanoscale materials and interfacial systems. Our simulations provide a unifying description of excited state dynamics on nanoscale, resolve highly debated issues, and generate theoretical guidelines for development of novel systems for solar energy harvesting and utilization.



DOE Sponsored Publications 2010-2013

Reviews and Feature Articles

1. A. A. Akimov, A. J. Neukirch, O. V. Prezhdo “Theoretical insights into photoinduced charge transfer and catalysis at metal oxide surfaces”, *Chem. Rev.*, accepted.
2. V. V. Chaban, O. V. Prezhdo “Ionic and molecular liquids: hand in hand for robust engineering”, *J. Phys. Chem. Lett.*, accepted.
3. H. M. Jaeger, K. Hyeon-Deuk, O. V. Prezhdo “Exciton multiplication from first principles”, *Acc. Chem. Res.*, accepted.
4. K. Hyeon-Deuk, O. V. Prezhdo “Photoexcited electron and hole dynamics in semiconductor quantum dots: phonon-induced relaxation, dephasing, multiple exciton generation and recombination”, *J. Phys. Cond. Matt.*, **24**, 363201 (2012).
5. S. A. Fischer, C. M. Isborn, O. V. Prezhdo, “Excited states and optical absorption of small semiconducting clusters: dopants, defects and charging”, *Chem. Science*, **2**, 400 (2011).

Regular Articles

6. S. V. Kilina, A. J. Neukirch, B. F. Habenicht, D. S. Kilin, O. V. Prezhdo “Quantum Zeno effect rationalizes the phonon bottleneck in semiconductor quantum dots”, *Phys. Rev. Lett.*, accepted.
7. H. Wei, C. M. Evans, B. D. Swartz, A. J. Neukirch, J. Young, O. V. Prezhdo, and T. D. Krauss “Colloidal semiconductor quantum dots with tunable surface composition”, *Nano Lett.*, **12**, 4465 (2012).
8. S. Kilina, K. A. Velizhanin, S. Ivanov, O. V. Prezhdo, S. Tretiak, “Surface ligands increase photoexcitation relaxation rates in CdSe quantum dots”, *ACS Nano*, **6**, 6515 (2012).
9. A. J. Neukirch, Z. Guo, O. V. Prezhdo “Time-domain ab initio study of phonon-induced relaxation of plasmon excitations in a silver quantum dot”, *J. Phys. Chem. C*, **116**, 15034 (2012).
10. H. M. Jaeger, S. Fischer, O. V. Prezhdo “The role of surface defects in multi-exciton generation of lead selenide and silicon semiconductor quantum dots”, *J. Chem. Phys.*, **136**, 064701 (2012).
11. K. Hyeon-Deuk, O. V. Prezhdo “Multiple exciton generation and recombination dynamics in small Si and CdSe quantum dots: an ab initio time-domain study”, *ACS Nano*, **6**, 1239 (2012).
12. R. Long, O. V. Prezhdo “Ab initio nonadiabatic molecular dynamics of the ultrafast electron injection from a PbSe quantum dot into the TiO₂ surface”, *J. Am. Chem. Soc.*, **133**, 19240 (2011).
13. S. V. Kilina, D. S. Kilin, V. V. Prezhdo, O. V. Prezhdo “Theoretical study of electron-phonon relaxation in PbSe and CdSe quantum dots: evidence for phonon memory”, *J. Phys. Chem. C*, **115**, 21641 (2011).
14. L. L. Chen, H. Bao, T. Z. Tan, O. V. Prezhdo, X. L. Ruan “Shape and temperature dependence of hot carrier relaxation dynamics in spherical and elongated CdSe quantum dots”, *J. Phys. Chem. C*, **115**, 11400 (2011).
15. K. Hyeon-Deuk, O. V. Prezhdo, “Time-domain ab initio study of Auger and phonon-assisted Auger processes in a semiconductor quantum dot”, *Nano Lett.*, **11**, 1845 (2011).

16. S. R. Fischer, B. F. Habenicht, A. B. Madrid, W. R. Duncan, O. V. Prezhdo, "Regarding the validity of the time-dependent Kohn-Sham approach for electron-nuclear dynamics via trajectory surface hopping", *J. Chem. Phys.*, **134**, 024102 (2011); Jan. 24, 2011 issue of *Virt. J. Nanoscale Sci. & Tech.*
17. V. V. Chaban, O. N. Kalugin, B. F. Habenicht, O. V. Prezhdo, "The influence of the rigidity of a carbon nanotube on the structure and dynamics of confined methanol", *J. Phys. Soc. Japan*, **79**, 064608 (2010).
18. V. V. Chaban, T. I. Savchenko, S. N. Kovalenko, O. V. Prezhdo, "Heat-driven release of a drug molecule from carbon nanotubes: a molecular dynamics study", *J. Phys. Chem. B*, **114**, 13485 (2010); Journal Cover.
19. A. Ueta, Y. Tanimura, O. V. Prezhdo, "Distinct infrared spectral signatures of the 1,2- and 1,4-fluorinated single-walled carbon nanotubes: A molecular dynamics study", *J. Phys. Chem. Lett.*, **1**, 1307 (2010).

Sensitization of Single Crystal Semiconductor Electrodes with Dyes, Quantum Dots and Polymers

Justin Sambur, Dae Jin Choi, John G. Rowley, Yongqi Liang, Alec Nepomnyashchii,
Kevin Watkins, Theodore Kraus and Bruce Parkinson

Department of Chemistry and School of Energy Resources
University of Wyoming
Laramie, WY 82071

Recent results from our work on spectral sensitization of single crystal semiconductor electrodes will be presented. We have performed a series of investigations on sensitizing both n and p type gallium phosphide single crystals. Anomalous photocurrents were measured where the same dye was able to produce sensitized photocurrents on both n and p type GaP crystals. Numerous scenarios where this could happen were considered but it was determined that sensitization of the p-type crystals was from normal hole injection into the GaP valence band whereas the sensitized photocurrents from the same dye on the n-type crystals was a result of a sensitized photocorrosion reaction. Photoetching of the n-type GaP produced high area electrodes with correspondingly higher photocurrents.

We have also been continuing our sensitization studies on semiconducting metal oxide single crystals. ZnO single crystal electrodes were fabricated into internal reflection prisms to test our long-standing assumption that the photocurrent yields we measure for dye monomers and dye aggregates on the crystal surfaces were proportional to their coverage on the electrode surface or that monomer and aggregates had the same quantum yields for photocurrent production. Our initial results for a model dicarboxylated thiocyanine dye indicates that our assumption was valid at least in the case of this dye. We have also been studying the influence of the doping density of the semiconducting oxide substrate on the yields of sensitized photocurrents. Preliminary results indicate that there is an optimum doping level where the electrical field gradient from the space charge layer is high enough to rapidly separate the injected electron and eliminate the back reaction where the electron returns to the photo-oxidized dye. These results are being compared to a model developed by Spitler that predicted the yields and current voltage behavior¹. Currently high temperature vacuum annealing or reduction with hydrogen is used to change the doping density of these crystals. Substitutional doping is the preferred method for doping these materials since it results in less strain and formation of trap states. We have had success with the growth of homoepitaxial layers of titanium dioxide with atomic layer deposition (ALD) where ordered single crystal layers are templated on either rutile or anatase substrates. Substitutional doping of these layers with niobium should produce higher quality substrates for fundamental studies of sensitization.

We will also discuss recent results from our collaboration with the Schanze Group at the University of Florida. We were able to verify that a poly(phenylene ethylene) conjugated polyelectrolyte, that was specifically synthesized to avoid aggregation, can photosensitize n-type zinc oxide (0001) single crystals and was demonstrated not to aggregate by both photocurrent spectroscopy and AFM imaging at the single polymer molecule level.

DOE Sponsored Publications 2009-2012

1. Dae Jin Choi, John G. Rowley, Mark Spitler and B. A. Parkinson, "Dye Sensitization of Four Low Index TiO₂ Single Crystal Photoelectrodes with a Series of Dicarboxylated Cyanine Dyes", *Langmuir*, submitted
2. A. B. Nepomnyashchii and B. A. Parkinson, "The Influence of the Aggregation of a Carbazole Thiophene Cyanoacrylate Sensitizer on Sensitized Photocurrents on ZnO Single Crystals", *Langmuir*, submitted
3. Douglas Shepherd, Justin Sambur, Yong-Qi Liang, Bruce A. Parkinson, Alan Van Orden, "*In-Situ* Studies of Photoluminescence Quenching and Photocurrent Yield in Quantum Dot Sensitized Single Crystal TiO₂ and ZnO Electrodes", *J. Phys. Chem. C*, 116, 21069-21076, (2012)
4. Carrick M. Eggleston, Justin R. Stern, Tess M. Strellis and Bruce A. Parkinson, "A Natural Photoelectrochemical Cell for Water Splitting: Implications for Early Earth and Mars", *American Mineralogist*, 97, 1804-1807, (2012)
5. Jennifer D. Schuttlefield, Justin B. Sambur, Melissa Gelwicks, Carrick M. Eggleston and B. A. Parkinson, "Photooxidation of Chloride by Oxide Minerals: Implications for Perchlorate on Mars", *J. Am. Chem. Soc.*, 133(44), 17521-17523, (2011)
6. B. A. Parkinson, "Combinatorial Identification and Optimization of New Oxide Semiconductors for Photoelectrochemical Hydrogen Production, *Electronic Materials: Science & Technology*", Volume 102, Part 2, 173-202, (2012)
7. Dae Jin Choi, John G. Rowley and B. A. Parkinson, "Dye Sensitization of n and p type Gallium Phosphide Photoelectrodes", *J. Electrochem. Soc.*, 159(11), H846-852, (2012)
8. Yongqi Liang, James E. Thorne, B. A. Parkinson, "Sensitization of ZnO Single Crystal Electrodes with CdSe Quantum Dots", in preparation
9. F. E. Osterloh and B. A. Parkinson, "Recent developments in solar water-splitting photocatalysis", *MRS Bulletin*, 36(1), 17-22, (2011)
10. C. M. Eggleston, B. A. Parkinson and E. S. Bramlett, "The hematite-pyrite tandem cell: Avenue to understanding Mars photochemical water oxidation?" *Geochimica, et Cosmochimica Acta*, 74(12), A261, (2010).
11. Justin B. Sambur, Christopher M. Averill, Colin Bradley, Jennifer Schuttlefield, Seung Ho Lee, John R. Reynolds, Kirk S. Schanze and B. A. Parkinson, "Interfacial Morphology and Photoelectrochemistry of Conjugated Polyelectrolytes Adsorbed on Single Crystal TiO₂", *Langmuir*, 27, 11906-11916, (2011)
12. Jianghua He and B. A. Parkinson, "A Combinatorial Investigation of the Effects of the Incorporation of Ti, Si, and Al on the Performance of α -Fe₂O₃ Photoanodes", *ACS Combinatorial Science*, 13, 399-404, (2011)
13. Justin B. Sambur, Thomas Novet and B. A. Parkinson, "Multiple Exciton Collection in a Sensitized Photovoltaic System", *Science*, 330, 63-66, (2010)
14. Justin B. Sambur and B. A. Parkinson, "CdSe/ZnS Core/Shell Quantum Dot Sensitization of

- Low Index TiO₂ Single Crystal Surfaces”, J. Am. Chem. Soc., 132 (7), 2130–2131, (2010)
15. Justin B. Sambur, Shannon C. Riha, Dae Jin Choi and B. A. Parkinson, “ The Influence of Surface Chemistry on the Binding and Electronic Coupling of CdSe Quantum Dots to Single Crystal TiO₂ Surfaces”, Langmuir, 26(7), 4839–4847, (2010)
 16. Mark T. Spitler and B. A. Parkinson, “Dye Sensitization of Single Crystal Semiconductor Electrodes”, Accounts of Chemical Research, 42, 2017-2029, (2009)
 17. Michael Woodhouse and B. A. Parkinson, “Combinatorial Approaches for the Identification and Optimization of Oxide Semiconductors for Efficient Solar Photoelectrolysis”, Chemical Society Reviews, 38(1), 197-210, (2009)
 18. Zhu, X. Z., Nepomnyashchii, A. B., Parkinson, B. A. and Schanze, K. S., “Imaging and Photoelectrochemical Properties of Single Molecules of a Poly(Phenylene Ethylene) Conjugated Polyelectrolyte on ZnO Single Crystals Surfaces” in preparation

Session IX

Dye Sensitized Systems

Bisphenanthrolinecopper(I) in Photoinduced Charge Separation and DSSC Dyes

C. Michael Elliott, L. N. Ashbrook, and M.S. Lazorski

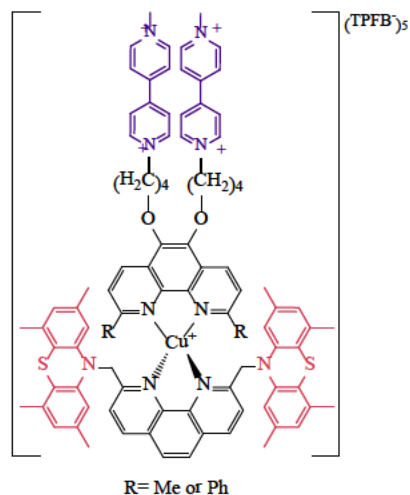
Department of Chemistry
Colorado State University
Ft. Collins, CO 80523

Photoinduced Charge-Separated State Formation in $[\text{Cu}(\text{P})_2]^+$ -based Donor-Chromophore Acceptor Assemblies.

Bisphenanthrolinecopper(I) complexes, $[\text{Cu}(\text{P})_2]^+$, have a number of desirable photophysical properties that mirror those of trisbipyridineruthenium(II). For example, the extinction coefficient for MLCT absorption of $[\text{Cu}(\text{P})_2]^+$ at ca. 550 nm is relatively large and the resultant MLCT excited state is quite a strong reductant, much stronger in fact than $[\text{Ru}(\text{bpy})_3]^{2+*}$. However, efforts to design and study donor-chromophore-acceptor supermolecular assemblies based on $[\text{Cu}(\text{P})_2]^+$ chromophores have been limited relative to $[\text{Ru}(\text{bpy})_3]^{2+}$ or other similar chromophores, largely because of the numerous challenges presented by the coordination chemistry of Cu(I). First, upon either excitation to the MLCT state or oxidation to Cu(II), the complex undergoes Jahn-Teller distortion towards a square-planar geometry which can result in an increase in the coordination number and a concomitant decrease in the excited-state energy. Second, unlike $[\text{Ru}(\text{bpy})_3]^{2+}$, $[\text{Cu}(\text{P})_2]^+$ complexes are typically labile; therefore, different strategies must be developed if the goal is to assemble heteroleptic complexes in which the donor and acceptor moieties are appended to different ligands. Third, $[\text{Cu}(\text{P})_2]^{2+}$ is a relatively weak oxidant, thus more easily oxidized donors are required than in $[\text{Ru}(\text{bpy})_3]^{2+}$ -based charge separation assemblies.

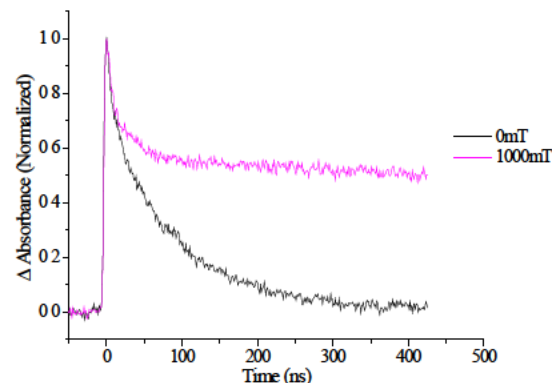
We have prepared a series of $[\text{Cu}(\text{P})_2]^+$ -based D-C⁺-A²⁺ assemblies which undergo efficient, long-lived photoinduced charge-separated state formation--an example is shown here. As we demonstrated from earlier studies of related $[\text{Ru}(\text{bpy})_3]^{2+}$ -based D-C-A assemblies, the ability of the donor to associate with the chromophore via π - π interaction is essential in achieving large CSS-formation quantum yields. By design, locating the donors on the 2,9-positions of one phenanthroline allows for a similar π -stacking interaction with the second phenanthroline and provides steric bulk which helps thermodynamically favor the formation of the desired heteroleptic complex.

A critical aspect of the CSS lifetime (and likely its formation) is its spin chemistry. As is true for ruthenium analogs, the initial formed ¹MLCT undergoes rapid intersystem crossing. As a consequence, the observed charge-separated state is formed as a triplet-correlated radical cation pair (³CSS, D^{•+}-C⁺-A^{•+}); thus, recombination to the singlet ground state is spin-forbidden. As a consequence, the recombination kinetics are strongly perturbed by the presence of even modest magnetic fields. For example, in 1,2-difluorobenzene the decay of the ³CSS is approximately a single exponential with a life time of $\tau \approx 94$ ns. In an applied field of a few mT the decay becomes biexponential. At 1 T the lifetime of



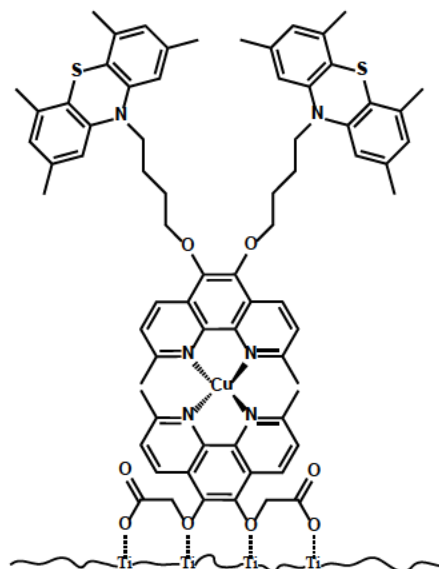
slow component (which comprises ca. 2/3 of the total CSS population) is approximately $\times 60$ longer than in zero field ($\tau_{1000\text{mT}} \approx 5.8 \mu\text{s}$). Moreover, the field dependant behavior of the copper assemblies are considerably more complex than for their $[\text{Ru}(\text{bpy})_3]^{2+}$ -based counterparts. For example, the CSS formation quantum yield depends on the field strength, but not for $[\text{Ru}(\text{bpy})_3]^{2+}$ -based assemblies. Detailed magnetic field studies on these assemblies are currently under way in an effort to understand their complex spin chemistry.

Effect of a Magnetic Field on the TA Decay of the of the $[\text{Cu}(\text{P})_2]^{+5}$ D-C-A at 560 nm in 1,2-Difluorobenzene



$[\text{Cu}(\text{P})_2]^{+}$ -Based DSSC Dyes.

For the same reasons that $[\text{Cu}(\text{P})_2]^{+}$ can function as a chromophore in D-C-A charge-separation assemblies, it can also function as a dye in DSSCs. Constable and co-workers have reported reasonable efficiencies from conventionally configured Grätzel cells in which the traditional ruthenium-based dyes were replaced with Cu(I) complexes of 6,6'-dimethyl-4,4'-diCOOH-2,2'-bipyridine. Unfortunately, $[\text{Cu}(\text{L})_2]$ complexes lack even intermediate term chemical and photochemical stability in I^-/I_3^- electrolyte; however, the same stability issue do not exist with $[\text{Co}(\text{bipy})_3]^{2+/3+}$ mediators. Because of the lability of $[\text{Cu}(\text{P})_2]$ in solution, it is possible to use a stepwise approach to assemble heteroleptic Cu(I) complex dyes on TiO_2 surfaces which exhibit good stability. An example of such a complex, $[\text{Cu}(\text{P})(\text{P-D})]^{+}$, which comprises both a Cu(I) chromophore with COOH binding moieties and a secondary electron donor, is shown here. The J-V behavior of cells incorporating this $[\text{Cu}(\text{P})(\text{P-D})]^{+}$ dye is significantly improved relative to analogs lacking the appended donor. Transient absorption experiments indicate that the hole is transferred from the oxidized Cu(II) to the donor within a few nanoseconds after photo injection.



The presence of certain solution additives common in traditionally configured Grätzel-type DSSCs, specifically 4-*t*-butylpyridine (TBP), causes dramatic changes in the cell behavior with these copper dyes. For example, TBP significantly reduces the apparent photoinjection efficiency for all of the dyes studied. For the dyes lacking the appended donor, the presence of TBP causes significant decay in the photocurrent under constant illumination over 10s of seconds. However, the process is reversible and the initial photocurrents fully recovers after several minutes in the dark. Also, similar photocurrent decays are not observed for the $[\text{Cu}(\text{P})(\text{P-D})]^{+}$ dye. We have interpreted these observations as: (1) in the case of reduced photoinjection efficiency, competition for binding sites on the TiO_2 between TBP and the ether oxygens of the surface binding phenanthroline and (2) in the case of the photocurrent decay, reversible incorporation of the TBP into the coordination sphere of the photooxidized Cu(II).

DOE Sponsored Publications 2010-2013

1. H-K Seo, C.M. Elliott, H-S Shin. "Mesoporous TiO₂ Films Fabricated Using Atmospheric Pressure Dielectric Barrier Discharge Jet," ACS Applied Materials & Interfaces, DOI: 10.1021/am100731w (Nov. 2010).
2. H-K Seo, H-S Shin, E-K Suh, C.M. Elliott. "A Novel Approach for the Synthesis of Rutile Titania Nanotubes at Very Low Temperature," J Vacuum Sci & Technology B, 29:2, 021019, DOI: 10.1116/1.3554737 (March 2011).
3. H.-K. Seo, E. R. Fisher, and C. M. Elliott, "Fast One-Step Method to Synthesize TiO₂ Nanoparticle Clusters for Dye Sensitized Solar Cells, , J. Nanosci. Nanotechnol. 12:8, 6276-6282 (2012).
4. Megan S. Lazorski, Riley H. Gest, and C. Michael Elliott, " Photoinduced, Multi-Step, Charge Separation in a Heteroleptic Cu(I) bis-Phenanthroline Based Donor-Chromophore-Acceptor Triad," J. Amer. Chem Soc. (2012), 134 (42), pp 17466–17469 DOI: 10.1021/ja3085093
5. Ammon P. Lehnig, Megan S. Lazorski, Michael Mingroni, Kimberly A. O. Pacheco, and C. Michael Elliott, "Oxidation of 2,9-Diphenyl-1,10-phenanthroline to Generate the 5,6-Dione and its Subsequent Alkylation," J. Heterocycl. Chem., Submitted: March 2013 .
6. Gaddie, Ross; Moss, Christopher; Elliott, C. Michael. "Cyclic Voltammetric Study of Cobalt Poly-4-*t*-butylpyridine Ligand Complexes on Glassy Carbon Electrodes: Electrolyte Dependence and Mechanistic Considerations" Langmuir (2012), DOI: 10.1021/la304262a
7. Ashbrook, Lance; Elliott, C. Michael. "Dye Sensitized Solar Cell Studies of a Donor-Appended Bis(2,9-dimethyl-1,10-phenanthroline) Cu (I) Dye Paired with a Cobalt-Based Mediator" J. Phys Chem. C (2012), DOI: 10.1021/jp3123693.
8. Seo, Hyung-Kee; Elliott, C. Michael; Ansari, S.G. "Enhanced Photocatalytic Properties of Nanoclustered P-Doped TiO₂ Films Deposited by Advanced Atmospheric Plasma Jet" J. Nanosci. Nanotechnol. 12:9, 6996-7001 (2012).
9. Xue, Di; Ashbrook, Lance N.; Gaddie, Ross S.; Elliott, C. Michael "Tris(4,4'-*di-t*-butyl-2,2'-bipyridine)cobalt: Cation Effects on the Voltammetry at ITO and on Mediator Performance in Dye Sensitized Solar Cells" J. Electrochem Soc. (2013) DOI: 10.1149/2.115306jes
.
.
.

Model Dyes for Study of Molecule/Metal Oxide Interfaces and Electron Transfer Processes

E. Galoppini,¹ A. Kopecky,¹ K. Chitre,¹ A. Batarseh
R. A. Bartynski,² S. Rangan,² S. Coh,² C. Ruggieri²
G. J. Meyer,³ P. Johansson,³ R. M. O'Donnell³

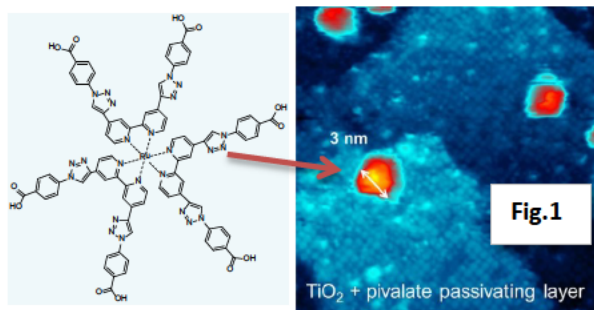
¹Department of Chemistry, Rutgers University, Newark, NJ

²Department of Physics and Astronomy, Rutgers University, New Brunswick, NJ

³Department of Chemistry, Johns Hopkins University, Baltimore, MD

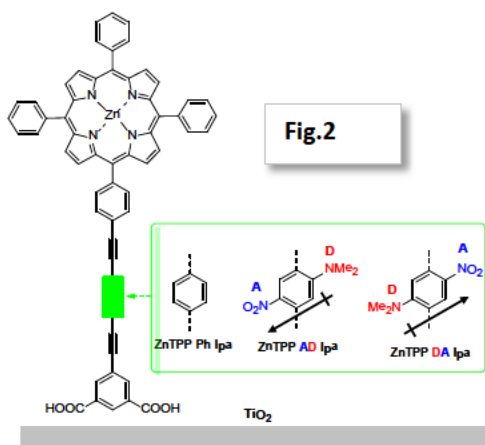
The objective of this research is to control, at the molecular level, binding, orientation, distance, and dipole orientation of model dyes on oxide semiconductor surfaces and to study how such parameters influence interfacial charge transfer processes that are relevant to solar energy conversion. The talk will describe our progress in the following three areas of research.

1. Star Ru(II) Complexes (*Galoppini, Bartynski, Meyer*). We have developed molecular sensitizers capable of providing enhanced control of surface binding and interfacial electronic properties. We synthesized nano-sized (2 to 4 nm diameter) homoleptic complexes of Ru(II) (“Stars”), where the linker units shield the metal center from the heterogeneity of the semiconductor surface,



resulting in reduced binding uncertainty and an unprecedented control over the charge transfer processes (slower recombination). Homoleptic ($[\text{Ru}(\text{L})_3]^{2+}$) and complexes carrying rigid ligands (L), comprised of oligophenylethyne units (OPE) or 1,2,3-triazole groups and a designated anchor group, Fig. 1, have been synthesized by cross-coupling reactions or click chemistry, respectively, and studied computationally, and experimentally in solution and on metal oxide surfaces. To elucidate the nature of binding to the surface, and determine the electronic structure and interactions with the oxide surface, we have studied Star complexes adsorbed on well-characterized single crystal TiO₂(110) surfaces under ultrahigh vacuum conditions. Scanning tunneling microscopy images (Fig. 1) show that the Star complexes do not form extensive islands, nor do they preferentially bind at step edges. Rather, they appear on the surface either as individual molecules or as small two- or three-member clusters. X-ray photoelectron spectra

indicate that the molecule remains intact upon adsorption. Photoemission and inverse photoemission spectra show that the molecular HOMO lies within the TiO₂ band gap, 1.0 eV above the valance band maximum, that the LUMO is degenerate with the conduction band, and that an interface dipole of 1.3 eV is present in this system. Further studies on morphologically rough surfaces such as ZnO(11-20), that offer multiple bonding opportunities to tether the ligands, are underway.

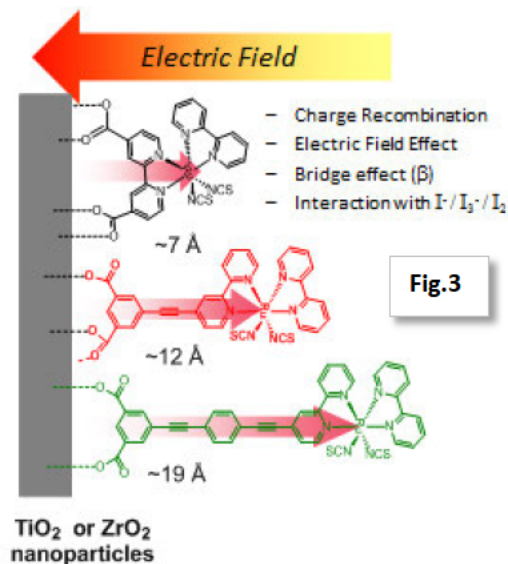


2. Sensitizers with Built-in Dipoles in Linkers. (*Galoppini, Bartynski*) Energy alignment between the molecular orbitals of adsorbed dye molecules and an

oxide semiconductor substrate is a key factor in photo-induced charge transfer processes. Typically, this alignment is governed by the nature of the molecule-oxide bond. However, by employing dye molecules with a head-linker-anchor architecture, where the HOMOs and LUMOs are on the head group, one can incorporate dipoles on the linker group that can be used to tailor energy level alignment. We have synthesized and studied a series of porphyrins with a built-in dipole in the linker. The presence of an electron donor (D) and acceptor (A) substituent on opposite sides of the linker phenyl provides a permanent intramolecular dipole with a component that is perpendicular to the surface, Fig.2. Photoemission and inverse photoemission spectra have been obtained from single crystal $\text{TiO}_2(110)$ surfaces sensitized with the porphyrins shown in Fig.2. In one set of measurements, the molecules have D and A groups on the linker, in the other set, those groups are absent. *Initial spectroscopic studies show that the energy levels of molecule with the internal dipole, in particular the levels associated with the porphyrin head group, are shifted to higher energy as compared to those of the molecule whose linker is not functionalized.* Further studies, investigating the effects of reversing the positions of the D and A groups on the linker (i.e., reversing the direction of the dipole), as well as varying the degree of charge transfer effected by the D and A groups (i.e., varying the magnitude of the dipole) are underway. In addition, the effects of linker on the energy alignment and separation of chromophore levels will be studied.

3. Distance and Electric Field Effects of Electron Transfer of Ru(II) N3-type complexes.

(Meyer, Galoppini). Electrons injected into nanostructured metal oxide semiconductors generate a significant electric field, yet the role this field plays in charge transfer processes at illuminated molecular-semiconductor interfaces remains poorly understood. Three ruthenium complexes, **AK0**, **AK1** and **AK2**, Fig. 3, and containing a linker made of $(\text{OPE})_n$ units with $n = 0, 1, 2$ between the bpy and an isophthalic acid group, were synthesized. These were bound to TiO_2 films to quantify interfacial charge transfer at variable distances (from ~ 7 to $\sim 19 \text{ \AA}$) from the surface electric field. The injection of electrons in TiO_2 resulted in a blue shift of the MLCT absorption band consistent with a Stark effect. The electric field experienced by the chromophoric end of the compounds decreased as the number of OPE spacers increased. After photoinduced electron injection, the fast ($10^{-8} - 10^{-5} \text{ s}$ time scale) charge recombination dynamics were found to be dependent on the number of OPE units, behavior that was most pronounced when the steady state illumination, $\text{TiO}_2(e^-)$ concentration, and/or the laser power were increased. These and other experiments that will be discussed indicate that charge recombination can be inhibited with increased distance particularly when the number of injected electrons is large, i.e. in the conditions that are relevant to the operational power of solar cells. Interestingly, longer, compounds exhibited increased open circuit photovoltage, V_{oc} , and very high ideality factors, a behavior ascribed to slower recombination. The incident photon-to-current efficiencies of dye sensitized solar cells based on these compounds decreased markedly for **AK1** and **AK2** because of formations of adducts with iodine.



DOE Sponsored Publications 2010-2013

PUBLISHED

1. *Energy alignment, molecular packing and electronic pathways: zinc(II) tetraphenylporphyrin derivatives adsorbed on TiO₂(110) and ZnO(1120) surfaces* S. Rangan, S. Coh, R. Allen Bartynski, K. Chitre, E. Galoppini, C. Jaye, D. Fischer *J. Phys. Chem. C* **2012**, *116*, 23921-23930. DOI: [10.1021/jp307454y](https://doi.org/10.1021/jp307454y)
2. *Synthesis of Homoleptic Ruthenium 'Star' Complexes via Click Reaction* Chitre, K. P.; Guillén, E.; Soojin Yoon, A. Elena Galoppini *European Journal of Inorganic Chemistry* **2012**, *33*, 5461-5464. DOI: [10.1002/ejic.201200896](https://doi.org/10.1002/ejic.201200896).
3. *Light-harvesting and electronic contacting capabilities of Ru(II) Ipa rod and star complexes - first principles predictions*, Persson, P; Knitter, M.; Galoppini E. *RSC Advances* **2012**, *2*, 7868-7874. DOI: [10.1039/C2RA21240D](https://doi.org/10.1039/C2RA21240D)
4. Fluorescence Enhancement of Di-p-tolyl Viologen by Complexation in Cucurbit[7]uril M. Freitag, L. Gundlach, P. Piotrowiak, E. Galoppini* *J. Am. Chem. Soc.*, **2012**, *134* (7), 3358–3366 DOI: [10.1021/ja206833z](https://doi.org/10.1021/ja206833z)
5. *Slow Q1 excited state injection and charge recombination at star-shaped ruthenium polypyridyl compounds—TiO₂ interfaces* Patrik G. Johansson, Yongyi Zhang, Maria Abrahamsson, Gerald J. Meyer and Elena Galoppini *Chem Comm*, **2011**, *47*, 6410-6412. DOI: [10.1039/c1cc11210d](https://doi.org/10.1039/c1cc11210d)
6. *Homoleptic star-shaped Ru(II) complexes* Y. Zhang, E. Galoppini, P. G. Johansson and G. J. Meyer *Pure and Applied Chemistry*, **2011**, *83*, 861-868.
7. **invited perspective** *Molecular Host-Guest Complexes: Shielding of Guests on Semiconductor Surfaces* M. Freitag, E. Galoppini, *Energy Environ. Sci.* **2011**, *4*, 2482-2494.
8. *Solar Energy Conversion – Natural to Artificial* H. Němec, E. Galoppini, H. Imahori, V. Sundstrom Elsevier series of books on Nanoscience: Comprehensive Nanoscience and Technology. Ed. D Andrews. Elsevier 2010
9. *Synthesis of Strapped Porphyrins: Towards Insulation of the Chromophore on Semiconductor Surfaces*. C.-H. Lee, E. Galoppini *J. Org. Chem.* **2010**, *75*, 3692-3704. DOI: [10.1021/jo100434t](https://doi.org/10.1021/jo100434t)
10. *Synthesis of Capped Tetrachelate Porphyrins*. Chi-Hang Lee, Keyur Chitre and Elena Galoppini *Journal of the Chinese Chemical Society* **2010** special issue, *57*, 1-8
11. *Decreased interfacial charge recombination rate constants with N3-type sensitizers*. M. Abrahamsson, P.G. Johansson, A. Kopecky, E. Galoppini G. J Meyer *J. Phys. Chem. Lett.* **2010**, *1*, 1725 DOI: [10.1021/jz100546y](https://doi.org/10.1021/jz100546y)
12. *Modular Synthesis of Ruthenium Tripodal System with Variable Anchoring Groups Positions for Semiconductor Sensitization*. C-H Lee, Y. Zhang, A. Romayanantakit, . E. Galoppini, *Tetrahedron* **2010**, *22*, 3897-3903.
13. *Influence of electron-cation interaction on electron mobility in dye-sensitized ZnO and TiO₂ nanocrystals: A study using ultrafast terahertz spectroscopy* H. Němec, J. Rochford, O.

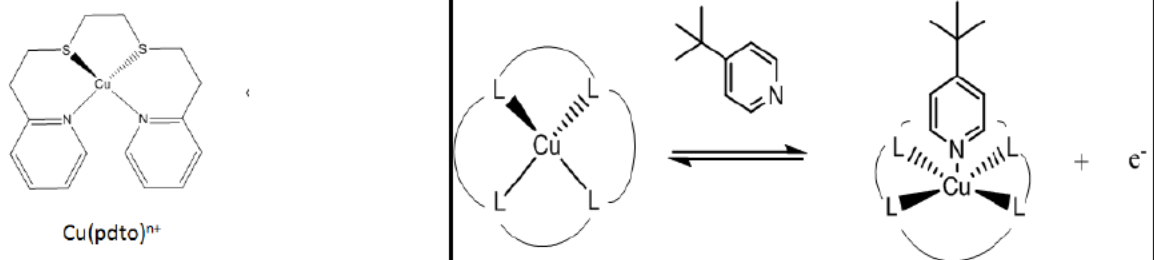
- Taratula, E. Galoppini, P. Kužel, T. Polívka, A. Yartsev, V. Sundström *Phys. Rev. Lett.* **2010**, *104*, 197401 DOI: 10.1103/PhysRevLett.104.197401.
14. *Efficient preparation of photoswitchable dithienylethene-linker-conjugates by palladium-catalyzed coupling reactions of terminal alkynes with thienyl chlorides and other aryl halides* Marc Zastrow, Sujatha Thyagarajan, Saleh A. Ahmed, Paul Haase, Sabine Seedorff, Dmitri Gelman, Josef Wachtveitl, Elena Galoppini and Karola Rück-Braun *Chemistry an Asian Journal* **2010**, *5*, 1202-12.
 15. **Invited review** *Organic aromatic hydrocarbons as sensitizing dye models for semiconductor nanoparticles* Y. Zhang, E. Galoppini *ChemSusChem* **2010**, *3*, 410-428.
 16. *Energy levels alignment of a Zinc(II) Tetraphenylporphyrin dye adsorbed onto TiO₂(110) and ZnO(1120) surfaces* S. Rangan, R. Thorpe, R.A. Bartynski, J. Rochford, E. Galoppini *J. Phys. Chem. C* **2010**, *114*, 1139-1147
 17. *“Energy level alignment of catechol molecular orbitals on ZnO(11-20) and TiO₂(110) surfaces,”* Sylvie Rangan, Jean-Patrick Theisen, Eric Bersch, and R. A. Bartynski, *Applied Surface Science* **2010**, *256*, 4829-4833.

Fundamental Studies of Light-induced Charge Transfer, Energy Transfer, and Energy Conversion with Supramolecular Systems

Joseph T. Hupp
Dept. of Chemistry
Northwestern University
Evanston, IL 60208

This project seeks to exploit supramolecular chemistry: a) to interrogate and understand fundamental aspects of light-induced charge transfer and energy transfer, and b) to construct solar energy conversion systems that make use of unique assembly motifs to address key conversion efficiency issues. The project focuses specifically on developing, investigating, and understanding at a fundamental-science level the behavior of promising new light harvesters and redox shuttles in DSC environments.

Redox shuttles. New redox shuttles based on macrocyclic complexes of Cu(I) and Cu(II) have been examined. An example is shown below. In these systems, desired dark-current-suppression/back-ET-inhibition is achieved via oxidation-state-dependent coordination and release of a solvent molecule or auxiliary ligand. The degree of dark-current suppression is tunable based on the strength of the Cu(II)-(auxiliary ligand) interaction, with stronger interaction causing greater back-ET inhibition. These systems lack the high-driving-force requirements of the iodide/tri-iodide system, as well as its corrosiveness and its undesirable propensity to associate with highly polarizable organic light-harvesters. Furthermore, the copper shuttles are more stable than the archetypal fast redox shuttle, ferrocene⁺⁰, and diffuse faster than tris-polypyridyl cobalt shuttles. Also being studied are new organic redox shuttles.

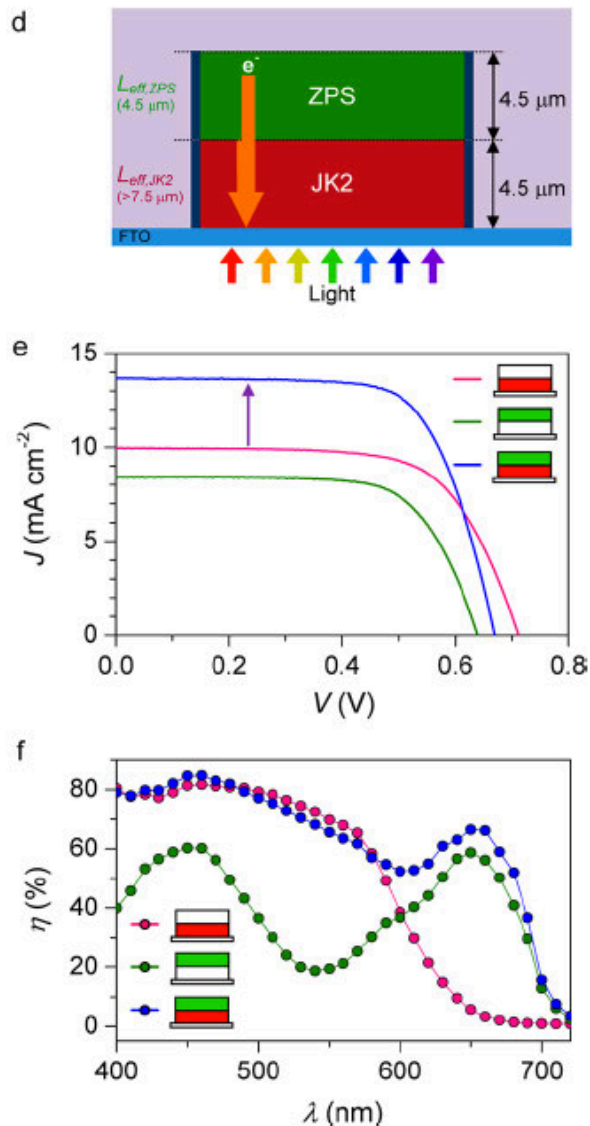


Light harvesters: Strategy and organizational rule for panchromatic sensitization based on complementary chromophores. Dye-sensitized solar cells, especially those comprising molecular chromophores and inorganic titania, have shown promise as an alternative to silicon for photovoltaic light-to-electrical energy conversion. Co-sensitization (the use of two or more chromophores having complementary absorption spectra) has attracted attention as a method for harvesting photons over a broad spectral range. If implemented successfully, then cosensitization can substantially enhance photocurrent densities and light-to-electrical energy conversion efficiencies. In only a few cases, however, have significant overall improvements been obtained. In most other cases, inefficiencies arise due to unconstructive energy or charge transfer between chromophores or because of modulation of charge-recombination behavior. Spatial isolation of differing chromophores offers a solution. We recently reported a new and versatile method for

fabricating two-color photoanodes featuring spatially isolated chromophore types that are selectively positioned in desired zones. Exploiting this methodology, we found that photocurrent densities depend on both the relative and absolute positions of chromophores and on "local" effective electron collection lengths. One version of the two-color photoanode, based on an organic push pull dye together with a porphyrin dye, yielded high photocurrent densities ($J(\text{sc}) = 14.6 \text{ mA/cm}^2$) and double the efficiency of randomly mixed dyes, once the dyes were optimally positioned with respect to each other. (See examples at right.) We believe that the organizational rules and fabrication strategy will prove transferrable, thereby advancing understanding of panchromatic sensitization as well as yielding higher efficiency devices.

Light harvesters: Extended chromophoric arrays.

Given that energy (exciton) migration in natural photosynthesis primarily occurs in highly ordered porphyrin-like pigments (chlorophylls), equally highly ordered porphyrin-based metal-organic frameworks (MOFs) might be expected to exhibit similar behavior, thereby facilitating antenna-like light-harvesting and positioning such materials for use in solar energy conversion schemes. We recently reported the first example of directional, long-distance energy migration within a MOF. Two MOFs, namely **F-MOF** and **DA-MOF** that are composed of two Zn(II) porphyrin struts [5,15-dipyridyl-10,20-bis(pentafluorophenyl)porphinato]zinc(II) and [5,15-bis[4-(pyridyl)ethynyl]-10,20-diphenylporphinato]zinc(II), respectively, were investigated. From fluorescence quenching experiments and theoretical calculations, we found that the photogenerated exciton migrates over a net distance of up to 45 porphyrin struts within its lifetime in **DA-MOF** (but only 3 in **F-MOF**), with a high anisotropy along a specific direction; see cartoon at right. The remarkably efficient exciton migration in **DA-MOF** is attributed to enhanced π -conjugation through the addition of two acetylene moieties in the porphyrin molecule, which leads to greater Q-band absorption intensity and much faster exciton-hopping (energy transfer between adjacent porphyrin struts). The long distance and directional energy migration in **DA-MOF** suggests promising applications of this compound or related compounds in solar energy conversion schemes as an efficient light-harvesting and energy-transport component.



DOE Sponsored Publications 2010-2013

1. "Photoinduced Electron Transfer from Rail to Rung within a Self-assembled Porphyrin Oligomeric Ladder," C. She, S.-J Lee, J. E. McGarrah, J. Vura-Weis, M. R. Wasielewski, H. Chen, G. C. Schatz, M. A. Ratner and J. T. Hupp, *Chem. Commun.*, **2010**, 46, 547-549.
2. "Dye-Sensitized Solar Cells: Sensitizer-Dependent Injection into ZnO Nanotube Electrodes," R. A. Jensen, H. Van Ryswyk, C. She, J. M. Szarko, L. X. Chen, J. T. Hupp, *Langmuir*, **2010**, 26, 1401-1404.
3. "Excess Polarizability Reveals Exciton Localization/Delocalization Controlled by Linking Positions on Porphyrin Rings in Butadiyne-Bridged Porphyrin Dimers," C. She, S. Easwaramoorthi, P. Kim, S. Hiroto, I. Hisaki, H. Shinokubo, A. Osuka, D. Kim, J. T. Hupp, *J. Phys. Chem.*, **2010**, 114, 3384-3390.
4. "Dye Sensitized Solar Cells: TiO₂ Sensitization with a Bodipy-Porphyrin Antenna System," C. Y. Lee, J. T. Hupp, *Langmuir*, **2010**, 26, 3760-3765.
5. "Dye-Sensitized Solar Cells: Driving-Force Effects on Electron Recombination Dynamics with Cobalt Based Shuttles," M. DeVries, M. J. Pellin, J. T. Hupp, *Langmuir*, **2010**, 26, 9082-9087.
6. "Ni(III)/(IV) Bis(dicarbollide) as a Fast, Non-Corrosive Redox Shuttle for Dye-Sensitized Solar Cells," T. Li, A. Spokoyny, C. She, O. K. Farha, C. A. Mirkin, T. J. Marks, J. T. Hupp *J. Am. Chem. Soc.*, **2010**, 132, 4580-4582.
7. "Electronic Tuning of Ni-based Bis(dicarbollide) Redox Shuttles In Dye-Sensitized Solar Cells," A. M. Spokoyny, T. C. Li, O. K. Farha, C. W. Machan, C. She, C. L. Stern, T. J. Marks, J. T. Hupp, and C. A. Mirkin, *Angew. Chem. Int. Ed.*, **2010**, 49, 5339-5343.
8. "Porphyrin Sensitized Solar Cells: TiO₂ Sensitization with a π -extended Porphyrin Possessing Two Anchoring Groups," C. Y. Lee, C. She, N. C. Jeong, and J. T. Hupp, *Chem. Commun.* **2010**, 46, 6090 - 6092.
9. "SiO₂ Aerogel-Templated, Porous TiO₂ Photoanodes for Enhanced Performance in Dye-Sensitized Solar Cells Containing a Ni(III)/(IV) Bis(dicarbollide) Shuttle," T. C. Li, F. Fabregat-Santiago, O. K. Farha, A. M. Spokoyny, S. Ruiz, J. Bisquert, C. A. Mirkin, T. J. Marks, and J. T. Hupp, *J. Phys. Chem. C*, **2011**, 115, 11257-11264.
10. "The Role of Electronic Couplings in Linear Porphyrin Arrays Probed by Single-Molecule Fluorescence Spectroscopy," J. Yang, J. Lee, C. Y. Lee, N. Aratani, A. Osuka, J. T. Hupp, D. Kim, *Chem. Eur. J.*, **2011**, 17, 9219-9225.

11. “Light-Harvesting Metal-Organic Frameworks (MOFs): Efficient Strut-to-Strut Energy Transfer in Bodipy and Porphyrin-based MOFs,” C. Y. Lee, O. K. Farha, B. J. Hong, A. A. Sarjeant, S. T. Nguyen, J. T. Hupp, *J. Am. Chem. Soc.* **2011**, *133*, 15858–15861.
12. “Luminescent Infinite Coordination Polymer Materials from Metal-terpyridine Ligation,” O. K. Farha, C. Stern, O. C. Compton, J. T. Hupp, S. T. Nguyen, *Dalton Trans.*, **2011**, *40*, 9189-9193.
13. “Effective Panchromatic Sensitization of Electrochemical Solar Cells: Design Rules and Strategy for Spatial Separation of Complementary Light-Harvesters on High-area Semiconductor Surfaces,” N. C. Jeong, C. Prasittichai, H-J. Son, R. A. Jensen, C. Y. Lee, O. K. Farha, J. T. Hupp, *J. Am. Chem. Soc.*, **2012**, *134*, 19820-19827
14. “Light Harvesting and Ultrafast Energy Migration in Porphyrin-Based Metal-Organic Frameworks,” H-J. Son, S. Jin, S. Patwardhan, S. J. Wezenberg, N. C. Jeong, M. So, C. E. Wilmer, A. A. Sarjeant, G. C. Schatz, R. Q. Snurr, O. K. Farha, G. P. Wiederrecht, J. T. Hupp, *J. Am. Chem. Soc.*, **2013**, *135*, 862-869.
15. “Energy Transfer from Quantum Dots to Metal-Organic Frameworks for Enhanced Light Harvesting,” S. Jin, H-J. Son, O. K. Farha, G. Wiederrecht, J. T. Hupp, *J. Am. Chem. Soc.* **2013**, *135*, 955-958.

Posters

Electronic Transport via Stokes-Shifted Dark States in Colloidal Quantum Dot Solids

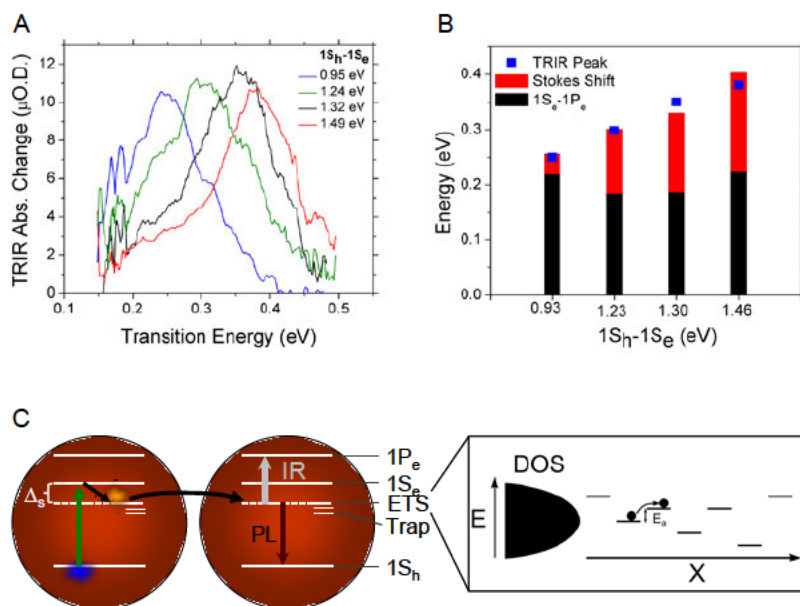
John B. Asbury

Department of Chemistry
The Pennsylvania State University
University Park, PA16802

An outstanding question regarding the mechanism of charge transport in quantum dot solids is resolved by revealing the existence of Stokes shifted electron transport states within the optical bandgap of nanocrystalline quantum dots. The mechanism of charge conduction and the influence that ligand-nanocrystal interactions have on the transport states are examined with a combination of ultrafast infrared spectroscopy and transient photocurrent measurements. By probing mid-infrared (mid-IR) electronic transitions of photo-excited charges on femtosecond to microsecond time scales, a comprehensive view of charge transport and recombination is obtained that enables unprecedented clarity regarding the nature and origin of transport states in quantum dot solids.

Figure 1A represents transient infrared absorption spectra measured 500 ns following bandgap excitation of PbS quantum dots arrayed in a nanocrystalline solid. The average frequencies of the mid-IR electronic transitions depend sensitively on the bandgaps of the quantum dots as has been previously observed by others. Quantitative analysis of the mid-IR transition energies reveals that they cannot be explained by transitions among conventional quantum confined band states such as $1S_h-1P_e$ intraband transitions. Instead, the transition energies are quantitatively described by the sums of $1S_h-1P_e$ transition energies and Stokes shift energies, Δ_s , of the quantum dots (Figure 1B).

Following bandgap excitation, excitons/charge carriers rapidly cool to band edge states at the Stokes shift energy below the $1S_e$ quantum confined levels of nanocrystals. Electrons need not be thermally promoted back up to $1S_e$ states to undergo charge transport. Instead electrons hop via an activated process among Stokes shifted electron transport states (ETS, Figure 1C). The activation energy arises from inhomogeneity in site energies of the transport states due to polydispersity of the quantum dot bandgaps. The origin of the Stokes shifted transport states, their implications for solar energy transduction, and the influence ligand-nanocrystal interactions have on their properties and energies are discussed.



Diode Linkers for the Covalent Attachment of Mn Catalysts to TiO₂ Surfaces

Christian Negre, Laura J. Allen, Rebecca L. Milot, Karin Brumback,
Gary W. Brudvig, Charles A. Schmuttenmaer, Robert H. Crabtree and Victor S. Batista
Department of Chemistry
Yale University
New Haven, CT 06520-8107

We characterize the electronic rectification properties of molecular linkers that covalently bind Mn catalysts to TiO₂ surfaces. Our focus is on Mn-complexes with phenylterpyridine ligands attached to 3-phenyl-acetylacetonate anchors via amide bonds.¹ We find that a suitable choice of the amide linkage yields directionality of interfacial electron transfer, essential to suppress recombination. Our findings are supported by calculations of current-voltage (I-V) characteristics at metallic atomic junctions, based on first-principles methods that combine non-equilibrium Green's function techniques with density functional theory.^{2,3} Our computational results are consistent with EPR measurements, confirming an asymmetry of electron transfer rates

for linkers with significant rectification. In addition, the computed molecular conductance of organic linkers is found to be directly correlated to the photoinduced interfacial electron transfer in sensitized TiO₂ surfaces. The reported studies are particularly relevant for the development of photovoltaic, or photocatalytic, devices based on functionalized TiO₂ thin-films where the overall performance is affected by recombination processes competing with interfacial electron injection.

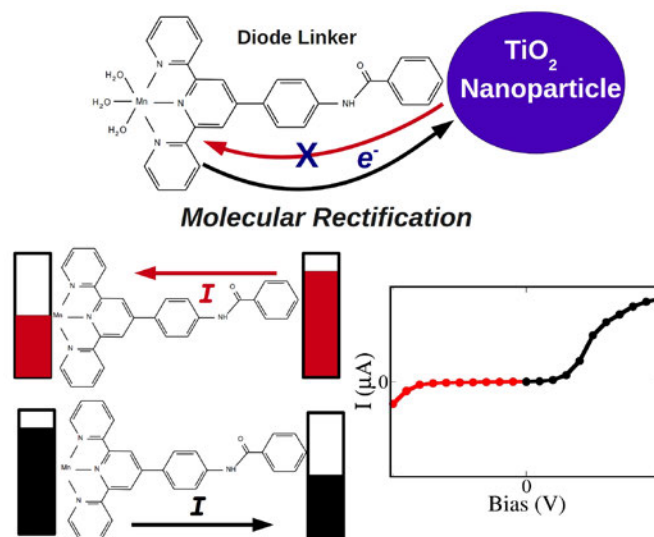


Figure 1: Top: Schematic illustration of a molecular linker that covalently binds a Mn catalyst to TiO₂ surfaces and yields directionality of interfacial electron transfer. Bottom: Molecular rectification found by the calculated electron transport properties of the Mn-complex between metallic electrodes.

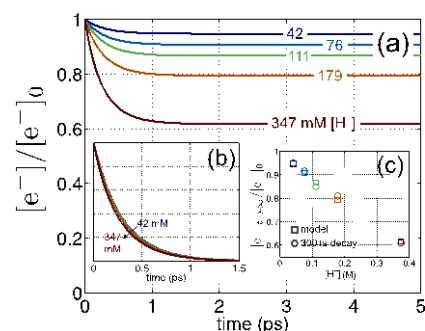
1. McNamara, W. R.; Snoeberger, R. C., III; Li G.; Schleicher, J. M.; Cady, C. W.; Pyatos, M.; Schmuttenmaer, C. A.; Crabtree, R. H.; Brudvig, G. W.; Batista, V. S. *J. Am. Chem. Soc.* **2008**, 130, 14329-14338.
2. Rocha, A. R.; Garcia-Suarez, V.; Bailey, S. W.; Lambert, C. J.; Ferrer, J.; Sanvito, S. *Phys. Rev. B* **2006**, 73, 085414
3. Palma, J. L.; Cao, C.; Zhang, X.-G.; Krstic, P. S.; Krause, J. L.; Cheng, H.-P. *J. Phys. Chem. C* **2010**, 114, 1655-1662.
4. Linker Rectifiers for Covalent Attachment of Transition Metal Catalysts to Metal-Oxide Surfaces, Negre, C.; Palma, J. L.; Allen, L. J.; Young, K. J.; Milot, R. L.; Schmuttenmaer, C. A.; Brudvig, G. W.; Crabtree, R. H. and Batista, V. S. *J. Am. Chem. Soc.* **2013**, submitted.

Electron Dynamics in pyrrolidinium bis(trifluoromethylsulfonyl)amid ionic liquids

Benjamin FitzPatrick, Andrew T. Healy, Francesc Molins, and David A. Blank
Department of Chemistry
University of Minnesota
Minneapolis, MN and 55455

The use of room temperature ionic liquids, RTILs, continues to expand across a broad range of energy related technologies. In many of these applications, for example solar and nuclear energy conversion, stability of the liquid under photolytic and radiolytic conditions becomes an important consideration. Some of the most commonly employed RTILs have an aromatic cation, which reacts readily with excess electrons. In contrast, aliphatic RTILs such as pyrrolidinium-based examples have proven to be more stable in the presence of excess electrons.

When compared with more common solvents, RTILs exhibit dilation of some solvent reorganization time scales. Temporal expansion of the solvation process enhances the influence of non-equilibrium electron reactivity following both radiolysis and photo-ionization. In radiolysis experiments with 15 ps time resolution, Wishart and coworker measured the trapping of the electron and demonstrated that electron reactivity declines with time.¹ These experiments also demonstrated that significant reactivity was lost much faster than 15 ps. Using photodetachment we have measured the dynamics on sub-ps time scales.² Transient absorption of the electron and the hole were measured throughout the visible and most recently extended into the near-IR. The results agree well with the computational predictions of Margulis et al. for the initial “dry” electron and hole,³ and exhibit interesting similarities and differences when compared with the radiolysis experiments. In the presence of perchloric acid we found a significant, previously unobserved sub-ps component in the reactivity of the electrons. The amplitude of this component depended linearly on the acid concentration, however the sub-ps apparent rate was independent of the acid concentration (see figure). This was explained by electron reactivity that was controlled by solvation. The results indicate a rate for electron scavenging that directly reflects solvent reorganization. By comparing a homologous series of pyrrolidinium cations, increasing the size of the non-polar alkane tail from 4 to 10 carbons, we are able to probe the influence of RTIL structure⁴ on the electron dynamics.



[Py₁₄⁺][NTf₂⁻] (a) Loss of photo-detached electrons as a function of quencher concentration. (b) Comparison after subtraction of the long time offset. (c) Comparison between the solvent controlled model and the measured asymptotic quenching.

¹ J. F. Wishart, A. M. Funston, T. Szreder, A. R. Cook, and M. Gohdo, Electron solvation dynamics and reactivity in ionic liquids observed by picosecond radiolysis techniques, *Faraday Discuss.* **154**, 353-363 (2012).

² F. Molins, B. FitzPatrick, A. T. Healy, and D. A. Blank, Photodetachment and electron reactivity in 1-methyl-1-butyl-pyrrolidinium bis(trifluoromethylsulfonyl)amide, *J. Chem. Phys.*, **137**, 034512 (2012).

³ C. J. Margulis, H. V. R. Annapureddy, P. M. De Biase, D. Coker, J. Kohanoff, and M. G. Del Popolo, Dry Excess Electrons in Room-Temperature Ionic Liquids, *J. Am. Chem. Soc.* **133**, 20186-20193 (2011).

⁴ C. S. Santos, N. S. Murthy, G. A. Baker, and E. W. Castner, X-ray scattering from ionic liquids with pyrrolidinium cations, *J. Chem. Phys.*, **134**, 121101 (2011).

Semiconductor-electrocatalyst contacts: theory, experiment, and applications to solar water photoelectrolysis

Shannon W. Boettcher, Fuding Lin, Thomas J. Mills
Department of Chemistry
University of Oregon
Eugene, OR 97403

Photoelectrochemical water-splitting cells incorporate semiconductors coupled with electrocatalyst films in aqueous electrolytes. The common picture for the operation of such semiconductor/catalyst/solution (SCS) systems is that the semiconductor absorbs light and separates charge while the catalyst increases the rate of the hydrogen- or oxygen-evolution reaction (HER or OER, respectively). Experiments, however, show that after deposition of OER catalysts onto n-type semiconductors the photoelectrode characteristics, e.g. the photovoltage, photocurrent, and fill-factor, change in a manner not always consistent with this simple model. Competing hypotheses have attributed this behavior to changes in surface recombination, band-bending, interface charge-trapping, optical effects, or kinetics. The goal of this work is to develop a complete microscopic picture of electron transfer to describe SCS systems.

We report a theory of SCS systems that accounts for the kinetics of charge transfer between the semiconductor, catalyst, and solution for catalysts with different ion permeability and electronic density of states.¹ This is important because catalysts can be dense metals, hydrous/porous ion-permeable oxyhydroxides, or molecules. We apply the theory using numerical simulations to predict the behavior of illuminated n-type semiconductor photoelectrodes in contact with such catalysts. We show that for ion-permeable materials the effective barrier for electron injection across the semiconductor/catalyst interface increases as the film is oxidized to its operational state. This allows ion-permeable catalysts to compensate for slow catalyst rate constants by increasing their chemical potential to maintain the photocurrent. We also report a method to quantify parasitic optical absorption in the catalyst layer and predict optimal catalyst loading.²

To support the theory and simulations, we developed a dual-electrode voltammetry test-architecture to probe the potential of the catalyst layer in model SCS systems as a function of illumination, the semiconductor potential, and the catalyst structure.³ Experimental results are in accord with theory, showing that ion-permeable catalyst layers exhibit unpinned interfacial barriers and improved performance relative to dense catalysts.

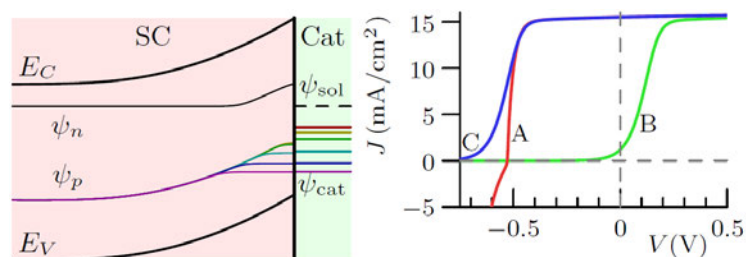


Fig 1. Simulation results of ion-permeable OER catalyst showing changes in catalyst potential and surface hole concentrations as a function of the catalyst kinetics.

- (1) Mills, T. J.; Boettcher, S. W. Theory and simulations of electrocatalyst-coated semiconductor electrodes for applications in solar water splitting. *To be submitted*. **2013**.
- (2) Trotochaud, L.; Mills, T. J.; Boettcher, S. W. An optocatalytic model for semiconductor-catalyst water-splitting photoelectrodes based on in situ optical measurements on operational catalysts. *J. Phys. Chem. Lett.* **2013**, *4*, 931-935.
- (3) Lin, F.; Boettcher, S. W. The role of adaptive interfaces in composite semiconductor-electrocatalyst solar water-splitting cells. *In preparation*. **2013**.

Photoelectrochemical Oxidation of a Turn-On Fluorescent Probe Mediated by a Surface Mn^{II} Catalyst Covalently Attached to TiO₂ Nanoparticles

Alec C. Durrell, Gonghu Li, Matthieu Koepf, Christian F. A. Negre, Laura J. Allen, William R. McNamara, Hee-eun Song, Victor S. Batista, Robert H. Crabtree, and Gary W. Brudvig

Department of Chemistry
Yale University
New Haven, CT 06520-8107

A manganese complex covalently attached to a TiO₂ electrode via a light-absorbing organic linker (**L**) was used in the photooxidation of 2',7'-dihydrodichlorofluorescein (H₂DCF). Significant and sustained photocurrent was observed upon visible-light illumination on the fully assembled anode in the presence of the substrate. The two-electron, two-proton oxidation of H₂DCF yields the fluorescent compound, 2',7'-dichlorofluorescein (DCF). Our studies suggest that the Mn^{II}-**L**-TiO₂ architecture is an effective photoanode for multielectron chemistry, as production of DCF under visible-light illumination exceeds yields observed for bare TiO₂ as well as Zn^{II}-**L**-TiO₂ anodes. The turn-on fluorescent behavior of H₂DCF upon oxidation makes it an excellent substrate for the study of new photoanodes. The high fluorescence quantum yield of DCF allows for nanomolar sensitivity and real-time monitoring of substrate oxidation. Additionally, illumination of the sensitized electrode in a 1% solution of 2-propanol results in similar sustained currents, suggesting the Mn^{II}-**L**-TiO₂ electrode may be competent for the photoelectrochemical oxidation of 2-propanol to acetone.

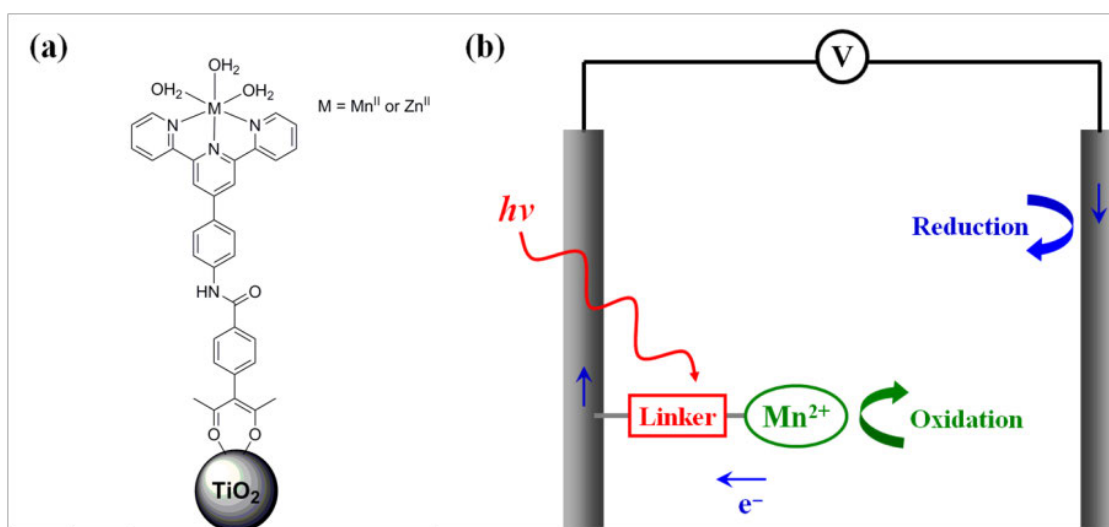


Figure 1. (a) The structure of a molecular Mn^{II} catalyst attached to a TiO₂ surface via a terpy-acac ligand (**L**), and (b) the schematic of a photoelectrochemical cell containing a light-absorbing linker and a Mn^{II} catalyst.

Towards Solar Fuels Enabling Cuprous Phenanthroline Complexes

Catherine E. McCusker and Felix N. Castellano*
Department of Chemistry & Center for Photochemical Sciences
Bowling Green State University
Bowling Green, Ohio 43403

Earth abundant copper(I) diimine complexes represent a renewable and economically feasible alternative to commonly used heavy metal containing chromophores. In the metal-to-ligand charge transfer (MLCT) excited state, copper(I) diimine complexes typically undergo a significant structural rearrangement, leading to molecules with large Stokes shifts and very short excited state lifetimes, thereby limiting their usefulness as sensitizers in bimolecular electron and triplet energy transfer reactions. Strategically placed bulky substituents on the coordinating phenanthroline ligands have proven useful in restricting the transiently produced excited state Jahn-Teller distortion, leading to longer-lived excited states. By combining bulky *sec*-butyl groups in the 2- and 9- positions with methyl groups in the 3-,4-, 7-, and 8- positions, a remarkably long-lived (2.8 μs in DCM) copper(I) *bis*-phenanthroline complex, $[\text{Cu}(\text{dsbtmp})_2]^+$, has been synthesized and characterized. Unlike other copper(I) diimine complexes, $[\text{Cu}(\text{dsbtmp})_2]^+$ also retains a μs lifetime in coordinating solvents such as acetonitrile and water as a result of the cooperative sterics inherent in the molecular design. Preliminary results on the use of this complex in hydrogen-forming homogeneous photocatalysis will be presented. Photon upconversion based on sensitized triplet-triplet annihilation (TTA) represents a photochemical means to generate high-energy photons (or high-energy chemical products) from low-energy excitation, having potential applications in solar energy conversion and solar fuels producing devices. For the first time, synthetically facile and earth abundant Cu(I) MLCT sensitizers have been successfully incorporated into two distinct photochemical upconversion schemes, affording both red-to-green and orange-to-blue wavelength conversions.

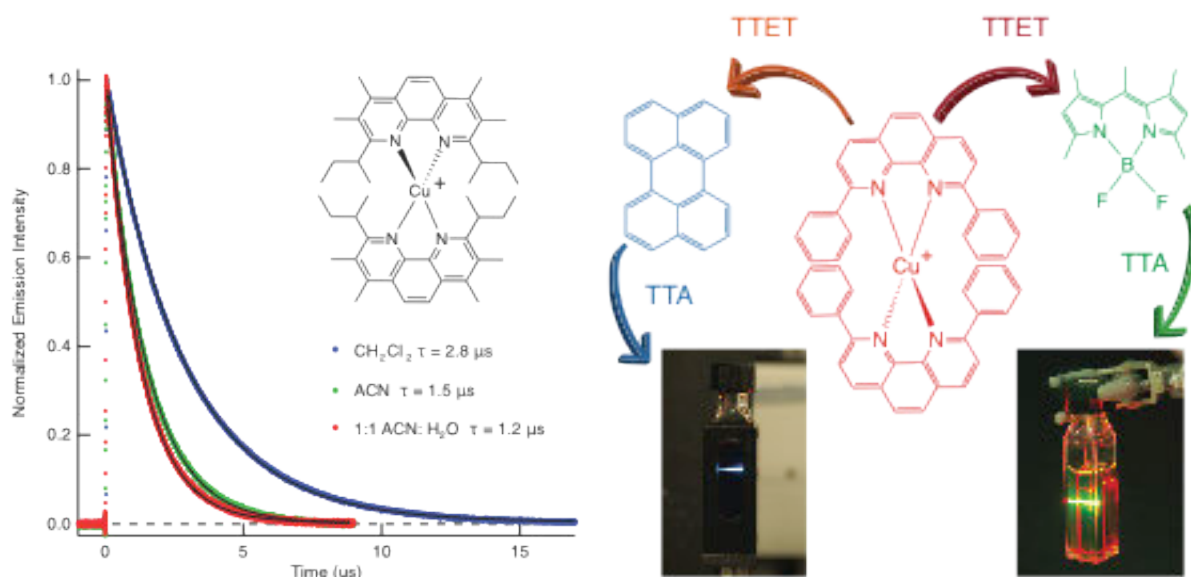


Photo-Induced Electron-Transfer and Solute-Ion Interactions in Ionic Liquids

Sufia Khatun, Min Liang, Marie F. Thomas and Edward W. Castner, Jr.
Department of Chemistry and Chemical Biology
Rutgers, The State University of New Jersey
Piscataway, NJ 08854

Two inter-related projects will be presented from our recent work on electron-transfer chemistry in ionic liquids. In the first project, we study photo-induced electron-transfer chemistry in ionic liquids using electron-donating anions. These anions comprise following the set of cyanates: selenocyanate (SeCN), thiocyanate (SCN), tricyanomethide (C(CN)₃) and dicyanoamide (N(CN)₂). Initial studies have used these anions paired with the 1-ethyl-3-methylimidazolium cation (C[2]-mim⁺). Using Stern-Volmer quenching analysis for the cyanate anion reductively quenching the excited state of 9,10-dicyanoanthracene, we observe diffusion-limited quenching behavior for SeCN and C(CN)₃ in CH₃CN solution. As has been observed previously, when an ionic liquid solvent (C[2]-mim⁺/NTf₂⁻) is used for the same photoreaction, the higher viscosity does retard the reaction rate, but when scaled for viscosity, the reaction is significantly faster than predicted by hydrodynamic laws. The self-diffusion of each species is measured using PG-SE NMR experiments.

The second project applies 2D nuclear Overhauser effect NMR spectroscopy to study the specific interactions between the protons on a redox-active solute, such as ferrocene, cobaltocenium or Ru²⁺(bpy)₃, and each of the ¹H cation spins and the ¹⁹F spins on the anion. More specifically, ROESY studies elucidate the specific interactions between the protons on the solute and the cation, and ¹H-¹⁹F HOESY spectra reveal the specific interactions between the anion and the solute. As the chain length of the alkyl substituent is varied from a shorter ethyl or butyl chain to a longer octyl or decyl chain, the intermediate range order of the liquid is changed. For short chains, both cation and anion interactions are clearly observed, as illustrated for solute-anion interactions in Fig. 1. Significant differences in observed NOE peak volumes are observed in the ROESY and HOESY spectra for longer-chain alkyl substituents on the cations. In this case, the alkyl tails begin to dominate the solute-ion interactions, and a three-fold reduction in the peak volumes for anion-solute interactions is observed.

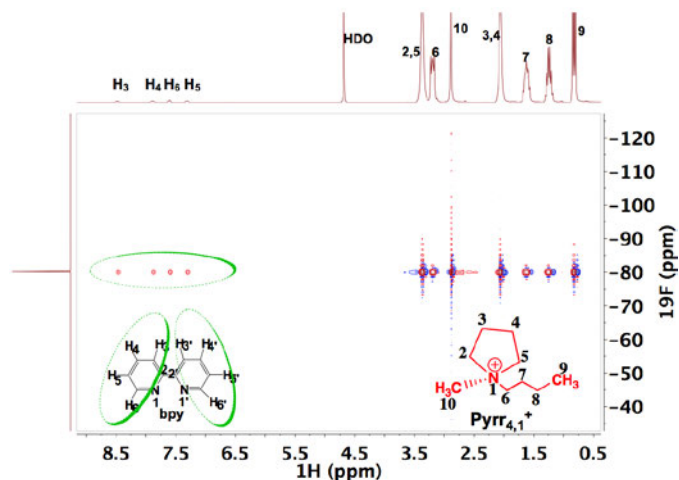


Fig. 1. ¹H-¹⁹F HOESY spectrum for Ru²⁺(bpy)₃ in Pyr_{1,4}⁺/NTf₂⁻, 120 ms mixing time and 295 K.

Physical Properties of Doped and Sensitized Polyoxotitanate Nanostructures

Philip Coppens, Jesse Sokolow, Yang Chen and Elzbieta Trzop
Chemistry Department
University at Buffalo, State University of New York
Buffalo, NY, 14260-3000

We will present the synthesis of novel nanoclusters by both solvothermal and ambient pressure solution methods, followed by crystallographic, spectroscopic and theoretical analysis.

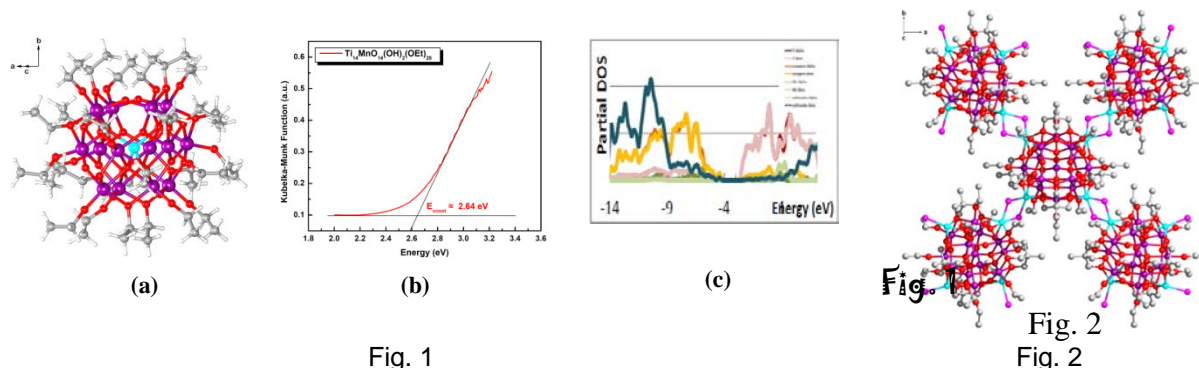


Fig. 1

Fig. 2

Doping of nanoclusters. Doping of the nanoclusters with 14-28 titanium atoms with Na, Li, Mn, Be, Sr, Ba and Pr leads to a considerable reduction of the bandgap compared with undoped clusters. Structure, reflection spectroscopy and calculated DOS for $\text{Ti}_{14}\text{MnO}_{14}(\text{OH})_2(\text{OEt})_{28}$ are illustrated in Figs. 1a, b, c resp. NEXAFS measurements show the tetrahedrally coordinated Mn to be 2+. Related structures and their properties will be presented and compared.

Connecting clusters into larger frameworks.

$\{\text{Ti}_{13}\text{Mn}_4\text{O}_{16}[\text{MeC}(\text{CH}_2\text{O})_3]_4(\text{OEt})_{12}\text{Br}_4\}_\infty$ consists of an infinite framework of clusters connected by Br atoms (Fig. 2). The band gap is observed to be 2.57 eV. A second approach to obtain polymeric frameworks is the use of linkers to connect individual clusters as shown in Fig. 3.

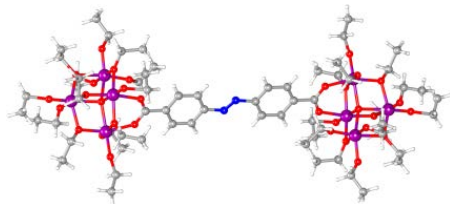


Fig. 3

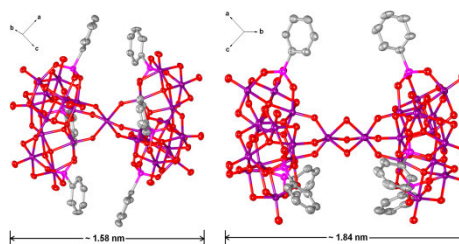


Fig. 4

Sensitizer binding modes. Whereas previous studies revealed both the chelate-bridging and the chelate-bidentate mode in a series of sensitized clusters, two new clusters functionalized with phenylphosphonic acid, $\text{Ti}_{25}\text{O}_{26}(\text{PhenylPO}_3)_6(\text{OEt})_{36}$ and $\text{Ti}_{26}\text{O}_{26}(\text{PhenylPO}_3)_6(\text{OEt})_{39}^+$, exhibit a novel tridentate mode, at variance with predictions made in the literature (Fig. 4).

Comments. The availability of detailed structural information allows theoretical calculations of band structure and the dynamics of electron injection. New infinite framework structures have the potential to lead to fully defined novel anode materials. Supported by DE-FG02-02ER15372.

Modular assembly of high-potential Zn porphyrin sensitizers attached to TiO₂ with a series of anchoring groups

Lauren A. Martini, Gary F. Moore, Rebecca L. Milot, Lawrence Z. Cai,^a Stafford W. Sheehan, Charles A. Schmuttenmaer, Gary W. Brudvig, and Robert H. Crabtree
Department of Chemistry and Energy Sciences Institute
Yale University
New Haven, CT 06520-8107

High-potential photoanodes (HPPAs) are essential for photoelectrochemical cells and where water splitting is the goal, the molecular components of an HPPA have to be stably attached to the semiconductor electrode surface in water as solvent. The standard anchors used at present are –COOH and –PO₄H₂ but the first detaches in water and the second shows poor performance in transmitting photoinjected electrons from a sensitizer.

We earlier introduced 2,4-pentanedione as a water-stable anchor that is stably attached to TiO₂ in water and efficiently mediates interfacial electron transfer. Although the bound 2,4-pentanedionate is robust, work in the most recent grant period indicates that deacetylation of the 2,4-pentanedione can occur particularly when certain groups, such as 4-pyridyl, are attached at the 3 position. We have therefore looked for other anchors that combine water-stability and good interfacial electron injection properties while avoiding easy decomposition.

We now find that hydroxamate not only fulfils all these needs but is also very easily available from RCOOH or RCOOEt by any one of a number of simple functionalization procedures. The compound shown in Fig 1 carries the same 4-pyridyl group that proved problematic in the 2,4-pentanedione derivatives but behaves well here.

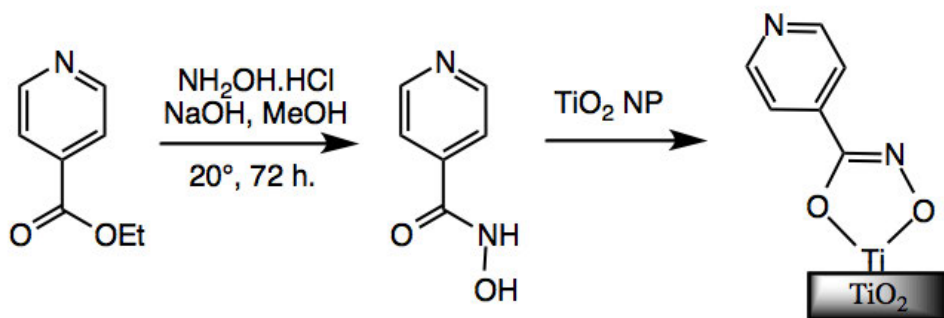


Fig. 1 Functionalization procedure and attachment to TiO₂ nanoparticle.

The THP protected version of the hydroxamate is equally easily synthesized and has the merit of spontaneously deprotecting and binding to TiO₂. This is allowing us to prepare derivatives with sensitive functionality and introduce metal ions without risk of them binding to the hydroxamate. We have also built T-shaped assemblies of the type discussed in the Schmuttenmaer abstract, but using hydroxamate as anchor—these operate in a very satisfactory manner and give promise for future development.

Computational and Experimental Strategies to Achieve, Control, and Understand Singlet Fission in Molecular and Thin Film Systems

Niels H. Damrauer, Paul Vallett, Jamie Snyder, Bijan Paul, Jasper Cook, Thomas Carey, and Ryan Michael
Department of Chemistry and Biochemistry
University of Colorado at Boulder
Boulder, CO 80309

The experiments and computational results to be discussed herein are motivated by previous work in our laboratory where singlet fission (SF) yields in polycrystalline tetracene thin films were modulated by shaped laser fields affecting low-frequency intermolecular (inter-monomer) motions impacting the interaction of π -systems.

These observations motivated the design of bi-chromophoric bis-tetracene molecules in a face-to-face configuration where interchromophore coupling can be synthetically controlled. In this poster we show results of DFT methods that determine the thermodynamics of a series of tetracene dimers that are held in various configurations using polynorbornene bridges (Fig 1). Attaching the bridge to a side position (BT1-t, BT1-c) versus an end position (BT1) results in a decrease in energy of the T_1 state relative to the S_1 state and a subsequent significant increase in SF driving force. In addition, a Davydov splitting (a hallmark of interchromophore coupling) of 87 meV was calculated for BT1-c, a value that is larger than the 34 meV calculated for BT1, and comparable to 78 meV as observed in thin films of tetracene where SF readily occurs. Further computational analysis of the series of dimers shows that the through-bond and through-space coupling can be independently controlled based on dimer geometry and bridge distance, allowing us to explore the effects of the different methods of coupling on SF once synthesized.

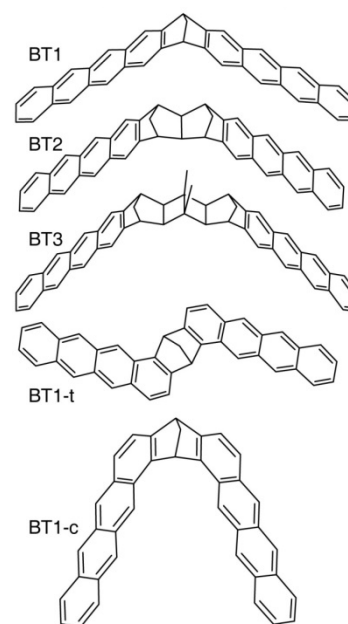


Fig 1. Tetracene dimers under study.

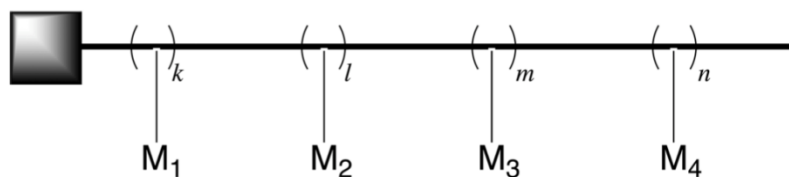
We will describe synthetic progress on the monomers and dimers currently underway in our laboratory. Two strategies have been identified and both are being pursued. The more recent strategy represents a potentially more efficient route towards the monomer and dimers of BT1 utilizing sequential double Wittig reactions to form the tetracene framework.

Finally, we will present exploration into shaped laser fields that can enhance and suppress observed vibrational motions, along with results utilizing more complex shaped fields than simple pulse trains to control SF. Preliminary results implicate a suite of low frequency lattice modes may be present that can affect SF yield in thinner (~50 nm) tetracene films.

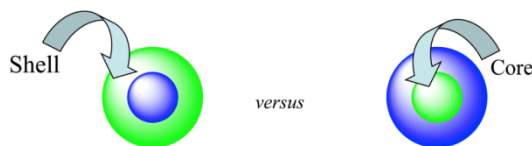
Multicomponent Arrays for Multiple-Redox and Multiple-Excited-State Interactions in Molecular Aggregates

Marye Anne Fox and James K Whitesell
Department of Chemistry and Biochemistry
University of California, San Diego
La Jolla, CA 92305

For several years, we have sought to devise molecular models that contain large numbers of dyes, producing ground states with high extinction coefficients. The resulting multi-component array can efficiently absorb incident light, produce excited states that initiate efficient electron exchange, and drive electron or energy transfer along a desired direction. In such complex arrays, production of multiple electron transfers within a single aggregate can drive light harvesting in multi-electron photoconversion devices.



We focus on those structural features that describe photoinduced electron transfer in polymers and nanocrystals that bear high dye densities. The quantum efficiencies of such devices are quite high when anchored in a specified geometry on a synthetic platform, and the photophysical properties of these arrays may predict those components that can achieve optimal solar utilization and catalysis. Here we describe catalysis or photocatalysis in self-assembled monolayers (SAM), in reactive shell-core clusters (SCC), in functional polymers, and in dendrimers. Each multi-component aggregate is designed to include structural features that can accommodate multiple charges when properly functionalized.



Differences in:

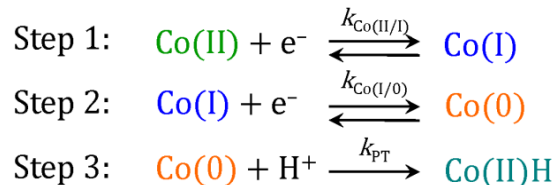
- surface binding sites**
- charge carrier trapping in core**
- surface band edge energetics**

In order to achieve controlled redox chemistry, we must define how physical dispersal of dyes in these arrays affect the excited states of fully loaded aggregates, how directionality toward a target must be included in molecular design, and which competing paths influence the long-term stability of the whole array. We also compare these aggregates with single molecule models used in photosensitization schemes. The scaffold onto which the chromophores are bound can then be compared with other supports encountered when the interacting dyes are imbedded as single entities in sol gels or attached as single adsorbates to a flat metallic surface.

Proton-coupled electron transfer kinetics of the hydrogen evolution reaction

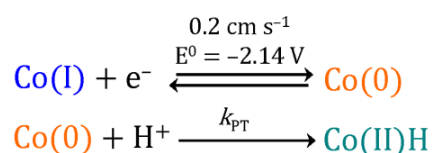
Daniel G. Nocera
Department of Chemistry and Chemical Biology,
Harvard University, Cambridge, MA 02138
dnocera@fas.harvard.edu

Cobalt hangman porphyrins with a xanthene backbone and a carboxylic acid hanging group have been shown to promote the hydrogen evolution reaction (HER). The hangman group is observed to facilitate HER by mediating a proton-coupled electron transfer (PCET) pathway that leads to a hydridic Co(II)H species, which has been shown to be the key intermediate. This species reacts with protons in an ensuing rate determining PT step, leading directly to H₂ generation. The mechanism has been interrogated by electrokinetic analysis according to the following steps:



Analysis and fitting of the electrochemical data yields a heterogeneous rate constant of $k_{0\text{Co(II/I)}} = 0.012 \text{ cm s}^{-1}$. Analysis of step 2 has been aided by the isolation of a Co(0) porphyrin not possessing a hanging group. The electron transfer rate constant of $k_{0\text{Co(I/0)}} = 0.2 \text{ cm s}^{-1}$ is an order of magnitude greater than the Co(II/I) couple, indicative of greater electron delocalization of the electron on the porphyrin ring in a reduced state.

The proton transfer reaction has been examined, step 3, with the following model,

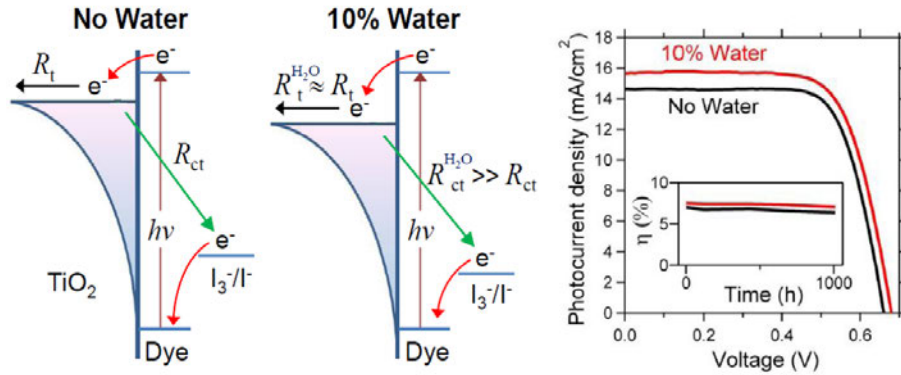


The electrochemical scan rate analysis for the hangman system yields the tunneling proton transfer rate constant for the HER reaction. A rapid intramolecular PT from the carboxylic acid hanging group to the reduced Co(0) center occurs at a rate of $k_{\text{PT}} = 8.5 \times 10^6 \text{ s}^{-1}$, providing a facile pathway for the formation of the Co(II)H species. Conversely, in the case of systems lacking an internal proton relay (non-hangman porphyrins), intermolecular PT rate constants on the order of $1000 \text{ M}^{-1} \text{ s}^{-1}$ were calculated (data will be shown on poster) for the reaction between the Co(0) center and an external acid source (benzoic acid). In comparison to these intermolecular rate constants, the measured intramolecular PT rate constant indicates that the presence of a pendant proton relay proximate to the metal center gives rise to a rate enhancement that is equivalent to an *effective* benzoic acid concentration >3000 M, thus establishing the first quantitative metric for the importance of a proton relay in the HER reaction.

Effects of Water on the Charge-Carrier Dynamics, Photoelectrochemical Properties, and Stability of Dye-Sensitized Solar Cells

Kai Zhu, Song-Rim Jang, and Arthur J. Frank
Chemical and Materials Science Center
National Renewable Energy Laboratory
Golden, CO 80401

Water (or moisture) is one of several factors that are generally perceived as detrimental to the performance and long-term stability of thin film photovoltaics. Because the charge-carrier dynamics are major determinants of cell efficiency, it is likely that transport and recombination kinetics are critical in determining the changes in cell performance over time. In this study, we examine the influence of water on the relationship of the charge-carrier dynamics to the photocurrent density–photovoltage (J – V) characteristics and stability of dye-sensitized TiO_2 solar cells (DSSCs) containing two different commonly used solvents. Adding 10 vol% water to the solvent in the DSSCs was found to alter the energy level alignments at the electrode/electrolyte interface, retard the recombination of electrons in the TiO_2 films with oxidized iodide species in the electrolyte, and increase the dark exchange current density.

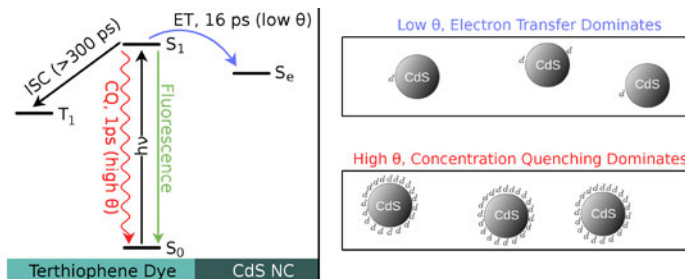


Surprisingly, the added water had no effect on electron transport as measured by electrochemical impedance spectroscopy. Changes in the J – V characteristics were shown to result from the effects of water on the energetics and kinetics of transport and recombination in the DSSCs. Regardless of the solvent used in the DSSCs, the added water had no observed effect on the cell stability during 1000 h of continuous illumination under full sunlight (AM1.5). Valuable insight was gained into the underlying mechanism that determined the relationship between the charge-carrier dynamics and the J – V properties and stability of DSSCs.

Excited State Quenching Mechanism of a Terthiophene Acid Dye Bound to Monodisperse CdS Nanocrystals: Electron Transfer vs. Concentration Quenching

Rajan Vatassery, Jon Hinke, Antonio Sanchez-Diaz, Ryan Hue, Kent R. Mann, David A. Blank, and Wayne L. Gladfelter
Department of Chemistry
University of Minnesota
Minneapolis, MN 55455

Oleate-capped CdS nanocrystals (NCs) dispersed in dichloromethane were found to quench the excited state fluorescence of the terthiophene derivative 3',4'-dibutyl-5''-phenyl-[2,2':5',2''-terthiophene]-5-carboxylic acid (**1-CO₂H**). Infrared and ¹H NMR spectroscopies provided evidence that **1-CO₂H** substitutes for oleate on the surface of the CdS NCs. Upon binding, the fluorescence of **1-CO₂H** is quenched, and the ¹H NMR lines from **1-CO₂H** are broadened. The importance of the carboxylate group in binding to the CdS NC was further established by examining the behavior of a similar fluorophore where the carboxylic acid group was replaced with a bromo substituent (**1-Br**). The CdS NCs had no influence on the fluorescence intensity or NMR lineshapes of **1-Br**. For **1-CO₂H**, Stern-Volmer plots indicated a nearly linear increase in I₀/I as the CdS NCs concentration was increased, but as the dye/NC ratio reached ~20/1, I₀/I reached a maximum of ~8 and began to decrease. By a dye/NC ratio of 2/1 the I₀/I reached a steady value of ~ 2.5. The peak in the Stern-Volmer plot at a 20/1 ratio was consistent with a maximum in the contribution from concentration quenching at this coverage. Based on the appearance of the dye's radical cation spectrum at low dye/NC ratios, ultrafast transient absorption spectroscopy confirmed electron transfer from the singlet excited state of the dye to the CdS NC with a lifetime of 16 ps. At higher dye/NC ratios, the signal from the radical cation was much less dominant, and the decay of the singlet excited state was dominated by the concentration quenching process having a 1 ps lifetime. The figure summarizes the events occurring upon excitation of the dye/NC dyads.



Given the widespread use of oligothiophenes in photovoltaics, and the detrimental effect that concentration quenching has on light-to-electricity conversion efficiency, rational dye design becomes an important consideration. Complicating the picture further is the fact that other groups have shown that certain aggregates not only participate in electron transfer, but also absorb a greater fraction of the solar spectrum due to aggregation-induced changes in their absorption spectra. To take advantage of aggregation as a benefit rather than a drawback, it will be necessary to study further the factors that affect the relative rates of electron transfer and energy dissipation in a variety of dyes.

Vatassery, R.; Hinke, J.; Sanchez-Diaz, A.; Hue, R.; Mann, K. R.; Blank, D. A. and Gladfelter, W. L. *J. Phys. Chem. C*, submitted for publication.

Molecular and Material Approaches to Overcome Kinetic and Energetic Constraints in Dye-Sensitized Solar Cells

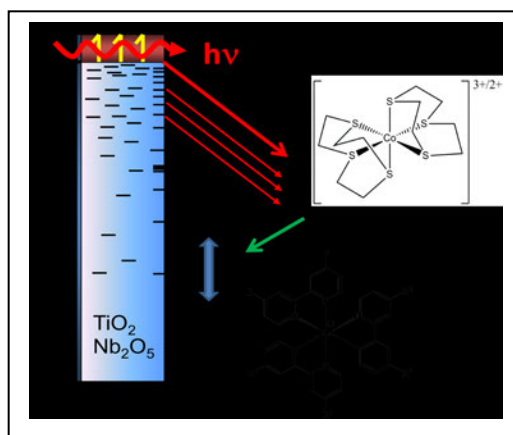
Jesse Ondersma, Yuling Xie, Suraj Soman, Dhritabrata Mandal and Thomas W. Hamann

Department of Chemistry
Michigan State University
East Lansing, MI 48824

The ultimate goal of our work is to redesign the dye-sensitized solar cell (DSSC). This is guided by systematic studies of each of the DSSC components: redox shuttle, photoanode, sensitizer, and solvent. Understanding the details of each component's role in key processes – injection, regeneration and recombination – will be used to overcome kinetic and energetic constraints of current generation DSSCs.

Redox shuttle: The primary limitation of current redox shuttles, I_3^-/I^- and cobalt tris-bipyridine, is the large driving force (ca. 500 meV) required to achieve quantitative regeneration. We will present recent results from our investigation of using a low spin cobalt(II) complex, cobalt bis-trithiacyclononane, $[Co(ttcn)_2]^{3+/2+}$ as a redox shuttle in DSSCs. This unique cobalt complex redox shuttle is stable, transparent, easy to synthesize from commercial ligands, and has attractive energetic and kinetic features for use in DSSCs. A series of photoelectrochemical and spectroscopic measurements were employed to understand the regeneration efficiency and recombination rates. These results indicate that $[Co(ttcn)_2]^{2+}$ is capable of quantitative dye regeneration with only a ~200 meV driving force. The recombination rates are an order of magnitude faster compared to cobalt tris-bipyridine, however, which reduces the electron diffusion length and overall charge collection efficiency. Initial attempts at overcoming recombination through sensitizer design and photoanode material will also be presented.

Photoanode: The photoanode plays a central role in charge injection, transport, and recombination. One potential way to control recombination is therefore to alter the photoanode material. We will present initial results of using Nb_2O_5 as a photoanode. The conduction band edge, E_{CB} , is arguably the most important physical property of the photoanode that determines the driving force and rate of recombination. We extended the method of variable temperature spectroelectrochemistry developed in our group to compare E_{CB} of Nb_2O_5 to TiO_2 . We found that the conduction band edge of Nb_2O_5 is ~100 meV lower than TiO_2 , consistent with previous estimates. The effect on recombination rates to $[Co(ttcn)_2]^{2+}$ will be presented.

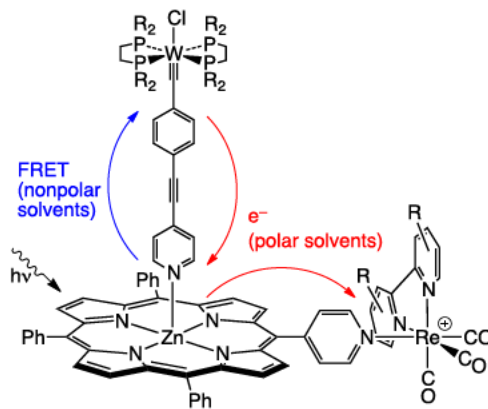


Sensitizer: The rates of regeneration with alternative redox shuttles, and injection with alternative photoanode materials, will also be affected by the energetics of the ground and excited states of the sensitizer, respectively. In addition, the rates of recombination can be partially controlled through adding steric bulk to the sensitizer. We have therefore synthesized a series of cyclometalated sensitizers to control the ground and excited state potentials as well as the steric bulk. Recent results of examining this series of sensitizers will also be presented.

Two-Catalyst Assemblies and Mixtures for Photochemical CO₂ Reduction

Davis B. Moravec, Nathan La Porte, and Michael D. Hopkins
Department of Chemistry
The University of Chicago
Chicago, IL 60637

This presentation will describe efforts to develop molecular artificial-photosynthetic systems for producing solar fuels from CO₂, in which renewable reducing equivalents replace conventional sacrificial donors. A common design element of these systems is the pairing of a hydrogen oxidation catalyst and CO₂ reduction catalyst with a chromophore that photosensitizes electron-transfer reactions between them. One portion of the work has focused on two- and three-component assemblies derived from metal-alkylidyne (MCR) building blocks, which possess highly reducing excited states and regenerative proton-coupled electron-transfer chemistry with H₂ relevant for CO₂ reduction reactions. Recent bimolecular quenching studies of W(CPh)(dppe)₂Cl and related compounds demonstrate that their long-lived dπ* excited states are as strongly reducing as sodium amalgam, and are characterized by small inner-sphere reorganization energies. In contrast to covalent assemblies we have previously studied, the MCR unit in the ZnPor/Re chromophore/CO₂-catalyst triad at right is incorporated as a dative metalloligand; the dative linkage allows exchange with free MCR in solution on the NMR time scale, potentially decoupling catalysis and charge recombination. Transient-absorption spectroscopic studies show that the relative rates and efficiencies of energy and electron transfer are subject to control via solvent polarity and porphyrin aryl substituents. Reactions of the components with CO₂ and H₂ under photochemical conditions will be described.



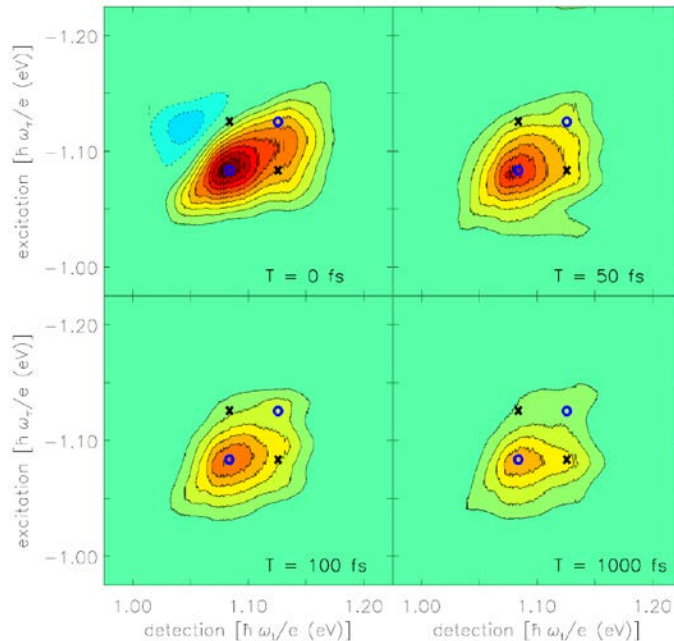
A second, recent thrust has been to study “unassembled” chromophore/two-catalyst systems—that is, mixtures of three different compounds in solution that operate via outer-sphere reactions. This eliminates the need for synthesis of assemblies and may enable diffusion/hole-trapping to outcompete charge recombination, but poses challenges in kinetically integrating photophysical and electron-transfer events. In this context, it has been found that the very long-lived T₁ states of Zn porphyrins ($\tau \sim 1$ ms) are valuable for photosensitizing inter-catalyst electron transfer. These chromophores have been paired with a variety of H₂-oxidation catalysts of types Cp*Cr(CO)₃, CpFe(P^R₂N^R₂)⁺, and Ni(P^R₂N^R₂)²⁺ (where P^R₂N^R₂ are the DuBois-type amino phosphine ligands). Appropriate pre-catalyst redox congeners of these compounds are shown to reductively quench the ZnPor T₁ state to produce ZnPor⁻; these reduced chromophores, in turn, may be oxidized thermally by Re(diimine)(CO)₃X compounds to initiate their the one-electron pathway for CO₂ reduction. Detailed transient-absorption spectroscopic measurements of the Cp*Cr(CO)₃⁻/ZnTPP/Re(bpy)(CO)₃Cl system in various relative concentrations and in different solvents has provided a complete picture mechanistic and kinetic picture of the photochemical and thermal bimolecular electron-transfer reactions. Under steady state photolysis conditions, preliminary evidence for CO₂ reduction has been found.

2D Electronic Spectra of PbSe Quantum Dots in the Short-Wave Infrared

Samuel D. Park, Dmitry Baranov, Byungmoon Cho, Vivek Tiwari, and David M. Jonas
Department of Chemistry and Biochemistry
University of Colorado
Boulder, CO 80309-0215

Next generation photovoltaics must have their bandgap in the short-wave infrared, which spans the 1-2 μm wavelength range. External quantum efficiencies exceeding 100% have been reported for lead selenide quantum dot solar cells and photocurrent quantum yields of almost two have been reported for lead sulfide quantum dots on TiO_2 , but the thresholds for the excess quantum yields are too high to boost energy conversion efficiency relative to conventional photovoltaics. Bulk lead chalcogenides have an interesting electronic structure, with their bandgap at the 4-fold degenerate (8-fold including spin) L -point of the first Brillouin zone. Depending on structure, this intervalley degeneracy may be lifted in quantum dots.

We have developed the first femtosecond two-dimensional Fourier transform spectrometer in this wavelength region and used it to record the 2D FT spectra of oleate capped colloidal lead selenide quantum dots in 2,2,4,4,6,8,8-heptamethylnonane. The quantum dots were prepared in our laboratory by a hot injection synthesis and kept under air and moisture free conditions throughout experiments. The synthesis is reported to produce lead rich surfaces, suitable for testing predictions about the intervalley splitting in spherical lead chalcogenide quantum dots. TEM indicates the quantum dots are ellipsoidal, with a 3.1 ± 0.3 nm short axis and a 4.4 ± 0.4 nm long axis; the short axis is consistent with the diameter deduced from a literature sizing curve and the first exciton absorption peak at 1.09 eV. The real 2DFT correlation spectra are shown below for 4 waiting times, T , between measurement of the excitation and detection frequencies.



Most interesting is the negative region above the diagonal at $T=0$. This could be a 2D signature of the phonon memory predicted by Prezhdov and co-workers, although the intervalley splitting of the bi-exciton states reached via excited state absorption is not yet understood and remains a potential explanation. Despite frequency calibration to within 0.1 meV, determination of any off-diagonal shifts (which are in opposite directions for the bi-exciton binding energy and the phonon Stokes' shift) is difficult because of a recently discovered need to subtract weak scattered light. At $T=1$ ps, the 2D spectra appear to show 3 peaks on a square, with hints of the fourth peak at $T=100$ fs (\times = cross-peak, \circ = diagonal peak) suggesting a 40 meV intervalley splitting.

Effects of Stranski-Krastanov Shells in the Charge Transfer Dynamics of ZnTe/CdSe Nanocrystals

Zhong-Jie Jiang and David F. Kelley
Chemistry and Chemical Biology
University of California, Merced
Merced, California 95343

ZnTe/CdSe core/shell nanocrystals with varying ZnTe core sizes and CdSe shell thickness have been synthesized. The absorption onset and photoluminescence (PL) wavelengths vary from the mid-visible into the near infrared range, as shown in figure 1, below. These particles are type-II, with the hole confined to the ZnTe core. The shell thickness inhomogeneity is determined from luminescence quenching dynamics with an adsorbed hole acceptor, phenothiazine (PTZ). Luminescence quenching results from hole tunneling, the rate of which depends critically on the shell thickness. The model used to describe the tunneling dynamics considers a Poisson distribution of acceptor numbers and includes shell thickness variability. The thickness-dependent hole tunneling rates are determined from calculated wavefunction penetration using the known core/shell energetics and effective masses. We find that the first approximately three layers of CdSe are deposited uniformly and that subsequent deposition results in Stranski-Krastanov (S-K) growth of shell islands. ZnTe and CdSe have very close to the same lattice constants and the interface therefore has very little lattice strain. However, cation interdiffusion changes the radial composition profile of the ZnTe-CdSe interface, leading to a large amount of lattice strain. Island formation minimizes the lattice strain energy, making the rough surface thermodynamically favorable. The conditions under which one gets S-K growth of nanocrystal shells and thin films can be understood in terms of elastic continuum calculations and surface energy considerations.

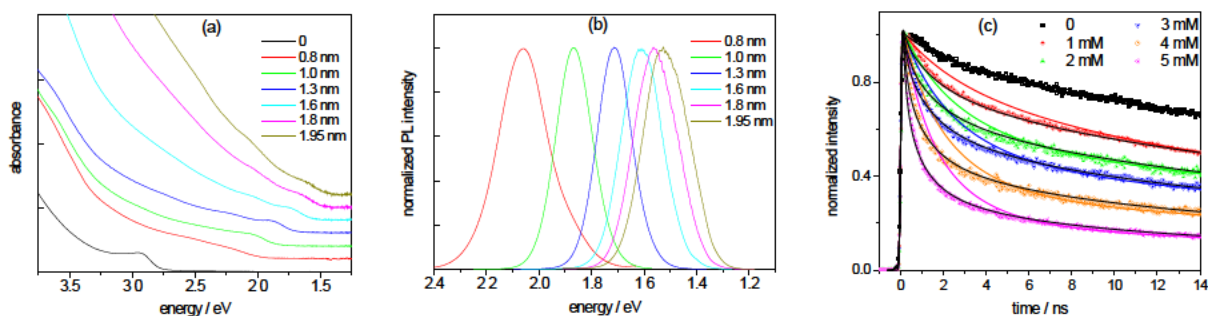


Figure 1. Absorption (a) and PL (b) spectra of 2.6 nm ZnTe core and ZnTe/CdSe core/shell nanocrystals. (c) PL kinetics of particles having a 1.2 nm CdSe shell deposited at 215 °C with different PTZ concentrations. The curves are calculated assuming uniform thickness shells (slower decaying color curves) and S-K growth of islands on three smooth shell monolayers (black curves).

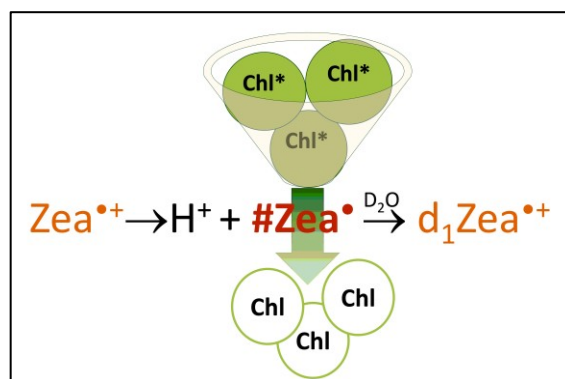
Neutral Carotenoid Radicals in Photoprotection

Adam Magyar,[†] Michael K. Bowman,[†] Peter Molnar,[‡] and Lowell D. Kispert*,[†]

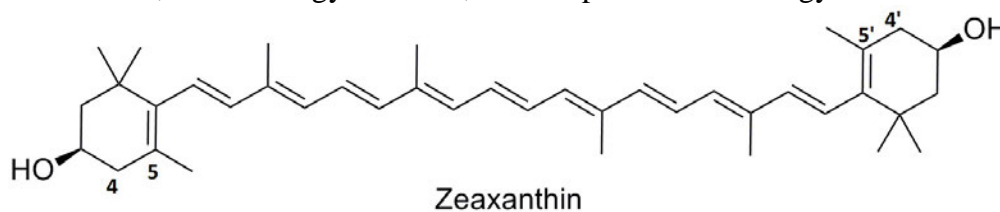
[†]Department of Chemistry, The University of Alabama, Box 870336
Tuscaloosa, Alabama 35487-0336

[‡]Department of Pharmacognosy, University of Pecs, Medical School, H-7624 Pecs, Rokus u. 2,
Pecs, Hungary

The deprotonation of naturally occurring zeaxanthin (Zea) radical cations (Zea^{•+}) to form neutral radicals (#Zea[•]) and their involvement in the qE portion of non-photochemical quenching (NPQ) is the subject of this presentation. Plants have several redundant mechanisms for protection from excess light, collectively known as non-photochemical quenching (NPQ).¹ One important form of NPQ is qE, which is characterized by a decrease in fluorescence. *Arabidopsis thaliana* mutants show a strong connection between the presence of (Zea) and the qE component of NPQ. During periods of excess light, a charge-transfer complex is formed between Zea and Chl generating Zea^{•+} (Zea^{•+}•••Chl⁻). Previous studies² have pointed out that Zea^{•+} are weak acids and the favorable formation of carotenoid neutral radicals occurs via proton loss at the terminal end (4 or 4') carbon for Zea and lutein (Lut) radical cations. This correlates with their ability to quench excess energy. Radicals have shown the ability to quench fluorescence and are the basis for detecting singlet and triplet oxygen. The cartoon given above



depicts the experimental scheme as well as how #Zea[•] may quench the excess energy from chlorophyll. To detect the deprotonation of naturally occurring (Zea^{•+}) to form (#Zea^{•+}) during qE, wild-type *A. thaliana* leaves were infiltrated with either D₂O or H₂O and exposed to light and analyzed via LC/MS. Only leaves exposed to light intensity that triggers qE in *A. thaliana* (>300 μE m⁻² s⁻¹) showed H/D exchange. This observation suggests that #Zea[•] can form by the deprotonation of the weak acid Zea^{•+} during qE and its role in qE activity in *A. thaliana* needs to be considered. This work was supported by the Office of Chemical Sciences, Geoscience and Biosciences Division, Basic Energy Sciences, U.S. Department of Energy.



1. Mozzo, M., et al. "Photoprotection in the Antenna Complexes of Photosystem II – Role of Individual Xanthophylls in Chlorophyll Triplet Quenching", *J. Biol. Chem.* **2008**, 283, 6184-6192.
2. Focsan, A. L., et al., "Structure and Properties of 9'-*cis*-Neoxanthin Carotenoid Radicals by Electron Paramagnetic Resonance Measurements and Density Functional Theory Calculations: Present in LHC II?", *J. Phys. Chem. B* **2009**, 113, 6087-6096.

Photoexcited Excitons in Charged Single Walled Carbon Nanotubes

Nicole M. Cogan, Sebastian Shaffer, Michael Odoi, Bradford Loesch, Julie Smyder, and Todd D. Krauss

Department of Chemistry and the Institute of Optics
University of Rochester
Rochester, New York 14627-0216

Semiconducting single-walled carbon nanotubes (SWNTs) display remarkably stable and size-tunable photoluminescence at near-infrared (NIR) wavelengths, making them fundamentally interesting and technologically relevant materials. However, individual SWNTs typically have a photoluminescence (PL) quantum yield (QY) of about a few percent, much less than other NIR emitting nanomaterials such as semiconductor quantum dots. It is currently not understood whether the poor QY of SWNTs is an intrinsic property or the result of extrinsic quenching mechanisms indicative of non-optimal sample quality, such as structural defects or dopants.

We will discuss several experiments designed to elucidate the nature of the PL emission in SWNTs. PL intensity time traces and spectra from individual NTs isolated on ITO while under a positive and negative electrochemical bias were acquired (Figure 1). Interestingly, for some NTs, PL intensity was quenched for appropriately large positive and negative applied bias voltages, likely due to filling of valence and conduction bands, respectively (Fig. 1B). However, for some NTs, PL quenching was observed for negative bias voltages, but PL enhancement was observed for positive bias voltages (Fig. 1C), suggesting that these NTs were intrinsically doped.

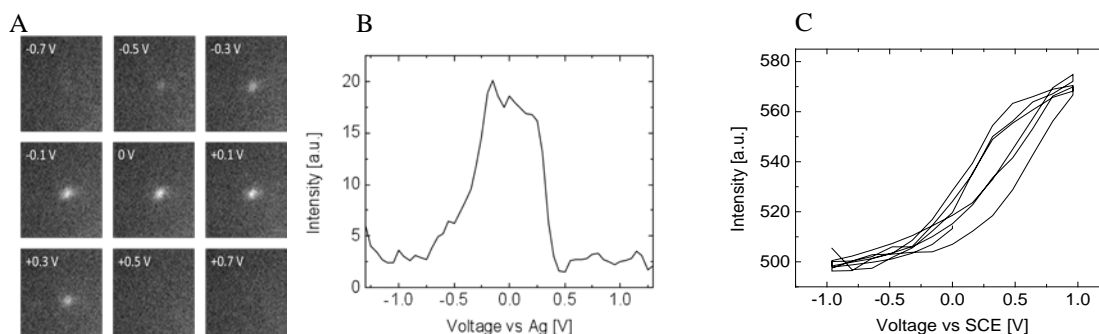


Figure 1. (A) PL images of a single NT while under an electrochemical bias. Average PL intensity versus applied bias for (B) the NT shown in (A) and for (C) a doped NT. The working electrode was Pt and the reference electrode was Ag/AgCl.

In a related study, correlated measurements of fluorescence and topography were performed for individual single-walled carbon nanotubes on quartz using epifluorescence confocal microscopy and atomic force microscopy (AFM). Surprisingly, only ~11% of all SWNTs were found to be emissive, while approximately 36% of the SWNTs displayed weak luminescence, in which PL spectra were not observed for corresponding bright pixels in the PL image. The rest of the NTs did not have any observable PL emission. Our data suggest that the low ensemble QYs for carbon nanotubes can be largely attributed to a small percentage of bright SWNTs in the ensemble, and not to a large population of poorly emitting SWNTs.

Exciton Dissociation Dynamics in Colloidal Triadic CdSe-CdS-Pt Nanorods

Kaifeng Wu, Haiming Zhu and Tianquan Lian
Department of Chemistry
Emory University
Atlanta, Georgia 30322

Triadic colloidal nanorods are emerging as a novel class of promising materials for solar-to-fuel conversion. These materials combine the light harvesting and charge separation ability of quantum-confined semiconductor nanorods with the catalytic activity of metallic nanoparticles. For example, in CdSe-CdS-Pt dot-in-rod nanorods (Figure 1a), the quasi type II band alignment in CdSe/CdS leads to ultrafast internal exciton dissociation across CdSe/CdS interface, which can facilitate efficient directional electron transfer to the Pt particle at the tip of the CdS nanorod (Figure 1b). The distance between the separated charges (with electron at the Pt tip and hole at the CdSe core) can be adjusted by the rod length to control the lifetime of the charge separated state. The energetics of the electrons and holes can be tuned by the choice of materials and the diameter of the rod through the quantum confinement effect in the radial direction. However, in CdSe-CdS-Pt nanorods prepared by colloidal seeded growth methods, both surface defects and non-uniform nanorod diameters along the rod direction often exist, leading to multiple long-lived excitonic states in these materials (Figure 1a and b). The optimization of charge separation properties in such nanorods requires the understanding of the spectral signature and dynamics of these excitons. In a recent series of study, we assigned the spectra and investigated the dynamics of excitonic states in CdSe-CdS-Pt nanorods by transient absorption spectroscopy. As shown in Figure 1c (upper panel) and d, the 1σ exciton bleach recovery is faster in CdSe-CdS-Pt than CdSe-CdS rods, indicating fast electron transfer to the Pt tip (with a half-life of ~ 100 ps). The charge separated state, which can be probed by the Stark effect induced exciton peak shift (Figure 1c lower panel), has a half-lifetime approaching 1 microsecond (Figure 1e). Ongoing studies are examining how the yield of charge separation and the lifetime of the charge separated state depend on the rod length and diameter and how these quantities correlate with their photocatalytic H₂ evolution performance.

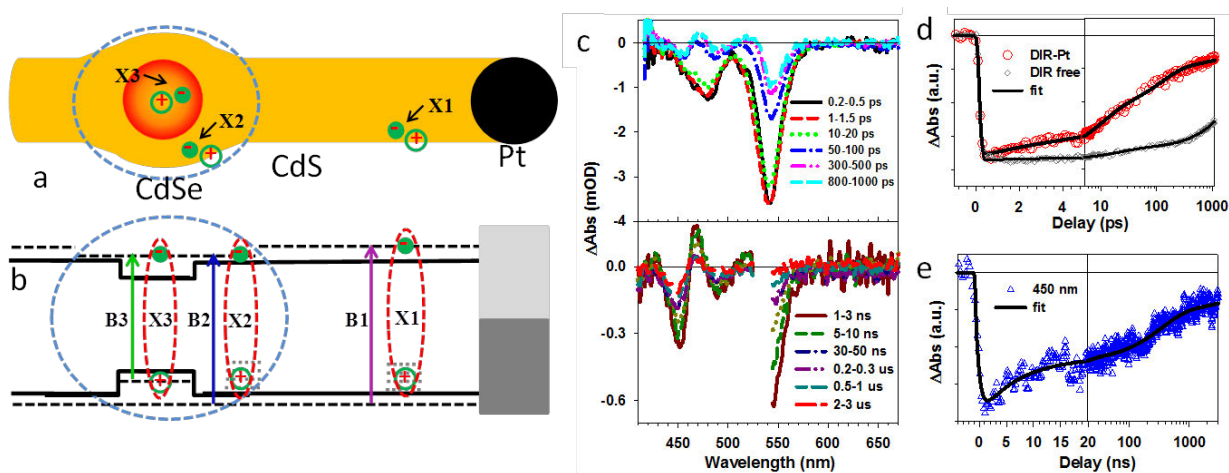


Figure 1. Colloidal triadic CdSe-CdS-Pt nanorods. a) Schematic structure, b) Energy level diagrams, c) Transient absorption spectra, d) Charge separation kinetics and e) Charge recombination kinetics.

Photochemical and Photovoltaic Properties of Conjugated Ionomers

Stephen Robinson, Ethan Walker, Chris Weber, and Mark Lonergan
Department of Chemistry
University of Oregon
Eugene, OR 97403

We report studies on the charge injection and transport properties, and photochemistry of ionically functionalized conjugated polymers (conjugated ionomers) and their junctions.

Unlike conventional organic photovoltaic systems, which rely on an asymmetry in frontier orbital positions to generate a photovoltaic effect, we have demonstrated a series of organic photovoltaic systems based on asymmetries in either doping type (like the conventional silicon p-n junction) or ionic composition. In regards to the former, we have detailed the properties of polyacetylene-based p-n junctions where the dopant density of the n-type region is systematically varied over the range 10^{19} to 10^{20} cm^{-3} . Variation of dopant density enables tuning of the junctions properties (see Figure 1), but the properties are distinct from classic inorganic p-n junctions in that they exhibit neither the voltage-dependent capacitance of a semiconductor depletion layer nor classic Shockley diffusion-based current-voltage behavior.

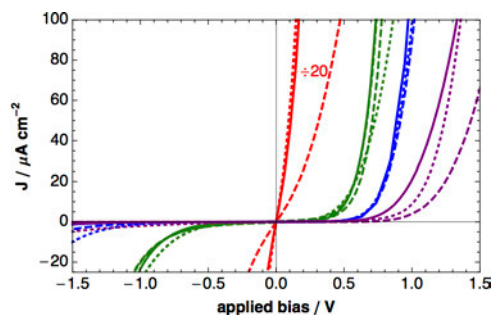


Figure 1 - Tuning current density (J)-voltage behavior of polyacetylene-based conjugated ionomer p-n junctions.

Studies on the photochemistry, charge injection, and transport in individual conjugated ionomers are being used to provide important insight into the properties of the photovoltaic systems described above and the dramatic effects of ionic functional groups. In regards to injection and transport, ionic functional groups impart mixed ionic/electronic character. Such character invalidates conventional approaches to determining basic parameters such as carrier mobility because of challenges in determining the density of injected charge, especially if the mobility is concentration dependent. We have used NIR absorbance as a direct, model-free approach to measure the density of injected charge in determining carrier mobility. These measurements have also enabled direct comparison of two-electrode and three-electrode electrochemical charge injection measurement in validating an electrochemical model of charge injection into conjugated ionomers (Figure 2).

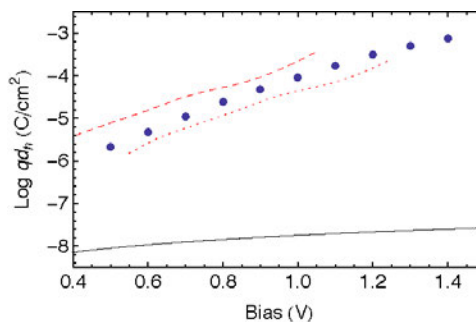


Figure 2 - Comparison of charge injected (qd_h) into a polyacetylene anionomer in a two-electrode system (blue circles) compared with the range expected (dashed red lines) from a three-electrode electrochemical experiment.

In regards to photochemistry, we have demonstrated that ionic functional groups result in a dramatic effect on the autoxidation of conjugated polymers. In particular anionic functional groups with alkali metal cations greatly stabilize the formation of an oxygen charge transfer complex that dramatically slows overall polymer photodecomposition.

Controlled seeding and growth of Ta:TiO₂ nanoforest and its performance as photoanode for dye sensitized solar cell devices

Yukihiro Hara, Timothy Garvey, Leila Alibabaei, Rudresh Ghosh, Rene Lopez

Department of Physics and Astronomy
University of North Carolina at Chapel Hill
Chapel Hill, NC, 27713

Efficient absorption of photons and effective carrier extraction are usually antithetical goals in traditional photovoltaic device configurations. Typical solar cell designs try to maximize photon capture by increasing the thickness of the absorbing layer. But this is detrimental to charge harvesting since increased transport path lengths lead to increased carrier recombination. The objective of our program is to comprehensively redesign the full opto-electronic properties of dye sensitized solar cells to develop the ultimate cell structure, at all length scales, that will enable DSSCs with perfect light capturing and electron harvesting.

Our approach is based on two developments that decouple carrier transport from optical absorption: 1) A novel high surface area oxide fabrication technique “nanoforest” of tantalum doped TiO₂ nanoparticle that allow us to achieve full dye loading and at the same time provide more direct paths for charge transport, reducing travel lengths and recombination opportunities. 2) The optical control allowed by non-invasive photonic micro-structuring.

Putting together this two independent technologies will allows us great latitude to understand and ultimately control in the optoelectronic properties of the dye sensitized photoanodes. For a first realization of this concept, a patterned array of indium tin oxide (ITO) micro-cones with 1.5 μm height was fabricated on fluorinated tin oxide (FTO) substrate via nanoimprint nanolithography and pattern transfer techniques. Tantalum doped TiO₂ was deposited on this patterned substrate by pulse laser deposition at high background pressure. The Ta:TiO₂ oxide layer grew in vertically separated bushes or trees out of the patterned ITO that provided a trunk-like seeds for this control growth. Dye-sensitized solar cells with the film on the patterned substrate as well as flat FTO for comparison were fabricated and tested. The devices with the patterned substrate showed 25 % increase in short circuit current (J_{sc}) compared to the one with flat FTO substrate. Optical and photoelectrochemical characterizations were performed to investigate the source of the improvement. The increase in J_{sc} was attributed to the enhancements of light absorption and effective electron collection by the patterned ITO.

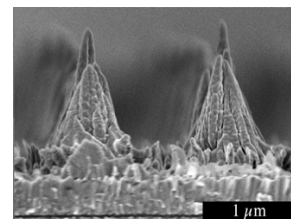


Fig.1 Electron cross sectional images of patterned substrates ITO features on FTO substrate.

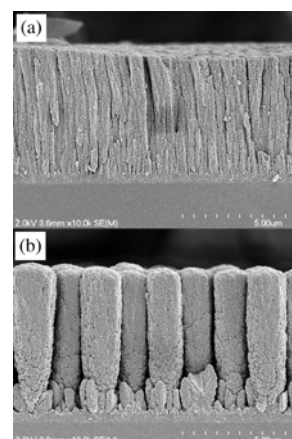


Fig.2 Electron cross sectional images of Ta:TiO₂ nanoforest film on (a) flat FTO and (b) patterned substrates after identical Ta:TiO₂ laser growth.

Sensitization of p-GaP Photoelectrodes with CdSe Quantum Dots: Light Stimulated Hole Injection

Zhijie Wang, Junsi Gu, Sabrina Peczonczyk, and Stephen Maldonado
Department of Chemistry
University of Michigan
Ann Arbor, MI 48109-1055

This presentation describes the first dataset illustrating light sensitized hole transfer between a photoexcited quantum dot and a p-type semiconductor photocathode immersed in an aqueous electrolyte. We demonstrate that cadmium selenide (CdSe) quantum dots have the capacity to sensitize p-type gallium phosphide (p-GaP) through light stimulated hole injection, i.e. the inverse process of the more familiar electron injection in ‘conventional’ dye sensitized systems. This work highlights several interesting features of this system, including sensitivity towards quantum dot size, surface composition, and a cathodic redox mediator (aquated $\text{Eu}^{3+}/^{2+}$). This work achieves two important goals. First, these data establish the p-GaP/CdSe platform as a new test-bed for fundamental study of light-stimulated charge transfer events at quantum dot materials. Second, these results demonstrate quantum-dot sensitized photocathodes can operate in simple aqueous electrolytes, suggesting the possibility of sensitized cells that generate chemical fuels instead of/in addition to electricity. Additional data will be presented illustrating the covalent modification of GaP interfaces for deliberate dye/quantum dot attachment.

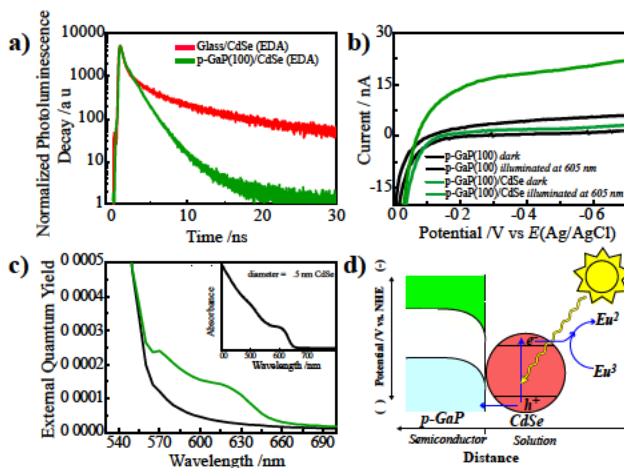


Figure 1. a) Time-resolved photoluminescence decay measured from a monolayer of CdSe (diameter = 4.5 nm) quantum dots on (red line) glass and (green line) p-GaP (100), respectively. b) Steady-state current-potential responses for a (black lines) mirror-polished, bare p-GaP(100) photoelectrode and (green lines) a mirror polished p-GaP(100) photoelectrode coated with a monolayer of CdSe quantum dots (diameter = 4.5 nm). Responses both (dashed lines) in absence of any illumination and (solid lines) under monochromatic illumination at 605 nm at 0.33 mW cm^{-2} are shown. c) External quantum yield spectra for (black) a bare p-GaP(100) photoelectrode and (green) a p-GaP(100) photoelectrode coated with a thin film of CdSe quantum dots. Inset: Absorption spectrum for the same CdSe quantum dots dispersed in hexane. d) Schematic depiction of the sensitized process.

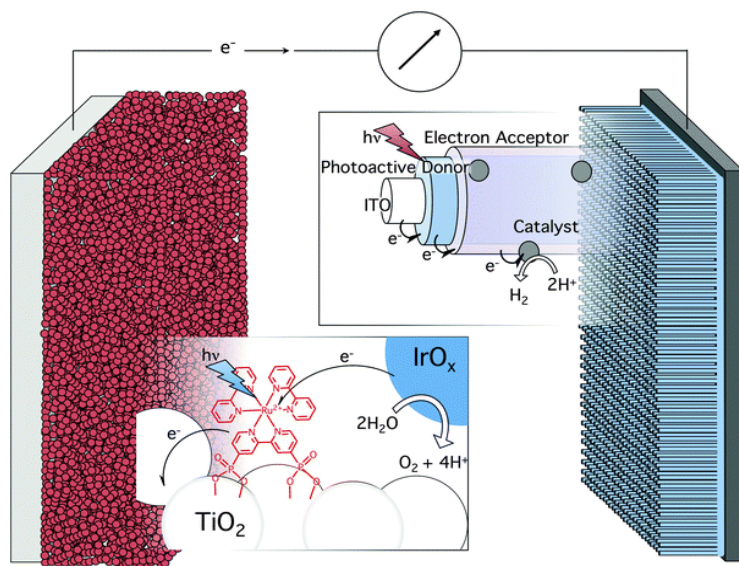
Nanostructured Photocatalytic Water Splitting Systems

Nella M. Vargas-Barbosa, John R. Swierk, Yixin Zhao, Nicholas McCool, Timothy P. Saunders
Jennifer L. Dysart, and Thomas E. Mallouk

Department of Chemistry, The Pennsylvania State University, University Park, PA 16802

Ana L. Moore, Thomas A. Moore, and Devens Gust

Department of Chemistry and Biochemistry, Arizona State University, Tempe AZ 85281



Our DOE-supported research investigates problems associated with overall water splitting in molecular photoelectrochemical systems. Our current efforts are focused on electron transfer processes in the anode and cathode assemblies illustrated in the cartoon at the left, and on membrane polarization processes that occur in photoelectrosynthetic cells.

One of the key problems for light-driven water splitting is the development of good water oxidation catalysts that can be directly linked to

electron transfer relays, semiconductor surfaces, and photosensitizers. Despite much past and current research on colloidal IrO_2 , the mechanism of nanoparticle formation from small molecule precursors is not well understood. We have identified two key intermediates in the synthesis of $\text{IrO}_x \cdot n\text{H}_2\text{O}$ nanoparticles, namely a colorless polymeric Ir(III) complex and a basic monomeric Ir(III) anion, which is tentatively formulated $[\text{Ir}(\text{OH})_5(\text{H}_2\text{O})]^{2-}$. It has not previously been appreciated that this anion adsorbs strongly but reversibly to $\text{IrO}_2 \cdot n\text{H}_2\text{O}$ and other oxide (TiO_2 , BiVO_4) surfaces. The anion can actually mediate back electron transfer at photoelectrodes catalyzed by $\text{IrO}_x \cdot n\text{H}_2\text{O}$ and thus deteriorate the performance of the photoanode. By hydrolyzing $[\text{IrCl}_6]^{2-}$ in the presence of phosphonate, carboxylate, or malonate ligands, it is possible to prepare size-controlled $\text{IrO}_x \cdot n\text{H}_2\text{O}$ capped by the appropriate ligand. Ligand-free $\text{IrO}_x \cdot n\text{H}_2\text{O}$ nanoparticles are highly active catalytically, but particles that are saturated with capping ligands are relatively inactive. We are currently working on strategies to partially cap the nanoparticles in order to achieve simultaneously high catalytic activity and covalent attachment of the nanoparticles to sensitizer or mediator molecules.

Flash photolysis studies have shown that the quantum yield of water splitting is determined largely by the kinetic competition between back electron transfer and water oxidation at the photoanode. We have made core-shell oxide electrodes and have incorporated electron transfer mediators into the photoanode to improve the balance of these rates. Using flash photolysis, we have studied the stepwise oxidation of $\text{IrO}_x \cdot n\text{H}_2\text{O}$ that leads to water oxidation. We are also modeling and measuring by conducting tip AFM the electron transfer kinetics of photoredox assemblies grown layer-by-layer for the cathode side of the photoelectrochemical cell.

Rotational Dynamics in Ionic Liquids – NMR & MD Studies

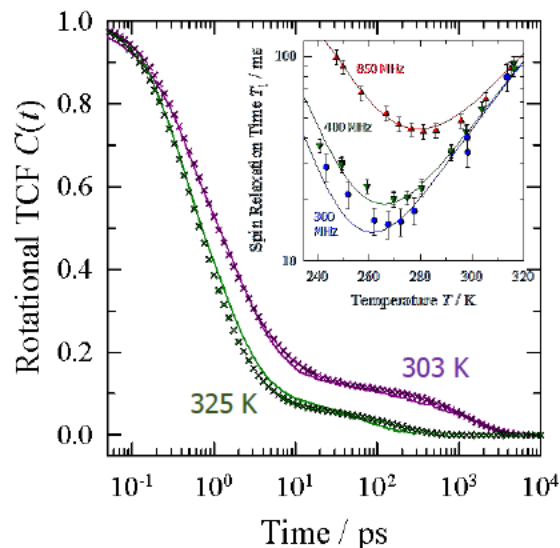
Anne Kaintz¹, Chris Rumble¹, Sharad K. Yadav², Claudio Margulis², and Mark Maroncelli¹
¹Department of Chemistry, The Pennsylvania State University, University Park PA 16802, and
²Department of Chemistry, The University of Iowa, Iowa City, IA 52242

For purposes of being able to more definitively model the kinetics of bimolecular electron transfer in ionic liquids¹ we have been trying to gain a quantitative understanding of solute translational and rotational dynamics in ionic liquids. We have completed an initial survey of solute translational diffusion, some of which we presented in a poster last year. Here we present the results of combined multi-frequency NMR measurements and molecular dynamics simulations focused on the rotational problem.

Early anisotropy measurements on fluorescent solutes² indicated that rotation in ionic liquids could be understood simply by extrapolating the behavior observed for a given solute in conventional solvents to the higher viscosities present in ionic liquids. However, dielectric relaxation measurements³ as well as some computer simulations suggested that the cations of imidazolium-based ionic liquids often rotate much more rapidly than would be expected based on simple hydrodynamic predictions, often exhibiting sub-slip rotation times. More recent ESR measurements using radical probes show a wide variety of rotational behavior, with times often well below the slip limit for dilute solutes.⁴

We have recently begun using ²H-NMR T_1 measurements to study the rotational dynamics of both dilute solutes and neat ionic liquid ions. Because NMR measurements only provide correlation times whereas simulations show that rotational time correlation functions (tcf) are often bimodal functions of time, we use molecular dynamics simulations to construct models for rotational tcf and their temperature/viscosity dependence. These models are used to guide the modeling of NMR data. When reasonable agreement between simulation and experiment is achieved, we can trust that the nature of the motions observed in simulation are representative of those of the real fluid. We will discuss the insights obtained thus far from such simulation – NMR comparisons.

1. Liang, M.; Kaintz, A.; Baker, G. A.; Maroncelli, M. *J. Phys. Chem. B* **2012**, *116*, pp 1370.
2. Ito, N.; Arzhantsev, S.; Maroncelli, M. *Chem. Phys. Lett.* **2004**, *396*, pp 83.
3. Huang, M.-M.; Bulut, S.; Krossing, I.; Weingärtner, H. *J. Chem. Phys.* **2010**, *133*, pp 101101.
4. Strehmel, V. *ChemPhysChem* **2012**, *13*, pp 1649.



Example fit of temperature-dependent multi-frequency ²H- T_1 data on C₆D₆ in [Im₄₁][BF₄] using model time-correlation functions derived from MD simulations. The inset shows the fit to NMR data and the main panel the rotational time correlation functions simulated (curves) and determined from the NMR fits at two temperatures.

Progress toward the Development of Iron-based Chromophores for Use In Solar Energy Conversion Strategies

Lindsey L. Jamula, Allison M. Brown, and James K. McCusker*

Department of Chemistry
Michigan State University
East Lansing, Michigan 48824

Our research program is focused on identifying, understanding, and ultimately overcoming the fundamental scientific problems undermining the use of molecular chromophores based on first-row transition metal ions in various solar energy conversion strategies, particularly in dye-sensitized solar cells (DSSCs). This research is being pursued on two fronts: (1) identification of the nuclear coordinate(s) that are coupled to the sub-ps charge-transfer (MLCT) to ligand-field (LF) state conversion we have previously identified as a key process leading to low efficiencies

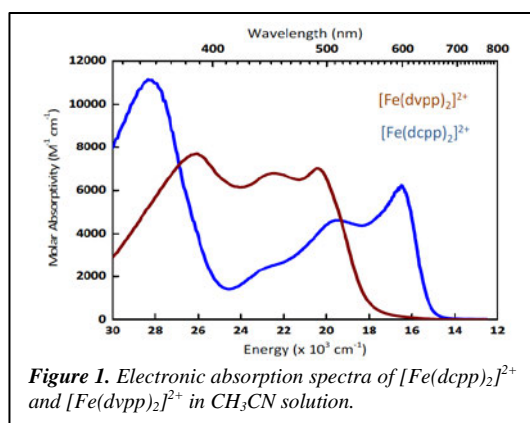


Figure 1. Electronic absorption spectra of $[\text{Fe}(\text{dcpp})_2]^{2+}$ and $[\text{Fe}(\text{dvpp})_2]^{2+}$ in CH_3CN solution.

of iron-sensitized DSSCs, and (2) the development of a new class of chromophores in which the relative energetics of the MLCT and LF states are inverted such that the former correspond to the lowest-energy excited states of the compound. This presentation will focus on the second branch of our program and will highlight progress we have made on the development of a promising new class of high-symmetry polypyridyl complexes.

Recent work from our group has resulted in the synthesis and characterization of an Fe(II) complex based on a modified tris pyridyl ligand, di-(2-carboxypyridyl)pyridine (dcpp). This compound is remarkable for several reasons: (1) the compound possesses near-perfect O_h symmetry, with six identical Fe-N bond lengths and *cis* and *trans* bond angles in the primary coordination sphere of $89(1)^\circ$ and $179(1)^\circ$, respectively; (2) the compound's absorption spectrum is characterized by a markedly red-shifted charge-transfer feature with a maximum at 620 nm (Figure 1); and (3) the Fe(II)/Fe(III) redox couple is shifted positive by nearly 700 mV, indicating a substantial stabilization of the t_{2g} orbitals of the metal center (Table 1). We believe these features conspire to place the lowest-energy charge-transfer and ligand-field states in close energetic proximity.

In an effort to understand what underlies the unique properties of $[\text{Fe}(\text{dcpp})_2]^{2+}$, we have prepared an analog in which the C=O group is replaced by an olefin. Despite the fact that the compounds are isostructural, the optical and electrochemical properties of $[\text{Fe}(\text{dvpp})_2]^{2+}$ are remarkably different (Figure 1 and Table 1). The photophysics of both of these compounds will be described in detail, as well as ongoing efforts to modify these systems further to allow for attachment to semiconductor nanoparticles and studies of their electron injection dynamics.

Table 1. Electrochemical data for a series of Fe(II) polypyridyl complexes. Potentials are reported relative to ferrocene.

Compound	$E_{1/2}$ [ox]	$E_{1/2}$ [red]
$[\text{Fe}(\text{bpy})_3]^{2+}$	0.665 V	-1.775 V
$[\text{Fe}(\text{terpy})_3]^{2+}$	0.715 V	-1.675 V
$[\text{Fe}(\text{dvpp})_3]^{2+}$	0.642 V	-1.166 V*
$[\text{Fe}(\text{dcpp})_3]^{2+}$	1.295 V	-0.965 V

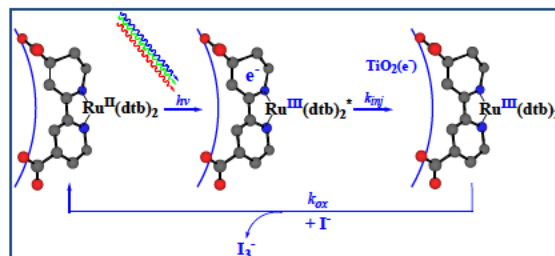
* irreversible

Electron Transfer Dynamics in Efficient Molecular Solar Cells

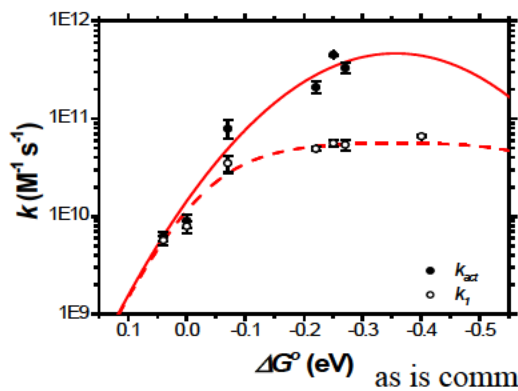
Atefeh Taheri, William Ward, Byron Farnum, and Gerald J. Meyer

Departments of Chemistry and Materials Science & Engineering,
Johns Hopkins University, Baltimore, MD 21218

The Ru(II) coordination compounds utilized in regenerative dye-sensitized solar cells quantitatively undergo three consecutive charge-transfer reactions shown schematically: 1) light absorption through metal-to-ligand charge transfer (MLCT) excitation; 2) excited-state electron injection into TiO₂; and 3) reduction through oxidation of an electron donor present in the solution electrolyte. In principle, immediately after completion of this cycle the sensitizer is “regenerated” and could repeat the “sensitization cycle” again. Under 1 sun illumination each sensitizer repeats this cycle on average about twice per second. This poster addresses the third charge transfer reaction and explored in fluid solution and reports iodide oxidation mechanisms in fluid solution and at metal oxide interfaces.



New Ru-tris(diimine) compounds were prepared that enabled systematic variation of the free-energy change for excited state hole transfer (ΔG°) to iodide over a 400 meV range. A strong driving force dependence was apparent with diffusion limited rate constants for exergonic



reactions and values on the order of $10^9 M^{-1} s^{-1}$ for $\Delta G^\circ \geq 0$ eV. Iodine atoms were identified as the reaction product. The temperature dependence was also quantified. After corrections for diffusion in CH₃CN, analysis of the activated rate constants, k_{act} , with Marcus theory provided insights into the factors that underlie the rapid electron transfer measured for endergonic reactions and indicate that iodine atoms cannot be ruled out as intermediates in dye sensitized solar cells based upon thermodynamic arguments alone as is commonly done.

In unpublished work, iodide oxidation mechanisms in low dielectric constant solvents where ion-pairing was clearly evident have been characterized. The photo-oxidation of iodide by Ru(deebq)(bpy)₂²⁺, where deebq is 4,4'-(CO₂Et)₂-2,2'-biquinoline, in thf revealed the immediate appearance of I₂⁻ and Ru(deebq)(bpy)₂⁺ under conditions where control experiments showed that the $I^- + I^- \rightarrow I_2^-$ reaction was much slower. This preliminary data suggests that I-I bond formation and electron transfer can occur in one concerted step from a molecular excited state. Electrocatalysis studies designed to identify conditions where concerted I-I bond formation might be initiated by an oxidized compound at metal oxide interfaces will also be presented. The electrochemical data provide compelling evidence that Ru and Os polypyridyl compounds anchored to metal oxide surfaces efficiently catalyze iodide oxidation.

Metal-to-Ligand Charge Transfer Excited States on Surfaces and in Rigid Media. Application to Energy Conversion

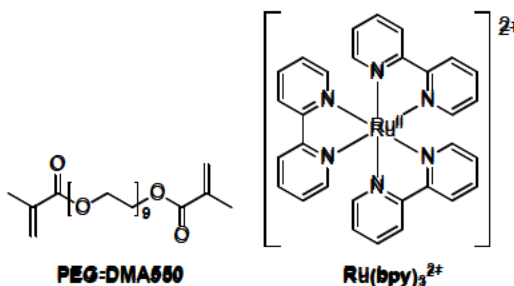
Akitaka Ito, John M. Papanikolas and Thomas J. Meyer

Department of Chemistry

The University of North Carolina at Chapel Hill

Chapel Hill, NC 27599

Poly(ethyleneglycol)dimethacrylate films and monoliths undergo thermal or photochemical polymerization to give optically transparent materials with features conformable to the nanoscale. We reported previously on the spectroscopic and photophysical properties of a series of polypyridyl ruthenium(II) complexes in a PEG-DMA containing nine ethylene glycol spacers (PEG-DMA550) in both fluid and film environments and have extended those measurements to a series of Os(II) complexes [1]. At the PEG-DMA550 fluid-to-film transition, the Metal-to-Ligand Charge Transfer (MLCT) emission energies and excited-to-ground state 0-0 energy gaps (E_0) increase due to a “rigid medium effect.” More recently, we have also reported long-range energy transfer from $\text{Ru}(\text{bpy})_3^{2+*}$ to two modified anthracenes by Dexter mechanism in semi-rigid PEG-DMA550 films and ultra-long-range energy transfer sensitization of electron transfer has been observed over $>90 \text{ \AA}$ in films containing complex, anthracene incorporated into the polymeric network, and added methyl viologen as an electron transfer trap [2].



We have extended the film-based dynamics studies to reductive electron transfer quenching of $\text{Ru}(\text{bpy})_3^{2+*}$ in PEG-DMA550 films, e.g., $\text{Ru}(\text{bpy})_3^{2+*} + \text{PTZ} \rightarrow \text{Ru}(\text{bpy})_3^+ + \text{PTZ}^+$ (PTZ is phenothiazine). In the polymerized film, emission quenching occurs by two kinetic pathways – rapid, static and slow, diffusional – similar to observations made earlier for energy transfer quenching. The kinetics of the rapid electron transfer quenching were analyzed as reported earlier [3]. Analysis of the distance dependence data for the rapid pathway demonstrated electron transfer of long distances with a distance attenuation factor, β , of $\sim 0.28 \text{ \AA}^{-1}$ with $k_{\text{ET}}(R) = k_{\text{ET}}^0 \exp(-\beta R)$ and k_{ET}^0 the electron transfer rate constant at $R = 0$, and R the internuclear separation distance. The β value was essentially independent of free energy change for electron transfer (ΔG_{ET}^0) while k_{ET}^0 varied with ΔG_{ET}^0 as predicted by electron transfer theory. Back electron transfer dynamics, $\text{Ru}(\text{bpy})_3^+ + \text{PTZ}^+ \rightarrow \text{Ru}(\text{bpy})_3^{2+} + \text{PTZ}$, are also distance dependent and were analyzed by power law kinetics.

References

- [1] Knight, T. E.; Goldstein, A. P.; Brennaman, M. K.; Cardolaccia, T.; Pandya, A.; DeSimone, J. M.; Meyer, T. J. *J. Phys. Chem. B* **2011**, *115*, 64.; Ito, A.; Knight, T. E.; Stewart, D. J.; Brennaman, M. K.; Meyer, T. J. manuscript in preparation.
- [2] Ito, A.; Stewart, D. J.; Fang, Z.; Brennaman, M. K.; Meyer, T. J. *Proc. Natl. Acad. Sci.* **2012**, *109*, 15132.; Ito, A.; Stewart, D. J.; Knight, T. E.; Fang, Z.; Brennaman, M. K.; Meyer, T. J. submitted for publication.
- [3] Wenger, O. S.; Leigh, B. S.; Villahermosa, R. M.; Gray, H. B.; Winkler, J. R. *Science* **2005**, *307*, 99.

Design of Structures Optimal for Singlet Fission

Josef Michl

Department of Chemistry and Biochemistry

University of Colorado

Boulder, CO 80309-0215

Singlet fission is a process in which a singlet excited chromophore shares some of its energy with a neighboring ground-state chromophore and both end up in their respective triplet states. It thus permits a single absorbed photon of sufficient energy to produce two electron-hole pairs. When the remaining lower-energy photons are used to produce one electron-hole pair each, the overall maximum theoretical efficiency exceeds the Shockley-Queisser limit by a factor of ~1.4. Very few solids are known to undergo singlet fission efficiently (e.g., tetracene and pentacene), and our project is to find structural design rules that would permit the discovery of additional efficient materials in order to make it easier to meet the numerous other conditions that a solar cell material needs to satisfy. In the past, we identified two classes of structures that are likely to serve as suitable chromophores, and demonstrated that a member of one of the classes, 1,3-diphenylisobenzofuran, actually affords the maximum possible triplet yield of 200% in the polycrystalline state. We have now also developed rules for efficient mutual coupling of chromophores (slip-stacking, with the slip in the direction of the HOMO-LUMO transition moment, is the optimal one so far and is indeed found in most of the known efficient systems, such as the polyacenes and 1,3-diphenylisobenzofuran). Our conclusion is that the direct term in the expression for the rate of singlet fission in a dimer is negligible relative to the mediated term that involves charge-transfer states of the dimer as virtual intermediates. We are currently engaged in the synthesis and testing of various types of covalent dimers of 1,3-diphenylisobenzofuran and cibalackrot. We have published direct observations of charge-transfer states of dimers in polar solvents (in non-polar solvents they remain virtual and are not observed).

Design of supramolecular cobaloxime-based photocatalyst assemblies

Karen L. Mulfort, Anusree Mukherjee, Oleksandr Kokhan, Jier Huang, Jens Niklas, Lin X. Chen, David M. Tiede

Division of Chemical Sciences and Engineering
Argonne National Laboratory
Argonne, IL 60439

Natural photosynthetic systems precisely position molecular light-harvesting and catalytic modules into complex, hierarchical protein host frameworks which create directional electron transfer pathways and stabilize long-lived charge separated states. Remarkably, these complex structures are composed wholly of earth-abundant elements and structurally bound by generally weak but specific supramolecular interactions. Supramolecular assembly techniques offer mechanisms to 1) stabilize traditional small molecule electrocatalysts, 2) promote efficient photoinduced electron transfer (PET) and stabilization of charge-separated states, and 3) enable dynamic self-healing pathways. This poster will describe our recent efforts to implement biological design principles to develop and discover new abiotic photocatalysts towards the goal of artificial photosynthesis.

In this poster we describe the synthesis and characterization of ground state structure and excited state dynamics of a new photocatalyst coordination motif based on the well-known cobaloxime proton reduction catalyst (Figure). The ground state structure of the new supramolecular photosensitizer-catalyst assembly was characterized by a variety of physical techniques including UV-Vis spectroscopy, Co K-edge X-ray absorption spectroscopy, and X-band EPR spectroscopy. Ultrafast and nanosecond transient absorption spectroscopy was used to show that equatorial coordination of Ru(II)polypyridyl photosensitizers to the cobaloxime macrocycle results in instantaneous formation of the mechanistically critical Co(I) state through ultrafast charge separation following visible light excitation. The Co(I) state persists for approximately 60 ps before decay to a bridging ligand based charge-separated state. Notably, slight modification of the photosensitizer-catalyst bridge results in dramatic differences in transient behavior. The photosensitizer-catalyst assemblies developed here are being extended and modified for incorporation into bio-hybrid assemblies using multi-heme c-cytochromes to provide architectures for multiple electron H₂ catalysis.

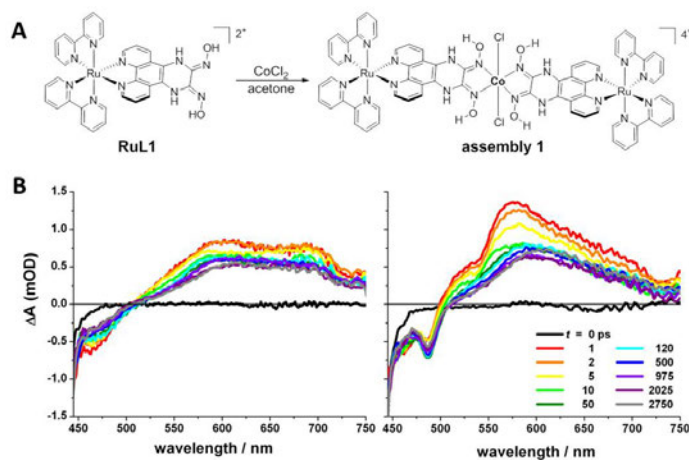


Figure. A) Chemical structure of dioxime-functionalized photosensitizer, **RuL1**, and Co(II)-templated assembly **1**. B) Difference spectra of **RuL1** (left) and assembly **1** (right) following 420nm excitation in CH₃CN.

Control of Optical Transitions in Colloidal Indium Nitride Nanocrystals via Chemical Oxidation

Peter K. B. Palomaki and Nathan R. Neale
Chemical and Materials Science Center
National Renewable Energy Laboratory
Golden, CO 80401

We are interested in chemical approaches to manipulate the fundamental photophysical properties of semiconductor nanocrystals (NCs). Over the past several years, we have focused on germanium NCs and demonstrated a novel route based on the mixed-valence precursor method that provided the first control of both the size and optical properties (band gap and NIR emission) of these colloidal species.¹ More recently, we extended this synthetic method to main group element-alloyed Ge NCs and uncovered unique surface chemistry that enabled the only reported long-range (25 μm) charge transport in group IV NC superlattices.²

We are also exploring III-V NCs due to their excellent light absorption and charge separation properties, which for many compositions stem from their combination of heavy effective mass electrons/holes and small, direct band gaps. Here, we will discuss our new results in synthesizing and manipulating the photophysics of colloidal indium nitride (InN) NCs.³ As has been revealed for InN thin films, surface states dope these nanostructures, moving the Fermi level above the conduction band minimum such that the Γ - Γ band transition occurs at energies well in excess of the band gap (the Burstein-Moss effect). We also will describe a characteristic optical feature for

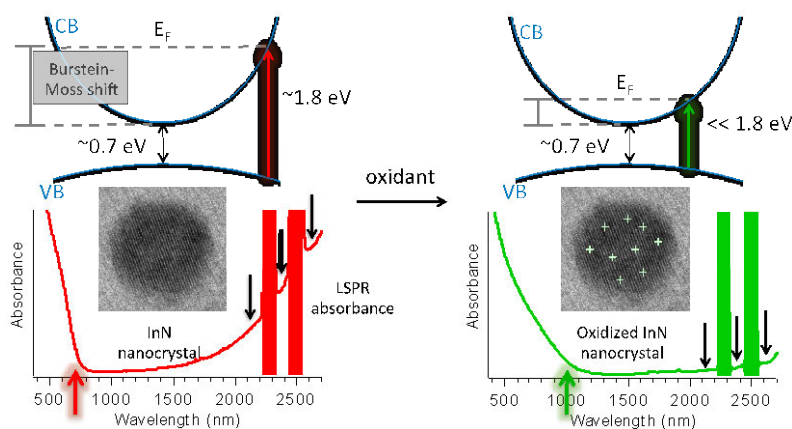


Figure 1. Tuning of the Γ - Γ band absorption onset from ~ 700 to ~ 1000 nm (colored arrows) and the plasmon absorption intensity (black arrows) in InN nanocrystals via chemical oxidation. The bold colored bars obscure solvent absorptions for clarity.

indium nitride in a localized surface plasmon resonance (LSPR) absorption in the infrared centered at ~ 3000 nm. Chemical oxidation is shown to modulate both the intensity of this LSPR and the band-to-band absorption onset (Figure 1). These results demonstrate control of carrier density in InN NCs through simple chemical oxidation, a strategy that can be applied more broadly to tuning the photophysical properties of other semiconductor nanostructures.

1. Daniel A. Ruddy, Justin C. Johnson, E. Ryan Smith, Nathan R. Neale *ACS Nano* **2010**, *4*, 7459-7466. (doi: 10.1021/nn102728u)
2. Daniel A. Ruddy, Peter T. Erslev, Susan E. Habas, Jason A. Seabold, Nathan R. Neale *J. Phys. Chem. Lett.* **2013**, *4*, 416-421. (doi: 10.1021/jz3020875)
3. Peter K. B. Palomaki and Nathan R. Neale, *Submitted*.

Formulation of D/A Coupling and the Role of Orthogonality

Marshall D. Newton
Chemistry Department
Brookhaven National Laboratory
Upton, New York 11973-5000

We consider the role of orthogonalization in the formulation of electronic coupling (H_{ij} , where H is the electronic Hamiltonian) in molecular electron transfer (ET), dealing specifically with linear DBA triads (where D, B, and A are, respectively, donor, bridge-mediating, and acceptor states/sites) as well as related diads DB, BA, and DA, with the goal of assessing the transferability of a given coupling magnitude (for both nearest-neighbor (NN) and next-nearest neighbor (NNN) pairs) between different molecular contexts. We also compare 2-state and multistate expressions for H_{DA} .

The diabatic states (D, B, and A) are generally defined as being maximally site-localized, based on some physical criterion. Often one employs a unitary transformation of the electronic eigenstates, thereby maintaining orthonormality (ON). Here, we use the familiar generalized Mulliken Hush (GMH) model (developed earlier in this Program with Robert Cave), maximizing the state centroid separations.

On the other hand, so-called ‘direct’ approaches generate D and A nonorthogonal (NO) D and A states via electronic symmetry breaking, leading to the familiar overlap adapted expression:

$$(H_{DA})' = H_{DA} - S_{DA} H_{D/A} / (1 - (S_{DA})^2) \quad (1)$$

where S_{DA} is the overlap element, and $H_{D/A}$ is generally the mean value of H_{DD} and H_{AA} .

NB: eq 1 does *not* express overall coupling between NO states. In fact, physically meaningful off-diagonal matrix elements must be expressed using ON states (to avoid arbitrary dependence on the zero of the relevant operator). The ON states implicit in eq 1 (D' and A') are easily expressed for symmetry equivalent D and A sites by determining the eigenstates of the 2-state Hamiltonian in the NO D, A basis and then taking the plus and minus combinations (normalized by $1/2^{1/2}$) of these eigenstates (*ie*, the localization step).

Another way to navigate from NO to ON states (in the ‘least motion’ sense) is to employ the Lowdin symmetrical orthogonalization scheme (LO), characterized by the transformation $S^{-1/2}$, where S is the overlap matrix. Here we apply LO to the fully site-localized (and thus NO) basis states, and then compare LO and GMH coupling magnitudes.

We explore the utility of a 1-dimensional delta function model (DFM), with potential energy operator at each site i , $V_i \delta(x-x_i)$, and $V_i < 0$, leading to one bound eigenstate for each isolated site (D, B, A). DFM eigenstates for DBA or the subunits DB, BA, and DA (with NN separation of $5 a_0$ and the NNN DA separation of $10 a_0$), were evaluated either exactly, or as basis set approximations (based on isolated DFM eigenstate basis states) and then subjected to LO and GMH localization. Salient results are as follows:

- Exact *vs* basis set and LO *vs* GMH coupling results: *excellent* agreement
- Transferability of coupling magnitude: *excellent* for all NN moieties; *very poor* for NNN (*ie*, DA), the consequence of orthogonality, which unavoidably involves the B state in the nominal direct DA coupling in DBA-- *ie*, the ‘orthogonality dilemma’.

New Approaches to Generating and Utilizing Multiple Excitons from Single Photons for Enhanced Photoconversion Efficiency

A.J. Nozik^{†,*}, J.C. Johnson[†], and M.C. Beard[†]

[†]National Renewable Energy Laboratory
Golden, CO 80401

and

*University of Colorado
Department of Chemistry and Biochemistry
Boulder, Colorado 80305

The generation of more than one electron-hole pair from single photons of sufficient energy to satisfy energy conservation can be achieved in semiconductor nanocrystals (quantum dots, quantum rods, and quantum wires) and in certain molecular chromophores that exhibit singlet fission. The photogenerated electron-hole pairs in these systems initially exist as excitons which must be subsequently dissociated and separated into free charge carriers for utilization in devices that convert solar irradiance into electricity or solar fuels. The solar power conversion efficiency of well-known semiconductors and singlet fission chromophores can be enhanced under 1-sun illumination through these carrier multiplication processes, but the degree of enhancement can be significantly increased further through the use of solar concentration, new phases of semiconductor photoconverters that have small values for their bulk bandgaps, and through buried junction and Z-scheme architectures. These various approaches will be discussed. Furthermore, the differences and similarities in the mechanisms of multiple exciton generation (MEG) in semiconductors and singlet fission in molecular chromophores, as well as in the device architectures of these two classes of exciton-multiplying photoconverters, will be described.

Single Molecule and Nanoparticle Spectroelectrochemistry for Understanding Interfacial Charge Transfer Events

Caleb M. Hill, Daniel A. Clayton, Jia Liu and Shanlin Pan

Department of Chemistry, The University of Alabama, Tuscaloosa, Alabama, 35487

We employed single molecule and single nanoparticle spectroelectrochemistry to reveal temporal and spatial heterogeneities in their charge transfer characteristics. For example, fluorescence “blinking” studies of single (4, 4'-difluoro-4-bora-3a, 4a-diaza-s-indacene) BODIPY dye molecules bearing two carboxylic acid groups at its 2 and 6 positions were carried out. Molecules self-assembled onto ordered TiO₂ nanostructures show the shortest ON duration times due to efficient interfacial charge transfer in comparison to molecules on bare glass and indium-tin oxide (ITO) surfaces, and to those embedded in a polystyrene matrix. Decreases in fluorescence stability or intensity due to charge transfer activity are revealed using single molecule spectroelectrochemical methods. Our study shows these molecules embedded in polystyrene have a heterogeneous half redox potential distribution of 1.80 (+/-0.18) V vs. SHE, which reflects the heterogeneity in charge transfer rates among single molecules (Figure 1). We also applied our single molecule spectroelectrochemistry method to

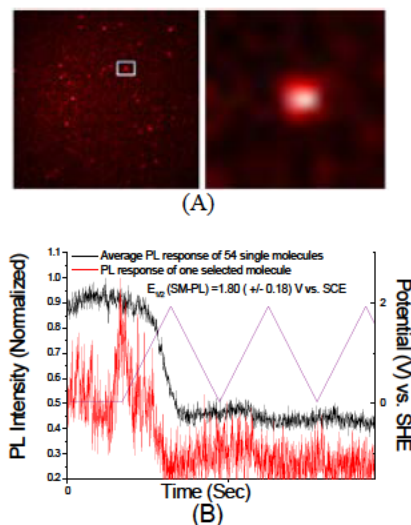


Figure 1: Single molecule fluorescence images (A), and responses to substrate potential (B).

probe the redox activities of individual noble metal nanostructures. Such metals, particularly Ag and Au, support strong plasmon resonance in the optical region of the electromagnetic spectrum, and have been shown to aid in the harvesting of solar energy by enhancing the absorption of visible light by dyes/semiconductors in close proximity. Here, the electrochemical synthesis of Ag nanoparticles is monitored *in situ* by dark-field scattering microscopy. After correlating the scattering measurements with scanning electron microscopy (SEM), Mie theory can be used to relate the scattering intensity for individual nanoparticles to their size. This enables the calculation of pseudo I-V curves (Figure 2) depicting the deposition of individual nanoparticles, a measurement not possible using traditional electrochemical techniques. The resulting heterogeneities in reactivity among a statistically significant population of nanoparticles (>2000) are presented and discussed. We also studied the photo-induced charge transfer events of individual metallic nanostructures on the surface of TiO₂ single crystals using combined electrochemical and optical spectroscopy methods. By taking advantage of the intrinsic fluorescence of silver, heterogeneities in charge transfer between different TiO₂ crystal facets and Ag⁺ ions in solution can be visualized.

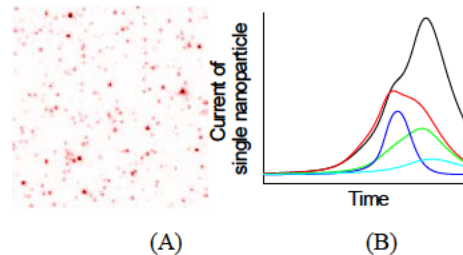


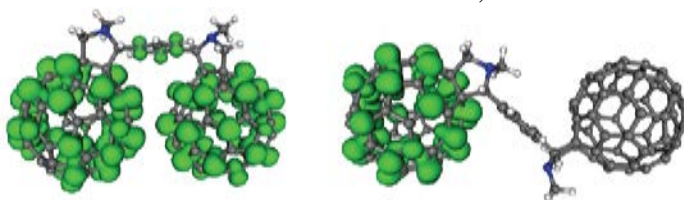
Figure 2: Dark field image of single silver nanoparticles (A), and current trajectories at several selected sites to form single silver nanoparticles (B).

Photoinduced Charge Separation Processes: From Natural Photosynthesis to Organic Bulk Hetrojunctions

Oleg Poluektov, Jens Niklas
Chemical Sciences and Engineering Division
Argonne National Laboratory
Argonne, IL 60439
Vladimir Dyakonov
Department of Experimental Physics
University of Würzburg
Würzburg, Germany D-97074

Advanced EPR spectroscopy, especially light-induced multi-frequency EPR, has been essential for understanding the mechanisms of the light generation, separation, and recombination of charge carriers in natural photosynthesis. The application of this technique to organic photovoltaic (OPV) materials demonstrates the significant similarities of charge transfer processes in OPVs and natural photosystems. Among them are: spatial delocalization of the positive cation radical after light-induced charge separation; sequential electron transfer between acceptor molecules; stabilization of charge separated states on the distances of ca. 25-30 Å. This analogy allows us to apply the suite of experimental and theoretical techniques, which were successfully developed for the study of photochemical reactions in natural and artificial photosynthetic systems, to OPV materials.

Here, we use EPR spectroscopy combined with DFT calculations to study charge separation and stabilization mechanisms in active organic PV materials based on composites of multiple polymers and fullerene derivatives of C₆₀ and C₇₀, including a C₆₀/C₇₀ heterodimer. Time-resolved EPR spectra show strong polarization pattern for all polymer-fullerene blends under study, which is caused by non-Boltzmann population of the electron spin energy levels in the radical pairs. Similar polarization patterns were first reported in natural and artificial photosynthetic assemblies, and were understood within the models of spin-correlated radical pairs and sequential electron transfer. These help us to describe the charge separation process like electron jumps or tunneling between neighboring fullerene molecules. The first step of the charge separation process is exciton dissociation and electron transfer to the fullerene molecule at the polymer interface. The life time of this state is no longer than few picoseconds. Forward electron transfer forms an intermediate radical pair, with the separation distance within 15-20 Å. The third step is electron transfer to the secondary radical pair with a separation of 25-30 Å which is stabilized for tens to hundreds of microseconds. No charge delocalization over several fullerene cages were observed in polymer-monomeric fullerene films. In contrast, in the fullerene heterodimer the anion state is delocalized over both cages in the film. The data presented here in combination with DFT calculations helps to improve our understanding of the mechanisms of charge separation processes in the active organic photovoltaic materials.



Theoretical calculation of spin density distribution in cis- and trans-conformers of C₆₀/C₇₀ heterodimer anion.

Miniature dispersive XES spectrometer for time resolved analysis of charge transfer

K. Davis, J. Seidler, Y. Pushkar
Department of Physics
Purdue University
West Lafayette, IN 47907

Removal of electrons from redox active metal centers results in charge separated states as well as in activated catalytic sites. For instance, the redox reactivity of Mn atoms is essential to the function of the oxygen evolving complex (OEC) of Photosystem II (PS II) and Mn-based artificial sunlight-to-energy assemblies. It has proven extremely challenging to follow the changes in the electronic structure of the Mn-centers in time as the system goes through the processes of light absorption, electron transfer and formation of new chemical bonds. Analysis of these processes with time resolved spectroscopic techniques is crucial for understanding the details of the underlying electron dynamic and the chemical bond formation. We proposed that laser pump/X-ray probe time resolved X-ray emission spectroscopy (TR-XES) is an efficient tool for time resolved analysis of electron structure dynamic at metal centers. Miniature X-ray emission spectrometer capable of dispersive detection of XES spectra at Mn K beta lines is well suited for TR-XES, Figure 1.

With miniXES we tested the paradigm of “detection-before-destruction” on the example of a metalloprotein complex exposed at room temperature to the high x-ray flux typical of third generation synchrotron sources. Following the progression of the x-ray induced damage by Mn K β XES, we demonstrated the feasibility of collecting room temperature data on the electronic structure of PS II. The determined non-damaging observation timeframe (about 100 milliseconds using continuous monochromatic beam, deposited dose 1×10^7 photons/ μm^2 or 1.3×10^4 Gy, and 66 microseconds in pulsed mode using pink beam, deposited dose 4×10^7 photons/ μm^2 or 4.2×10^4 Gy) is sufficient for the analysis of this protein’s electron dynamics and catalytic mechanism at room temperature. Reported time frames are expected to be representative for other metalloproteins. We also analyzed a time/dose progression of X-ray induced damage and proposed a kinetic model which fits experimental data.

Delivering a laser excitation (in the form of ns laser pulses) onto the sample and synchronizing laser pump and X-ray data collection we characterized light induced states such as S₂ state in the PS II, Figure 1 and metal to metal charge transfer process in all inorganic chromophores Zr(IV)-O-Mn(II) on the surface of nano-silica (in collaboration with H. Frei, LBNL).

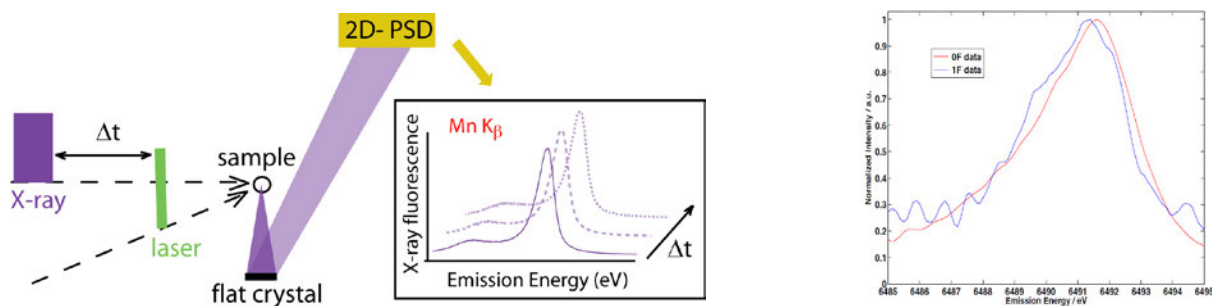


Figure 1. Left: scheme of the laser pump / X-ray probe experiment utilizing dispersive miniXES spectrometer. Right: PS II Mn K β XES of the dark stable S₁ state (0F- red) and S₂ formed with one laser flash (1F- blue). Light excitation: 8 ns, 532 nm laser pulse. Detection: 200 μsec after laser excitation by 40 μsec X-ray pulse with about 3×10^{11} photons. Measurement time: 25 min at 20Hz, 50000 X-ray pulses were averaged.

Photo-induced electron transfer in polymer solar photoconversion systems

Garry Rumbles, Obadiah Reid, Nikos Kopidakis, Bryon Larson, Andrew Ferguson
Chemical and Materials Sciences Center
National Renewable Energy Laboratory
Golden, Colorado and 80401

Although certified power conversion efficiencies for organic solar cells have now exceeded 10%, our knowledge of how these devices function remains rudimentary. Of particular interest, is the ability of the system to generate free charges in high yield when the primary product of photoexcitation is a bound electron-hole pair (exciton). The efficiency of charge generation far exceeds what would be predicted for the low dielectric medium comprised of a specific blend of conjugated polymer with, most frequently, a high electron affinity fullerene. Using the

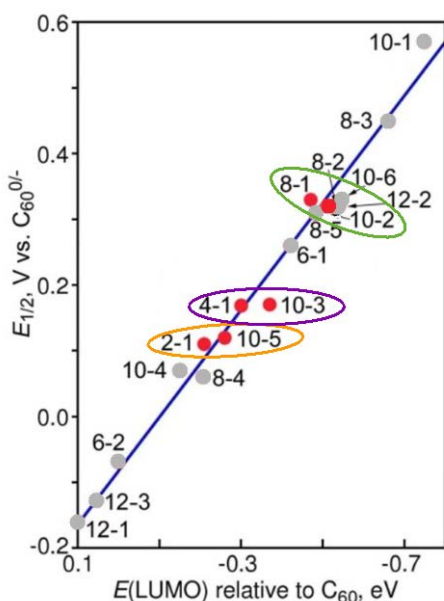


Figure 1 – Controlling the reduction potential of PFAFs using selective substitution patterns and number of $-\text{CF}_3$ groups on the fullerene (Popov, Strauss, Boltalina et al, J. Am. Chem. Soc.129 (2007) 11551).

electrodeless technique of time-resolved microwave conductivity (TRMC) we have examined the factors that control the generation of free carriers in two novel systems. The first builds upon our previous work that examined the influence of the driving force for electron transfer by controlling the electron affinity (more precisely, the reduction potential) of the fullerene. In this presentation we will report new results on 6 perfluoroalkyl fullerenes (PFAFs) that form 3 pairs with common reduction potentials, but significantly different substitution patterns (see Figure 1). This study has enabled us to determine not only the carrier yields, but also the role that the substitution pattern has on the electronic coupling between the clustered PFAFs.

In addition, we will report on a new bilayer platform for probing the role that the interface between the conjugated polymer and the fullerene plays in determining the relative efficiency of the formation of charge separated (CS) states and charge transfer (CT) states. Using a layer of precursor-route poly(*p*-phenylene vinylene), PPV, we have successfully vapour-deposited C_{60} to create an excellent bilayer construct that yields extremely low free carrier yields, even though the driving force for electron transfer is determined to be almost ideal. We will report new results on how this platform enables us to control the relative yields of CT and CS states.

Recent publications:

Coffey, D. C.; Larson, B. W.; Hains, A. W.; Whitaker, J. B.; Kopidakis, N.; Boltalina, O. V.; Strauss, S. H.; Rumbles, G. (2012). Journal of Physical Chemistry C. Vol. 116(16); pp. 8916-8923;
Blackburn, J. L.; Holt, J. M.; Irurzun, V. M.; Reasco, D. E.; Rumbles, G. (2012). Nano Letters. Vol. 12(3), 14; pp. 1398-1403;
Dayal, S.; Kopidakis, N.; Rumbles, G. (2012). Faraday Discussions. Vol. 155; pp. 323-337;

Formation and Characterization of Semiconductor Nanorod/Oxide Nanoparticle Hybrid Solids: Toward Vectoral Electron Transport

Neal R. Armstrong, Jeffrey Pyun, S. Scott Saavedra

Department of Chemistry/Biochemistry

University of Arizona

Tucson, Arizona 85721

Overview: The synthesis and characterization of a new class of photocatalytic heterostructured semiconductor nanorods will be discussed. We have developed robust and selective synthetic methods to deposit noble metal and cobalt oxide based nanoparticle as “tips” onto the termini of n-type CdSe@CdS nanorods (Fig. 1). The synthesis of nanorods with varying structural motifs (e.g., matchstick, dumbbell, asymmetric) and nanoscopic dimensions has been conducted to enable optimization of photocatalytic materials. Our recent research efforts have been focused on: (i) formation of new photocatalytic nanorods and nanostructured networks with electronically coupled semiconductor interfaces to metallic and metal oxide catalytic sites; (ii) the characterization of valence band energies (E_{VB}) of heterostructured photocatalysts by photoemission spectroscopies; (iii) spectroelectrochemical and photocatalytic characterization of heterostructured nanorod and network materials

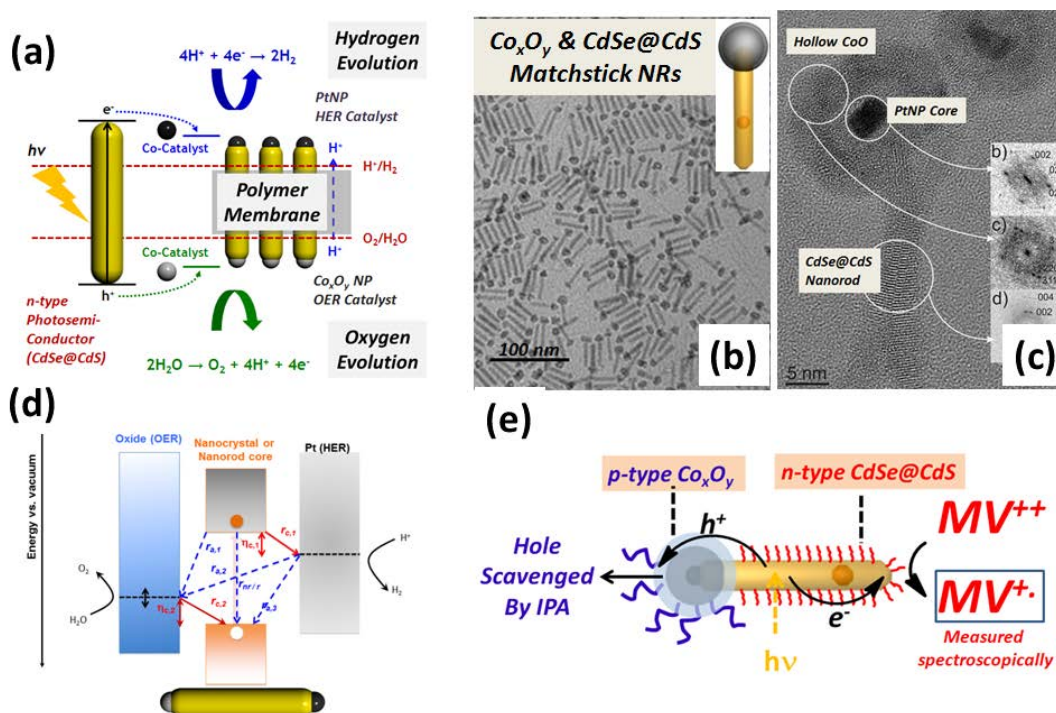


Figure 1: (a) proposed scheme for artificial photosynthesis using heterostructured nanorod photocatalysts (b) TEM of matchstick nanorods of Co_xO_y and CdSe@CdS (c) HRTEM of dumbbell Co_xO_y & CdSe@CdS (d) proposed energetics for nanorod materials measured via PES (e) photocatalytic studies with heterostructured nanorods.

Carrier Injection and Dynamics from Photoexcited Transition Metal Containing Porphyrins

Rebecca L. Milot, Gary F. Moore, Lauren A. Martini, Christian A. F. Negre, Victor S. Batista,
Robert H. Crabtree, Gary W. Brudvig, and Charles A. Schmuttenmaer

Department of Chemistry
Yale University
New Haven, CT 06520-8107

Terahertz spectroscopy has proven itself to be an excellent non-contact probe of charge injection and conductivity with sub-picosecond time resolution. I will describe the charge injection time scale and efficiency for a selection of high-potential photoanodes (HPPAs) for photoelectrochemical cells. The anodes consist of bis- and tris-pentafluorophenyl free-base and metallo-porphyrin sensitizers anchored to TiO_2 and SnO_2 nanoparticles. Photoelectrochemical measurements demonstrate that the photosensitizers extend the absorption of the bare anode well into the visible region. THz spectroscopic studies demonstrate the sensitizers used in these HPPAs are capable of injecting electrons into the conduction band of the metal-oxide materials in those cases where the energies of the donor (excited state dye) and acceptor (metal oxide conduction band minimum) components are appropriate. The time scales and efficiencies are interpreted in terms of the identities (singlet vs. triplet) and energetics of excited electronic states.

We have also investigated axially complexing bis-pentafluorophenyl Zn-porphyrin sensitizers to an isonicotinic acid anchor or variants thereof rather than binding them directly to the metal oxide surface. I will compare their binding stability in water, as well as their photoexcited interfacial electron transfer efficiency when using carboxylic acid, hydroxamate, acetylacetonate and phosphonate the anchoring group.

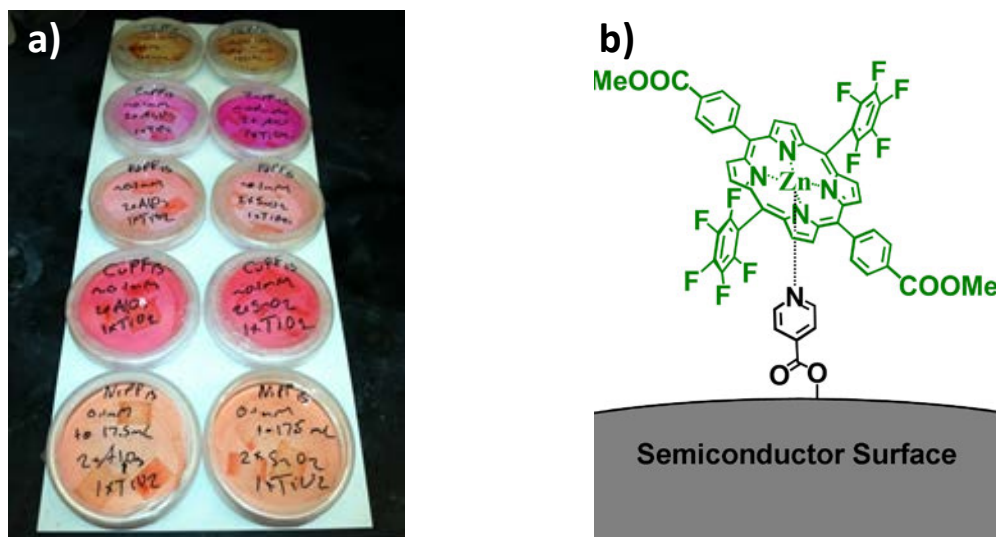


Figure 1. Part (a) shows dichloromethane solutions the tris-pentafluorophenyl metallo-porphyrins studied where $M = \text{Ni}^{2+}$, Cu^{2+} , Pd^{2+} , Zn^{2+} , and H_2 in going from the bottom to the top. Part (b) shows a high-potential Zn porphyrin complexed to isonicotinic acid that is anchored to a metal oxide surface.

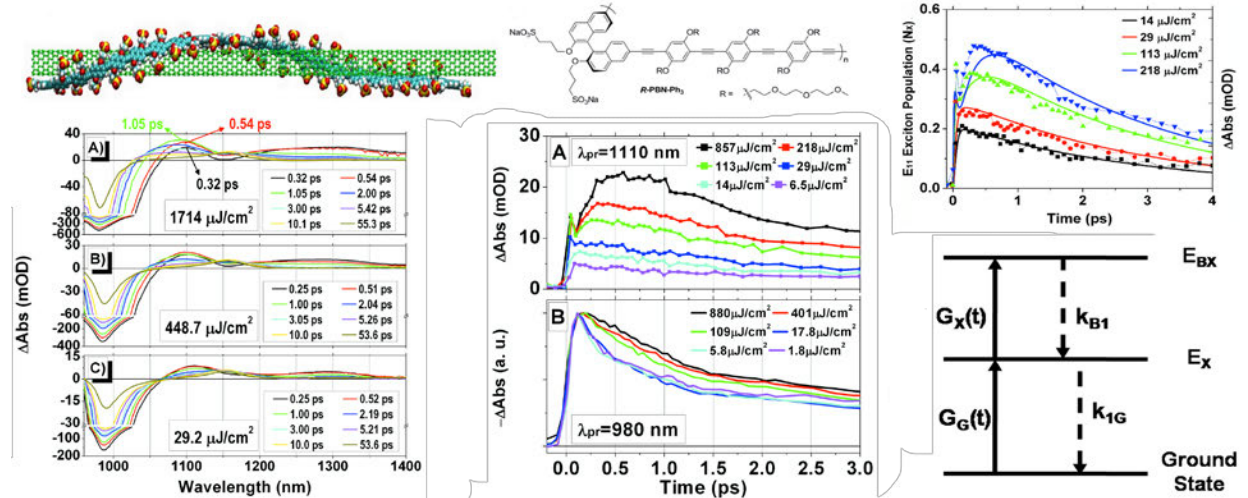
Fluence-Dependent Singlet Biexciton Dynamics in Chirality-Enriched Single-Wall Carbon Nanotubes

Jaehong Park^{a,b}, Pravas Deria^b, Jean-Hubert Olivier^b, and Michael J. Therien^b

^a Department of Chemistry, University of Pennsylvania, 231 South 34th Street, Philadelphia, PA 19104-6323, USA

^b Department of Chemistry, French Family Science Center, 124 Science Drive, Duke University, Durham, NC 27708-0346, USA

We utilize individualized (6,5) chirality-enriched single-walled carbon nanotubes (SWNTs), femtosecond transient absorption spectroscopy, and variable excitation fluences, to interrogate nanotube exciton/biexciton dynamics. For pump fluences below $30 \mu\text{J}/\text{cm}^2$, transient absorption (TA) spectra of (6,5) SWNTs reveal the instantaneous emergence of a TA at 1100 nm, suggesting that it derives from the E_{11} state; in contrast, under excitation fluences exceeding $100 \mu\text{J}/\text{cm}^2$, the corresponding TA manifests a rise ($\tau_{\text{rise}} \approx 250 \text{ fs}$) indicating that E_{11} state repopulation is required to produce this signal. These experiments demonstrate that relaxation of the E_{11} biexciton state ($E_{11,\text{BX}}$) gives rise to a substantial E_{11} state population, as increasing delay times result in a concomitant increase of $E_{11} \rightarrow E_{11,\text{BX}}$ transition oscillator strength. Notably under these experimental conditions, no fast relaxation component is observed for the ground state bleaching signal, indicating that contrary to perhaps commonly held expectations, exciton-exciton annihilation does not dominate SWNT relaxation dynamics under high excitation fluence conditions. Numerical simulations based on a three-state model are consistent with a mechanism whereby biexcitons are generated at high excitation fluences via sequential SWNT ground- and E_{11} -state excitation that occurs within the 980 nm excitation pulse duration. These experiments monitoring fluence-dependent TA spectral evolution show that SWNT ground $\rightarrow E_{11}$ and $E_{11} \rightarrow E_{11,\text{BX}}$ excitations are coresonant, and provide convincing evidence that $E_{11,\text{BX}} \rightarrow E_{11}$ relaxation constitutes a significant decay channel for the SWNT biexciton state, a finding that runs counter to assumptions made in previous analyses of SWNT biexciton dynamical data where exciton-exciton annihilation has been assumed to play a dominant role.



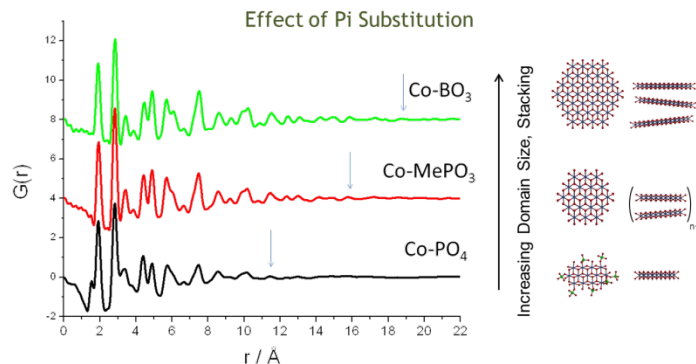
Amorphous Oxides as Models for the Design of Molecular Catalysts for Artificial Photosynthesis

David M. Tiede¹, Pingwu Du², Olesandr Kokhan¹, Karena Chapman³, Peter Chupas³, Karen L. Mulfort¹

¹Chemical Sciences and Engineering Division and Department and ³X-ray Science Division, Advanced Photon Source, Argonne National Laboratory, Argonne, IL 60439
and

²CAS Key Laboratory of Materials for Energy Conversion & Department of Materials Science and Engineering, University of Science and Technology of China, Hefei, China 230026

Efficient water oxidation chemistry is essential to achieve artificial photosynthesis for solar hydrogen or other fuels production. Electrolytically grown, self-assembled thin film oxygen evolving catalysts (OECs) of first row transition metals are of wide-spread interest for artificial leaf applications, and notable success has been achieved in the development of cobalt and nickel based films. Resolution of the fundamental chemistry underlying the self-assembly, repair, and catalysis of these amorphous metal-oxides provides can provide information needed for the design of efficient molecular catalysts for artificial photosynthesis applications that are based on first row transition metals. Towards this end, the structure of cobalt-phosphate oxygen evolving thin film catalysts, CoOECs, and the roles of the oxyanions used for the formation of these films was investigated using X-ray pair distribution function (PDF) analysis. X-ray PDF was applied to solve the structure of cobaltate domains within amorphous water splitting catalyst ex-situ films formed under three different buffer solutions (pH = 7.0, phosphate; pH = 8.0, methylphosphate, and pH = 9.2, borate). In each case the films are found to be composed of equivalent edge-sharing cobaltate lattice domains that differ in size, following the sequence of borate > methylphosphate > phosphate, with maximum atom-pair distances of approximately 19 Å, 16 Å, and 11 Å, respectively. In addition, the X-ray scattering measurements show that the changes in domain size are correlated to a transition to a disordered, layered domain structure and concomitant variation in the electrocatalytic activity. The results for the Co-OEC and for an analogous amorphous Ir-OEC¹ suggest a model where auxiliary ligands (Pi in the case of the Co-OEC, CP* poly-acid oxidation products in the case of the Ir-OEC) function to terminate growth of metal-oxide crystalline lattices and to provide acid-base functional groups to accelerate proton-coupled electron transfer catalysis.



(1) Blakemore, J. D.; Mara, M. W.; Kushner-Lenhoff, M. N.; Schley, N. D.; Konezny, S. J.; Rivalta, I.; Negre, C. F. A.; Snoeberger, R. C.; Kokhan, O.; Huang, J.; Stickrath, A.; Tran, L. A.; Parr, M. L.; Chen, L. X.; Tiede, D. M.; Batista, V. S.; Crabtree, R. H.; Brudvig, G. W. *Inorganic Chemistry* **2013**, *52*, 1860-1871

Fast Current Blinking in Semiconductor Quantum Dots

Klara Maturova, Sanjini U. Nanayakkara, Joseph M. Luther, and Jao van de Lagemaat
Chemical and Materials Sciences Center
National Renewable Energy Laboratory
Golden, Colorado, 80401

Single molecules and single semiconductor quantum dots (QDs) generally exhibit intermittency (i.e. blinking) of their fluorescence. Generally, it is theorized that Auger processes intermediated by an additional charge in the QD in either a trap state or in a bulk energy level cause the dots to be “off” while neutral dots are fluorescent. Analogously to luminescence blinking being caused by trapped charges, similar behavior might occur when the current through a single QD is measured in a scanning tunneling microscope or a conductive atomic force microscope (c-AFM).¹ This effect owes to the trapped charge inside the QD causing a Coulomb blockade and thus disabling current injection. Alternatively, the trapped charge can cause Auger processes to occur with injected charges from the tip.

In this contribution, we will show results of time-resolved, intermittent-contact, conductive atomic-force microscopy in the dark and under illumination on isolated CdSe and PbS semiconductor quantum dots covalently bound to gold substrates. Fast (microsecond to second scale) current intermittency of the tunneling current through the single QDs was observed in these experiments. The current switches on and off at timescales with power-law distributions for both the “on” and “off” times similar to observations of fluorescence intermittency as well as a distribution of discrete “on” levels at higher applied biases. We also observed additional current levels when the QDs were illuminated at low biases indicating photocurrent generation in the individual QDs. The observation of current intermittency due to Coulomb blockade effects has important implications for the understanding of carrier transport through extended arrays of quantum dots.

¹. Maturova, K.; Nanayakkara, S.; Luther, J. M.; van de Lagemaat, J. *Nanolett.* **2013**, doi:[10.1021/nl3036096](https://doi.org/10.1021/nl3036096)

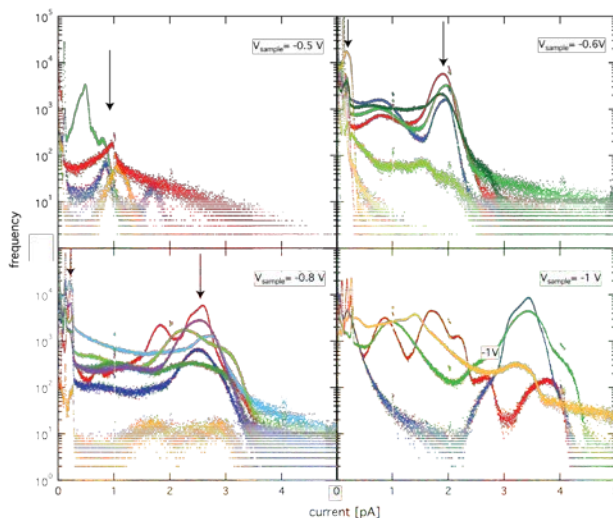


Fig. 1. Top: Maximal current intermittency histograms through single PbS QDs at different applied voltages. At high biases multiple current levels are observed

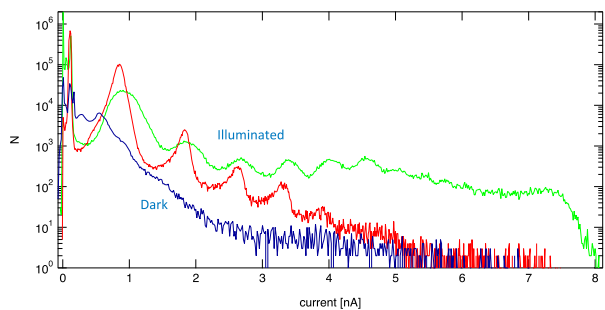


Fig. 2. Histogram of maximal current during a tap in the dark (blue) and light (green).

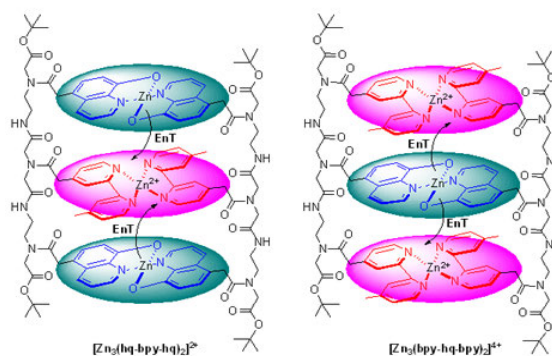
Tuning Photochemical Function of Multimetallic Assemblies Linked by Artificial Oligopeptide Scaffolds

Joy A. Gallagher, Meng Zhang, Sha Sun, Benjamin M. Biber and Mary Elizabeth Williams

Department of Chemistry
The Pennsylvania State University
University Park, PA 16802

Artificial oligopeptides with pendant ligands bind transition metal ions to form multi-metallic, heterofunctional structures capable of long-distance electron transfer and charge separation. Changing the ligands, metal ions, peptide backbone structure (e.g., insertion of a chiral center) and environment (e.g., solvent, anion) tunes the photochemical properties. In this poster we report recent studies on photoinduced electron/energy transfer in these structures and models for molecular switches. We have also recently inserted azobenzene into the oligopeptide to add a photoswitchable geometry and therefore interactions between metal complexes.

Heterofunctional tripeptides with pendant hydroxyquinoline (hq) and bipyridine (bpy) ligands were synthesized with two different sequences, hq-bpy-hq and bpy-hq-bpy. Coordination with Zn^{2+} forms trimetallic (Zn^{2+}) cross-linked tripeptide duplexes, in which emission of $[\text{Zn}(\text{hq})_2]$ is quenched by adjacent $[\text{Zn}(\text{bpy})_2]^{2+}$. A Dexter energy transfer quenching mechanism is supported by studies of the redox behavior and variable-temperature and solvent-dependent emission, as well as DFT calculations. We find that the interactions between unbridged but proximal metal complexes can be used to tune both the radiative relaxation rate and the wavelength of the emitted photon. $[\text{Zn}(\text{hq})_2]$ and $[\text{Cu}(\text{hq})_2]$ have also been linked to $[\text{Ru}(\text{bpy})_3]^{2+}$ to give heterometallic ‘hairpin’ structures in which the Zn or Cu species quench emission of $[\text{Ru}(\text{bpy})_3]^{2+}$ by different mechanisms. The photophysical data points towards an energy transfer from $[\text{Zn}(\text{hq})_2]$ to $[\text{Ru}(\text{bpy})_3]^{2+}$; however electron transfer quenching becomes the dominant mechanism when $[\text{Cu}(\text{hq})_2]$ is instead bound.



In separate experiments, a $[\text{Ru}(\text{bpy})_3]^{2+}$ oligopeptide complex with pendant bpy ligands was used to direct binding of 1 - 3 Pd^{2+} ions to form photocatalysts for the dimerization of α -methylstyrene. The excited state quenching mechanism of the Ru-Pd complexes was further studied by examining the details of the role of solvent dielectric, temperature, and addition of a sacrificial electron donor. These data together confirm an excited state electron transfer from Ru to Pd to generate the catalytically active species. This system is a good model for studying soft linkages between sensitizers and reaction centers that can be further applied to other reactions.

Bimolecular Electron Transfer Reactions in Ionic Liquids: Effects of Charge and Structure

Masao Gohdo and James F. Wishart

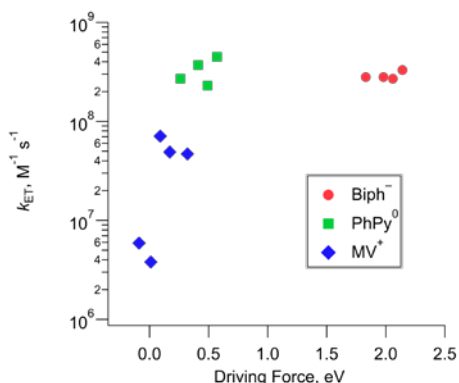
Chemistry Department, Brookhaven National Laboratory, Upton, NY 11973

Sufia Khatun and Edward W. Castner, Jr.

Dept. of Chemistry and Chemical Biology, Rutgers, The State University of New Jersey
Piscataway, NJ 08854

Ionic liquids (ILs) are useful media for many energy-related applications involving charge transport processes. However, their molecular-scale heterogeneity (polar/nonpolar domains, anion/cation interactions, etc.) sets them apart from conventional molecular solvents and confers unique combinations of properties. Kinetic and electrochemical studies have indicated that transport and reactivity of redox-active solutes in ILs depends on their charge types and sizes. In addition, redox-induced charge creation or annihilation may change the preferred solvation environment of the solute, adding additional complexity to the thermodynamic reaction profile.

We have been using pulse radiolysis techniques at the BNL LEAF picosecond pulse radiolysis facility to investigate the effects of reactant charge type on electron transfer reactions in the prototypical and widely studied ionic liquid *N*-methyl-*N*-butylpyrrolidinium bis(trifluoromethyl-



Plot of ET rate constants vs. driving force for three biaryl radicals reacting with four substituted benzoquinones.

sulfonyl)imide ($C_4mPyrr NTf_2$). We used pulse radiolysis to reduce biaryl redox species (biphenyl, *N*-phenylpyridinium cation and methylviologen dication) to produce quasi-isostructural biaryl radical electron adducts having respective charges of -1, 0, and +1 for electron transfer reactions with a series of substituted *p*-benzoquinone electron acceptors. Rate constants and activation parameters for the bimolecular ET reactions were obtained. DOSY Bipolar Pulse Pair STimulated Echo (DBPPSTE) NMR spectroscopy was used to measure diffusion coefficients of the biaryl solutes, and cyclic voltammetry at a boron-doped diamond electrode was coupled with simulations to estimate solute diffusion coefficients as well.

In general it was seen from these studies that diffusion of neutral biaryl species in $C_4mPyrr NTf_2$ is faster than for charged ones but not by a dramatic amount. This can be attributed to the fact that the redox solutes are of comparable size to the component ions of the ionic liquid and the butyl chains of the cations are too short to aggregate into an extensive nonpolar domain that could facilitate transport of neutral species. Recent X-ray scattering experiments and MD simulations on $C_nmPyrr NTf_2$ salts with chain lengths of $n = 4-10$ carbons by the Castner and Margulis groups as part of this SISGR collaboration show that such domains (evidenced by a “pre-peak” due to polar/nonpolar alternation) have an onset around $n = 8$ in this cation/anion system. Accordingly, these ET reactions are now being studied in $C_{10}mPyrr NTf_2$ and compared with our earlier results to look for explicit effects of the discrete polarity domains that exist in the longer-chain IL.

Dynamics of excess electrons and other solutes in room-temperature ionic-liquids

Jorge Kohanoff¹, Changhui Xu², Aleksander Durumeric², Hemant K. Kashyap², Sharad K. Yadav², Anne Kaintz³, Chris Rumble³, Mark Maroncelli³, Claudio J. Margulis²

¹Queen's University Belfast University Road Belfast BT7 1NN Northern Ireland

²Department of Chemistry, The University of Iowa, Iowa City, IA 52242

³Department of Chemistry, The Pennsylvania State University; University Park PA 16802

We are interested in understanding ionic transport as well as charge transport and transfer in room temperature ionic liquids. During the past year we have made significant progress in two areas, namely the early dynamics of excess electrons in different ionic liquids and the rotational and translational dynamics of solutes and ionic liquid solvents.

Our early studies on excess electrons¹ suggested that depending on the nature of cations and anions, electron localization could be very different. For example for imidazolium halide type of systems localization appears to be on the cations but instead in the case of alkyl-ammonium bis(trifluoromethylsulfonyl)amide systems an excess electron localizes on anions. Because the alkyl-ammonium systems that we studied are transparent in the typical UV and visible ranges commonly spectroscopically probed, at time zero absorption is solely due to excess electrons and holes. Our current studies indicate that initial subpicosecond dynamics produces large changes in the origin of electronic transitions in some of these systems with excess electrons. This is because the bis(trifluoromethylsulfonyl)amide anion is prone to dissociation and consequently the electronic structure of such systems significantly changes due to stabilization of the excess charge. This is quite relevant in light of recent experiments by David Blank and coworkers on these systems².

Another area that we have made significant progress in during this year is that of rotational dynamics of ionic liquids and solutes dissolved in them. One of the underlying questions we are trying to address is that of “anomalous” rotational diffusion (faster than hydrodynamic predictions). Computer simulations in the Margulis group in conjunction with NMR experiments and somewhat more simplistic computational models from the Maroncelli group are being used to understand whether dynamical heterogeneity or rotational diffusion via hopping are related to the observed phenomena. Current work in progress also addresses the difference in translational and rotational correlation times of solutes of the same size but different charge.

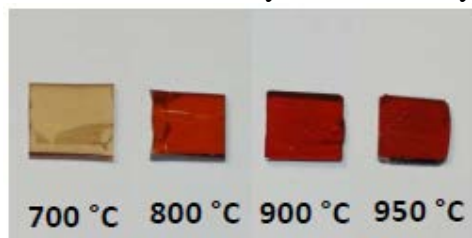
¹Claudio J. Margulis, Harsha V. R. Annapureddy, Pablo M. De Biase, David Coker, Jorge Kohanoff and Mario G. Del Pópolo. *J. Am. Chem. Soc.*, **2011**, 133 (50), 20186–20193

²Francesc Molins i Domenech, Benjamin FitzPatrick, Andrew T. Healy, and David A. Blank. *J. Chem. Phys.*, **2012**, 137, 034512

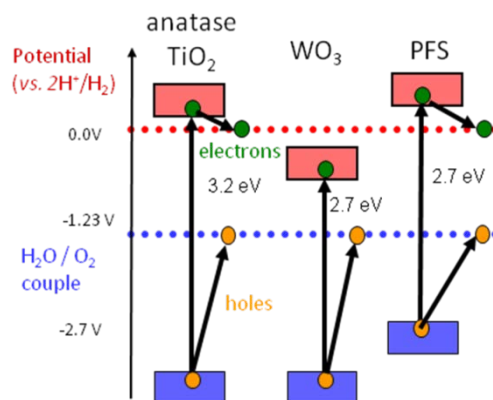
Perovskite oxynitrides and pyrochlore oxides: Light harvesting and surface chemistry of complex semiconductors

Polina Burmistrova, Limin Wang, Andrew Malingowski, Peter Khalifah
Department of Chemistry
Stony Brook University
Stony Brook, NY 11794-3400

Many prior measurements on LaTiO_2N have showed that this semiconductor has a band gap (~ 2.25 eV) which absorbs most of the visible light spectrum and also has band edge energies appropriate for driving both half reactions for overall water splitting. This system has not yet been shown to be capable of overall water splitting, but merits further investigation due to the tunable nature of its perovskite structure. Initial specular reflectivity data from spectral ellipsometry measurements suggested that these compounds have exceptionally high absorbance coefficients for visible light ($\alpha > 10^5 \text{ cm}^{-1}$), results which have been recently confirmed by absorption measurements collected in transmission geometry which are much more sensitive to energies near the band edge. These results have also been correlated with very high-level DFT calculations (w/ Mark Hybertsen, BNL), which are found to very accurately reproduce the structure and optical properties of this phase, as well as to give insights into their potential anisotropy. Based on these results, we have investigated the growth kinetics of these oxynitride compounds to enable the preparation of substantially thinner films than were studied previously, and demonstrate that the optical properties are minimally affected by film thickness. Prior films may have been an order of magnitude thicker than necessary to effectively harvest visible light photons, leading to unnecessarily high carrier recombination rates. Preliminary carrier transport measurements on these compounds will be presented. Collaborative surface science studies (John Lofaro, Michael White, SBU/BNL) show that the surface of LaTiO_2N films greatly differ from the bulk in valence and stoichiometry in a manner that is expected to adversely influence their photoelectrochemical activity, and provides insights into which surface treatment measurements for this substance (in thin film or powder form) are likely to succeed or fail.



We have recently demonstrated that pyrochlore-family semiconductors (PFS) such as $\text{AgBiNb}_2\text{O}_7$ ($E_g \sim 2.72$ eV) and $\text{Ag}_{1/2}\text{Bi}_{5/6}\text{Ta}_2\text{O}_{6.5}$ ($E_g \sim 2.96$ eV) are capable of effectively absorbing visible light yet still have a valence band edge which is suitably aligned for driving H_2 fuel production. Some unusual structural aspects of the ions comprising these structures have been determined. Efforts to prepare and characterize the thin films of these and other structurally related semiconductors with similar or smaller band gaps will be discussed.



List of Participants

Participants List – 35th Solar Photochemistry Research Meeting

Dawn Adin
U.S. Department of Energy
Dawn.adin@science.doe.gov

Neal Armstrong
University of Arizona
Dept. Chemistry and Biochemistry
Tucson, AZ 85721
520-730-7365
nra@email.arizona.edu

John Asbury
Department of Chemistry
Pennsylvania State University
University Park, PA 16801
814-863-6309
jasbury@psu.edu

Robert Bartynski
Rutgers University
136 Frelinghuysen Rd.
Piscataway, NJ 08854
732-445-5500
bart@physics.rutgers.edu

Victor Batista
Yale University
P.O. Box 208107
New Haven, CT 06477
203-432-6672
victor.batista@yale.edu

Matt Beard
National Renewable Energy Laboratory
15013 Denver West Parkway
Golden, CO 80401
303-384-6781
Matt.beard@nrel.gov

Jeffrey Blackburn
National Renewable Energy Laboratory
16253 Denver West Parkway
Golden, CO 80401
303-384-6649
jeffrey.blackburn@nrel.gov

David Blank
University of Minnesota
207 Pleasant St SE
Minneapolis, MN 55455
612-624-0571
blank@umn.edu

David Bocian
University of California, Riverside
Department of Chemistry
Riverside, CA 92521
951-827-3660
David.Bocian@ucr.edu

Shannon Boettcher
Department of Chemistry
University of Oregon
Eugene, OR 97403
541-346-2543
swb@uoregon.edu

Gary Brudvig
Yale University
P.O. Box 208107
New Haven, CT 06477
203-432-5202
gary.brudvig@yale.edu

Louis Brus
Columbia University
Chemistry Department
3000 Broadway
212-854-4041
leb26@columbia.edu

Emilio Bunel
Argonne National Laboratory
9700 S. Cass Avenue
Argonne, IL 60439
630-252-4309
ebunel@anl.gov

Participants List – 35th Solar Photochemistry Research Meeting

Ian Carmichael
Notre Dame Radiation Laboratory
University of Notre Dame
Notre Dame, IN 46556
574-631-4502
Carmichael.1@nd.edu

Felix N. Castellano
Department of Chemistry &
Center for Photochemical Sciences
Bowling Green State University
Bowling Green, Ohio 43403
419-372-7513
castell@bgsu.edu

Edward Castner
Rutgers University
610 Taylor Road
Piscataway, NJ 08854
732-445-2564
ecastner@rci.rutgers.edu

Philip Coppens
University at Buffalo SUNY Buffalo
732 NSc Complex
Buffalo, NY 14260-3000
716-645-4273
coppens@buffalo.edu

Robert Crabtree
Yale University
225 Prospect St.
New Haven, CT 06520
203-432-3925
robert.crabtree@yale.edu

Niels Damrauer
University of Colorado at Boulder
Dept. Chemistry and Biochemistry
Boulder, CO 80309
303-735-1280
niels.damrauer@colorado.edu

Linda Doerrer
Boston University
590 Commonwealth Ave.
Boston, MA 02139
617-358-4335
doerrer@bu.edu

C. Michael Elliott
Colorado State University
Department of Chemistry
Ft. Collins, CO 80523
970-491-5204
elliott@lamar.colostate.edu

Christopher Fecko
University of North Carolina
cfecko@unc.edu
919-962-0528

Susanne Ferrere
National Renewable Energy Laboratory
15013 Denver West Parkway
Golden, CO 80401
303-384-6502
Susanne.Ferrere@nrel.gov

Graham Fleming
Lawrence Berkeley National Laboratory
I Cyclotron Road
Berkeley, CA 94720
510-643-2735
grfleming@lbl.gov

Marye Anne Fox
University of California, San Diego
9500 Gilman Drive
La Jolla, CA 92093
858-534-3135
mafox@ucsd.edu

Participants List – 35th Solar Photochemistry Research Meeting

Arthur Frank
National Renewable Energy Laboratory
1617 Cole Blvd.
Golden, CO 80401
303-384-6262
Arthur.Frank@nrel.gov

Richard A. Friesner
Columbia University
Department of Chemistry
3000 Broadway, MC 3110
New York, NY 10027
212-854-7606
ec31@columbia.edu

Elena Galoppini
Rutgers University
73 Warren Street
Newark, NJ 07041
973-353-5317
galoppin@rutgers.edu

Bruce Garrett
Pacific Northwest National Laboratory
P.O. Box 999 (K9-90)
Richland, WA 99352
509-372-6344
bruce.garrett@pnnl.gov

Wayne Gladfelter
University of Minnesota
Department of Chemistry
Minneapolis, MN 55455
612-624-4391
wlg@umn.edu

Devens Gust
Arizona State University
Dept. Chemistry and Biochemistry
Tempe, AZ 85287
480-965-4547
gust@asu.edu

Thomas Hamann
Michigan State University
578 S. Shaw Lane, RM 411
East Lansing, MI 48824
517-355-9715
hamann@chemistry.msu.edu

Alexander Harris
Brookhaven National Laboratory
Building 555, P.O. Box 5000
Upton, NY 11973
631-344-4301
alexh@bnl.gov

Dewey Holten
Washington University
Chemistry Dept., One Brookings Dr.
St. Louis, MO 63130
314-935-6502
holten@wustl.edu

Michael Hopkins
The University of Chicago
Department of Chemistry
Chicago, IL 60637
773-702-6490
mhopkins@uchicago.edu

Libai Huang
University of Notre Dame
223 A Radiation Lab
Notre Dame, IN 46556
573-631-2657
luang2@nd.edu

Joseph Hupp
Northwestern University
2145 Sheridan Road
Evanston, IL 60208
847-441-0136
j-hupp@northwestern.edu

Participants List – 35th Solar Photochemistry Research Meeting

Justin Johnson
National Renewable Energy Laboratory
15013 Denver West Parkway
Golden, CO 80401
303-384-6190
justin.johnson@nrel.gov

David Jonas
University of Colorado
215 UCB
Boulder, CO 80309-0215
303-492-3818
david.jonas@colorado.edu

Prashant Kamat
University of Notre Dame
223 Radiation Laboratory
Notre Dame, IN 46556
574-631-5411
pkamat@nd.edu

David Kelley
University of California, Merced
5200 N. Lake Road
Merced, CA 95343
209-228-4354
dfkelley@ucmerced.edu

Peter Khalifah
Department of Chemistry
Stony Brook University
Stony Brook, NY 11794
631-632-7796
kpete@bnl.gov

Christine Kirmaier
Washington University
Dept. of Chemistry, Box 1134
St. Louis, MO 63130
314-725-6157
kirmaier@wustl.edu

Lowell Kispert
The University of Alabama
Box 870336
Tuscaloosa, AL 35487-0336
205-348-7134
lkispert@bama.ua.edu

Todd Krauss
University of Rochester
120 Trustee Road
Rochester, NY 14627-0216
585-275-5093
krauss@chem.rochester.edu

Frederick Lewis
Northwestern University
2145 Sheridan Road
Evanston, IL 60208
847-491-3441
fdl@northwestern.edu

Tianquan Lian
Emory University
1515 Dickey Drive NE
Atlanta, GA 30322
404-727-6649
tlian@emory.edu

Jonathan Lindsey
North Carolina State University
CB8204, 2620 Yarbrough Drive
Raleigh, NC 27695-8204
919-515-6406
jlindsey@ncsu.edu

Mark Lonergan
University of Oregon
1253 Department of Chemistry
Eugene, OR 97403
541-346-4748
lonergan@uoregon.edu

Participants List – 35th Solar Photochemistry Research Meeting

Rene Lopez
University of North Carolina at Chapel Hill
343 Chapman Hall, Physics Dept.
Chapel Hill, NC 27713
919-962-7216
rln@physics.unc.edu

Stephen Maldonado
University of Michigan
930 N. University
Ann Arbor, MI 48109-1055
734-647-4750
smald@umich.edu

Thomas Mallouk
Pennsylvania State University
Department of Chemistry
University Park, P A 16801
814-863-9637
tem5@psu.edu

Diane Marceau
U.S. Department of Energy
1000 Independence Ave., SW
Washington, DC 20585
301-903-0235
diane.marceau@science.doe.gov

Claudio Margulis
University of Iowa
118 TATL
Iowa City, IA 52242
319-335-0615
claudio-margulis@uiowa.edu

Mark Maroncelli
Penn State
I 04 Chemistry Building
University Park, PA 16802
814-865-0898
maroncelli@psu.edu

James McCusker
Michigan State University
578 South Shaw Lane
East Lansing, MI 48824-1322
517-355-9715
jkm@chemistry.msu.edu

Michael McGehee
Stanford University
mmcgehee@stanford.edu

Gail McLean
U.S. Department of energy
Gail.mclean@science.doe.gov

Thomas Meyer
University of North Carolina
Department of Chemistry
Chapel Hill, NC 27599-3290
919-843-8313
tjmeyer@unc.edu

Gerald Meyer
Johns Hopkins
3400 N. Charles St.
Baltimore, MD 21218
410-516-7319
meyer@jhu.edu

Josef Michl
University of Colorado
Dept. Chern. and Biochem., 215 UCB
Boulder, CO 80309-0215
303-492-6519
michl@eefus.colorado.edu

John Miller
Brookhaven National Lab
Chemistry 555
Upton, NY 11973
631 -344-4354
jrmiller@bnl.gov

Participants List – 35th Solar Photochemistry Research Meeting

John Miller
U.S. Department of Energy
1000 Independence Ave., SW
Washington, DC 20585
301-903-5806
John.miller@science.doe.gov

Ana Moore
Arizona State University
Dept. Chemistry and Biochemistry
Tempe, AZ 85287-1604
480-965-2747
amoore@asu.edu

Thomas Moore
Arizona State University
Dept. Chemistry and Biochemistry
Tempe, AZ 85287-1604
480-965-3308
tmoore@asu.edu

Karen Mulfort
Argonne National Laboratory
9700 South Cass A venue
Argonne , IL 60439
630-252-3545
mulfort@anl.gov

Nathan Neale
National Renewable Energy Laboratory
15013 Denver West Parkway
Golden, CO 8040 1
303-384-6165
nathan.neale@nrel. gov

Marshall Newton
Brookhaven National Laboratory
Chemistry Department
Upton, NY 11973
631 -344-4366
NEWTON@BNL.GOV

Daniel Nocera
Harvard University
dnocera@fas.harvard.edu

617-495-8904
Arthur Nozik
University of Colorado
215 UCB
Boulder, CO 80309
303-384-6603
anozik@nrel.gov

Shanlin Pan
The University of Alabama
Department of Chemistry
Tuscaloosa, AL 35487-0336
205-348-6381
spanl@bama.ua.edu

John Papanikolas
University of North Carolina
Department of Chemistry
Chapel Hill, NC 27599-3290
919-962-1619
john_papanikolas@unc.edu

Bruce Parkinson
University of Wyoming
1000 E. University
Laramie, WY 82071
303-766-9891
bparkin1@uwyo.edu

Oleg Poluektov
Argonne National Laboratory
9700 South Cass Ave.
Argonne, IL 60439
630-252-3546
Oleg@anl.gov

Dmitry Polyansky
Brookhaven National Laboratory
Chemistry Department
Upton, NY 11973
631-344-4315
dep@bnl.gov

Participants List – 35th Solar Photochemistry Research Meeting

Oleg Prezhdo
University of Rochester
Department of Chemistry
Rochester, NY 14627
585-276-5664
oleg.prezhdo@rochester.edu

Yulia Pushkar
Purdue University
525 Northwestern Avenue
West Lafayette, IN 97407
765-496-3279
ypushkar@purdue.edu

Jeffrey Pyun
University of Arizona
1306 E. University Blvd.
Tucson, AZ 85721
520-626-1834
jpyun@email.arizona.edu

Garry Rumbles
National Renewable Energy Laboratory
15013 Denver West Parkway
Golden, CO 80401
303-384-6502
garry.rumbles@nrel.gov

Scott Saavedra
University of Arizona
1306 E. University
Tucson, AZ 85721-0041
520-621-9761
saavedra@email.arizona.edu

Russell Schmehl
Tulane University
Department of Chemistry
New Orleans, LA 70118
504-862-3566
russ.schmehl@gmail.com

Charles Schmuttenmaer
Yale University
225 Prospect St.
New Haven, CT 06520-8107
203-432-5049
charles.schmuttenmaer@yale.edu

Mark Spitler
U.S. Department of Energy
1000 Independence Ave., SW
Washington, DC 20585
301-903-4568
mark.spitler@science.doe.gov

Michael Therien
Duke University
124 Science Dr. 5330 FFSC
Durham, NC 27708-0346
919-660-1670
michael.therien@duke.edu

David Tiede
Argonne National Laboratory
Chemical Sciences and Engineering
Argonne, IL 60439
630-252-3539
tiede@anl.gov

William Tumas
National Renewable Energy Laboratory
15013 Denver West Parkway
Golden, CO 80401
303-384-6502
Bill.tumas@nrel.gov

Jao van de Lagemaat
National Renewable Energy Laboratory
15013 Denver West Parkway
Golden, CO 80401
303-384-6143
jao.vandelagemaat@nrel.gov

Participants List – 35th Solar Photochemistry Research Meeting

Michael Wasielewski
Northwestern University
2145 Sheridan Rd.
Evanston, IL 60208
847-467-1423
m-wasielewski@northwestern.edu

Emily Weiss
Northwestern University
2145 Sheridan Rd.
Evanston, IL 60208-31 13
847-491-3095
e-weiss@northwestern.edu

Mary Beth Williams
Pennsylvania State University
Department of Chemistry
University Park, P A 16801
814-865-8859
mbw@chem.psu.edu

James Wishart
Brookhaven National Laboratory
Chemistry Department
Upton, NY 11973
63 I -344-4327
wishart@bnl.gov